



NEW CONCEPTS IN POLYMER SCIENCE

Radiation Chemistry of Biopolymers

A.S.

Y.A. Sharpatyi

Radiation Chemistry of Biopolymers

This page intentionally left blank

Radiation Chemistry of Biopolymers

V.A. Sharpatyi

///VSP///

CRC Press
Taylor & Francis Group
6000 Broken Sound Parkway NW, Suite 300
Boca Raton, FL 33487-2742

© 2006 by Taylor & Francis Group, LLC
CRC Press is an imprint of Taylor & Francis Group, an Informa business

No claim to original U.S. Government works
Version Date: 20120706

International Standard Book Number-13: 978-9-04-741867-2 (eBook - PDF)

This book contains information obtained from authentic and highly regarded sources. Reasonable efforts have been made to publish reliable data and information, but the author and publisher cannot assume responsibility for the validity of all materials or the consequences of their use. The authors and publishers have attempted to trace the copyright holders of all material reproduced in this publication and apologize to copyright holders if permission to publish in this form has not been obtained. If any copyright material has not been acknowledged please write and let us know so we may rectify in any future reprint.

Except as permitted under U.S. Copyright Law, no part of this book may be reprinted, reproduced, transmitted, or utilized in any form by any electronic, mechanical, or other means, now known or hereafter invented, including photocopying, microfilming, and recording, or in any information storage or retrieval system, without written permission from the publishers.

For permission to photocopy or use material electronically from this work, please access www.copyright.com (<http://www.copyright.com/>) or contact the Copyright Clearance Center, Inc. (CCC), 222 Rosewood Drive, Danvers, MA 01923, 978-750-8400. CCC is a not-for-profit organization that provides licenses and registration for a variety of users. For organizations that have been granted a photocopy license by the CCC, a separate system of payment has been arranged.

Trademark Notice: Product or corporate names may be trademarks or registered trademarks, and are used only for identification and explanation without intent to infringe.

Visit the Taylor & Francis Web site at
<http://www.taylorandfrancis.com>

and the CRC Press Web site at
<http://www.crcpress.com>

Radiation chemistry of biopolymers

V.A. Sharpatyi

Edited by Prof. E.G. Zaikov

2006

TABLE OF CONTENTS

	Page
Introduction	vi
Chapter 1. Radiation chemistry. Basic concepts of radiation chemistry	1
1.1. Types of radiation	1
1.2. The effect of ionizing radiation	2
1.3. Key terms of radiation chemistry	5
References	13
Chapter 2. Primary radiation-chemical processes	14
2.1. Ions and ionic reactions	14
2.2. Excited states and conversions of excited molecules	17
2.3. Free radicals and their conversions	23
References	25
Chapter 3. Detection methods for radiolytic products	26
3.1. Mass-spectroscopy method	26
3.2. Luminescence methods	28
3.3. The method of electron paramagnetic (spin) resonance	32
References	39
Chapter 4. Radiation chemistry of water and water solutions	40
4.1. Primary products of water radiolysis	40
4.2. Radiolysis of frozen-up aqueous solutions	44
References	49
Chapter 5. Basic regularities of solution radiolysis	50
5.1. Substances – the radical acceptors	50
5.2. Concentration dependence of dissolved substance dissociation yield	60
References	63
Chapter 6. The regularities of radiolysis of aqueous biopolymers and their components	64

6.1. Biopolymers as radical acceptors	64
6.2. Concentration dependence of dissolved substance conversion yield. Radiosensibilization effects	68
6.3. Radiolysis of frozen-up aqueous solutions of biopolymers	73
References	83
Chapter 7. The problems of radiation chemistry of protein molecules	85
7.1. Structure and composition of protein molecules	87
7.2. Basic radiolytic effects in proteins	88
7.3. Oxygen effect at protein radiolysis	107
7.4. Reactions of water radicals with side branches of polypeptide chain	109
7.5. Radiolysis features of aqueous solutions of proteid	115
7.6. Conclusion	117
References	119
Chapter 8. Radiation chemistry of polysaccharides	124
8.1. Structure of carbohydrates, polysaccharides	125
8.2. The role of •OH and electron in carbohydrate degradation	128
8.3. The origin of carbohydrate radicals	131
8.4. Primary macroradical transformations	138
8.5. Oxygen effect	153
8.6. Formation mechanisms for low-molecular products	160
8.7. The role of adsorbed water in formation and conversions of macroradicals; radiolysis of the structured starch–water system	191
8.8. Post-radiation effects in polysaccharides	206
References	213
Chapter 9. The radiolysis method for glycoproteids	219
9.1. Structure and properties of glycoproteids	219
9.2. Radiolytic properties of glycoprotein components	222
9.3. Formation and conversions of radicals in glycoprotein components	226
9.4. Radiolysis of glycoprotein and radical conversions	243
References	255

Chapter 10. Radiation chemistry of DNA aqueous solutions	257
10.1. DNA structure	257
10.2. Radiological effects	258
10.3. Macroradical conversions	264
10.4. Oxygen effect	271
10.5. About molecular mechanisms of radiation mutagenic action	280
References	284
Chapter 11. Chromatin DNP radiolysis	287
11.1. Composition and structure of DNP complex	287
11.2. Basic radiolytic effects	289
11.3. On the origin of DNP radicals	293
11.4. DNA fragment degradation	298
11.5. On the mechanism of radical conversions	303
11.6. DNA-protein crosslink formation	306
References	311
Chapter 12. Radiolysis in the cell. Primary stages of radiolysis	313
12.1. Problems in describing radiation-chemical processes proceeding in the cell	313
12.2. Low-temperature radiolysis of chlorella cells	314
12.3. Electron spin resonance (ESR) of irradiated chlorella cells	318
12.4. Low-temperature radiolysis of animal tissues	321
12.5. On the origin of free radicals in irradiated plant tissues ...	324
References	329
Chapter 13. The effects of radioprotection and sensibilization of radiation degradation of biopolymers in aqueous solutions	330
13.1. General principles of organics radioprotection in the condensed phase	330
13.2. On radioprotection of biopolymers at primary physical stages of radiolysis	333
13.3. The effects of radioprotection and radio-sensibilization of biopolymer degradation at the stages of radical formation and conversion	336

Conclusion	349
References	353

INTRODUCTION

In recent 20 – 25 years, the interest to investigations of the transformation mechanisms of biological macromolecules induced by ionizing radiation was continuously increased. This problem is touched upon in monographs and reviews on radiation chemistry of various systems, including biological systems, published in Russia and abroad. This is assignable, because the practice of ionizing radiation energy use poses the problem of effective control over radiation processes, for example, associated with processing and modification of natural raw stock, agriculture waste utilization – in industry and cattle breeding, and protection of the living cell and human organism from radiation – in radiobiology and medicine.

The resolution of these problems significantly depends the understanding of primary mechanisms of the radiation-chemical degradation of biopolymers, which are the basic components of natural raw stock and a cell, at their radiation in the composition of complex heterogeneous system as, for example, raw stock and industrial and agricultural wastes, and the more so the cell.

Among the broad literary data on radiation chemistry of various organic compounds, there are scanty works devoted to the study of primary mechanisms of biopolymer radiolysis. In this monograph, we classify the ideas about primary stages of radiation-chemical transformation of the main biopolymers, paying special attention to radiolysis of their aqueous solutions, formation and conversion mechanisms of macroradicals, synthesized in acts of solvent radical interaction with biopolymer molecules and in their natural complexes. In this connection in initial Chapters (1 – 6) the ideas about water radiolysis mechanism and the basic regularities of aqueous solution radiolysis of biologically valuable substances are discussed. The subsequent Chapters (7 – 12) are devoted to radiolytic properties of biopolymers – protein, polysaccharides, DNA, and their natural complexes – showing extending charts of their radiolysis mechanisms. The conclusive Chapter 13 presents data on the mechanisms and abilities of radioprotection and sensitizing of the radiation degradation of biomacromolecules.

This monograph includes, first of all, the data of Soviet (Russian) investigators, who have decisively contributed in the development of this field of knowledge (the schools headed by Academicians N.N. Semenov, N.M. Emanuel, N.K. Kochetkov, and many others).

The monograph is based on the course of lectures on radiation chemistry of biopolymers, read by the author to students specializing in physics, radiation biophysics and radiobiology.

Prof. G.E. Zaikov

Acknowledgement

The author is greatly thankful to Professor Gennady E. Zaikov for reviewing and editing the manuscript and Alex Yu. Borissevitch for translation and preparation of the book CRC.

Chapter 1. Radiation chemistry. Basic concepts of radiation chemistry

1.1. TYPES OF RADIATION

In physics, the term “*irradiation*” defines emission of electromagnetic waves (the field theory) or photons (the corpuscular theory), as well as other corpuscular emissions: α - and β -particles, neutrons, protons and nuclei. The class of electromagnetic radiation includes:

- 1) X-rays and γ -irradiation – electromagnetic emissions at the wavelength between 10^{-11} and 10^{-7} cm, which represent the short-wave region of the spectrum;
- 2) charged particles having kinetic energy enough for ionization act as they pass through the medium: electrons, protons, deuterons, α -particles, polyvalent ions, nuclear fission products of heavy elements.

Being electrically neutral particles, neutrons themselves passing through the medium may not induce ionization acts. As they interact with atoms of the medium, neutrons may produce the above-mentioned ionizing particles or photons, and electromagnetic emissions. The type of neutron interaction with the substance is defined by the energy of neutrons and the type of nuclei. The specific energy of ionizing radiation is electron-Volt (eV) equal energy obtained by electron (charged 1.602×10^{-19} C) as it passes the potential drop equal 1 Volt.

Sometimes, X-ray radiation is characterized by the wavelength. The quantum energy expressed in electron-Volts is related to the wavelength (λ , Å) by the following ratio:

$$E = \frac{12,400}{\lambda}.$$

1.2. THE EFFECT OF IONIZING RADIATION

As ionizing radiation hits the substance, it ionizes and excites atoms and molecules in the substance. The ionization act (electron removal from electron shell of an atom or molecule) is accompanied by occurrence of two oppositely charged ions: positively charged ions (an atom or a molecule which lost an electron) and negatively charged ion (an atom or a molecule obtaining electron).

Excited states of atoms of molecules are formed under the impact of ionizing radiation on them, which induces electron transition from basic to excited orbital. At the reverse transition from excited to basic orbital, the energy is emitted as photons of visible, ultraviolet light or X-rays.

Charged particle interaction with the matter

As passing through the matter, charged particles lose energy due to various processes. For heavy particles, the energy losses are generally caused by elastic occlusions with electrons of atoms from the medium and, the more so, by losses for irradiation and scattering. The energy scattering rate depends on the charged particle origin. For heavy charged particles, the average energy loss per specific path or the so-called stopping power of the matter (Erg/cm) is expressed by the Bethe formula:

$$-\frac{dE}{dx} = \frac{4\pi Z^2 e^4}{m\nu^2} N_A \rho \frac{Z}{A} \left[\ln \frac{2m\nu^2}{I(1-\beta^2)} - \beta^2 - \frac{\delta}{2} \right],$$

where Ze is the charge of moving particle, electrostatic units; e is the electron charge; m is the rest mass of electron, g; ν is the particle speed, cm/s; N_A is the Avogadro number; ρ is the medium density; A and Z are atomic weight and the number of atom; $\beta = \frac{\nu}{c}$, where c is the light speed; I is the average potential of the medium atom excitation; δ is a correction factor for polarization of the matter atoms in electrical field of moving particle; E is the kinetic energy of electron.

As shown by the current formula, the stopping power of the medium is proportional to its density. It is also shown that the lower the particle energy, the higher the stopping power of the matter. The distance that can be passed by a charged particle is called the free path of the particle, defined by the stopping power of the matter.

Interaction between X-rays and γ -radiation with the matter

X-rays and γ -radiation lose their energy in three basic processes: photoelectrical absorption, Compton scattering and pair production. Hence, as penetrating through the substance the radiation intensity decreases due to the following law:

$$I = I_0 \exp(-\mu x),$$

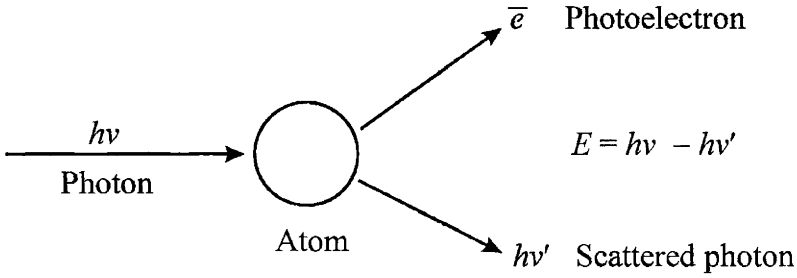
where x is the path length; $\mu = \mu_{\text{ph}} + \mu_{\text{C}} + \mu_{\text{p}}$ is the linear coefficient of energy absorption indicating, at which thickness x of the absorber I_0 intensity of γ -radiation is e -fold decreased due to photoeffect (μ_{ph}), Compton's effect (μ_{C}), or $e^- - e^+$ pair formation (μ_{p}), where μ_i are corresponding absorption coefficients. The relative contribution of each of these processes to general absorption of the medium depends on the irradiation energy and the medium origin. The photo effect dominates at low energy values, Compton's effect – at moderate energy values, and the pairing effect – at high energy of photons. Also, Compton's effect dominates in materials with low atomic numbers (biological media), in the range between 1 keV and 2 MeV.

The photoelectrical effect manifests itself as electron emission after photon absorption by the electron shell of the atom. Kinetic energy of this electron is

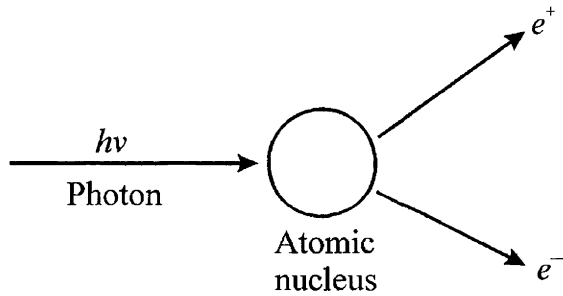
$$E = h\nu - E_{\text{b}},$$

where $h\nu$ is the photon energy; E_{b} is the electron bond energy in the atom.

At Compton's effect ($h\nu > 0.3$ MeV) photons are scattered due to elastic collisions with electrons of the medium and transmit a part of their energy to the latter.



The energy of Compton recoil electrons (photoelectrons) equals the difference between energies of the primary and scattered photons. As pairing proceeds, photon disappears in the atomic nucleus field with simultaneous of electron and positron. The photon energy $h\nu$ transits to masses at rest of these two particles and kinetic energies of electron (E_e) and positron (E_p).



Obviously,

$$E_p + E_e = h\nu - 2mc^2; 2mc^2 = 1.02 \text{ MeV.}$$

At higher photon energies, photonuclear reactions proceed, which contribution to total absorption by the environment is low.

As an X-ray or γ -quantum is absorbed with simultaneous excitation of atom, excitation energy may be internally redistributed (the internal conversion) and, as a result, electron is emitted from K-shell. At the second stage, electron from the upper shells, L-shell, for example, jumps to K-vacancy during 10^{-15} s. Hence, the energy excess, which is $(E_K - E_L)$ may stipulate for one more electron emission from the atom, already from its cover shell. This is the Auger effect (autoionization of atom).

Thus in all interactions of photons with the matter secondary particles (electrons) are formed, which may also cause ionization and excitation.

1.3. KEY TERMS OF RADIATION CHEMISTRY

Absorbed radiation dose, units of measurement

For the absorbed radiation dose we take the energy of ionizing radiation, absorbed by specific mass of radiated matter. Gray (Gy) is the unit of absorbed dose. The specific unit (1 Gy) equals absorption of 1 Joule of any kind of ionizing radiation by 1 kg of the matter. For X-rays and γ -radiation, absorbed and exposure doses are distinguished. The exposure dose is measured in Coulombs per kilogram (C/kg). The dose of X-rays and γ -radiation is the radiation measure based on its ionizing ability. Let us consider this more comprehensively, using the Gaussian system of units for higher visualization. In this system the exposure radiation dose is measured in roentgens (1 R = 2.58×10^{-4} C/kg). The specific dose of 1R corresponds to the dose, at which in 1 cm³ of air (e.g. 0.001293 g) radiation under normal conditions ($T = 273$ K, $P = 1,013$ hPa) ions carrying charges of 1 electrostatic unit of each sign are produced. As known from electrochemical data, 1 electrostatic unit of electricity equals 2.1×10^9 specific charge of each polarity e.g. this amount of ionic pairs is formed in 1 cm³ of air, which absorbed 1 R radiation dose. On average, formation of 1 ionic pair consumes 34 eV (1 eV = 1.6×10^{-12} erg). Thus at 1 R dose 1 cm³ of air absorbs $(2.1 \times 10^9) \times 34 = 0.114$ erg or 87 erg per air gram, respectively.

Previously published papers on radiobiology and radiation chemistry present such notions as Roentgen-equivalent-physical (Rep) and Roentgen-equivalent-man (Rem). Rep is the dose, at which water or tissue absorbs the same amount of energy, as under the impact of 1 R dose. Rem is the unit of radiation dose equivalent (the amount of any radiation type), which causes the same biological damage compared with 1 rad dose impact of X-rays (within the energy range between 100 and 1,000 keV). In the SI system the dose-equivalent is measured in Joule per kilogram (J/kg):

$$1 \text{ Gy} = 1 \text{ J/kg} = 100 \text{ rad} = 107.5 \text{ Rep} = 6.24 \times 10^{15} \text{ eV/g.}$$

The absorbed dose intensity represents energy of ionizing radiation absorbed by specific mass of radiated substance during specific time (Gy/s, Gy/min, Gy/h). In SI system, the intensity unit of exposure dose equals

Ampere per kilogram (A/kg). The relation between dose intensity and the dose value is presented by the formula:

$$P = \frac{D}{t}.$$

Radiation intensity is the radiation energy, which hits 1 cm² of the matter surface transversal to the radiation ray direction during 1 s.

Also, radiobiology studies dependence of biological organism survivability on radiation dose (survivability curves). Survivability curves are subdivided to linear, exponential, sigmoid, and combined curves. The combined curves are frequently represented by a sum of two components. The notion of radiation dose (D_{37}), under which the quantity of survived organisms equals 37% (the second case of survivability curves), is used for specification of radiosensitivity of organisms in the study of survivability curves.

Radiation-chemical yield

It is the main quantitative characteristic of any reaction proceeding under the impact of ionizing radiation. It is denoted as G and equals the number of molecules, ions, atoms and free radicals, formed or consumed as the system absorbs 100 eV of ionizing radiation. First of all, the radiation-chemical yield depends on the type of radiation-chemical reaction. For non-chain processes, G is low (8 – 15 molecule/100 eV as a maximum). For chain processes G may be much higher (ten and hundred thousands of molecules per 100 eV). The radiation-chemical yield is determined by the initial straight intersect of the product accumulation curve (or initial compound degradation curve) with respect to the absorbed dose, studied in the experiment:

$$G = N \times \frac{100}{D},$$

where N is the number of product molecules in the current volume of the matter; D is the dose (eV) absorbed by the current volume. If the effect – dose dependence under study is nonlinear, and due to methodological restrictions relatively low doses cannot be measured, G is determined with the help of analytical expression for the effect – dose dependence, similar to the example

that follows. At 77 K 10% aqueous deoxyribonucleic acid – DNA (with molecular mass (*MM*) equal 1×10^6) was radiated. The concentration of radicals in the samples was determined with the help of ESR method (Table 1.1). In this system, radical accumulation obeys the following dependence:

$$C = C_{\infty}[1 - \exp(-kD)] \text{ (Figure 1.1),}$$

where C and C_{∞} are concentrations of radicals R, initial and at high radiation doses, respectively; k is the constant of radical dissociation during radiation of the sample, determined by linear anamorphosis tangent in $\ln\left(\frac{C_{\infty}}{C_{\infty} - C}\right) - D$ coordinates.

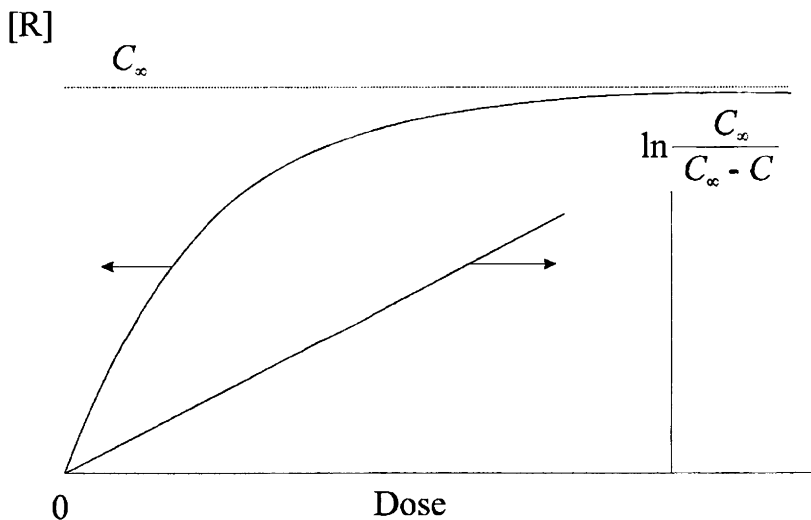


Figure 1.1. Radical accumulation in DNA aqueous solutions, irradiated at 77 K (refer to Table 1.1)

The value $G(\text{radical}/100 \text{ eV})$ is determined by the following expression:

$$G = \frac{dC}{dD_{D \rightarrow 0}} = kC = \frac{10.3 \cdot 10^{17} \cdot 0.26 \cdot 100}{6.24 \cdot 10^{19}} = 0.43.$$

Table 1.1

Accumulation of radicals in aqueous solutions of DNA, γ -radiated at 77 K

Dose $\times 10^4$, Gy	$C_R \times 10^{17}$, radical/g	$(C_\infty - C) \times 10^{17}$, radical/g	$\frac{C_\infty}{C_\infty - C}$	$\ln\left(\frac{C_\infty}{C_\infty - C}\right)$
0.8	2.1	8.2	1.26	0.2311
2.8	5.4	4.5	2.2	0.7500
6.2	7.8	2.5	4.13	1.4183
10.4	9.4	0.9	11.5	2.7081
∞	10.3	0	—	—

Primary processes and structure of ionization areas

As mentioned above, the ionizing radiation produces charged particles in the matter (molecular ions and electrons) and excited molecules. Conversion of these primary products of radiolysis causes formation of radicals, atoms, and final products of radiolysis. The interaction of ionizing radiation with the matter produces a large quantity of secondary electrons, which are the main transmitters of radiation energy to the matter. The energy spectrum of secondary electrons weakly depends on the radiation type and energy, as well as on the origin of radiated substance. A considerable part of secondary electrons has energy exceeding the ionization and excitation potential of molecules. Therefore, these electrons may also ionize and excite molecules. To determine the relative role of any processes in formation of radicals or molecular products, yields of primary active particles should be known. In the gas phase, energetic yield equals 3–4 ionic pairs and is prone to some increase with molecular mass of the gas and decreasing ionization potential. In the condensed phase, the ionization potential is decreased by 0.5 – 2 eV compared with the gas phase due to the medium polarization by cation and electron. The yield of ions in the condensed phase was determined indirectly with the help of different methods:

$$G(\text{ions}) = 3 - 4.$$

For various substances, the yield of primary excited molecules (including neutralization of charged particles) equals 1 to 3. For water, total yield of radiolized molecules (ionized and excited) reaches ~8.

In condensed media secondary electrons lose energy in the ionization zones: spurs, blobs, short and main tracks. This classification is based on the energy of electron, which forms the current area. Spurs represent the ionization zones, produced by electrons with energy below 100 eV. Blobs represent the retarding region of electrons with energy (E_e) of 100 to 500 eV. The upper energy limit is defined by the fact that an electron with $E_e \leq 500$ eV still remains in the range of Coulomb's field of the parent ion. The distance at which Coulomb's interaction becomes weaker than kT depends on dielectric permeability of the medium (kT is the measure of the mean heat energy, where

$$k = \frac{R_0}{N} = 1.3804 \times 10^{-16} \text{ erg/deg} = 8.6167 \times 10^{-5} \text{ eV/deg}.$$

Therefore, the upper border of electron energy, which forms a blob, is different for different substances. Hydrocarbons have $E_e = 500$ eV. Ionic density in spurs and blobs is almost equal. In short tracks, the electron energy varies within the range between 500 and 5,000 eV. The ionic density approaches that in spurs and blobs. In essence, a short track is the region of continuously overlapping spurs and blobs. Main tracks are ionic regions created by electrons with the energy $E_e \leq 5,000$ eV. The ionic regions do not overlap, and the main tracks consist of isolated spurs.

The above-shown classification of ionic regions is valid for radiation with low linear energy transfer (LET), which is γ -radiation, high-speed electrons, and X-rays. In the interaction of deuterons, high-energy protons and fission fragments, which represent types of radiation with high LET, only main tracks may be detected, because ionic density in them is similar to spurs, blobs and short tracks. The relative role of various ionic regions cardinally depends on the energy of radiation. For Compton electrons of γ -radiation, emitted from ^{60}Co , about 65% of energy is localized in spurs.

The local concentration of primary active particles – ions, excited molecules and low-speed electrons – in ionic regions depends on secondary electron retarding rate. The energy transfer mechanism from electron to the matter changes with electron retarding rate. If $E_e \geq E_{\text{exc}}$ (where E_{exc} is the excitation energy), the energy of electron is mainly consumed for ionization and excitation of molecules. Let r_1 be the electron track length in the condensed phase (paraffin oil), at which its energy decreases from E_e to 8 eV – the approximate lower level of electron excitation potential. If $E_{\text{exc}} \geq E_e \geq E_{\text{vibr}}$ (where E_{vibr} is the vibratory energy), the energy of electron is mainly consumed

for vibratory excitation of molecules. In hydrocarbon fluid the energy of electron decreases from 8 to 0.4 eV at a distance $r_2 \approx 17 \text{ \AA}$. If $E_{\text{exc}} \geq E_e \geq kT$, the electron energy decreases to thermal (thermalization) as a result of rotary degree of freedom excitation in molecules and intermolecular vibrations. These processes are rather ineffective. In hydrocarbon fluids or solids, the track length r_3 , when electron loses energy from 0.4 eV to thermal level, equals 50 – 70 \AA . In polar substances this length is shorter.

The above estimations give an opportunity to present distribution of primary active particles in a typical spur, formed by an electron with energy of 100 eV. Let a spur be sphere-shaped. The central zone of the spur ($r \leq r_1$) accumulates ions ($G_{\text{ion}} \approx 4$); the second zone ($r_1 + r_2 \geq r > r_1$) – vibration-excited molecules, mostly in the electronic ground state. Finally, the third zone ($r_1 + r_2 + r_3 \geq r > r_1 + r_2$) accumulates thermolized electrons ($G_e \approx 4$). If energy of the secondary electron, which forms the ionic region, differs from 100 eV, only radius of the central zone r_1 and the quantity of primary active particles are changed, whereas r_2 and r_3 are independent of E_e . This distribution is established during time $\tau \leq 10^{-13} \text{ s}$.

Linear energy transfer (LET)

As losing energy, ionizing particles form different number of ions and excited molecules on their way. For example, as is completely retarded, α -particle from ^{210}Po forms about 150,000 ionic pairs in the air. Chemical reactions and the yield of products depend on both the number of active products formed and their concentration in the track, which is defined by the radiation energy loss rate in the substance. The energy loss rate is measured in units of linear energy transfer, which are keV/ μm . Table 1.2 shows some mean path and LET values for α -particles in air and in water. LET depends on the energy of particles, increasing with their retarding. LET values shown in Table 1.2 were obtained by dividing the initial energy of α -particles by their mean path. Since the rate of the energy loss changes with the particle retarding, LET shows different values along the track. For various particles possessing equal energy, LET value increases in the following sequence:

γ -radiation \rightarrow high-speed electrons \rightarrow low-energy X-rays \rightarrow β -particles \rightarrow
 \rightarrow protons \rightarrow deuterons \rightarrow α -particles \rightarrow heavy ions \rightarrow nuclear debris

Table 1.2

The mean path and LET for α -particles

Nuclide	Energy, MeV	Mean path		LET in water
		In air, cm	In water, μm	
^{222}Ra	4.795	3.3	33.0	145
^{210}Po	5.30	3.8	38.9	136
^{222}Rn	5.49	4.0	41.1	134

Enhanced ionizing radiation and biopolymers

In radiobiological studies, carried out on cells and animals, and in medical practice (radiotherapy or radiodiagnostics), various radioactive nuclides (tritium ^3H , phosphorus ^{32}P , iodine ^{125}I , etc.) incorporated in the composition of biopolymers, such as proteins, nucleic acids and so on, are used as labels. They are the so-called incorporated irradiators. In all above-mentioned cases, the manifestation of the enhanced ionizing radiation effect with respect to short paths of ionizing particles in the medium, caused by either large mass of ionizing particle (recoil nucleus) or low energy of light particles (β -particles), should be taken into account.

The following radiolytic effects of incorporated irradiators are observed:

1. Radiation by particles emitted by a radionuclide, particularly, β -particles emitted by ^3H with the mean energy between 5 and 6 keV and ^{32}P with energy of ~ 1.7 MeV, and other β -particles, emitted by atomic nuclei at the interaction K-shell electrons, the so-called K-capture (^{125}I with energy of 100 keV). For example, β -particles emitted by tritium form an enhanced ionized cylinder with the mean track length shorter than $1 \mu\text{m}$ and the mean ionization index along the track equal 160. In the case of β -particles emitted by ^{32}P , a loosely ionized track is formed, $2,500 \mu\text{m}$ long, where 5.5 ionizing acts are implemented along the initial micron.
2. The radiation impact induced by recoil nuclei, which is so higher, the higher energy of a particle emitted by radioactive nucleus. For instance, the mean recoil energy of ^{32}P nuclei equals 30 eV at the mean path of

phosphorus nucleus of 10 Å, whereas ^3H has the energy of 1 eV at negligibly short path of H nuclei.

3. Radiation due to multiple ionization of an atom (the Auger effect). The K-vacancy at carbon, nitrogen and oxygen atoms shows energies of 280, 400 and 530 eV, respectively. It may be concluded about enhanced ionized track formation in this case, too. This should be accompanied by crucial degradation of biopolymer molecule in the vicinity of the current atom (or even in the neighbor molecules). According to literary estimations, radiation-chemical yield from nucleic acids, impacted by electrons or protons with 1 MeV energy, caused by the Auger effect, equals 0.03 that gives about 5% of total ionization index.

In this Section, one more type of biopolymer degradation induced by incorporated irradiators should be mentioned. It is the nucleus transmutation effect e.g. the change of the atomic nucleus origin. For example, β -decomposition of ^3H and ^{32}P produces helium and sulfur nuclei, which require balanced sets of electrons different from those in the source nuclei. Restructuring of electronic shells and changing of the number of valence electrons induce a considerable variation in the structure of biopolymer, in the area possessing these atoms, proceeding up to chemical bond break. For example, β -decomposition of $^{32}\text{P}_{15}$ produces $^{32}\text{S}_{16}$, and in DNA strand instead of pentavalent phosphorus tetravalent sulfur occurs. As a result, a bond between phosphorus and sugar unit in the nucleotide is broken e.g. a single-stranded break occurs (see Chapter 10 for details).

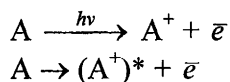
REFERENCES

1. Bugaenko L.T., Kuzmin M.G., and Polak L.S., *Chemistry of Higher Energies*, 1988, Moscow, Khimia, 336 p. (Rus)
2. Byakov V.M. and Nichiporov F.G., *Internal Track Chemical Processes*, 1985, Moscow, Energoatomizdat, 152 p. (Rus)
3. Ivanov V.S., *Radiation Chemistry of Polymers*, 1988, Leningrad, Khimia, 320 p. (Rus)
4. Kudryashov Yu.B., *Radiation Biophysics (Ionizing Radiation)*, 2004, Moscow, FIZMATLIT, 448 P. (Rus)

Chapter 2. Primary radiation-chemical processes

2.1. IONS AND IONIC REACTIONS

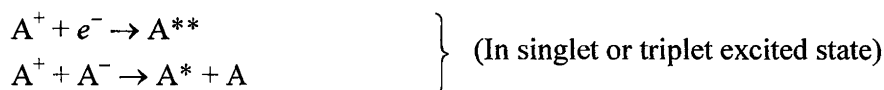
The primary acts accompanying the interaction between ionizing radiation and the matter are ionization and excitation of molecules of the matter. Ions are formed by the following reactions:



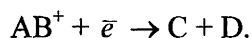
They are detected in gases using the mass-spectroscopy method and in the condensed phase with the help of express spectrophotometric method, ESR and radiothermoluminescence (see Chapter 3).

Ionic reactions

Recombination

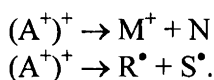


If ionized molecules are united in aggregates with other molecules or transient ion-molecular complexes, neutralization reaction of the following type may proceed:

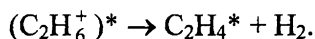


Dissociation

Positively charged ions, which are formed under the impact of ionizing radiation, are usually excited (possessing excessive vibratory motion): distances between atomic nuclei in ions are different from these in non-ionized molecules. Their decomposition by the following reaction is possible:

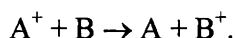


Both degradation products represent molecules or radicals, one of which is ionized. Charge is localized on the component with lower ionizing potential.

Example

Positive charge is transferred to ethylene. The ionizing potential of ethylene is $I = 10.5$ eV; $I_{H_2} = 15.4$ eV.

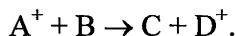
As excited ions of complex molecules dissociate, bonds break not necessarily in places of initial excitation (at molecule interaction with radiation), because the charge may quickly migrate in the molecule. Energy is redistributed in the molecule, and the weakest bonds are preferably broken. For example, in aliphatic haloid compounds the weakest carbon-halogen bond is usually broken (dissociation of complex ions is retarded to 10^{-5} s). Ions may be restructured before or during dissociation. Hence, the products are formed, which may not be produced by simple bond break in the primary ion. For example, ethylene formation from $C_2H_6^+$ is stipulated by intramolecular migration of hydrogen atom.

Charge transfer (or electron transfer from molecule to ion)

Hence, $I_B < I_A$. Excessive energy may convert to vibratory or electron excitation energy of reaction products. Sometimes the energy of excitation is so high that is able to induce secondary dissociation of formed ions, for example:



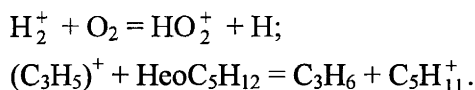
Ion-molecular reactions



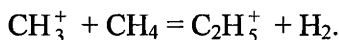
Examples:

1. $\text{H}_2\text{O}^+ + \text{H}_2\text{O} = \text{H}_3\text{O}^+ + \text{OH};$
2. $\text{CH}_4^+ + \text{CH}_4 = \text{CH}_5^+ + \text{CH}_3.$

The process may proceed with participation of protons (H^+) or H^- :

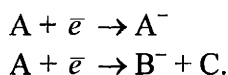


Radical and carbon-carbon bond formations:

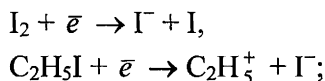


Exothermal ion-molecular reactions require no activation energy. They proceed at a very high rate even at low temperature.

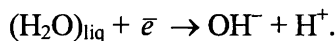
Addition of electron



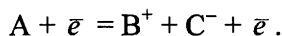
The reaction is defined by electron affinity energy of the molecule A, which high value is of importance for halogens, molecular oxygen, liquid water, alcohols, etc.:



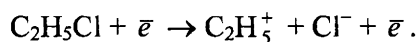
In liquid water:



The third alternative of electron addition is the following:



For example:



2.2. EXCITED STATES AND CONVERSIONS OF EXCITED MOLECULES

The ground state energy is exceeded by: the electron excitation energy, approximately, by 3 eV; vibratory energy – by 0.01 – 1 eV (Ir-spectroscopy area, 10^4 K); rotary energy – by 10^{-4} – 10^{-2} eV (the microwave area, 10^2 – 10^4 μm).

Figure 2.1a presents energy diagram of two-atomic molecule; ρ is the distance between two nuclei; ρ_e is the equilibrium distance; $q = \rho - \rho_e$. As ρ approaches infinity, we obtain two atoms with total electronic energy equal

$$\varepsilon_{\text{el}}(\infty) = \varepsilon_{\text{el}}^{(1)} + \varepsilon_{\text{el}}^{(2)}.$$

As ρ approaches zero, ε_{el} will tend to infinity due to repulsion between nuclei: the repulsion energy equals $Z_1 Z_2 \bar{e}^2 / \rho$, where $Z_1 e$ and $Z_2 \bar{e}$ are charges of nuclei. The molecule is stable, when there is ρ , at which $\varepsilon_{\text{el}}(\rho)$ dependence has a minimum. If approach of atoms produces no minimum of energy, this means that stable molecule 2 is not formed. D_e is the molecule dissociation energy;

$U(q)$ is potential energy of the movement of nuclei; $T(q)$ is the kinetic energy of relative movement of nuclei.

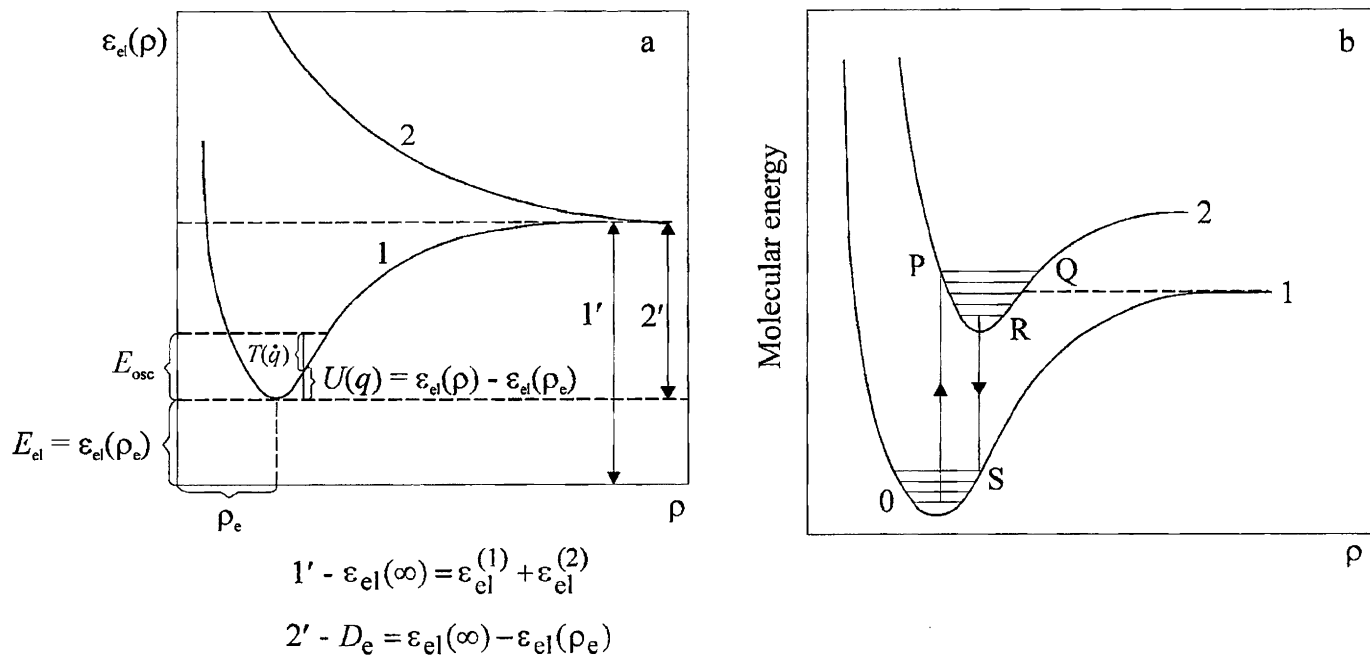


Figure 2.1. Potential energy curves for two-atomic molecules:
 a – stable molecule formation (1), no stable molecule formed (2);
 b – ground (1) and electron-excited (2) states of the molecule

Total vibration period equals 10^{-13} s, and the molecule excitation transfer – 10^{-15} s. Nuclei are much heavier than electrons. Transition to a new electronic state proceeds at such high rate that nuclei are unable to change their location during this time (the Frank–Condon principle). In Figure 2.1b, in the point *P* of the diagram, the excited molecule is compressed, begins vibrating with amplitude *PQ*, converts energy to heat, and then transits to the level *R*. Then after photon emission (with *RS* energy) the molecule returns to the ground state *S*. This process is fluorescence (with semifluorescence period $\ll 10^{-8}$ s). The molecule loses energy in collisions and returns to the state *O*.

The process of excited molecule conversion is the following:



Transition probabilities between two current levels at light absorption and emission are identical; however, spectra are different. Intensities of bands are defined by both transition probability and population of the initial levels (the ground state for absorption spectrum and the excited state for emission spectrum).

To express intensity of the absorption band, the oscillator force *f* is used:

$$f = 4.315 \times 10^{-9} \int \varepsilon \, d\nu.$$

Molar index of extinction ε ($\text{cm}^{-1}\text{M}^{-1}$) equals

$$\varepsilon = \frac{1}{lC} \log \frac{I_0}{I},$$

where *I* is the light intensity penetrated through light-absorbing substance layer; ν is frequency expressed in wave numbers. For allowed transition, $f = 1$. Peaks of $f = 0.1 - 1$ correspond to molar index of extinction equal 10,000 – 100,000 with respect to the band width. For a single symmetrical peak, *f* may be approximated as

$$f \cong 4.6 \times 10^{-9} \cdot \varepsilon_{\max} \Delta\nu_{1/2}.$$

For transition between states a and b , integral intensity of the absorption band is determined as

$$I = \left| \int_{-\infty}^{+\infty} \psi_b^* \mathbf{M} \psi_a^* d\nu \right|^2,$$

which is the transition moment integral, where ψ_a^* and ψ_b^* are wave functions of the excited and ground states, respectively; \mathbf{M} is the electric dipole moment proportional to the difference of electron dipole moments of the ground and excited states (due to different electron distribution); $d\nu$ is the specific volume element. \mathbf{M} is a vector and, therefore, I may be factorized. The allowed transition requires even a single non-zero factor.

The internal conversion occurs in the case, if potential energy curve of the excited state of the molecule approaches or crosses the ground state curve. This process proceeds within a single oscillation act (10^{-13} s). Such transitions may be implemented at different levels of molecules and, as a result, fluorescence from the lower level happens.

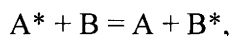
Intramolecular (internal) transitions

In this case, fluorescence becomes lesser intensive, whereas phosphorescence period increases to $10^{-4} - 10^{-3}$ s or even to several seconds. Retarded fluorescence is observed in cases of $T \rightarrow S$ transition in the vibration act and collision of molecules. Triplet lifetime increases as transiting to highly viscous or solid systems, because collisions of molecules become more infrequent and deactivation by collisions with solvent molecules decreases. Hence, the medium has no effect on singlet excited states. Phosphorescence is not observed in nonviscous solutions, where triplet states are deactivated in Auger (nonradiant) interactions with solvent molecules. The internal conversion of singlet and triplet states is much easier in the presence of paramagnetic atoms or heavy nuclei in the environment, because this shortens the lifetime of triplet states. Triplet states play a significant role for radiation chemistry because of their long lifetime. They are of biradical origin and, therefore, manage to react. Quickly moving charged particles produce optically allowed transitions (from singlet ground to singlet excited state). Slowly

moving (at neutralization, too) charged particles may induce optically forbidden transitions.

Nonradiant energy transmission

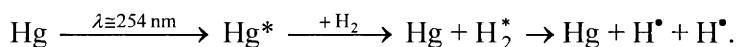
It represents a process:



which is possible, if the excitation energy of B is less than or equal the excitation energy of A.

1. Collisions (collisions of the second kind)

In gas



Here Hg excitation energy is 113 cal/mol, and H–H bond energy is 103 cal/mol.

In liquids (an example with scintillating fluids)

The energy is absorbed by solvent and transmitted to an organic compound dissolved in it, which then fluoresce.

2. Nonradiant resonance conversion or dipole-dipole interaction between two molecules

The necessary condition is overlapping of A* irradiation and B absorption spectra. The range is 50 – 100 Å (immediate proceeding in gases, liquids and solids).

3. Energy may be transmitted, if excited molecule is somehow regulated with the surrounding ones, as, for example, excited molecule in a crystal. The electronic excitation (exciton) is quickly transmitted from one molecule to another, remaining each molecule in the excited state for a very short time (about a single vibration period). The lifetime of exciton equals $\sim 10^{-8}$ s (in solids, activated admixtures, scintillating fluids, crystals, polymeric molecules, and less frequently in liquids). For many cases, to explain high exciton transmission rate in some scintillating fluids, the existence of domains – small regulated groups of molecules (10 – 15 molecules each) – was suggested. Collision with

any molecule in a domain containing excited molecule is equivalent to collision with the excited molecule itself.

The role of excited states in biological processes

There are many familiar biological processes having transition to electronic excited of molecules as the initial stage: photodynamic effect, photolytic protein inactivation, photodimerization of nucleic acid bases, vision, bioluminescence, and photosynthesis. Properties of molecules in singlet and triplet excited states are different due to differences in electronic structures (distribution of charges, spin density, and π -electronic exchange symmetry). This reasons the differences in donor-acceptor properties of molecules, reactivity, and the lifetime of excited states.

Chemical properties of excited molecules

Chemical properties of molecules depend on states of electrons present on antibonding orbits. In the ground state, these electrons are paired. As two molecules approach one another, potential energy increases due to repulsion of electronic shells. To obtain a new configuration, a molecule must be provided with the energy enough for overcoming this repulsion.

As radiated, molecules transit to the excited state and their reactivity increases due to the following reasons:

1. Excited electron remained on the orbit after removal of the first electron from it is not paired yet. Any other molecule with unpaired electron may form a bond with the excited molecule as soon as their orbits begin overlapping. The potential barrier of the reaction decreases.
2. Excited electron is present on the orbit, which occupies the greater part of the space, and is weaker bound to the rest of the molecule. Therefore, this electron may be much easier detached by another electrophilic agent.
3. Since excited electrons, sometimes, are inactive in chemical bond formation, nuclei in excited molecule are not so strongly bound compared with unexcited one. Therefore, the excited molecules dissociate much easier than unexcited ones.

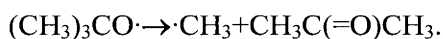
2.3. FREE RADICALS AND THEIR CONVERSIONS

Radicals represent particles, atoms and parts of molecules having unpaired valence electrons. This definition indicates that such particles are formed at radiation impacting of substances due to the act of ionization (electron removal from a molecule or an atom) and excitation with subsequent bond break in the molecule. The next Chapter discusses the nature and properties of radicals more comprehensively. As electron is detached from or added to neutral molecule, charged particle with unpaired electron is formed: cation-radical or anion-radical.

Radical reactions

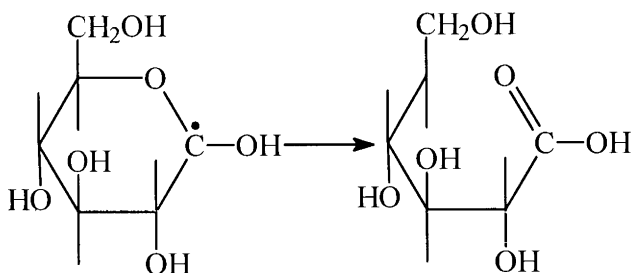
Dissociation of radicals

The most typical example is represented by dissociation with formation of simpler radical and a molecule with unsaturated bond. For instance, in the case of tertiary butoxy-radical in the gas phase the following high-temperature dissociation takes place:



Intraradical rearrangement and radical isomerism

In these acts, radicals with more stable structures are formed, for example, in the case of primary radicals' isomerism in carbohydrates obtained at radiolysis of their frozen aqueous solutions (refer to Chapter 8).

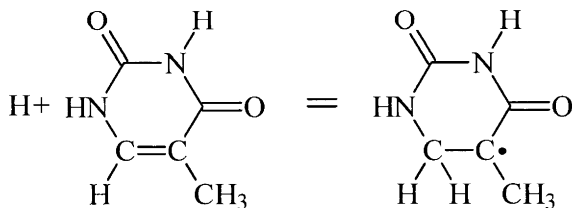


Migration of hydrogen atoms, haloids and methyl groups is most frequently observed.

Interactions of radicals with substances

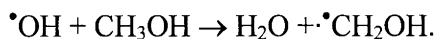
Addition of radicals

The most typical case is the interaction of radicals with π -electrons of unsaturated systems. Hence, a new radical is produced in this process:



Substitution reactions

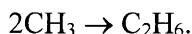
These reactions may compete with reactions of addition of radicals to unsaturated bonds:



Radical recombination reactions

Radical recombination or dimerization

This process represents linking of two radicals with covalent chemical bond formation. In gases these processes proceed at high rate. For example, for methyl radicals, almost every collision produces ethane molecules:



In solutions the recombination rate changes with respect to the diffusion rate up to 10^6 l/(mol×s) level.

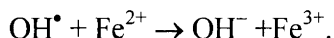
Disproportionation of radicals

Disproportionation of radicals proceeds with formation of saturated and unsaturated molecules:



Redox reactions

The typical example of these processes is one-electron transition in reactions of radicals with ferrous iron ions:



REFERENCES

1. Kayushin L.P., Pulatova M.K., and Krivenko V.G., *Free Radicals and Their Conversions in Radiated Protein*, 1976, Moscow, Atomizdat, 272 p. (Rus)
2. Bensasson R.V., Land E.J., and Truscott T.G., *Flash Photolysis and Pulse Radiolysis. Contributions to the Chemistry of Biology and Medicine*, Pergamon Press, Oxford, 1983.
3. Pulatova M.K., Rikhireva G.T., and Kuropteva Z.V., *Electron Spin Resonance in Molecular Radiobiology*, 1989, Moscow, Energoatomizdat, 232 p. (Rus)

Chapter 3. Detection methods for radiolytic products

Radiolytic conversions of various substances are generally defined by the radiation conditions (phase state of the medium, ionizing radiation intensity, composition and concentration of solutions, etc.). Therefore, determination of the radiolytic conversion mechanism for the system under study and control of the reactions in it require recording moments of occurrence and conversion of primary products of radiolysis – ions, excited states and radicals, which are highly reactive particles. The simplest case is presented radiolysis of gaseous substances. Under these conditions, the interaction between molecules is minimal. Ions may be registered directly in the gas phase, for example, using the mass-spectrometry method. Spectroscopic methods may help in tracking formation and conversions of intermediate compounds having absorption bands in various ranges of wavelengths. In the condensed phase at direct registration of ions, luminescence and ESR methods may help in tracking formation and conversions of ions and excited states, and ESR and spectroscopy methods help in tracking radical conversions. Let us briefly discuss physical grounds of these methods of investigation.

3.1. MASS-SPECTROSCOPY METHOD

The mass-spectrometric method determining the origin of ions and studying their properties is based on the principle of ion acceleration by electrostatic field between condenser plates with accelerating potential V and their emission to evacuated system, placed in magnetic field with intensity H . Magnetic field is transversal to the electron motion direction. In magnetic field ions are moving by circular orbits of radius r . The semicircle radius r depends on the accelerating potential V , mass of ion m , ion charge e , and magnetic field intensity H .

Potential energy of the ions converted to kinetic energy $\frac{mv^2}{2}$, and at complex acceleration

$$eV = \frac{mv^2}{2}.$$

In magnetic field, the centrifugal force $\frac{mv^2}{r}$ is balanced by centripetal force Hev :

$$\frac{mv^2}{r} = Hev,$$

wherefrom

$$v = \frac{Her}{m}.$$

Thus, substituting the velocity expression into the above formula of energy conservation, we get:

$$Hev = \frac{mH^2e^2r^2}{2m^2}.$$

From this expression, we deduce that

$$\frac{m}{e} = \frac{H^2r^2}{2v}.$$

Values of H , v and r can be determined in the experiment that gives an opportunity to obtain $\frac{m}{e}$ value.

Ions occurring on the detector are formed by the following reaction:

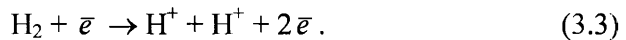


The quantity of positive ions is expressed in ionic current units and depends on potential V_i , which accelerates the ionizing electron. For example, ion H_2^+ is

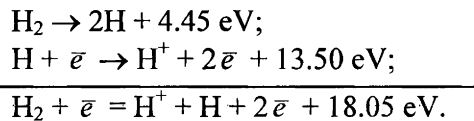
not formed until potential reaches 15.4 V level (the ionizing potential of molecular hydrogen), which is necessary for running the reaction



As energy of electrons exceeds the ionization potential, hydrogen molecule may dissociate into two atoms, one of which is ionized:



The potential at which H^+ ions occur equals 18.05 V. This potential equals the sum of H–H bond break energy and the ionization potential of hydrogen atom. Of course, this is true under the condition that the products formed are present in the ground state:



This method may be applied to determination of bond break energies of many molecules.

In mass-spectrometer the lifetime of ions is up to 10^{-5} s (up to 10^{-13} s in the liquid phase).

3.2. LUMINESCENCE METHODS

The method is based on substance luminescence registration at transition of particles from the excited to the ground state. The luminescence spectrum represents a dependence of luminescence intensity on the wavelength of irradiated luminescent light:

$$I_{\text{lum}} = f(\lambda_{\text{lum}}).$$

At photoluminescence (luminescence excitation by photoimpacting of the sample) luminescence intensity I_{lum} at current wavelength of exciting light is

measured. For radioluminescence, the excitation source is ionizing radiation. In the case of chemiluminescence, luminescence occurs due to proceeding of chemical reactions, in which products in the excited state are formed. The excitation spectrum (the case of photoluminescence, the luminescence action spectrum) shows the dependence of luminescence intensity on the wavelength of exciting light:

$$\frac{I_{\text{lum}}}{I_{\text{exc}}} = f(\lambda_a),$$

where I_{exc} is the exciting light intensity, expressed in quantum/(cm²s). The quantum yield of luminescence φ equals the ratio of the number of luminescence quanta to the quantity of absorbed quanta:

$$\varphi = \frac{I_{\text{lum}}}{I_q(1-T)},$$

where I_q is the quantity of quanta hitting the sample; T is the sample transmittance.

The important characteristic of the method is the luminescence damping time, from which lifetime of the excited state of the molecule is determined. If the lifetime of excited molecule is 10⁻⁸ s or shorter, we are speaking about fluorescence; if the lifetime time is longer, we mean phosphorescence. More strictly, the first case represents luminescence at transition from the excited singlet state to the ground state; the second case represents luminescence at transition from the excited triplet state to the ground state.

For instance, the luminescence methods are applied to investigations of biopolymer structure and changes in it under the effect of various factors (reagents, radiation, etc.) in the studies of energy intra- and intermolecular migration processes. The measurement technique for radiochemiluminescence is used in the study of radiolytic conversion mechanism of dissolved substances.

The radiothermoluminescence (RTL) method used for detection of primary products of radiolysis, which are ions, is based on a physical phenomenon – the formation of excited states of molecules in acts of recombination of oppositely charged ions. Of course, such measurements can be implemented, if the recombination act is accompanied by luminescence,

registered, for example, by a photoelectron multiplier. In the general case, the RTL method includes the following sequence of operations:

- substance radiation at low temperature, usually, liquefied nitrogen temperature;
- irradiated substance of system heating up;
- luminescence registration by appropriate devices.

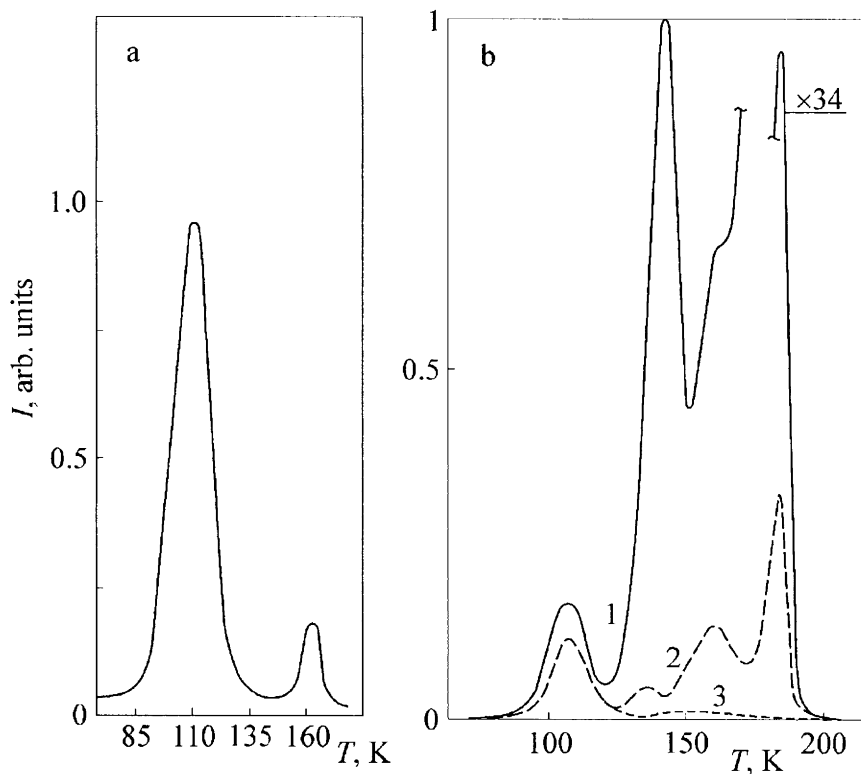


Figure 3.1. Photon emission curves for solutions radiated at 77 K:

- (a) vitreous 10 M KOH solution containing thymine (0.001 M), radiation dose 16 kGy;
- (b) 4.6 M NaH_2PO_4 solutions containing glucose, radiation dose 2.4 kGy: 1 – without glucose; 2 – 0.01 M glucose; 3 – 0.1 M glucose

The right branch of the curve 1 is recorded at amplification 0.03

Radiation of substances at low temperature, when the majority of molecular movements in the system under study are suppressed, induces capture of oppositely charged ions, formed in the primary acts, by any traps – the defects of molecular structure, if the systems represent solutions, polymers, etc. Heating up of irradiated samples initiate mobility of some components of the system, traps are destroyed, and charges are released from them, recombining and forming excited states. The latter luminesce, simultaneously. Typical photon emission curve (RTL curve) is shown in Figure 3.1. The maximum in the low-temperature range indicates occurrence of mobility of the system components or recombination of primary ions:



The luminous intensity depends on the number of recombining ions and luminosity or the luminescence activator concentration. The application of this technique to the study of acceptor properties of various compounds in relation to primary products of radiolysis of water, biopolymer components, protectors or radiosensitizers was the most successful.

Figure 3.1b presents photon emission curves for hydrophosphate solutions containing different concentrations of glucose. The measurement data for these samples, obtained by the RTL technique, indicate a decrease of luminous intensity in the solution in high-temperature area ($T = 170 - 180 \text{ K}$) with increasing glucose concentration. This is explained by drifting of recombining particles – OH^- radical and electron – in the reaction with glucose.

The spectrophotometry method

The spectrophotometry method represents a particular case of ion detection in the condensed phase – solids or solutions. This method is based on particle detection using optical absorption spectra. For monochromatic light, absorption in the sample is described by the Bouguer-Lambert law:

$$I = I_0 \exp(-\varepsilon Cl),$$

where I_0 and I are intensities of incident light and after penetrating through the sample, respectively; C is the concentration of particles or molecules, cm^{-3} ; l is

the sample thickness, cm; ε is index of absorption per specific unit e.g. specific index of absorption.

The relation between luminous flux penetrating through the sample to incident luminous flux is called transmission:

$$T = \frac{I}{I_0},$$

and the value $(1 - T)$ is absorption. The value

$$D = -\log T = \log \frac{I_0}{I}$$

is called optical density. If C is expressed in gram-moles per liter at the sample thickness equal $l = 1$ cm, the index of absorption ε (the molar extinction) is determined by the equation:

$$\log \frac{I_0}{I} = D = \varepsilon Cl.$$

Thus if we know the molar absorption index of any particle, its concentration in the current system may always be determined. Many works on radiation chemistry were devoted to the study of properties and reactions with the substances of solvated (hydrated in the case of aqueous solutions) electron. For this purpose, the express method of spectrophotometering combined with pulsed irradiation of solution.

3.3. THE METHOD OF ELECTRON PARAMAGNETIC (SPIN) RESONANCE

The method of electron paramagnetic (spin) resonance (the so-called EPR or ESR, discovered by E.K. Zavoisky in 1944, in Kazansky University) is applied to registration of intermediate products having uncompensated spin. The particular case is its application to detection of ions (anions or cations), if they also have uncompensated spin. The method is based on the Zeeman effect,

which concludes in splitting of energy levels of particles having electrons with uncompensated spin in magnetic field. According to the theory of magnetism, the matter is presented by two classes of substances:

- paramagnetic, represented by atoms or molecules possessing magnetic moment;
- diamagnetic, represented by atoms or molecules having no constant magnetic moment.

The method of electron paramagnetic (spin) resonance (ESR) is used for detection of paramagnetic particles. As a paramagnetic substance is placed to constant magnetic field H , elementary magnetic dipoles in particles are oriented at a definite angle to the external magnetic field direction. Every orientation has its own energy of dipole interaction with the field equal

$$E_{\text{magn}} = -\mu_J H \cos \theta,$$

where θ is the angle between the field intensity vector and the magnetic moment of dipole μ_J ; J is the total quantum number of many-electron particle:

$$J = L + S.$$

Here $L = \sum l_i$; $S = \sum S_i$, where L and S are orbital and spin quantum numbers, respectively. Total magnetic moment of electron equals the vector sum

$$\mu_{\text{H}} = \mu_{\text{L}} + \mu_{\text{S}},$$

where $\mu_{\text{L}} = -\frac{le\hbar}{2mc} = -l\beta$, β is the Bohr magneton, when $l = 1$ e.g. electron is

located on p -orbital of the atom; $\mu_{\text{S}} = -\frac{Se\hbar}{mc}$. Since the magnetic moment of the particle is determined by the value of J , its projection to the field direction (magnetic quantum number) has discrete values only: $J, J-1, J-2, \dots, -J$. As a consequence, every energy level in magnetic field is split to $(2J+1)$ magnetic levels.

Let us consider a substance, consisting of particles having one unpaired electron. Let us also assume that this unpaired electron has no orbital moment. Thus interaction of the substance with external magnetic field will produce two

energy levels corresponded to two possible orientations of spin 1/2 in constant magnetic field:

$$\begin{aligned} E_1 &= -\mu_1 H \cos \theta; \\ E_2 &= -\mu_2 H \cos \theta; \\ \mu &= -g\beta\hbar; \\ E_1 &= 1/2 g\beta H; \\ E_2 &= -1/2 g\beta H, \end{aligned}$$

where g is the spectroscopic splitting factor, which is the dimensionless value equal 2.0023 for free electron – the proportion factor taking into account ESR line location in the spectrum. In the general case,

$$g = 1 + \frac{J(J+1) - L(L+1) + S(S+1)}{2J(J+1)}.$$

As constant magnetic field is applied to the sample, it becomes heat equilibrated, and the levels are populated with respect to the Boltzmann distribution law. The relation between populations of the upper and the lower levels equals

$$\exp\left(-\frac{g\beta H}{kT}\right),$$

where k is the Boltzmann constant; T is the absolute temperature.

As electromagnetic field of the frequency providing $h\nu = g\beta H$ is applied to a system, two processes may take place:

- absorption of electromagnetic radiation quantum;
- its induced emission.

These processes are equiprobable, but excessive population of the lower level causes absorption of electromagnetic radiation. Figure 3.2 shows the simplest dependence of UHF power absorption on the intensity of constant magnetic field.

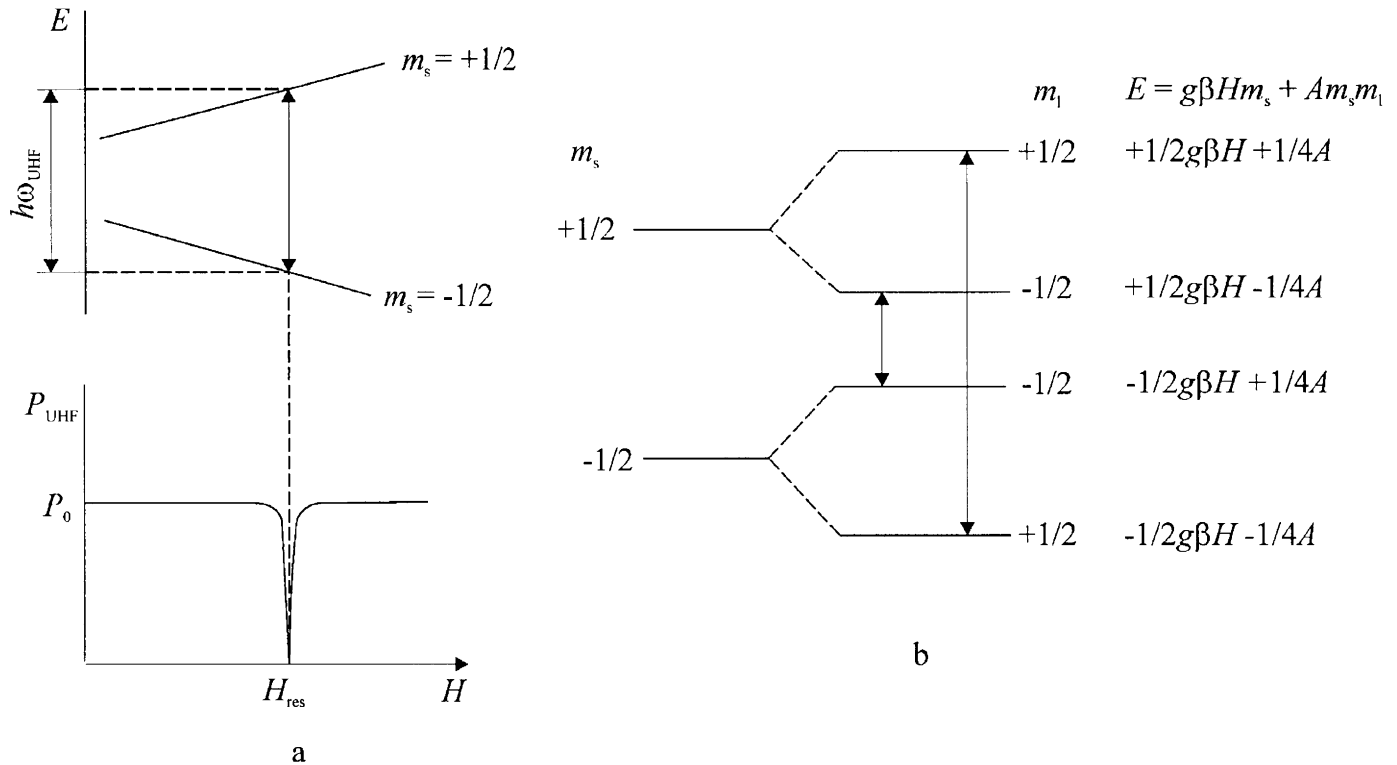


Figure 3.2. Diagrams showing splitting of energy levels:

(a) for paramagnetic particle having $l = 0$ and $S = 1/2$;

(b) for unpaired electron at interaction of its magnetic moment with magnetic moment of the nucleus $I = 1/2$

P_{UHF} is the UHF power; H_{res} is the intensity of magnetic field at resonance absorption

For the majority of paramagnetic particles, the resonance absorption represents a complex curve, which is ESR spectrum characterized by the following parameters: band intensity, width and shape, g -factor value, and hyperfine structure (HFS) of the spectrum. These parameters define the origin and structure of paramagnetic particles, their interaction with one another and the environment.

The interaction between μ_e and external magnetic field is expressed by Hamiltonian as follows:

$$H = -\mu_e \text{ or } H = g\beta HS_z.$$

The interaction between a nucleus and electron (hydrogen atom is the simplest example) is described by the following Hamiltonian:

$$H_0 = g\beta HS_z - g_N \rho_N H I_z,$$

where I_z is the Z-axis component of the nuclear spin. Magnetic moments of electrons and nuclei interact by the contact interaction (Fermi) mechanism:

$$H_1 = a\mathbf{IS} = a(I_x S_x + I_y S_y + I_z S_z),$$

where hyperfine interaction constant is $a = (8\pi/3)g\beta g_N \beta_N |\psi_0|^2$. Hence, Hamiltonian of dipole interaction is

$$H_2 = -g\beta g_N \beta_N \left[\frac{\bar{I}\bar{S}}{r^3} - \frac{3(\bar{I}r)(\bar{S}r)}{r^5} \right],$$

where \vec{r} is the radius-vector from μ_e to μ_N ; r is the distance between appropriate magnetic moments. Thus, the general Hamiltonian is the following:

$$H_0 = g\beta HS_z - g_N \beta_N H I_z + H_1 + H_2.$$

Hyperfine splitting

The energies of levels are expressed as follows:

$$E = g\beta H m_s + A m_s m_I.$$

For hydrogen atom: the nuclear moment is $m_I = \pm 1/2$ and spin electron moment is $m_s = \pm 1/2$. The selection rules for ESR spectra are $\Delta m_s = \pm 1$, $\Delta m_I = 0$.

Figure 3.2 shows that the energy of two transitions observed equals

$$E = g\beta H \pm A/2,$$

where A is the distance between neighboring bands. Taking the equation

$$h\nu = g\beta H$$

and substituting values of h and β , and $g_e = 2$ into it, and moreover assuming $H = 10^3$ G, we get the frequency of electromagnetic energy equal $\sim 10^{10}$ Hz, which falls within the ultrahigh frequency (UHF) range.

ESR band intensity

This parameter is defined as the area under the resonance absorption curve and is proportional to the quantity of paramagnetic particles in the sample. Their absolute quantity is estimated by comparing intensities of spectra measured for the sample under study and the standard.

Band shape

The band shape in ESR spectrum is compared with Lorentz's and Gaussian band shapes, which are for Lorentz shape:

$$y = \frac{a}{1 + bx^2},$$

and for Gaussian:

$$y = a e^{-bx^2}.$$

Band width

The band width ΔH_{\max} is related to the half-height ($\Delta H_{1/2}$) by the following expression:

$$\Delta H_{\max} = (2\sqrt{3}) \Delta H_{1/2} \text{ (the Lorentz shape)}$$

and

$$\Delta H_{\max} = \left(\frac{2}{\ln 2} \right) \frac{1}{2} \Delta H_{1/2} \text{ (the Gaussian shape).}$$

Usually, real bands are of an intermediate shape (Lorentz in the middle and Gaussian at the borders).

Relaxation times

Relaxation times t_1 and t_2 define the resonance band width as follows:

$$\Delta H_{1/2} \sim \frac{1}{t_1} + \frac{1}{t_2}.$$

Here t_1 is the lifetime of the excited electron spin. For organic radicals t_1 may reach several seconds. The main contribution into the band width is made by relaxation processes related to spin-spin interactions, proceeding during t_2 time, which is inversely proportional to $\Delta H_{1/2}$.

Due to the information content, the ESR method offers considerable possibilities of investigating primary and intermediate processes of radiolytic conversions of the matter, because it detects particles with uncompensated spin, free radicals (including cation- and anion-radicals), and, moreover, particles in the triplet excited state. All the above-mentioned products are formed at the substance radiation, produced by the interaction of ionizing radiation with the matter transiting to ionized and excited states due to complete and incomplete removal of electrons from molecular orbits. Further on, these states of molecules change due to dissociation producing (similar to some cases of ion conversion in the gas phase) free radicals. Under common

conditions (in solutions), short-living free radicals may be quite easily detected at low temperature of the irradiated sample. This technique helps in registering and studying properties of radicals of many radiated systems, including frozen-up solutions. This will be discussed in more detail on the example of radiolysis of biopolymers (Chapters 7 – 12).

REFERENCES

1. Pshezhetskii S.Ya., Kotov A.G., Milinchuk V.K., Roginsky V.A., and Tupikov V.I., *ESR of Free Radicals in Radiation Chemistry*, Moscow, Khimia, 1972, 480 p. (Rus)
2. *Experimental Methods of Chemical Kinetics*, Ed. N.M. Emanuel and G.B. Sergeev, Moscow, Vysshaya Shkola, 1980, 375 p. (Rus)
3. Partridge R.H., 'Thermoluminescence of polymers', In: *Radiation Chemistry of Macromolecules*, vol. 1, Chapter 10, Ed. M. Dole, New York-London: Academic Press. 1972.
4. E.B. Burlakova, K.E. Kruglyakova, and L.N. Shishkina, *Studying Synthetic and Natural Antioxidants in vitro and in vivo*, Moscow, Nauka, 1992, 110 p. (Rus)

Chapter 4. Radiation chemistry of water and water solutions

4.1. PRIMARY PRODUCTS OF WATER RADIOLYSIS

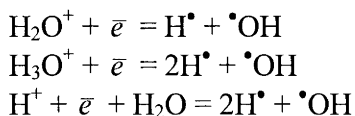
Mass-spectrometric studies of water vapor radiolysis allowed experimental detection of the majority of primary products of water molecules. Table 4.1 shows ionic composition formed after water vapor radiation, reactions of ion formation, potentials of their occurrence and relative yield. Clearly, H_3O^+ , HO^+ and H^+ ions are most popular. The intensity of H_3O^+ ion peak is proportional to square pressure of water vapor in the ionic source. Therefore, this ion is formed in a secondary biomolecular reaction. The yield of negatively charged ions is very low. Water radiolysis produces neutral radicals H and OH, and molecular products H_2 and H_2O_2 .

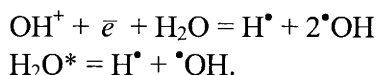
Table 4.1

Basic ions formed in water vapor according to mass-spectrometry data

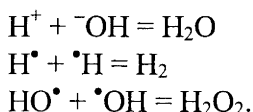
Ion	Occurrence potential, V	Relative intensity		Reaction
		at 50 V	at 100 V	
H^+	4.8; 5.6	–	0.6	$\text{H}_2\text{O} + \bar{e} \rightarrow \text{H}^- + \text{OH}$
O^-	7.4; 7.5	–	0.15	$\text{H}_2\text{O} + \bar{e} \rightarrow \text{O}^- + 2\text{H}(\text{O}^- + \text{H}_2)$
H_2O^+	12.61; 13; 12.67	100	100	$\text{H}_2\text{O} + \bar{e} \rightarrow \text{H}_2\text{O}^+ + 2\bar{e}$
H_3O^+	10.8; 18.1; 18.7	20	–	$\text{H}_2\text{O}^+ + \text{H}_2\text{O} \rightarrow \text{H}_3\text{O}^+ + \text{OH}$
$\text{OH}^+\cdot\text{O}^+$	18.5; 18.8; 19.6	20	23	$\text{H}_2\text{O} + \bar{e} \rightarrow \text{OH}^+ + \text{H} + 2\bar{e}$
H^+	19.5; 29.15; –	2	2	$\text{H}_2\text{O} + \bar{e} \rightarrow \text{O}^+ + \text{H}_2 + 2\bar{e}$

Radicals H^\bullet and $\bullet\text{OH}$ are formed by the following reactions:

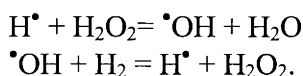




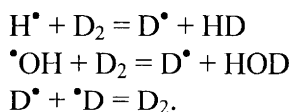
Molecular products are formed in the interaction of radicals in the absence of radical acceptors in the gas phase on the vessel walls or near water molecules:



Proceeding of the following reactions is also possible:



It has been proven (by Firestone) that D_2 is a good acceptor of H^\bullet and $^\bullet\text{OH}$ radicals. For instance, at water vapor radiolysis by β -particles from tritium the following reactions proceed:



Since the numbers of H^\bullet and $^\bullet\text{OH}$ radicals equal one another and equal the number of dissociated water molecules, then HD yield may be expressed as follows ($T < 150^\circ\text{C}$):

$$G(\text{HD}) = G(-\text{D}_2) = G(\text{Y}) = G(^\bullet\text{OH}) = G(-\text{H}_2\text{O}) = 11.7.$$

In water vapor, up to 3.5 ionic pairs per each 100 eV are formed. For irradiation of water vapor by 10 keV electrons, it has been found that total yield of dissociated water equals:

$$G(-\text{H}_2\text{O}) = G_{\text{ionized molec.}} + G_{\text{excited molec.}} = 2.91 + 4.96 = 7.87.$$

Note that the same ultimate yield of water dissociation, corresponded to complete invoking oxidative or reduction component of water radiolysis e.g. $G \cong 8$, may also be reached in the case of radiolysis of concentrated aqueous solutions of acceptor of any of these components, if conditions suppressing the inverse reactions of primary water radical recombination are obeyed in the experiment. For example, in strong alkaline solutions of sodium nitrate (1 M) the yield of nitrate ion dissociation equals $G = 4 - 4.5$ (it is determined by nitrite-ion accumulation; two reduction equivalents are consumed for each nitrate ion).

Liquid water radiolysis

Table 4.2 shows water radiolysis products and types of reactions, in which these products are formed under the effect of ionizing radiation on water and as a result of primary particle conversions in the following 10^{-12} s. The Table is composed with respect to data on vaporized water radiolysis.

Table 4.2

Reactions possible in liquid water after radiation impact

Primary particle and maximal energy of optical absorption or appearance potential, eV	Reaction products and relative intensity of the appearance peak (the mass-spectrum at electronic impact, $E = 100$ eV)
H_2O^* (7.4 eV)	$\cdot\text{OH} + \text{H} + \sim 2$ eV
H_2O (9.2)	$\cdot\text{OH}^* + \cdot\text{H}$
$\text{H}_2\text{O} + \bar{e}$ (12.56) unpaired electron or $\text{H}-\text{O}-\text{H}\dots^+\text{O}-\text{H}_2$	(100) $\text{H}_3\text{O}^+ + \cdot\text{OH} + \bar{e}$
$\text{H}_2\text{O} + * + \bar{e}$ (~ 18.7)	$\text{OH}^+ + \cdot\text{H} + \bar{e} + E_{\text{kin}}$ (23)
(-19.5)	$\text{H}^+ + \cdot\text{OH} + \bar{e}$ (5)
(-18.6 and 26)	$\text{O}^+ + \cdot\text{H} + \bar{e}$ (2 and 1.7)
H_2O (singlet) + \bar{e}	H_2O (triplet) + \bar{e}
\bar{e} (5.6 eV) + H_2O	$\text{H}^- + \cdot\text{OH}$ (0.6)
\bar{e} (7.5 eV) + H_2O	$\text{O}^- + 2\text{H}^\cdot$ (1.5)

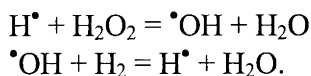
The differences in radiolysis of liquid and vaporized water are the following: ions and excited molecules are closer to one another in liquid water; LET is several thousand times higher; ions are hydrated.

Table 4.3

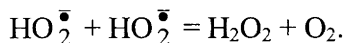
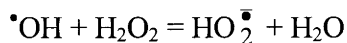
Time scale for radiation chemistry of water

Time, s	Process, lifetime of particles
10^{-18}	Molecule closing by an electron with 1 MeV energy
10^{-16}	Molecule closing by an electron with 5 eV energy
10^{-15}	Vertical excitation
10^{-14}	Ion-molecular reactions. Molecular vibrations; dissociation; electron thermolysis and its capture by a spur in liquid: $\text{H}_2\text{O}^* \rightarrow \text{H}^+ + \text{}^-\text{OH}$
10^{-13}	Particle collisions in the liquid; internal conversion $\text{H}_3\text{O}^+ + \bar{e} \rightarrow \text{H}^\bullet + \text{H}_2\text{O}$
10^{-12}	Radical breakthrough at diffusion ($d \sim 2$ to $8 \times 10^{-5} \text{ cm}^2 \text{ s}^{-1}$)
10^{-11}	Dipole relaxation; electron capture time in liquid ($\bar{e} \rightarrow \bar{e}_{\text{hydr}}$)
10^{-10}	Period between collisions in gas under 1,013 hPa (1 atm) pressure
10^{-9}	Radical recombination in a cylindrical track. Singlet excitation lifetime (in organic systems)
10^{-8}	Radical recombination in spherical spurs
10^{-5}	Radical reactions with dissolved substances of 1 M concentration (with activation energy equal 5 kcal/mol)
10^{-4}	Diffusion of radicals between spurs in tracks of electrons with 1 MeV. Triplet excited state lifetime
$10^{-1} - 1$	O_2^\bullet lifetime
Total:	$\text{H}_2\text{O} \xrightarrow{h\nu \ 10^{-18}-10^{-15}} \text{H}_2\text{O}^+, \text{H}_2\text{O}^* \xrightarrow{10^{-12}} \text{H}, \text{OH}$ $\bar{e}_{\text{hydr}} \xrightarrow{10^{-8}-10^{-7}} \text{H}_2, \text{H}_2\text{O}_2, \text{H}_2\text{O}, \text{}^\bullet\text{H}, \text{}^\bullet\text{OH}, \bar{e}_{\text{hydr}}$

In the absence of dissolved compounds in encapsulated systems the following reactions proceed with high yield:



In open systems H_2 is released and hydrogen peroxide is accumulated. Then with water radiation the following processes should proceed:



Duration of water radiolysis active product formation and conversion are shown in Table 4.3.

4.2. RADIOLYSIS OF FROZEN-UP AQUEOUS SOLUTIONS

The specific character of low-temperature radiation method is stipulated by difficulties in recording radiolytic phenomena in a multiphase system, represented by frozen-up aqueous solution.

However, if during freezing glasses are formed e.g. chaotic disposition of solvent and dissolved substance molecules is preserved, the yield of water radiolysis primary products will approach its value for the liquid-phase radiolysis.

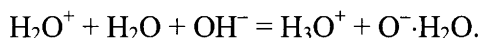
For such solvents–matrices, used for observation of radiolytic properties of substances, acid, alkaline and mixed salt solutions are taken – organic compounds and water solutions forming transparent quasi glassy-like structures at quick freezing (by steeping to liquefied nitrogen). Variation of the composition of these matrices creates conditions for accumulating one water radiolysis product or another with the maximum yield and inspecting their interactions with the substances under study.

In the investigations of glassy-like frozen-up aqueous solutions, we managed to determine the origin and discover properties of the majority of the primary products obtained at the water radiolysis (except for H_2^+ and H_2O^+) their radiation-chemical yield and, consequently, compose the material balance of the primary products of the water radiolysis.

Contrary to the liquid-phase radiolysis, such determinations were performed by direct measurements. For this purpose, low-temperature ESR and spectrophotometry methods have been used.

Radiation-chemical yields of the primary products of water radiolysis were determined. They were stabilized in various glassy-like matrices –

alkaline and acid frozen-up solutions. For instance, radiolysis of frozen-up aqueous alkaline solutions (KOH, 10 M) was studied by tracking accumulation of radicals \bar{e}^*_{st} , H^+ and O^- . The latter is formed in the following reaction proceeding in strongly alkaline medium:



It has been found that \bar{e}^*_{st} and O^- yields in the alkaline KOH 10 M solution are identical:

$$G(\bar{e}^*_{st}) = G(O^-) = 3.4 \pm 0.2.$$

We may also introduce a correction per recombination of radicals e_{st} and O^- at low temperature due to tunneling of electrons during the time passed after irradiation till registration of these particles. In this case, the value may reach ~ 5 e.g. the value for the liquid-phase radiolysis. As we apply the method of short-term pulse radiation (dozens of picoseconds), for pure water the following values were recorded:

$$G(\bar{e}_{hydr}) = 4.3.$$

In the case of radiolysis of frozen-up concentrated acid solutions (4.5 – 6 M H_3PO_4) at 77 K, we succeeded in registering only e and H_2O^+ conversion products: H atoms, $\bullet OH$ radicals, and radicals formed from ions of diluted acids interacting with H_2O^+ . In the presence of phosphoric acid, which in 1 M concentration is effective acceptor of electrons, nitrate ions, in the glassy-like solution, primary radicals can be invoked in the reactions and register total yield of radicals (H atoms and $\bullet OH$ radicals, phosphate and nitrate radicals) equal 7. If we introduce a correction for the radical recombination reaction with time, this value should be expanded to values corresponding to that observed for radiation impact on vitrified solutions of concentrated alkaline.

Thus the balance of water radiolysis primary products is fulfilled for concentrated alkaline and acid solutions and coincides with the measurement results for radiation of pure liquid water. These results confirm the unity of origins of the processes proceeding in all three types of aqueous systems and, which of the same importance, allow for a conclusion about appropriateness of frozen-up aqueous solution application as model systems for studying regularities of aqueous solution radiolysis for various substances.

The example of application of low-temperature radiation method to the study of the radiolysis mechanism for dissolved compounds is presented by the data on accumulation of primary radicals in lactose and disaccharide solutions (refer to Chapter 8). Table 4.4 shows concentrations of primary radicals (water radiolysis products) H^+ and O^- and total concentration of radicals in lactose solutions irradiated at 77 K (^{60}Co , γ -radiation, 50 kGy).

Table 4.4

Concentration of radicals (radical/g) in frozen-up aqueous alkaline solutions (10 M KOH) of lactose

Lactose concentration, M	Total concentration of radicals, $\times 10^{18}$	Radical H^+ concentration, $\times 10^{16}$	Radical O^- concentration, $\times 10^{18}$
0.126	1.4	5.5	1.1
0.350	1.5	2.0	0.7
0.700	4.7 (2.8)	1.1	0.4 (0.25)

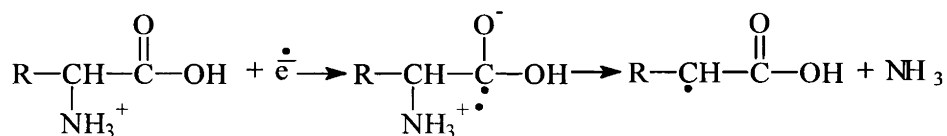
Note: Shown in brackets are concentrations of $\bullet OH$ radicals in neutral solutions.

As may be concluded from these data, disaccharide molecule interacts with the oxidant component of water radiolysis and H^\bullet radicals: the concentration of these radical products, stabilized at 77 K, decreases with increasing concentration of carbohydrate in solution. Such method of radiation impact on frozen-up aqueous solutions was also used in the studied of the primary stages of biopolymer radiolysis (refer to Chapters 8 – 11).

The use of low-temperature radiation technique for water solutions allows for both observation of the primary stages of radiolysis of dissolved compounds and the study of the following stages of conversion, for example, for radicals to which dissolved compounds dissociate. These data may also be related to detectable final effects of solution radiation. For example, the study of amino acid deamination, radiated at different temperatures (77 and 195 K) and pH, indicated electron participation in this reaction. As transiting from 77 to 195 K e.g. to conditions, when besides electron $\bullet OH$ radicals are also mobile in the solution, ammonia yield does not practically change (Table 4.5). Vice versa, as amino acid solution is added by inositol – $\bullet OH$ radical acceptor, the yield tends to increase (radiosensitization effect, refer to Chapter 13).

In the process under discussion, the primary act is capture of an electron by carbonyl group and corresponding formation of anion-radical. The ammonia

(e.g. anion-radical) yield depends on the fact, if carboxylic group is dissociated or not (refer to data on glutamic acid, Table 4.5). Further on, anion-radicals degrade with ammonia release. The general process proceeds according to the following scheme:



Chapters 7 – 11 present more detailed information on the radical formation and conversion mechanisms under the radiation impact on aqueous solutions of biopolymers, obtained by the low-temperature radiolysis method.

Table 4.5

Amino acid deamination yield $G(\text{NH}_3)$, analyzed by Conway, at irradiation of their frozen-up aqueous solutions (0.05 M at 77 K)

Irradiated substance	$G(\text{NH}_3)$
Glycine (pH 6.1) $\begin{array}{c} \text{H} \\ \\ \text{H}-\text{C}-\text{COOH} \\ \\ \text{NH}_2 \end{array}$ [2.4]* [9.8]	0.035 ± 0.15 $0.035 \pm 0.02^{**}$
Leucine (pH 6.8) $(\text{CH}_3)_2\text{CHCH}_2-\underset{\text{NH}_2}{\text{CH}}-\text{COOH}$ [2.36] [9.6]	0.03 ± 0.01
Lysine (pH 6.8) $\text{H}_2\text{N}-(\text{CH}_2)_4\underset{\text{NH}_2}{\text{CH}}-\text{COOH}$ [2.18] [10.53] [8.95]	0.1 ± 0.02
Arginine (pH 8.0) $\text{H}_2\text{N}-\overset{\text{NH}}{\parallel}{\text{C}}-\text{NH}-(\text{CH}_2)_3-\underset{\text{NH}_2}{\text{CH}}-\text{COOH}$ [2.17] [12.48] [9.04]	0.02 ± 0.01

REFERENCES

1. Allen A.O., *The Radiation Chemistry of Water and Aqueous Solutions*, Toronto - New York - London: D. Van Nostrand Company, Inc. Princeton, New Jersey, 1959, 204 p.
2. Amiragova M.I., Duzhenkova N.A., Krushinskaya N.P., Mochalina A.S., Savich A.V., and Shal'nov M.I., *Primary Radiobiological Processes*, Moscow, Atomizdat, 1973, 336 p. (Rus)
3. Sharpatyi V.A., *Uspekhi Khimii*, 1961, vol. **30**(5), p. 645. (Rus)
4. Sharpatyi V.A., *Uspekhi Khimii*, 1963, vol. **32**(6), p. 737. (Rus)
5. Kochetkov N.K., Kudryashov L.I., and Chlenov M.A., *The Radiation Chemistry of Carbohydrates*, Moscow, Nauka, 1978, 288 p. (Rus)
6. Korotchenko K.A. and Sharpatyi V.A., *Radiat. Biologia. Radioekologia*, 2000, vol. **40**(2), p. 133. (Rus)

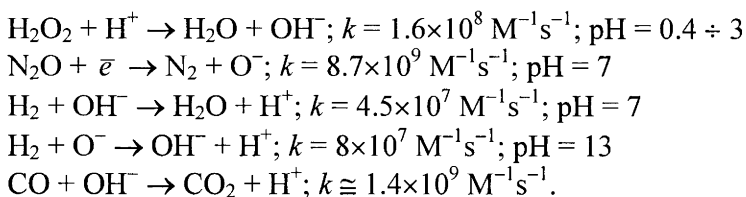
Chapter 5. Basic regularities of solution radiolysis

5.1. SUBSTANCES – THE RADICAL ACCEPTORS

Determination of reaction rate constants

Water and solution radiolysis products are results of the interaction of radicals formed from water with one another and dissolved substances. All water-soluble substances may be considered as water radical acceptors. Interacting with water radicals, they form radicals of dissolved compounds. As interacting with oxidative radicals ($\bullet\text{OH}$, H_2O^+), they oxidize the substance (detach electron or H^+ or add $\bullet\text{OH}$), whereas the interaction with reduction components of water radiolysis (H^+ and e^-) causes reduction of dissolved compound.

To implement the process by one of these directions, radiation chemistry uses the method of introducing substances consuming the “unwilling” component of water radiolysis in their reactions and producing the component necessary for the process proceeding into the solution. These compounds are, for example, H_2O_2 , Na_2O , H_2 and CO :

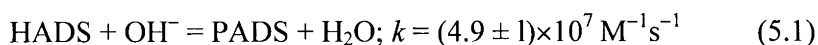


For making the process proceed in the desired (for example, oxidative) direction for dissolved substance X, the following condition must be fulfilled:

$$k[\text{H}][\text{H}_2\text{O}_2] \gg k_x[\text{H}][\text{X}].$$

This means that the reaction rate of reduction radicals with the additive compound must be much higher than the interaction rate of these radicals with the dissolved substance.

Determination of relative reaction rate constants is based on the principle of competition kinetics. The solution contains potassium hydroxylamine disulfonate (HADS), $\text{HON}(\text{SO}_3\text{K})_2$, and tested substance X, for which the rate constant of the reaction with OH^- radicals should be determined. It is known that dissolved HADS reacts with OH^- radicals forming only potassium peroxyamine disulfonate (PADS), $\text{O}=\text{N}(\text{SO}_3\text{K})_2$, radical stable in water. The selection of HADS and X concentrations may create conditions for preferable proceeding of two processes in the solution:



PADS accumulation in the solution may be observed by ESR or spectrophotometry method (the absorption spectrum of PADS falls within the range of λ between 220 and 260 nm).

Let us present the balance equation. The substance (HADS indicator) conversion rate equals:

$$W = G(-\text{HADS}) \times I = G(\text{PADS}) \times I = k_1[\text{HADS}][\text{OH}^-], \quad (5.3)$$

where I is the radiation intensity;

$$[\text{OH}^-] = \frac{G(\text{PADS}) \times I}{k_1[\text{HADS}]}. \quad (5.3a)$$

Under stationary conditions, the variation rate of radical $\bullet\text{OH}$ concentration equals zero, i.e. the number of $\bullet\text{OH}$ radicals formed equals the number of them consumed in the reaction:

$$-\frac{d(\bullet\text{OH})}{dt} = G(\bullet\text{OH}) \times I - k_1[\text{HADS}][\bullet\text{OH}] - k_2[\text{X}][\bullet\text{OH}] = 0; \quad (5.4)$$

after separation of variables, we get:

$$G(\bullet\text{OH}) \times I = \{k_1[\text{HADS}] + k_2[\text{X}]\}[\bullet\text{OH}]. \quad (5.5)$$

As we substitute (5.3a) into (5.3), the following expressions are deduced:

$$G(\bullet\text{OH}) \times I = G(\text{PADS}) \times I \frac{k_1[\text{HADS}] + k_2[\text{X}]}{k_1[\text{HADS}]}; \quad (5.6)$$

$$\frac{I}{G(\text{PADS})} = \frac{1 + \frac{k_2[\text{X}]}{k_1[\text{HADS}]}}{G(\bullet\text{OH})}. \quad (5.7)$$

This means that in $\frac{1}{G(\text{PADS})} \sim \frac{[\text{X}]}{[\text{HADS}]}$ coordinates PADS accumulation dependence is linear (Figure 5.1b):

$$\text{tg} \alpha = \frac{k_2}{G(\bullet\text{OH})k_1}.$$

By k_1 and $G(\bullet\text{OH})$ values the reaction constants k_2 of the reaction (5.2) may be determined, similar to how it has been made for the radiolysis of aqueous solutions of compounds – biopolymer components and biopolymers themselves. The tests have studied the dependence of stable PADS radical accumulation on the radiation dose (Figure 5.1a). From initial linear areas of PADS accumulation curves $G(\text{PADS})$ was determined. The dependence of $G(\text{PADS})$ on concentration of compound X was studied (Figure 5.1b). The linear anamorphism of $G(\text{PADS})$ dependence curve on the concentration of compound X was composed in the dashed bound area in Figure 5.1b, and from its tangent the rate constant of X reaction with $\bullet\text{OH}$ radicals was determined (Figure 5.1c).

Table 5.1 shows rate constants of $\bullet\text{OH}$ radical reactions with the components of the main biopolymers and biopolymers themselves. The compounds-indicators of oxidant radicals were potassium hydroxylamine disulfide (the alkaline medium) and the nitroso base (accelerene, the neutral medium). Table 5.2 presents rate constants of water radical reactions with compounds used as radioprotectors in radiobiology. These values were determined with the help of various indicator systems.

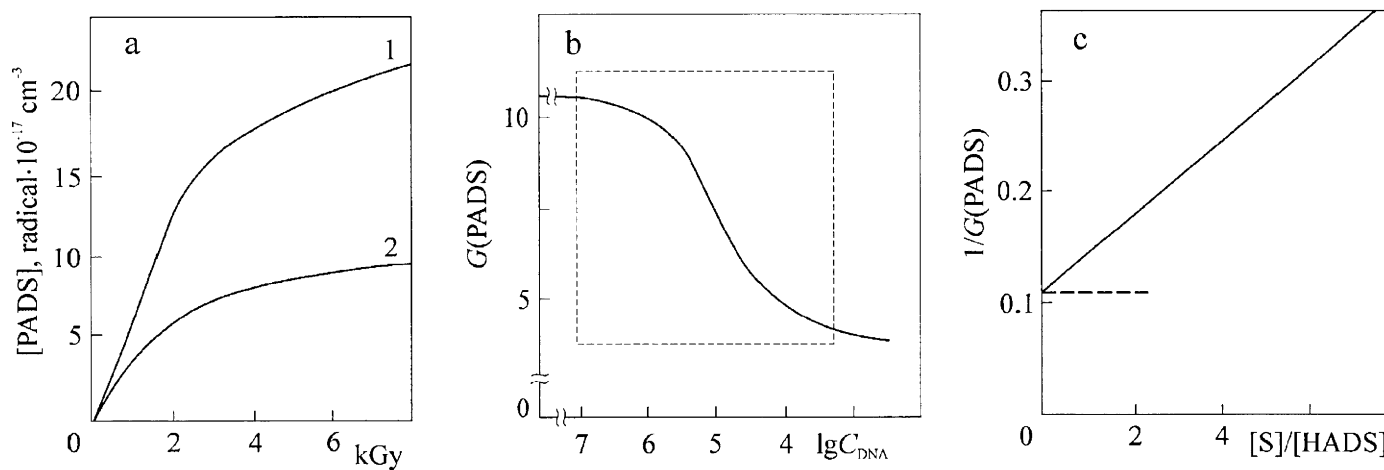


Figure 5.1. Accumulation (a) and yield of stable PADS radicals (b, c) at HADS solution radiation (see text) by accelerated electrons (1.6 MeV):

- (1) HADS 0.1 M solution without any additive; (2) the same in the presence of DNA (8.3×10^{-3} M, molecular mass equals 300 atomic units);
- concentration dependence of $G(\text{PADS})$ at radiation of HADS and DNA;
- linear anamorphosis of the concentration dependence

Table 5.1

The rate constants of $\bullet\text{OH}$ reactions with compounds, determined with the help of indicator systems PADS + $\bullet\text{OH}$ (pH = 12, 8.8)* and RNO + $\bullet\text{OH}$ (pH = 6.5**) [1, 2]

Compound	k ($\bullet\text{OH}$ + compound), $\text{M}^{-1}\text{s}^{-1}$
DNA	$(7 \pm 1.7) \times 10^{10}$
	$(5.6 \pm 1.1) \times 10^9$ *
	$(2.2 \pm 0.4) \times 10^{10}$ **
RNA	$(1.9 \pm 0.3) \times 10^9$ **
Thymine	$(7.6 \pm 1.5) \times 10^9$
	$(4.4 \pm 0.9) \times 10^9$ *
	$(1.4 \pm 0.1) \times 10^9$ **
Thymidine	$(2.7 \pm 0.5) \times 10^9$
Thymidylic acid	$(6.9 \pm 0.2) \times 10^8$
Uracyl	$(4.2 \pm 0.8) \times 10^9$
	$(6.9 \pm 1.3) \times 10^9$ **
Uridine	$(2.4 \pm 0.5) \times 10^9$
	$(2.4 \pm 0.1) \times 10^9$ **
Uridylic acid (2',3')	$(1.9 \pm 0.5) \times 10^9$
	$(2.5 \pm 0.3) \times 10^9$ **
5-Aminouracyl	$(8.8 \pm 1.7) \times 10^9$
Cytosine	$(2.9 \pm 0.6) \times 10^9$
Cytidine	$(2.5 \pm 0.4) \times 10^9$
Deoxycytidine HCl	$(6.4 \pm 2.7) \times 10^9$
Deoxycytidylic acid	$(8.5 \pm 2.3) \times 10^9$
Hypoxanthine	$(4.2 \pm 0.8) \times 10^9$
Adenine	$(4.9 \pm 1.0) \times 10^9$
Adenosine	$(2.8 \pm 0.3) \times 10^9$
Adenylic acid	$(3.6 \pm 1.4) \times 10^9$
Deoxyadenosine	$(2.0 \pm 0.4) \times 10^9$
Guanine	$(4.1 \pm 0.3) \times 10^9$
Deoxyguanosine (pH 11)	$(1.25 \pm 0.37) \times 10^9$
Deoxyguanylic acid NH_4^+ (pH 11)	$(2.3 \pm 0.6) \times 10^8$
	$(9.6 \pm 2.9) \times 10^8$
2-Deoxyribose	$(8.8 \pm 1.9) \times 10^8$

Table 5.1 (continued)

Ribose	$(1.36 \pm 0.45) \times 10^9$
	$(4.4 \pm 0.4) \times 10^8$ **
Disubstituted potassium glucose-1-phosphate	$(4.2 \pm 0.7) \times 10^7$
	$(1.6 \pm 0.4) \times 10^8$ **
Na ₂ HPO ₄	$(1.6 \pm 0.3) \times 10^8$
NaH ₂ PO ₄	$(8.2 \pm 0.2) \times 10^7$
Human serum albumin	$(4.0 \pm 0.8) \times 10^8$ *
	$(9.4 \pm 2.2) \times 10^7$ **
β-Phenylalanine	$(3.7 \pm 0.7) \times 10^9$
	$(2.8 \pm 0.6) \times 10^9$ **
Tyrosine	$(1.2 \pm 0.35) \times 10^{10}$
	$(5.6 \pm 2.6) \times 10^9$
Tryptophane	$(4.3 \pm 0.9) \times 10^{10}$
Cysteine	$(5.6 \pm 1.9) \times 10^9$
Cystine	$(5.7 \pm 0.9) \times 10^{10}$
	$(3.1 \pm 0.3) \times 10^8$ **
Cystine (pH 11)	$(4.4 \pm 0.8) \times 10^9$
Alanine	$(9.8 \pm 1.9) \times 10^7$
Glycine	$(5.5 \pm 1.7) \times 10^8$
	$(3.7 \pm 1.9) \times 10^8$ **
Deoxyphenylaniline	$(3.9 \pm 0.8) \times 10^9$
DNP (deoxyribonucleic protein)	$(1.36 \pm 0.3) \times 10^{10}$
Benzene (pH 11)	$(2.3 \pm 0.2) \times 10^9$
Phenol	$(2.4 \pm 0.5) \times 10^{10}$
	$(7.7 \pm 1.5) \times 10^{10}$
Indole	$(4.7 \pm 0.8) \times 10^{10}$
Corn starch	$(2.9 \pm 0.5) \times 10^8$ **
Waxy starch	$(2.5 \pm 0.4) \times 10^8$ **
Glucose	$(9.5 \pm 1.9) \times 10^7$
	$(3.8 \pm 1.1) \times 10^8$ **
Cellobiose	$(4.9 \pm 1.0) \times 10^8$
	$(3.6 \pm 0.1) \times 10^9$ **
Melibiose	$(3.8 \pm 1.2) \times 10^9$ **
Lactose	$(2.4 \pm 0.2) \times 10^9$ **

Table 5.1 (continued)

Methyl glycoside	$(2.4 \pm 0.3) \times 10^9$ **
Methyl galactoside	$(1.6 \pm 0.1) \times 10^9$ **
Methyl arabinoside	$(2.4 \pm 0.5) \times 10^9$ **

The comparison of data in Tables 5.1 and 5.2 induce the following conclusions:

1. The most probable places of damaging by $\cdot\text{OH}$ in biopolymers are the following: in the protein molecule – sulfur-containing and aromatic amino acid residues, particularly, their aromatic rings (this is also true for H atom reaction); in nucleic acid molecules – nitric bases.
2. In molecules of nucleic acids about 80 – 90% of $\cdot\text{OH}$ radicals attack bases, and 10 – 20% – sugar phosphate fragment.
3. Substances-radioprotectors are among the most effective acceptors of both oxidant and reduction radicals. It may be suggested that one of manifestations of the protective effect in the biological system is induced by their competing with biopolymers for water radiolysis products (see Chapter 13).

Therefore, the investigations of reactivity of flavonoids, which are natural (vegetable) substances, nontoxic phenols and potential radioprotectors, in relation to oxidant $\cdot\text{OH}$ radicals are of special interest. Flavonoids possess several extraordinary pharmacological properties: they are antioxidants, antimicrobial, antiviral and anti-inflammatory agents, has positive effect on vision, release heavy metal salts from the organism. They are also used for prophylaxis of cardiovascular system diseases: hypertension, thrombophlebitis, and atherosclerosis. These compounds possess antiradical activity (radical $\cdot\text{OH}$, \bar{e} , HO_2^{\cdot} and other peroxide radical acceptors [3 – 5]). Table 5.3 presents the rate constants of reactions for several flavonoids and allied compounds (refer to Figure 5.2 for corresponding structures) in relation to radicals $\cdot\text{OH}$, obtained with the help of the above-considered method of competitive kinetics [5]. Para-nitrosodimethylaniline with $k(\text{RNO}^{\cdot} + \cdot\text{OH}) = (1.25 \pm 0.25) \times 10^{10}$ l/mol·s was used as the indicator substance. As shown in Table 5.3, all the above-mentioned natural compounds possess effectiveness as $\cdot\text{OH}$ radical acceptors, the same as synthetic sulfur-containing radioprotectors mercaptoethylamine (MEA) and mexamine.

Table 5.2

**Rate constants of radioprotector reactions with oxidant and reduction
components of water radiolysis**

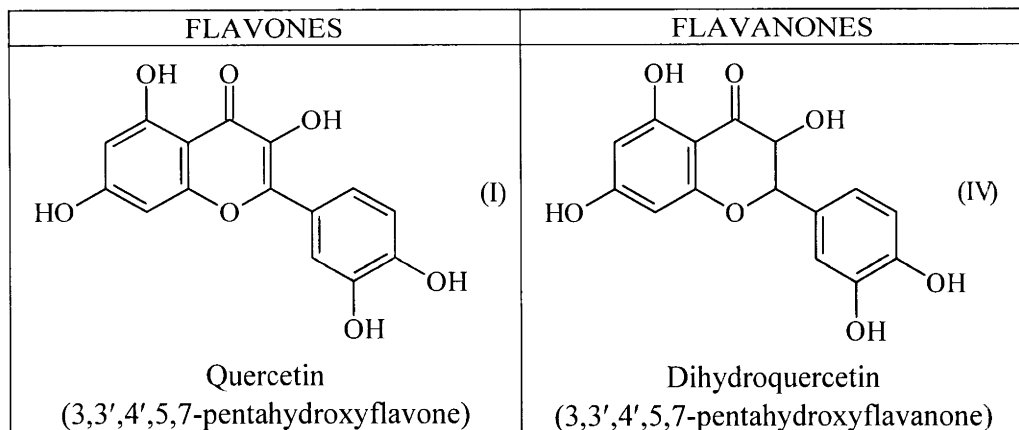
Radioprotector	$k_{rp+\cdot OH}, M^{-1}s^{-1}$	$k_{rp+e_{hydr}}, M^{-1}s^{-1}$
Meso-inositol	$(1.0 \pm 0.12) \times 10^9$	–
Propyl gallate	$(1.2 \pm 0.2) \times 10^{10}$	$(5.5 \pm 5.2) \times 10^5$
3-Oxypyridine	$(6.7 \pm 0.6) \times 10^9$	–
2,4,6-Trimethyl-3-oxypyridine	$(2.5 \pm 0.4) \times 10^9$	$(2.0 \pm 0.2) \times 10^7$
4-Ethyl-6-methyl-3-oxypyridine	$(1.4 \pm 0.1) \times 10^9$	–
<i>d,l</i> -Penicillamine	4.7×10^9	5.1×10^9 (pH 6.5)
Penicillamine disulfide	6.5×10^9	–
2-Mercaptoethylamine (cysteamine)	1.49×10^{10} (pH 1) 3.9×10^{10} (for H, pH 2)	–
2-Mercaptoethylamine (cystamine)	–	2×10^{10} (pH 6.9) 4×10^{10} (pH 7.3)
2-Mercaptoethanol	$(6.5 - 5.1) \times 10^9$ 2×10^9 (for H)	– 1.2×10^{10} (pH 6.5)
Mercaptoethylguanidine reduced –SH oxidized –S–S–	– –	2×10^{10} (pH 6.74) 2×10^{10} (pH 7.4)
2,2'-Dithiobisethylamine	1.1×10^{10} (pH 1)	–
β -aminoethylisothiuronium (AET)	$\geq 1 \times 10^{10}$	–
Thiourea	4.7×10^9 (pH 7)	–
Selenourea	$(7.2 - 5.5) \times 10^9$ (pH 7) $(7.5 - 6.3) \times 10^8$ (for H)	4.0×10^9 (pH 6 - 11)

Table 5.3

Reaction rate constants of flavones and flavanones* with $\cdot\text{OH}$ radicals [5]

Compound	pH	$k_{\cdot\text{OH}}$, l/mol·s
Quercetin (I)	6.0	$(2.3 \pm 0.3) \times 10^{10}$
	7.2	$(1.3 \pm 0.1) \times 10^{10}$
Luteolin (II)	6.0	$(2.2 \pm 0.5) \times 10^{10}$
	7.2	$(1.3 \pm 0.1) \times 10^{10}$
Saliphoside (III)	6.0	$(2.0 \pm 0.5) \times 10^{10}$
	7.2	$(1.3 \pm 0.2) \times 10^{10}$
Dihydroquercetin (IV)	6.0	$(5.7 \pm 0.2) \times 10^9$
	7.2	$(7.3 \pm 0.5) \times 10^9$
Phellavin (V)	6.0 – 7.2	$(7.8 \pm 0.5) \times 10^9$
Anthocyanin (VI)	7.2	5×10^9
Alpizarine (VII)	6.0 – 7.2	$(6.1 \pm 0.6) \times 10^9$
MEA	6.0 – 7.0	$(1.6 \pm 0.2) \times 10^{10}$
Mexamine	6.0 – 7.4	$(6.3 \pm 0.3) \times 10^9$

Note: Digits in brackets represent numbers of structures in Figure 5.2.



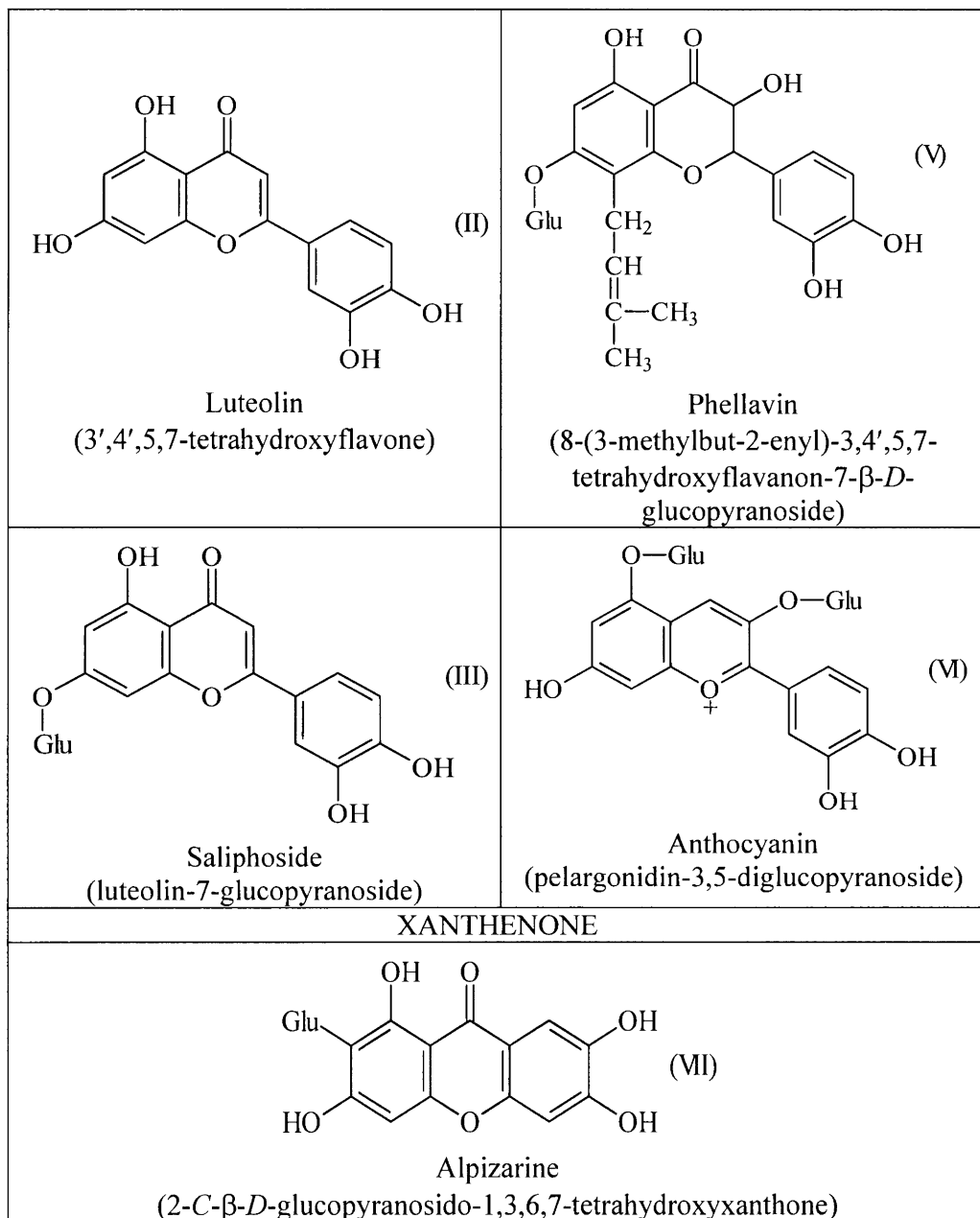


Figure 5.2

Concluding the consideration of the possibilities of the method for determination of the substance reactivity based on the application of competition kinetics principles, let us indicate that the technique discussed using a water-stable radical as the indicator substance may also be applied to natural nontransparent systems, such as blood, cells, etc.

Other systems – the reactivity indicators – are also discussed in the literature. The apparent advantage of these systems is relative quickness of getting information about reactivity of the compounds under study in relation to any radicals. The general disadvantage of these systems is possible proceeding of secondary reactions between the indicator substance and radiolysis products of the irradiated system. Therefore, for the purpose of excluding such secondary effects in determination of the compound reactivity the investigator must use a set of indicator substances.

5.2. CONCENTRATION DEPENDENCE OF DISSOLVED SUBSTANCE DISSOCIATION YIELD

The radiation-chemical yield G is the main characteristic of radiolytic conversion of any dissolved compound. For aqueous compounds of the same compound, this value may vary from thousandth parts to 10 or more converted molecules or ions with respect to radiolysis conditions per 100 eV absorbed by the solution. The radiolytic decomposition rate of dissolved compounds is defined by two reasons: the number of radiolyzed water molecules (8 as a maximum) participating in the process and activity e.g. reactivity of intermediate products of dissolved compound radiolysis in relation to molecules of the initial compounds. In both cases, these “start-up” reasons of G variation may be masked by secondary processes and inverse reactions. For example, for radiolysis of biopolymers with various functional groups it is not so easy to determine why one of the processes initiated by the radiation impact proceeds with higher yield, whereas another proceeds with relatively lower yield. Nevertheless, the general reasons determining degradation of biopolymer and maximal (under sensitization conditions) and minimal (under protection conditions) yields of the processes should be known, because in practice processes must be controlled towards both maximal degradation of this component (radiosensitization therapy, for example) and suppression of the

radiation damage (which is important for searching the most effective protection). Let us determine and discuss the reasons for changing the radiation-chemical yields of the main biopolymer conversions. The first reason is conditions of injecting primary products of the water radiolysis into the reaction. M.A. Proskurin has formulated the basic principles for creating conditions involving water radiolysis products into the reactions [6]:

1. Since compound concentration in the solution increases, active products of water radiolysis are gradually injected: firstly, ionized (about four) radiolysis products or the products of their conversion and, secondly, excited or conversion products of H^\bullet and $\bullet\text{OH}$ radicals (about four also) due to suppression of the radical recombination process proceeding in the cell:



This is reflected in the character of the two-stage concentration curves of radiolysis product yield. The levels at these curves correspond to full involvement of two various types of water radiolysis products into the reactions. The maximal yield of dissolved substance conversion, carried out in this way, equals 8.

The geometrical image of the track indicating diffusion of active particles participating in recombination reactions with dissolved compounds changes with time. The curve of radiolysis product yield under discussion displays the final picture of passed reactions with the track development, the part of active water-derived products, included in the reaction with dissolved compound, compared with the general quantity of active reagents. The concentration dependence of compound degradation yield possesses a plateau (Figure 5.3) and reflects the effectiveness of dissolved compound in relation to water radiolysis products. Curve 4 corresponds to the most reactive reagent.

2. Water represents rather structured liquid. As the solvent absorbs energy, excited water molecules are formed. Excitation may migrate in the system (via channels formed by the liquid structure), and it is definitely probable that excitation may be localized on water molecules present in the places, where the structure of water is distorted – in hydrate covers of dissolved substances, for example. The interaction level of excited water molecules neighboring the dissolved compound

to molecules of the dissolved compound (e.g. their relation) and reactivity of the dissolved substance in relation to H and OH radicals are the reasons, which finally determine, if the excitation energy is to be transferred to dissolved compound or water molecule dissociates to H and OH radicals, which then will react with the dissolved compound.

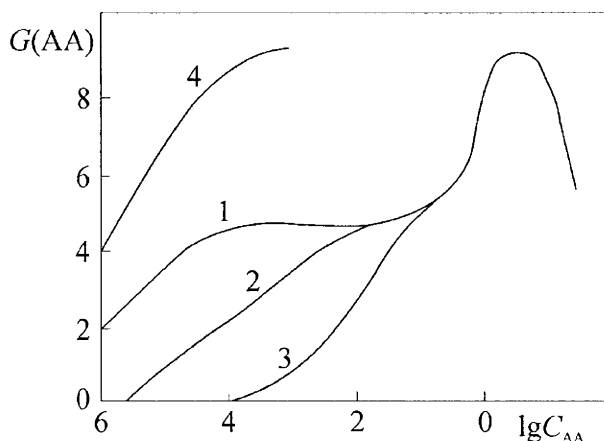
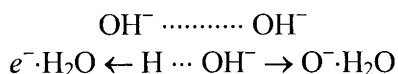


Figure 5.3. The dependence of radiation-chemical conversion yield of dissolved compounds on their concentration [6]:

1 – the most effective radical acceptor; 2, 3 – less active acceptors; 4 – in the presence of “accessory” radical acceptor (conjugated according to M.A. Proskurin)

3. Dissociation of water molecules into radicals and their involvement into reactions becomes much simpler at simultaneous radiation impacting of two compounds in the solution (conjugated radical acceptors, according to M.A. Proskurin). One of these compounds preferably accepts one of the water radiolysis components, and another compound accepts the opposite component. In the presence of conjugated acceptors, high conversion is provided for lower concentrations of the above compounds compared with their separate radiation. The conjugated acceptors may act in rather diluted solutions e.g. at rather long distances between molecules of dissolved compounds from one another.

The process of excited water molecule injection into the reaction in the presence of compounds showing high proton affinity and, therefore, changing the chemical origin of irradiated particles, for example, in the case of strongly alkaline solutions, may be presented as follows:



Note also that all above-mentioned conditions may, principally, be fulfilled in the case of cell radiation e.g. in the cell microareas representing a liquid phase (a fluid or an aqueous solution) or to be more appropriate, a selection of solutions in the range from the most diluted ones to rather concentrated gels of compounds possessing several functional groups, if these groups may also compete with one another in the molecule and conjugated acceptors.

REFERENCES

1. Zakatova N.V. and Sharpatyi V.A., *Izv. AN SSSR, Ser. Khim.*, 1968, No. 7, pp. 1642 – 1644. (Rus)
2. Zakatova N.V., Nikonorova G.K., and Sharpatyi V.A., *KhVE*, 1970, No. 1121-69, Dep. VINITI, pp. 1 –18. (Rus)
3. Revina A.A., *Doctor Dissertation Thesis*, Moscow, 1995, N.N. Semenov Institute of Chemical Physics. 198 p. (Rus)
4. Sharifillina L.R., *Candidate Dissertation Thesis*, Moscow, 2004, L.Ya. Karpov Research Physicocemical Institute, 121 p. (Rus)
5. Kondakovaa N.V., Sakharova V.V., Ripa N.V., Kolkhir V.K., and Tyukavkina N.A., *KhVE*, 1998, vol. 32(2), pp. 106 – 111. (Rus)
6. Proskurin M.A., *Doklady AN SSSR*, 1960, vol. 135(6), pp. 1446 – 1449. (Rus)

Chapter 6. The regularities of radiolysis of aqueous biopolymers and their components

6.1. BIOPOLYMERS AS RADICAL ACCEPTORS

The interest raised in 1950ies to radiolysis of aqueous biopolymers and other biologically active compounds was mostly defined by the tasks of radiobiology: a living cell protection against ionizing radiation and vice versa stimulation of its decomposition, for example, in the case of cancer therapy. To solve these problems, the primary stages of radiolytic processes proceeding in all microareas of the living cells must be known.

Aqueous solutions of biopolymers represent a suitable model for radiobiological investigations, because on average a cell contains up to 80%, and some parts of it represent a set of organic and inorganic compounds in different concentrations. At the same time, the cell also contains components forming a solid phase and interphases form membranes. Therefore, the task of taking into account radiolytic processes proceeding in this complex heterogeneous system, the living cell, for the above-formulated purposes of practical radiobiology and medicine must be reduced to estimation of direct and indirect (via water radicals) action of irradiation in all components of the system.

Biopolymers represent water radical acceptors, formed by the radiation impact. The information about the role of water radiolysis products in conversion of biopolymers were obtained with the help of various methods used in radiation chemistry:

- the method of competing radical acceptors;
- the registration method for water radiolysis molecular products - H_2 and H_2O_2 ;
- by radiolysis products of dissolved substances;
- the method of direct observation for primary radiolysis product reactions with dissolved substances at express spectrophotometry combined with the pulse radiation technique.

The method of competing radical acceptors

The method of competing radical acceptors is based on a technique of studying radiation-chemical kinetics of dissolved substance (an indicator) dissociation in the presence of the compound under study (refer to Chapter 5). This method was applied to the study of the reactivity of many biological substances, by which the reaction rate constants of these compounds with reduction and oxidation water radiolysis radicals were determined, for biopolymers with $\cdot\text{OH}$ radicals, in particular (refer to Table 5.1).

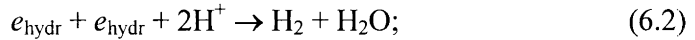
First of all, the data shown in Table 5.1 indicate that biopolymers under study and their precursors really behave themselves as typical $\cdot\text{OH}$ radical acceptors. When estimating reactivity of biopolymers in relation water radicals, one should pay attention to the fact that their rate constants, determined with the help of the competing radical acceptor method, are usually overestimated compared with the rate constants for lowmolecular analogues of the polymers. One of the reasons for this is probable loss of mobility by the indicator substance in the biopolymer solution either due to the structure of macromolecules or fixing at any functional groups of this biopolymer.

Moreover, as comparing the reactivity of biopolymers and their lowmolecular analogues, one also should take into account the fact that the macromolecule reactivity estimated from reactivity of each component of this polymer (for example, in the case of human serum albumin) appears higher than the value obtained in the experiment (Table 5.1). The reason is that $\cdot\text{OH}$ radicals in precursor solutions (amino acids and oligopeptides) mostly react with the functional groups, which compose macromolecules of the biopolymer.

The registration method for molecular products

The registration method for molecular products of radiolytic dissociation of water (H_2 and H_2O_2) in aquatic solutions of biomolecules allowed for obtaining data on the participation of water radiolysis components in reactions under the conditions, when the influence of the secondary processes of H_2 and H_2O_2 formation is eliminated.

As accepted for the application of this method, if the water radiolysis components do not react with the dissolved substance, they recombine and form H_2 and H_2O_2 . In neutral solutions, these products are formed in the following reactions:



The concentration dependence of molecular product yield (G_m) at aquatic solution radiolysis is the following:

$$G_m \sim G_m^0 - B \cdot [\text{Ac}]^{1/3}.$$

It reflects the competitive processes of radical recombination formed in the ionizing particle tracks. An intersect of the axis of ordinates, cut off by a straight line (in $G_m \sim [\text{Ac}]^{1/3}$ coordinates) at extrapolation of the acceptor concentration to zero, represents the maximum yield of molecular products H_2 и H_2O_2 for the ideal case, when all H^\bullet and $\bullet\text{OH}$ radicals formed in the track are involved in recombination of the same radicals, exclusively.

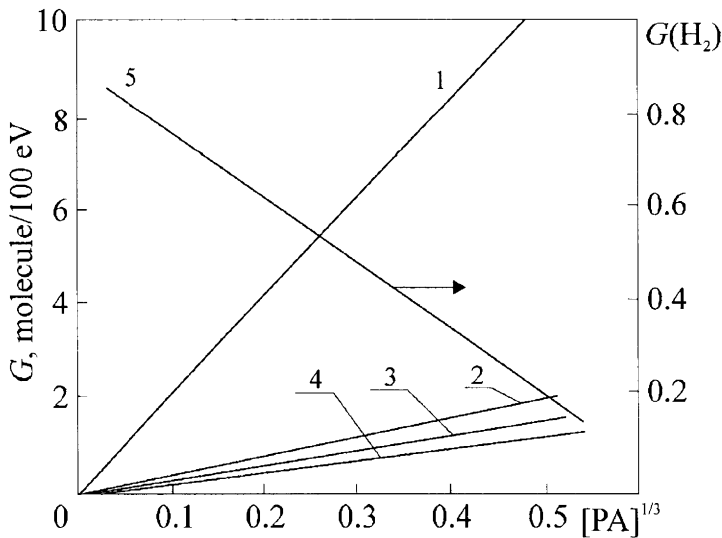


Figure 6.1. Concentration dependencies of the yield of:

1 – phenylalanine dissociation; 2 – ammonia formation; 3 – tyrosine; 4 – phenylethyl amine; 5 – molecular hydrogen; phenylalanine solution irradiation in the absence of O_2 [1, 2]

In the case of radiolysis of biopolymers and their components, the above-mentioned concentration dependence (of the cubic root degree) was determined for the yield of both water radiolysis molecular products and dissolved substance radiolysis products. As an example, the regularity discussed is observed for the case, when the main reactions consuming H^\bullet and $\bullet\text{OH}$ radicals are addition reactions, for instance, to aromatic rings of amino acids (Figure 6.1). Hence, if the processes of the following type proceed in the system:



the type of the concentration dependence is preserved, and upper limit of H_2 yield must two-fold increase as compared with the first case. The measurements of molecular oxygen yield at the radiolysis of aqueous solutions of amino acids and glucose indicated a possibility of such processes in biopolymers having aliphatic amino acid residues and monosaccharide units in their structure. Radiolysis of aqueous thymine solutions of different concentrations showed H_2 yield equal 0.46 or lower. For 0.03 wt.% DNA solution, $G(\text{H}_2) = 0.37$. This indicates that, firstly, in DNA solutions of this concentration, e_{hydr} formed are completely captured by the biopolymer and, secondly, in DNA solutions atomic hydrogen is not consumed by the reaction (6.4), but, obviously, participates exclusively in addition reactions by double bonds.

A technique for radiolysis product analysis

A technique for radiolysis product analysis mainly represents a direct method for determination of the participation of water radiolysis products in reactions. For example, the chromatographic method has determined the products of OH addition to double bonds in the bases of nucleic acids, phenylalanine (tyrosine), tyrosine (deoxyphenylalanine). The results of chemical and physicochemical methods for analyzing the composition of radiolysis products of nucleic acids and lowmolecular analogues provide for a conclusion that $\bullet\text{OH}$ radicals attack both nitric bases and C–H bonds of DNA sugar fragment (Chapter 10).

The direct registration method of water radiolysis primary products and observation for reactions with their participation during irradiation is generally extended to the reactions with participation of hydrated electron (e_{hydr}), because this particle may be reliably detected from optical absorption spectra in the visible region. Multiple works were devoted to determination of e_{hydr} reactivity in relation biological objects via determination of the reaction rate constants. Among the biopolymers under study (protein, DNA, polysaccharides), the highest rate constant in relation to e_{hydr} is displayed by a protein molecule. In the protein molecule, the sites for e_{hydr} attack are presented by sulfur-containing and aromatic amino acid residues (Chapter 7). Also, high activity in relation to e_{hydr} is manifested by nitric bases in the molecules of nucleic acids.

The methods of pulse radiation and express spectrophotometry gave an opportunity not only to study primary stages of e_{hydr} involving into the reaction with dissolved substance, but also to track the conversion of an intermediate product, formed in the primary act: for instance, electron transfer to substances possessing radioprotector or radiosensibilizer properties. It has been found that the rate constants of electron transfer from DNA components to some radioprotectors are close to diffusion ones, i.e. $k \sim 10^{10} \div 10^{11} \text{ M}^{-1} \cdot \text{s}^{-1}$. Apparently, in the native systems these processes are of great importance.

6.2. CONCENTRATION DEPENDENCE OF DISSOLVED SUBSTANCE CONVERSION YIELD. RADIOSENSIBILIZATION EFFECTS

There are multiple data in the literature describing the studies of radiolysis of biopolymer and lowmolecular analogue aqueous solutions in a broad range of concentrations ($10^{-5} \div 0.1 \text{ M}$). The concentration dependence curves for the yield of radiolytically dissociating initial compounds or the yield of the products of their radiolysis are shaped similar to the saturation curves. The plateau on these curves shows involvement of all water radiolysis products into the reactions with dissolved substances. If any dissolved substance predominantly reacts with one of the water radiolysis component, e_{hydr} , for example, its dissociation yield at the plateau will equal ~ 3.5 , and in the case of two components – ~ 7 . Figure 6.2 presents concentration curves for the yield of radiolysis products of two compounds: glucosamine (glucoproteid “precursor”) and lactose (sisaccharide), which are malonic aldehyde (MA) and deoxy-sugar,

respectively. Both these products are formed as a result of $\cdot\text{OH}$ radical interaction with the initial compounds. As is observed, glucosamine solutions saturated with nitrous oxide show $G(\text{MA})$ values almost twice higher in the plateau area of concentrations compared with the case of irradiated solution saturation with an inert gas, because N_2O , the e_{hydr} acceptor, under experimental conditions captures about 80% electrons, hence, forming $\cdot\text{OH}$ radicals.

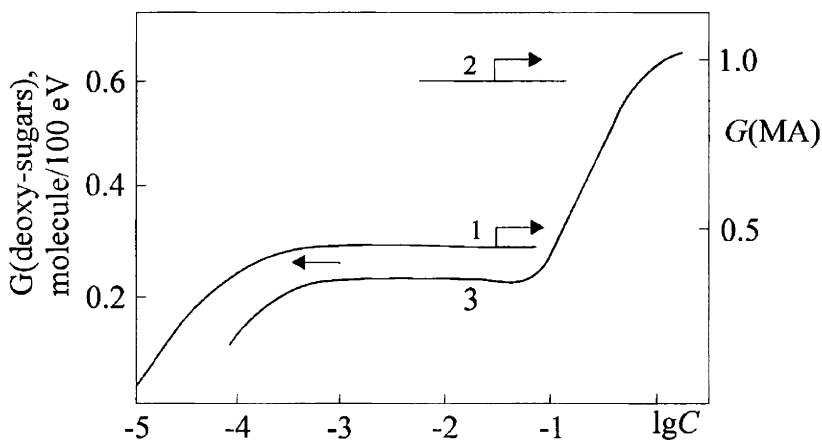


Figure 6.2. Concentration dependencies of malonic aldehyde (1, 2) and deoxy-sugars (3) yield at irradiation of glucosamine and lactose solutions saturated by: 1 – argon; 2 – nitrous oxide; 3 nitrogen [2]

At the radiolysis of lactose solutions in the concentration range from 10^{-4} to 0.67 M, it has been found that the concentration dependence of one of the main lactose dissociation product yield (deoxy-sugars) represents a typical two-stage curve with a plateau in the concentration range of $10^{-3} \div 8 \times 10^{-2}$ M and at concentrations above 0.1 M. Such shape of the concentration dependence is explained by participation of $\cdot\text{OH}$ radicals, produced from ionized and excited water molecules, in the reactions (Chapter 5). It is of interest that G values at the steps are approximately two-fold different, i.e. identically to radiolysis of aqueous solutions of inorganic compounds.

The dissociating lactose yield observed in the concentrated solutions is also two-fold higher than G values for lactose (4.27 ± 0.44), recorded at the first step. The comparison of data by $G(-\text{carbon})$ for various mono- and disaccharides, obtained in the range of concentrations corresponded to the first

step indicates a change of this value at transition from one type carbohydrate to another. Therefore, it becomes evident that this value is determined by conditions of the radiolysis proceeding: by involving radiolyzed water molecules, which mostly depends on the ratio of rates of consecutive reactions of dissociated carbon primary radical conversions.

In the current concentration range, the maximum dissociation of dissolved sugar, observed for some studied compounds, equals 3.3 (in centimolar cellobiose solutions). If we assume that the participation of electron in these systems is negligible, then the yield of dissociated sugar, determined in solutions of the same concentrations (at the first step), saturated with nitrous oxide, equals $G = 6.5$, which precisely corresponds to complete involvement of $\bullet\text{OH}$ radicals formed from ionized water molecules into the reactions, $G_{\text{ion}} = 3.4$.

The discussed regularity is clearly observed only in the case of usual non-chain reactions of radiolytic conversion of the dissolved substance. On the contrary, the curve of substance dissociation yield has no plateau, and G may reach tens or hundreds converted molecules per 100 eV of absorbed energy. For example, in the case of glucosamine solution irradiation (in the absence of O_2), G (-glucosamine) value reaches 400 molecules per 100 eV of absorbed energy [3].

Similar curves may be plotted for aqueous solutions of biopolymers – DNA, proteins, etc. However, these concentration curves with steps are true for the experimental conditions, when post-radiation processes are excluded, similar to DNA solutions: hydroperoxide dissociation into radicals leads to additional degradation of the biopolymer.

The study of radiolysis of DNA, which is a multifunctional organic compound, in a broad range of concentrations using methods able to detect any degradation products, determines concentration $G(\text{products})$ curves, the steps on which correspond to the use of various types of radiolyzed water molecules in the reactions. For example, the study of decomposition of nitrous compounds in the DNA structure with respect to decreasing optical density in the wavelength area of $\lambda = 260 - 265$ nm (chromophore group degradation) and DNA concentration in the solution, it has been found that in the plateau area $G(-\text{chromophore groups}) = 2 - 3$. This G value indicates full consumption of $\bullet\text{OH}$ radicals and e_{hydr} , formed at water radiolysis.

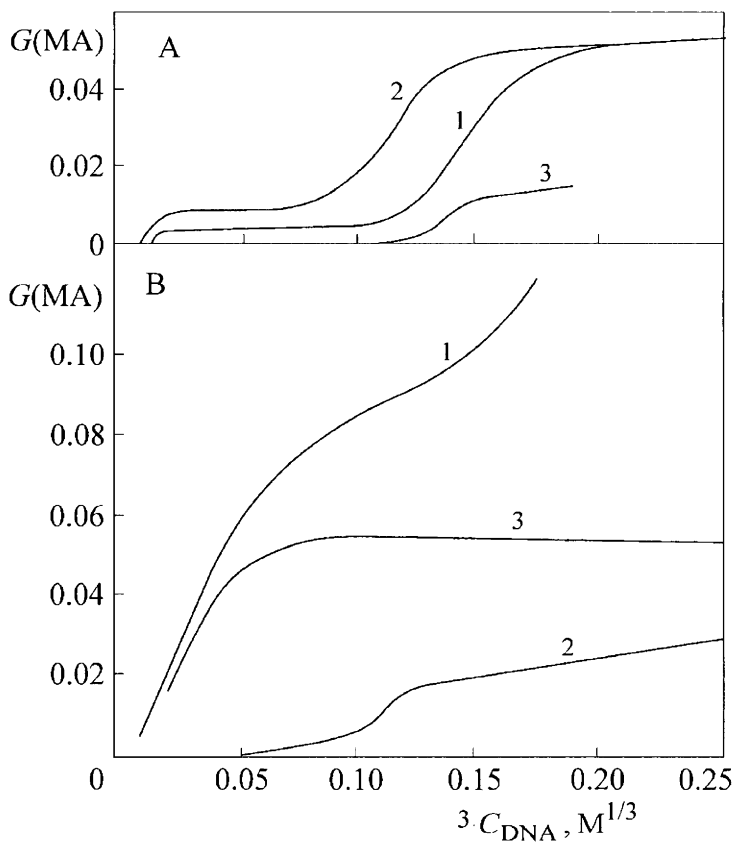


Figure 6.3. The concentration dependence of malonic aldehyde yield at DNA solution irradiation under different conditions:

- A) solutions saturated by: 1 – argon; 2 – nitrous oxide; 3 – nitrous oxide in the presence of myoinositol;
 B) solutions saturated by O_2 : 1 – in the absence of myoinositol; 2 – in the presence of myoinositol; 3 – myoinositol is injected to the solution after irradiation termination [4]

The yield of chromophore group degradation is determined by the prehistory of the DNA preparation used, the “completeness” – more precisely, the degree of the initial DNA structure preservation at its extraction from the tissue. The highest $G(-\text{chromophore group})$ value is observed for denatured preparations (i.e. those with broken hydrogen bonds between cords).

As studying the yield of one of the degradation products of DNA sugar unit – the analogue of malonic aldehyde, with respect to the DNA concentration in solution, typical concentration dependence with two steps was obtained. This is possible in the case, if in the experiment all post-irradiation polymer degradation processes are eliminated (Figure 6.3). The substitution of inert gas by nitrous oxide causes two-fold increase of MA yield in the plateau area (MA is formed due to $\cdot\text{OH}$ radicals). It should also be noted that if radiolysis is performed in the presence of O_2 , the obtaining of a characteristic curve requires injection of a radical acceptor into the irradiated solution. This substance inhibits the chain process of post-irradiation degradation. In present case (refer to Figure 6.3), the irradiated DNA solution was added by myoinositol – the acceptor of radicals formed a hydroperoxide dissociation and reacting with DNA molecules.

The studies of aqueous protein substance radiolysis also determine a plateau of the concentration dependence for the biopolymer degradation yield. In this case, the most demonstrative are the results of observation for biological activity of enzymes. As protein molecules are attacked by water radicals, the whole system defining the main protein function is “totally disturbed”. The radiation-chemical yield of the enzyme inactivation depends on the enzyme origin and may vary from 0.009 to 0.55. As these solutions are saturated with nitrous oxide, the enzyme inactivation yield is twice increased, i.e. it is mainly induced by $\cdot\text{OH}$ radicals (Chapter 7).

When in experiments with aqueous solutions of proteins and complex proteins – the enzymes, physicochemical properties were registered reflecting the radiolysis stages close to the primary ones, in relation to dissolved substance concentration (oxygenated hemoglobin oxidation to metahemoglobin, ferrocytochrome C reduction, ferricyanide ion recombination in solution – the gelatin gels) the G value was found equal 3 – 6 molecule/100 eV. These yield values were recorded for the concentration range corresponded to the plateau at the concentration curves and reflect full involvement of water radical pairs into the reactions.

The values different from the average level $G = 4.5$ may be explained by any processes proceeding in these systems, in which water radiolysis products are consumed in parallel with the registered one or dissociation of one molecule of the initial compound requires two or more radicals rather than one, which represents the case of G value underestimation. Hence, the “overestimation” may relate to either introduction of an additional amount of radiolized water molecules (radicals formed from excited molecules) into the

reaction or participation of their radiolysis products in the substance dissociation.

6.3. RADIOLYSIS OF FROZEN-UP AQUEOUS SOLUTIONS OF BIOPOLYMERS

The participation of \bar{e} , H and $\cdot\text{OH}$ in reactions with dissolved biopolymers is directly observed in the method of low-temperature irradiation of substances applied in combination with the registration methods of intermediate products: ESR, RTL, spectrophotometry, which was discussed in the previous Chapters. Observing for accumulation of these products in solutions-matrices and in the presence of biopolymers in them with respect to the irradiation dose, the changes in e_{st} , H and $\cdot\text{OH}$ yields may be related to participation of these primary particles in the reactions with dissolved substances. Table 6.1 shows the yield values for e_{st} , H, $\cdot\text{OH}$ and O^- in the solvents-matrices for the studies of DNA radiolysis. Obviously, in contrast with O^- , in the presence of DNA the yields of e_{st} and H are considerably reduced with increasing DNA concentration. It may be concluded that even at 77 K DNA reacts with reduced component of water radiolysis.

Table 6.1

The yield of water radicals in alkaline and acidic DNA solutions irradiated at 77 K [2]

Matrices	Radicals	DNA content, wt.%				
		0	0.3	1	5	10
10 M KOH	\bar{e}_{st}	3.4	3.4	3.1	2.2	0.8
	O^-	3.4	3.0	3.0	3.0	3.0
	H	0.1	—	0.05	—	0
	$\Sigma\text{R (except } \text{O}^-)$	3.4	3.0	3.6	3.6	3.6
4.5 M H_3PO_4	H	0.8	0.6	0.4	0.15	0.15
	DNA radicals	0	0.8	1.0	2.2	2.4
	$\Sigma\text{R (except H)}$	1.9	2.7	3.1	4.1	4.3

Similar to the case of the liquid-phase radiolysis, creating conditions for proceeding of competing reactions (hence, one of them is taken for the indicator reaction), the reactivity of dissolved substances in relation to water radiolysis products may be determined.

Table 6.2

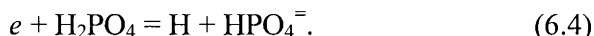
**Relative reaction rate constants of substances (S) with electron
(pH 3) [2, 4]**

Substance	$\frac{k_{S+\bar{e}}}{k_{H_2PO_4+\bar{e}}}$
Glycosamine	128
Lysine	34 ± 1
Arginine	38 ± 4
Leucine (pH 1.3)	103 ± 12
Glutamine	78 ± 22
Glutamic acid:	77 ± 15
pH 1.3	49 ± 10
pH 3.0	28 ± 6
pH 4.4	47 ± 5
Glycine	58 ± 12
Glycyl-glycine NO ₃ ⁻	220
Guanine*	$2,620 \pm 400$
Uracyl*	$1,680 \pm 250$
Thymine*	$1,250 \pm 180$
Adenine*	$1,200 \pm 180$
Cytosine*	800 ± 120
Inositol	12 ± 2
Cystamine*	170 (310 ± 30)
1,2-Bisdiazoacetyethane**	280 ± 30
1,3-Bisdiazoacetylpropane**	50 ± 5
1,4-Bisdiazoacetylbutane	300 ± 50

Notes: * In 6 M H₃PO₄.

** Solvents were irradiated in the presence of 5% ethanol.

Thus, the reactivities of some compounds to electron were determined (Table 6.2). Hence, for the “indicator reaction” the reaction of H atom formation was assumed:



Similarly, in frozen-up solutions the reactivity of chemical substances in relation to e , $\cdot\text{OH}$, $\cdot\text{H}$ and H_2O^+ cation-radicals can be determined. Let us consider this fact on the example of the study of some antioxidants-radioprotectors reactivity in relation to the mentioned radicals with the help of RTL and ESR techniques.

RTL method for determining antiradical activity of substances

As already mentioned in Chapter 3, the RTL method is based on the observation of luminescence of the studied substances, irradiated at low temperature, at their subsequent annealing. To study the acceptor properties of compounds in relation to e and $\cdot\text{OH}$, the solvent-matrix was represented by 10% gelatin solution, added by various concentrations of substances-antioxidants. As the luminescence factor, thymine was added to the initial solution. After sample irradiation by 10 kGy dose from a cobalt source at 77 K the measures by RTL method were performed on a thermoluminograph according to common technique. Typical luminescence curves for irradiated solutions are shown in Figure 6.4. Obviously, these curves have a single peak at $T_{\text{max}} = 105 \text{ K}$ (Figure 6.4a). The presence of the studied substances in the solution-matrix affects neither the luminescence curve shape, nor the luminescence peak location; hence, the luminescence intensity and the peak height change (Figure 6.4b).

The decrease of total luminescence and the increase of the peak at introduction of substances into the solution compared with the initial gelatin solution (the control) may be explained by capturing of electron by these compounds during the sample irradiation and, as a consequence, reduction of the quantity of stabilized electrons in the solution-matrix. Vice versa, an increase in intensity of sample luminescence compared with the initial matrix is explained by increasing e_{st} concentration as a consequence of effective reactions between additives and $\cdot\text{OH}$ (H_2O^+) radicals, which are then eliminated from recombination with e .

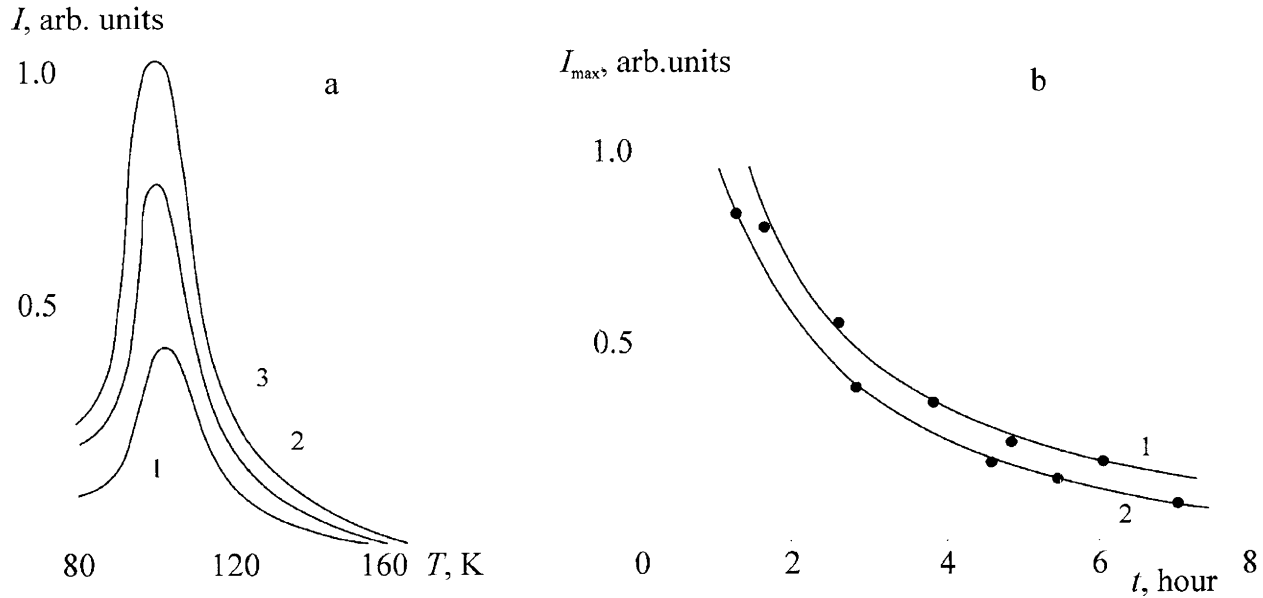


Figure 6.4. The temperature dependence of RTL intensity of samples irradiated at 77 K

- a: 1 – 10% gelatin solution + 0.025 M thymine; 2 – 10% gelatin solution + 0.025 M thymine + 0.1 M CH_3COOH ; 3 – 10% gelatin solution + 0.025 M thymine + 0.1 M CH_3COOH + 0.1 M glucose. The curves were plotted 90 min after termination of irradiation. The dose was 10 kGy
- b: The dependence of luminescence intensity at $T = (105 \pm 2)$ K for 10% gelatin and 0.025 M thymine solutions on the sample storage time in liquefied nitrogen: 1 – without additives; 2 – in the presence of glutathione

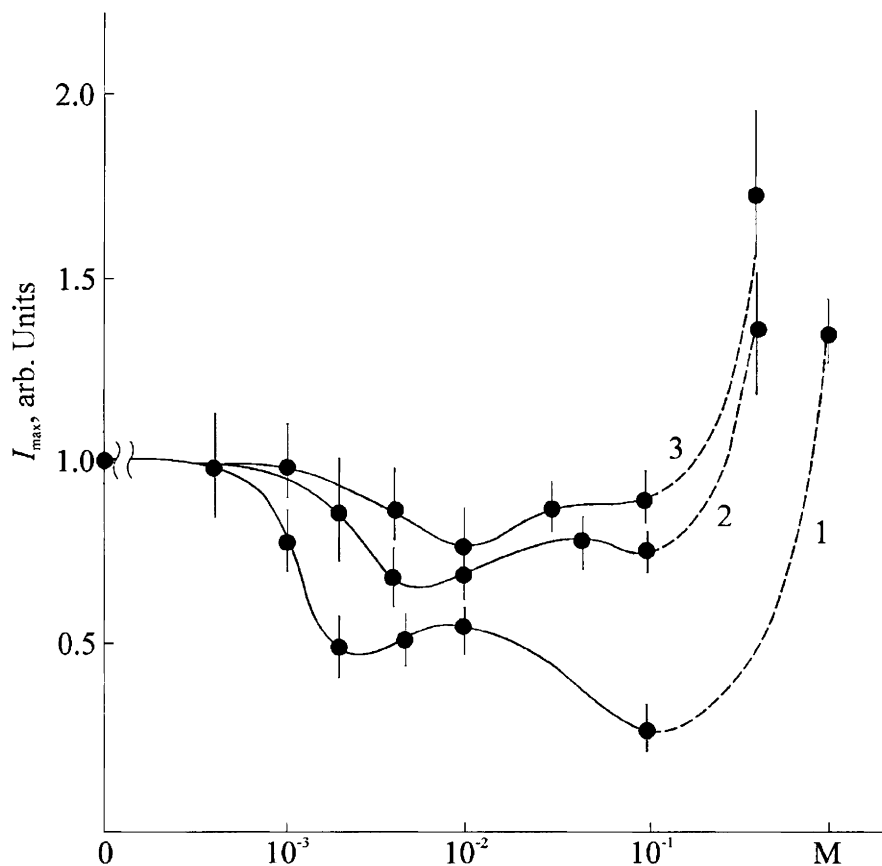


Figure 6.5. The change of luminescence intensity by RTL curves at $T_{\max} = (105 \pm 2)$ K with respect to the concentration of oxypyridines: 1 – 3-oxypyridine; 2 – 6-methyl-2-ethyl-3-oxypyridine; 3 – 2,6-dimethyl-3-oxypyridine in 10% gelatin and 0.025 M thymine solution. Cryostat heating rate is (16 ± 2) deg/min at the dose equal 10 kGy [5, 6]

The alternating increases and decreases of luminescence intensity peaks on the curve at T_{\max} with respect to concentration of injected substance (Figure 6.5) is explained by the presence of several sites for e and $\cdot\text{OH}$ attack, various functional groups, in a molecule of the studied substance. The action of the most “active” functional groups is displayed in the area of lower concentrations

of these compounds. For such systems, the following expression for the reaction rate is assumed valid:

$$w = k_{AA+e}[e][AA], \quad (6.5)$$

where k_{AA+e} (by analogy with k_{AA+OH}) is a coefficient proportional to the reaction rate constant in the liquid phase. It is suggested that at comparison of the efficiency of various functional groups equal change of the intensity ΔI_{\max} (a decrease or an increase) for two substances may testify about equal rate of e (or $\bullet OH$) elimination from the reaction. Then

$$w_1 = w_2 = k_1[e][AA_1] = k_2[e][AA_2] \quad (6.6)$$

and

$$k_2 = k_1 \frac{[AA_1]}{[AA_2]}. \quad (6.7)$$

As accepting for specific reactivity, for example, the case of glycine (the lowest reactive compound among those under study in relation to e and $\bullet OH$), one may compare the effectiveness of these compounds in relation to radicals and directly their relative functional groups (Table 6.3).

Table 6.3

Relative interaction rate constants of antioxidants and other chemical compounds with primary water radiolysis radicals at 77 K [5, 6]

Compound	Rate constants of interactions with	
	\bar{e}	$\bullet OH$
3-Oxypyridine (I)	7	20
6-Methyl-2-ethyl-3-oxypyridine (II)	4	3
2,6-Dimethyl-3-oxypyridine (III)	3	3
Spurdog liver extract	200	30
Peginol	15	50
Glutathione	300	500
Glucose	0.3	1
Glycine	1	1

Figure 6.5 shows concentration dependence curves of the luminescence intensity peak changes at T_{\max} for irradiated gelatin solutions in the presence of

additives I, II and III. For all three compounds, the initial drop of luminescence intensity is explained by their acceptor properties in relation to electron. As follows from the analysis of curves 1 – 3 in the concentration range of 0.001 – 0.1 M, the reactivity of these compounds in relation to \bar{e} is ranked as follows:

$$I > II > III.$$

Using the equation (6.7) and assuming that $k_1(\bar{e}) = 1$, one may determine relative rate constants of \bar{e} reactions with the substances II and III:

$$k_{II}(\bar{e}) \sim 0.5k_1(\bar{e}); k_{III}(\bar{e}) \sim 0.25k_1(\bar{e}).$$

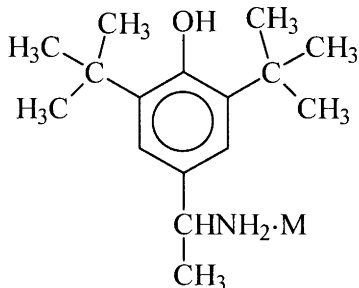
Further run of the curve in the concentration range between 0.002 – 0.1 M reflects proceeding of two processes in the irradiated system. The first process represents the interaction between dissolved substance and $\cdot\text{OH}$, which results in the luminescence intensity increase. The second process represents an additional capture of electrons, which yield is increased due to $\cdot\text{OH}$ radical elimination from reactions with them. The ratio of the rates of these two processes define the shape of curves 1 – 3. For compound I, the rates of these processes are significantly different, whereas for compounds II and III these differences are lower, in the descending order. If one suggests that reaching of the maximum in the concentration range between $5 \cdot 10^{-3}$ – $5 \cdot 10^{-2}$ M means total involvement of $\cdot\text{OH}$ (H_2O^+) radicals in the reactions with the studied substances, then for the concentration range with $\Delta I = \text{const}$ the following sequence is observed:

$$k_I(\text{OH}):k_{II}(\text{OH}):k_{III}(\text{OH}) = 10:1:1.$$

ESR studies of atomic hydrogen reactions with any substances at 77 K

This technique applies instability of H atoms (the tunneling effect), generated by γ -irradiation at 77 K in a glassy-like matrix, represented by 6 M H_3PO_4 solution. Using typical ESR spectra of radicals formed in the post-radiation period, this technique may help in the study of the reactivity of various functional groups of substances in relation to H atoms. Let us discuss this fact on the example of 4-oxy-3,5-di-*tert*-butyl- α -methylbenzylamine,

which is the compound of the class of spatially hindered phenols [7], used as a therapeutic measure, including the radiation damage of the organism [8].



ESR spectra of irradiated solutions I and II, recorded at 77 K directly after irradiation and storage of samples in liquefied nitrogen are shown in Figure 6.6 [9]. They represent the totality of ESR-lines of atomic hydrogen (a doublet with $a \sim 50$ mT), “matrix” and dissolved substance radicals: R_1 – phenoxyl radical (H detachment from phenol hydroxyl group, extended singlet), R_2 – radical-H adduct by C_2 or C_6 in the ring (splitting of 4.9 mT doublets, 0.35 mT), and R_3 – H detachment radical from C_α (the splitting quartet 1:3:3:1 ~ 2 mT). All these radicals are formed in the reactions of H atoms with corresponding functional groups of the compound directly at the solution irradiation or in the post-irradiation period: Concentration of H atoms with time of the sample storage liquefied nitrogen decreases, whereas of R_1 – R_3 radicals increases (Figures 6.7, Table 6.4). Integration of these radical spectra allowed determination of the values of their parallel yields and, subsequently, estimate the relative reactivity of atomic H in reactions with the mentioned functional groups of the current phenol:

$$[R_1]: [R_3]: [R_2] = 10: <3: 1.$$

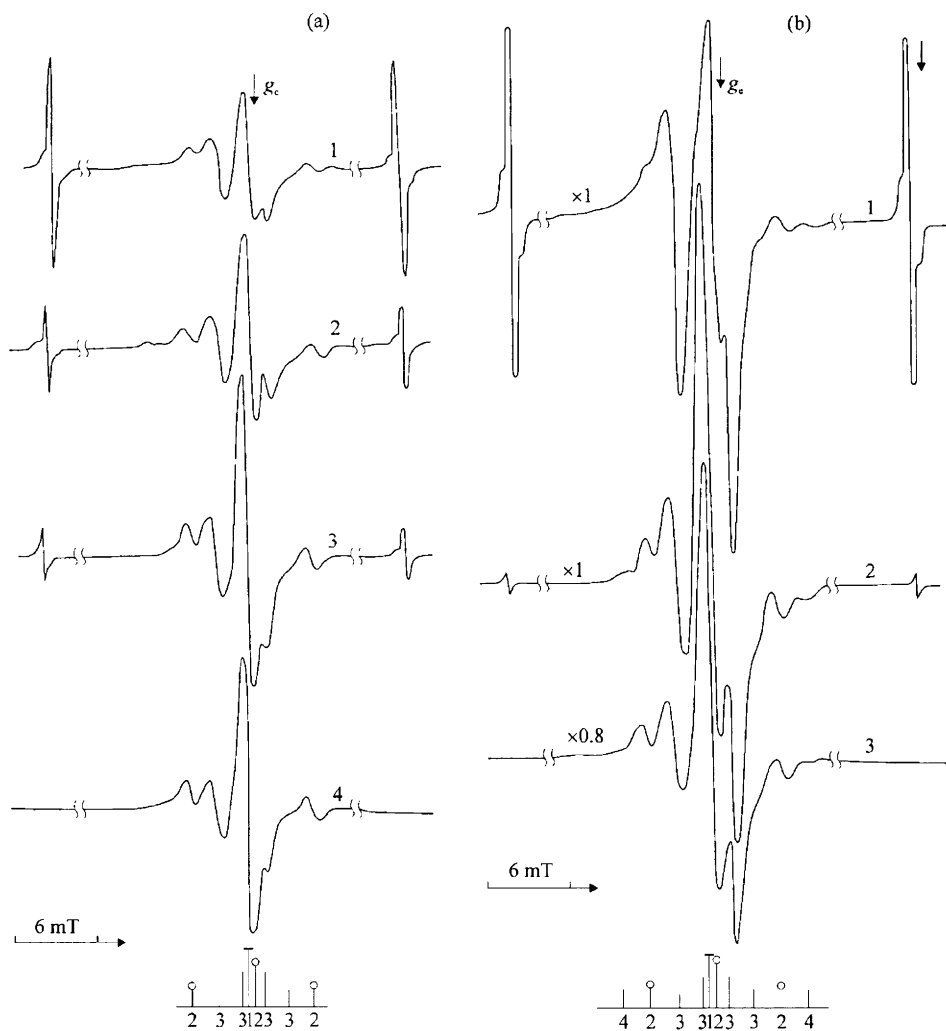


Figure 6.6. ESR spectra of phenol hydrochloride (I) and tartrate (II) of the mentioned structure (77 K), irradiated in 6 M H_3PO_4 solution, recorded at 77 K

a: 1 – 40 min after; 2 – 4 h after; 3 – one day after; 4 – three days after;

b: 1 – 3 h after; 2 – 8 days after; 3 – 40 days after;

$P_{UHF} \leq 0.015$ mW; “ $\times 0.8$ ” – amplification; below the spectra – dashed simulation of spectra of the identified radicals

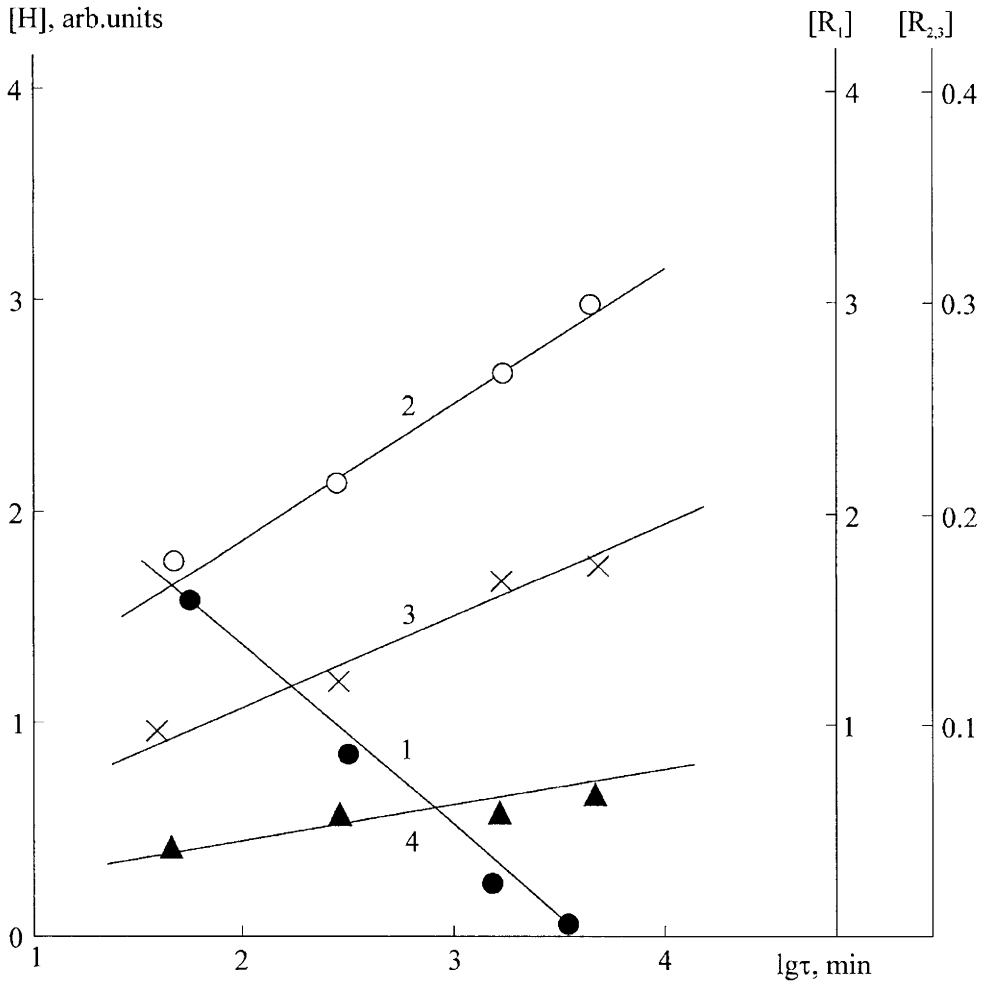


Figure 6.7. The change in radical concentration in the irradiated sample I (5 kGy dose) with the storage time in liquefied nitrogen: atomic hydrogen (1), and radicals R_1 (2), R_2 (3), and R_3 (4)

Table 6.4

Radical concentration change (relative units) in the sample I during storage in liquefied nitrogen (refer to legends of Figures 6.6 and 6.7)

Radical	At the irradiation day	8 days after	40 days after	$[R]_{40} - [R]_0$
ΣR , except for H^\bullet	650	510	360	-290*
R_1	80	185	190	110
R_2	27	45	37	10
R_3	—	—	—	$\leq 30^{**}$
$\bullet OH$	460	210	80	-380*

Notes: * Minus means a decrease of the radical concentration;

** R_3 concentration was determined by integrating the spectrum, reconstructed by the boundary spectrum components with suggested quartet HFS (1:3:3:1)

REFERENCES

1. Brodskaya G.A., "Radiolysis of phenylalanine and tyrosine aqueous solutions", *Candidate Dissertation Thesis*, Tashkent, TGU, 1967, 151 p. (Rus)
2. Sharpatyi V.A., *Radiation Chemistry of Biopolymers*, Moscow, Energoizdat, 1981, 168 p. (Rus)
3. Kochetkov N.K., Kudryashev L.I., and Chlenov M.A., *Radiation Chemistry of Carbohydrates*, Moscow, Nauka, 1978, 288 p. (Rus)
4. Zakatova N.V., "Radiolytic conversion of DNA in aquatic solutions", *Candidate Dissertation Thesis*, Moscow, Institute of Electrochemistry AS USSR, 1973, 132 p. (Rus)
5. Svanidze E.O., "The features of free radical conversions at the radiolysis of frozen-up gelatin solutions", *Candidate Dissertation Thesis*, Moscow, IKhF RAN, 1992, 189 p. (Rus)
6. Svanidze E.O. and Sharpatyi V.A., In Coll.: *The Studies of Synthetic and Natural Antioxidants Bot in vitro and in vivo*", Ed. E.B. Burlakova, K.E. Kruglyakova, and L.N. Shishkina, Moscow, Nauka, 1992, p. 43. (Rus)

7. Ershov V.V., Nikiforov G.A., and Volod'kin A.A., *Spatially Hindered Phenols*, Moscow, Khimia, 1972, 351 p. (Rus)
8. Emanuel N.M., *Uspekhi Khimii*, 1981, vol. **50**(10), p. 1721. (Rus)
9. Minkhadzhidinova D.R. and Sharpatyi V.A., *Khimia Vysikhikh Energyiy*, 1996, vol. **30**(5), p. 352. (Rus)

Chapter 7. The problems of radiation chemistry of protein molecules

Proteins represent high-molecular organic compounds with molecular weight varying from dozens to hundreds of thousand units. They are the main components of cells and are accumulated in seeds and eggs in the form of nutrients. Protein molecules in the cell perform various functions (immunity, respiration, muscular contractions, enzymatic catalysis, etc.) [1]. As radiation affects the cell, the energy received is finally absorbed by protein molecules (total concentration of dry protein in the cell reaches 60 wt.%, on average). Therefore, the knowledge of initial damage localization in protein molecules and the mechanism of propagation by them is important for forecasting the cell radiation consequences and cell radioprotection, i.e. for the purposes of applied radiobiology. We also face the problem of the radiation action estimation in case of food preservation [2]. Hence, of importance is to know the origin and the quantity of protein radiolysis products formed, some of which may be toxic.

The dose ranges of ionizing radiation used for radiation treatment of protein systems are related to the so-called doses of biological range: from thousandth parts to units Gy. The exclusion is for microbial flora annihilation, when the radiation dose may reach hundreds Gy or more. However, practice also requires the use of higher doses absorbed by protein system, which may reach dozens kGy, for industrial purposes, such as wool upgrading or sterilization of corresponding materials used in medicine by radiation treatment. In all cases, the questions of the control for radiation-chemical processes in irradiated proteins are urgent.

For all these examples, the integrating factor is formation and conversion of free radicals, because free-radical processes are predominant in both radiation damaging of proteins and radiation modification of protein systems: total yields of the radiolysis final products of and primary free radicals are comparable (refer to Section 7.4). Therefore, the first and foremost question to be discussed in this Chapter is the role of free radicals in the radiation degradation of proteins. On some particular examples the author considers their conversion till formation of final radiolytic effects. In relation to free-radical mechanism, let us formulate the second topic to be discussed in this Chapter – the role of free-radical products of water radiolysis in the

radiation damage of proteins. In addition, we'll try to determine the regularities of radiolysis of their aqueous solutions.

Analysis of the strategy for the study of protein radiation chemistry indicates the following:

1. Aqueous solution of a polymer is irradiated.
2. We are dealing with radiation chemistry of polymers and separately with radiation chemistry of water and aqueous solutions.

Seemingly, if we take into account all basic laws of radiolysis of polymers and aqueous solutions, we may gain an impression of the mechanism of radiolytic conversion of protein molecules in the protein–water system. Primarily, this is stipulated by a complex structural organization of this system and manifestation of radiolytic features of both components of the system:

1. Protein is a polymer containing no monomeric units of constant chemical composition, but contains residues of 20 amino acids with various functional groups.
2. In protein molecules, amino acid residues interact differently with one another and the solvent molecules, wherefrom microheterogeneity of the system, the presence of clusters formed by polar and non-polar (hydrophobic) amino acid radicals, a possibility of collective responses to external energy depositions.
3. The existence of supermolecular organization (the hierarchy of structures) is typical of protein molecules. This particularly provides for their variable biological activity, which is extremely sensitive to the radiation effects even in the low dose range.

So far as concerns the features of water radiolysis in proteins, they are mostly induced by the interaction between water molecules and functional groups of amino acid residues, which, in turn, structure water. Therefore, strictly speaking, even in the case of irradiation of native proteins, but not their only their solution, the radiolysis of structured water (water from hydrate covers and water molecules in the cluster composition) should be considered. As a consequence of these factors the estimation of manifestation of direct and indirect irradiation effects on the protein–water system is hindered. Here we may speak about the mechanisms of directed transfer of the energy absorbed by the system from the solvent molecules to functional groups of macromolecules,

generally predetermined by supermolecular structural organization of biopolymer.

7.1. STRUCTURE AND COMPOSITION OF PROTEIN MOLECULES

A protein molecule is a polypeptide consisting of amino acid residues, linked by $-C(=O)-NH-$ peptide bonds. Amino acid residue radicals form branches from the polypeptide chain. The variety of radicals by chemical and physical properties (the radical chain length, volume, and configuration and, therefore, the shape and relief of the protein particle surface) promotes multifunctionality and specific features of proteins.

The primary protein structure represents a sequence of amino acid residues in one or several polypeptide chains composing the protein molecule. The so-called secondary structure is formed by a system of hydrogen bonds between polypeptide groups locating in the neighbor folds of a helix-shaped molecule (α -helix sections) and between molecules (β -layer formation).

The tertiary structure of proteins represents location of molecular chains in space, fixed by:

- a) Van-der-Waals interaction forces between side radicals of amino acid residues;
- b) hydrogen, ionic or disulfide bonds;
- c) interactions between amino acid residues and water molecules.

Thus, the latter are structured by functional groups of proteins and together with biomacromolecules form the integrated natural complex possessing definite biochemical functions. By the quaternary structure of the protein we mean a totality of a definite number polypeptide chains (subunits) located in strictly fixed position in space resulting local interaction forces between functional groups, located on the surface of protein globules, for example, Coulomb's interaction of dissimilar charged groups.

The proteins are most demonstrative showing the dependence of their properties on the molecule shape, defined by intermolecular or intramolecular energy interactions. An abrupt change in the properties of some native proteins induced by various impacts is related to the molecular shape change from globular to linear, which is stipulated by destruction of intramolecular bonds.

Enzymes are protein substances, too. Beside protein fragments, they sometimes contain residues of other organic compounds – co-enzymes, metal ions and nonmetals (ionic co-enzymes). All these groups form the so-called active site of the enzyme and endue it with specific catalytic activity.

For the most extent, the composition of protein molecules is interesting for us with respect to answering the following questions:

- a) what the protein molecule fragments are damaged first of all at the radiation impact on the protein solutions;
- b) what the origin of primary macroradicals formed is;
- c) what the sites in the biopolymer for water radicals are;
- d) how these initial damages (unpaired electrons) in the molecules transform to final radiolytic effects.

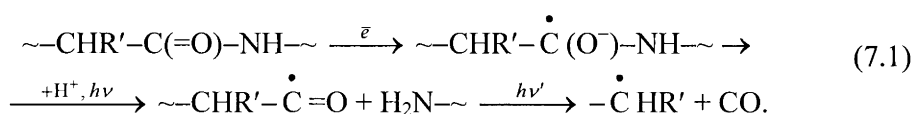
7.2. BASIC RADIOLYTIC EFFECTS IN PROTEINS

The basic radiolytic effects in proteins may be classified as follows: polymer backbone degradation, crosslink (chemical bond) formation, modification of amino acid residue radicals, the change in conformation and crystallinity degree of the protein, oxidative degradation (in the presence of O₂), formation of low-molecular products, and damaging of an active site in the enzymes.

Degradation of the polypeptide chain

The specificity of the protein molecule radiolysis is stipulated by the presence of peptide bonds: one peptide bond is accounted for one monomeric unit (of variable chemical composition) of this biopolymer. To put it differently, the protein molecule possesses greater quantity of peptide bonds. The peptide bond is characterized conjugation of electrons from nitrogen, carbon and oxygen atoms that makes it similar to the double bond -NH-C(=O)- . This is manifested in decreasing of its length (1.325 Å) compared with C–N bond length (1.46 Å). Oxygen and hydrogen atoms bond to N and C atoms, which form a peptide bond, are located in the same plane. The carboxylic group at the peptide bond is affined to electron. As dry

preparations [3, 4] or aqueous solutions of protein [5] are irradiated, the electrons released hit these carboxylic groups and are captured by them then forming anion-radicals. In the presence of water, anion-radical are protonated, and the energy gain reaches 3 eV per bond. Since each monomeric unit contains one peptide bond, one may conclude about predominance of peptide bond carbogroup attack by electron in the protein molecule. In anion-radicals, the peptide bond affected by the light wavelength $\lambda = 365$ nm is decomposed [6]. Hence, acyl radical is formed, which degrades releasing carbon oxide under the effect of $\lambda = 520$ nm radiation.



In aqueous solutions, the basic role in protein degradation is devoted to $\cdot\text{OH}$ radicals. The sites for their attacks are functional groups of amino acid residues (see Section 7.4). Hence, the forecasting of the radiation damage localization sites in the protein molecule was based only on the information about reactivity of individually irradiated amino acids and peptides in relation to radical products of water radiolysis [7]. Beside the peptide bond, the repeating unit of the protein contains -HC(-R)- fragment, where R is the amino acid residue radical. It should be expected that beside the peptide bond is one of the basic sites of localization of the primary radiation damage. Actually, the ESR method applied to proteins irradiated at room temperature [8, 9] and their frozen-up solutions after low-temperature irradiation (77 K) and further annealing below 180 – 200 K in the absence of O_2 [5] has registered free radicals, formed at H atom detachment from C atom. In frozen-up solutions, this process is induced by $\cdot\text{OH}$ radical: the irradiation of glassy gelatin solutions, annealed in liquefied nitrogen in the temperature range of 85 – 130 K, indicates the antibatte shape of $\cdot\text{OH}$ radical (decreasing) and C_α (R_{gly} and R_{ala} , refer to Table 7.2) radical concentration dependencies at the total concentration of radicals [10] unchanged (within the measuring accuracy) in the sample:

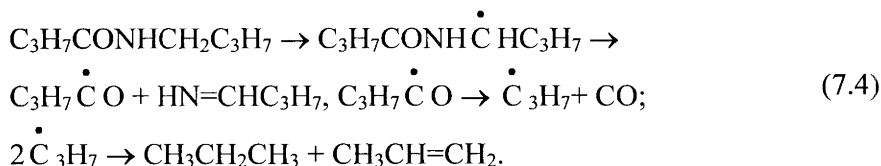


where RH is the protein molecule.

As demonstrated on the example of low-molecular model compounds of $R-C(=O)NHR'$ structure and polyamides of general formula $-CONH-(CH_2)_n-CONH-$, where $n = 1 - 10$, C_α type radicals, in which unpaired electron is localized at the amino group, may be formed under the effect of H atoms [11, 12]:



Basing on these data a conclusion about possible proceeding of the reaction (7.3) in the case of protein radiolysis (at least at dry substance irradiation) was made. The process of radical C conversion in the absence of O_2 is accompanied by polypeptide bond break. The data on model system (amides and polyamides) radiolysis clearly illustrate the latter fact [11, 12]. The proceeding of the reaction (7.3) is confirmed by relatively high yield of molecular oxygen: $G \sim 2$ molecules per 100 eV comparable with CO yield. At irradiation of N-d-butyric acid amide and N-(ethyl-2d-) butyric acid amide (the compounds modeling fragments of polyamides) propane and propylene were detected, which total yield equaled a half of carbon oxide yield. This allowed for the following scheme of formation and conversion of radicals:



It is clear that carbon oxide is a specific indicator of the radiation cleavage of peptide bond.

Turning back to the protein molecule radiolysis in aquatic solutions, let us dwell on two processes concerning the entity of the polypeptide chain, in which $\bullet OH$ and \bar{e} take part (in the absence O_2), on the example of radiolysis of aqueous solutions containing various gelatin (Glt) and human serum albumin (HSA) concentrations. The concentration dependence of molecular hydrogen yield in irradiated gelatin air-free solutions [2] is linearized well in $G(H_2) - [Glt]$ coordinates. As extrapolated to zero protein concentration, such straight line cuts an intersect $G(H_2) = 0.45$ on the axis of ordinates. This means [13] that molecular hydrogen is formed in recombination acts of primary water radiolysis products, and reactions between biopolymer molecules and H_2

precursors in tracks proceed at rather high rates. The presence of saccharose in irradiated solutions (1 – 8%) has no effect on the concentration dependence of H₂ yield. This is no wonder, because saccharose (Sch) is an effect [•]OH acceptor, and its reactivity with \bar{e} is four orders of magnitude lower [14].

Table 7.1

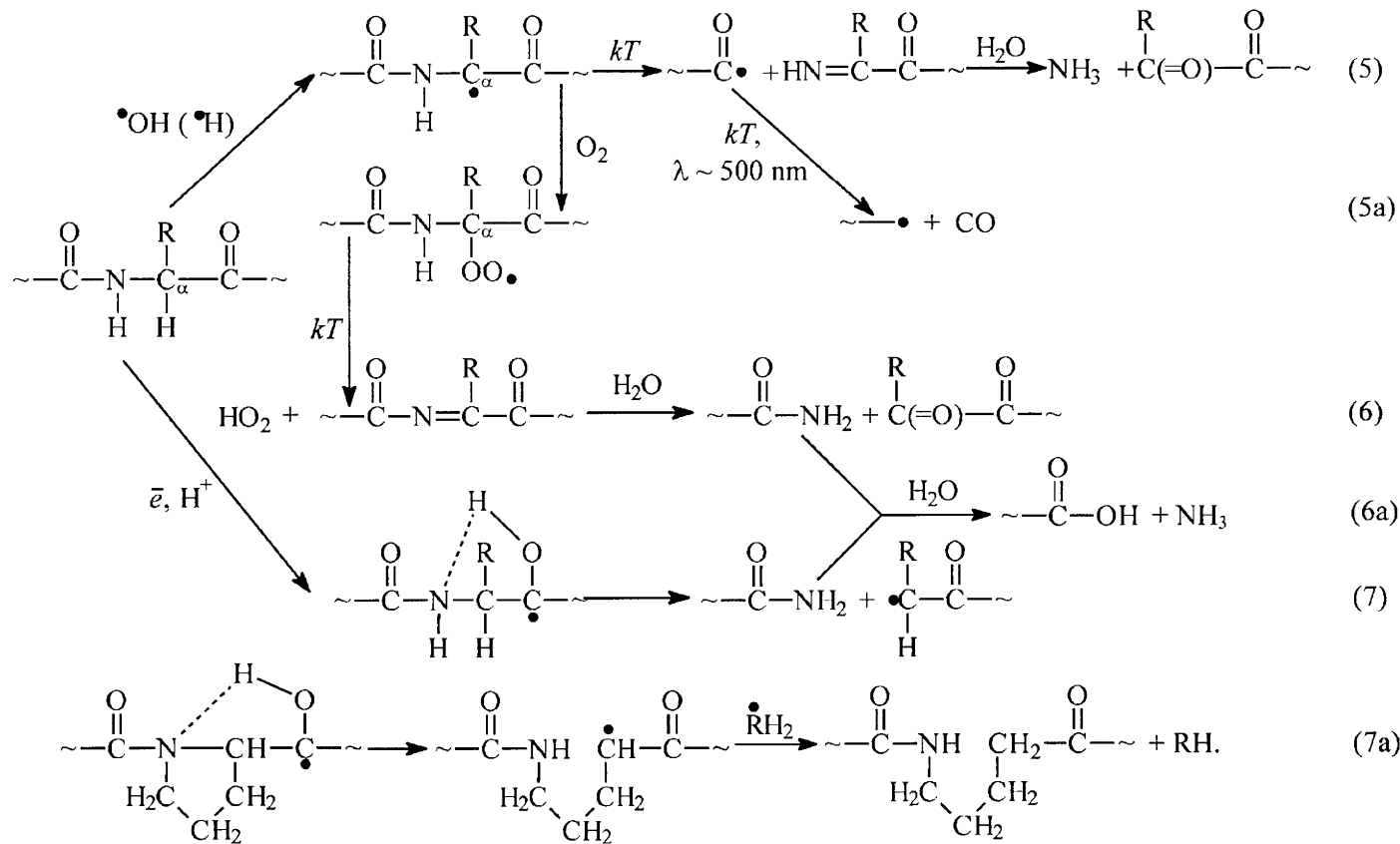
Radiation-chemical yield of H₂ and CO from irradiated (*D* = 45 kGy) evacuated gelatin solutions (Glt, *M_w* = 68,000) [2] and the gelatin protection by saccharose (Sch) against degradation [15]

Solutions	<i>G</i> (H ₂)	<i>G</i> (CO)	Gelatin protection by saccharose, %
1% Glt (1.5×10 ⁻⁴ mol/l) + + 8% Sch (0.23 mol/l)	0.32	0.01	80
6% Glt (9×10 ⁻⁴ mol/l)	0.25	0.09	0
10% Glt (1.5×10 ⁻³ mol/l) + + 1% Sch (0.029 mol/l)	0.21	0.08	20
Sch (dry preparation)	0.002	0.003	–

Sch considerably decreases CO yield, which is one of the protein degradation products (Table 7.1). If we take into account that at irradiation of aqueous solutions the accumulation of [•]OH radical conversion products should also follow the analogous regularity:

$$G_m = G_0 - qC,$$

where *q* is a coefficient related to the track parameters, the type of radiation, and radical acceptor origin [15], then according to the estimation protein radioprotection by saccharose against degradation, induced by [•]OH, in irradiated solutions varies in the range between 20 and 80%. The validity of this regularity for estimating biopolymer oxidative degradation is indicated by the results of irradiation of another water-soluble protein – human serum albumin (HSA), namely, oxidative deamination in HSA concentration range between 0.001 and 0.2%. In this case, in the absence of O₂, when the interaction between \bar{e} and protein is impossible and oxidative degradation of



Scheme 7-1

this protein is initiated exclusively by $\cdot\text{OH}$ radicals, the yield in deamination process (ammonia release) obeys the linear dependence:

$$G(\text{NH}_3) \sim [\text{HSA}] \text{ [16].}$$

The diagram below (Scheme 7.1) presents the scheme of NH_3 and CO formation processes proceeding at protein irradiation in solutions [17].

Contrary to CO , ammonia amide is released at irradiation of both air-free and oxygen-saturated protein solutions. In the first case, total deamination of protein is mainly contributed by $\cdot\text{OH}$ radicals: as transiting from $\bar{\epsilon}$ and $\cdot\text{OH}$ reagents (HSA solution saturated with argon) to $2\cdot\text{OH}$ (the solution is saturated with nitrous oxide: $\bar{\epsilon} + \text{H}_2\text{O} + \text{H} = \text{OH} + \text{N}_2$), ammonia yield increases more than two times [18]. This process of deamination represents hydrolytic cleavage of $\text{C}(=\text{O})\text{-NH}_2$ amide bonds (Scheme 7.1, reaction (6a)).

Thus, it should be noted that:

- 1) formation of both carbon oxide and ammonia amide at irradiation of protein solution indicates cleavage of peptide bonds;
- 2) CO is formed only due to conversions of primary C-type radicals.

Polypeptide chain breaks may also occur as a result of isomerization of primary anion-macroradicals, synthesized at the electron attack on carbo-groups in peptide bonds. The role of electron and the role of this process of the polypeptide chain break should become more urgent in case of irradiation of dry protein preparations. The formation of breaks due to anion-macroradical conversions is not accompanied by CO release. The latter may be released only resulting photolytic impact on the anion-macroradical [3, 6].

A possibility of reaction (7a) proceeding is proved by ESR data, obtained for gelatin and bovine thymus histone solutions irradiated at 77 K and then thermally annealed [18 – 21]. Primary $\cdot\text{R}_{\text{pb}}$ radicals (doublet spectrum, Table 7.2) with increasing temperature of the sample transform into R (quintet spectrum, Table 7.2; in Figure 7.1, the radical with unpaired electron in proline residue is marked by vertical arrows) in gelatin with the yield 5 times higher compared with total thymus histone. These values correlate with molar content of proline residues in gelatin and histone (30 and 6%, respectively).

Table 7.2

Characteristics of free radicals identified by ESR spectra in wool fiber samples, γ -irradiated by ^{60}Co source at 77 K [27]

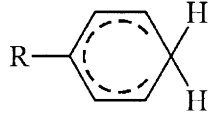
Radical, number of HFS components	Total spectrum width, mT	a , mT	g -factor	Radical content, G (%)	Supposed radical structure and formation reaction	Temperature range of recording, K
1	2	3	4	5	6	7
R_1 (R_{lys}), 6 (1:3:4:4:3:1), sextet	12.5	$a_\alpha = a_\beta^1 = 2.2$	2.003	> 10	$\cdot\text{CH}_2\text{-CH}_2\text{-}$	77 – 150
		$a_\beta^2 = 4.5$		0.1	$\bar{e} + \text{NH}_3^+ \text{CH}_2\text{CH}_2\text{-} \rightarrow R_1 + \text{NH}_3$	
R_2 (R_{ar}), 9 triplet (1:2:1) triplets (1:2:1)	~10	$a_\alpha = 4.2$	2.003	7		77 – 300
		$a_0 = a_n^{**} = 0.8$		~0.1	$\bar{e} + \text{R-} \langle \text{benzene ring} \rangle + \text{H}^+ \rightarrow R_2^*$	
R_3 (R_{ps}), 2, doublet (1:1)	~3	–	2.00	25 } 0.3 <10 }	$-\dot{\text{C}}(\text{O}^-)\text{C}_\alpha\text{HRNH-}$	77 – 220
					$\bar{e} + -\text{C}(=\text{O})\text{CHRNH-} \rightarrow R_3$	
R_4 , 5, quintet (1:2:2:2:1)	9	$a_\alpha = a_\beta^1 = 2.2$	2.003	<10	$-\text{C}(=\text{O})\dot{\text{C}}_\alpha\text{H}(\text{CH}_2)_3\text{NH-}$	300 – 340
		$a_\beta^2 = 4.5$				

Table 7.2 (continued)

1	2	3	4	5	6	7
R ₅ (R _{ala} + R _{gly}), 4 (1:7:7:1)	~6			20		
R _{ala} , 4 (1:3:3:1)		~1.5	2.00		$-\text{NH}\dot{\text{C}}_{\alpha}\text{CH}_3\text{C}(=\text{O})\text{NH}-$	77 - 360
				0.2	$\dot{\text{H}} + -\text{NHCHCH}_3\text{C}(=\text{O})\text{NH}- \rightarrow \text{H}_2 + \text{R}_{\text{ala}}$	
R _{gly} , 2 (1:1)		~2	2.00		$-\text{NH}\dot{\text{C}}_{\alpha}\text{HC}(=\text{O})\text{NH}-$	77 - 360
					$\dot{\text{H}} + -\text{NHCH}_2\text{C}(=\text{O})\text{NH}- \rightarrow \text{H}_2 + \text{R}_{\text{gly}}$	
R ₆ , 2 (1:1), doublet	3	-	2.003	40	$[\text{RSSR}]^{\bullet}, \bar{e} + \text{RSSR} \rightarrow \text{R}_6$	77 - 360
				0.4		
R ₇ (RS [*]), asymmetrical spectrum	10	-	$g_1 = 2.002$ $g_2 = 2.029$ $g_3 = 2.057$		$\text{RS}^{\bullet}, [\text{RSSR}]^{\bullet} \xrightarrow{kT} \text{RS}^{\bullet} + \text{RS}^{-}$	220 - 425

Notes: * H-adduct of Phen or Tyr aromatic ring.

** ST cleavage constants on *ortho*- and *para*-atoms of hydrogen.

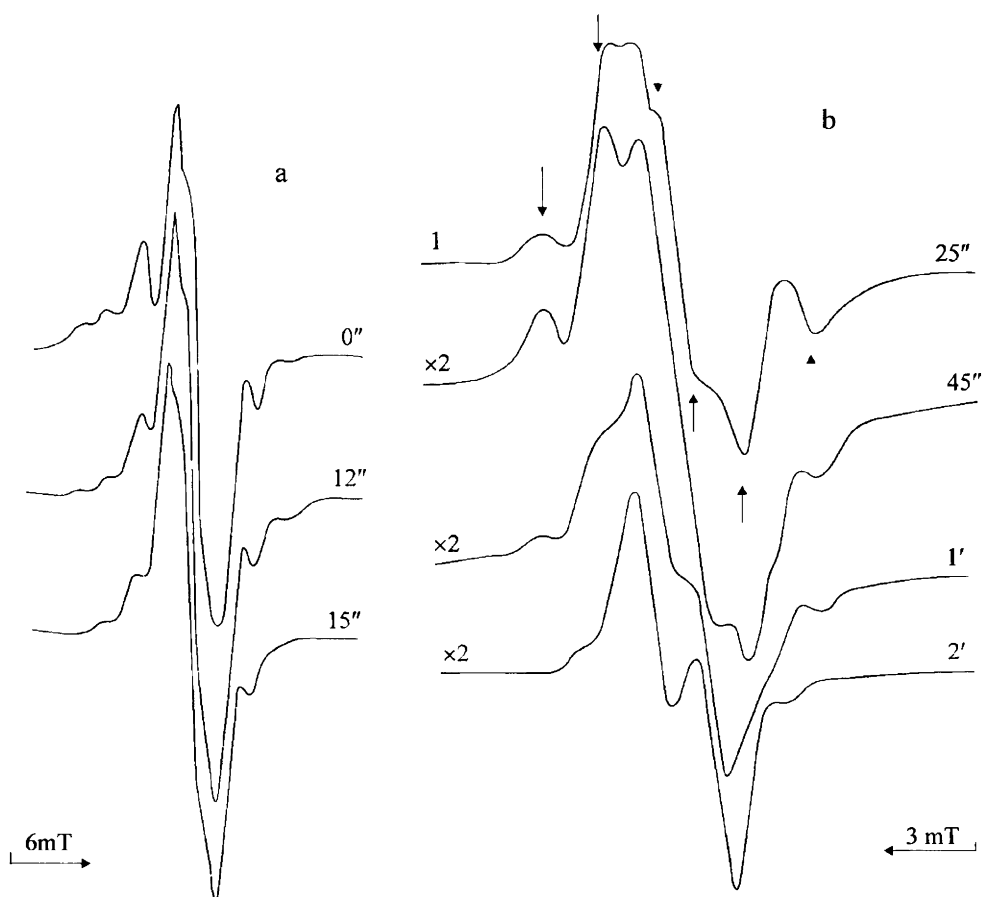


Figure 7.1. ESR spectra of gelatin solution (24%, 50 kGy dose), γ -irradiated at 77 K and recorded immediately after irradiation and then after annealing at $T \sim 300$ K during the period of time, indicated at the right of the spectra

Finally, as follows from reactions (5) – (7a), the conversion sequence of “proline” radicals (reaction (7a)) is not accompanied by polypeptide chain cleavage, but just by the change in conformation of the initial macromolecule.

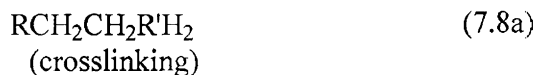
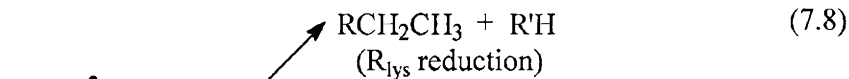
Macroradicals and final products of radiolysis and cross-linking

Despite multiple works on protein radiolysis [3, 4, 22 – 25], literary data on the conversion mechanisms of protein free radicals by stages are absent. General picture of the conversion mechanisms for primary macroradicals in irradiated proteins may be obtained from the analysis of ESR data on protein samples, prepared at low temperature and then thermally annealed: gradually heated up to temperatures, at which the whole relaxation spectrum of molecular mobility in the polymer is subsequently realized [26, p. 178]. Free radicals stabilized at low temperatures subsequently with the occurrence of one type of molecular mobility or another in polymer fragments enter reactions, isomerize and recombine. Hence, the yields of free radicals and final molecular products in the same samples, irradiated at low temperature, and breaks and crosslink yields can be compared. To the greatest extent, such analysis was performed in the study of low-temperature radiolysis of “dry” protein preparation – wool keratin [27, 28] and frozen-up aquatic gelatin solutions [10]. Let us discuss these systems.

ESR spectra obtained for the wool fiber irradiated at 77 K (Figure 7.2) allowed for identification of several types of free radicals (Table 7.2), which are also detected in other proteins. The variety of spectra observed for the irradiated proteins of similar amino acid composition is explained by different fractional yields of primary macroradicals.

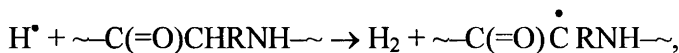
All these radicals are formed due to proceeding of uniform primary processes at the interaction of \bar{e} and H^\bullet with amino acid residues in macromolecules (sulfur-containing fragments, aromatic rings, amino and carboxylic groups, carbogroups of peptide bonds) and at C–H bond cleavage in the peptide chain under the influence of H^\bullet and $^\bullet OH$.

As a sample is annealed in the temperature range between 150 and 180 K, the sextet components with $\Delta H = 12.5$ mT related to R radicals (R_{lys} , Table 7.2) disappear from the spectrum. These radicals are formed at the interaction of \bar{e} with protonated amino groups of lysine and guanidyl group in arginine, which is also deamination process [27, 29]. As a result of R_{lys} radical conversion and consequent reactions, additional hydrophobic groups or crosslinks in macromolecules may be formed [28]:

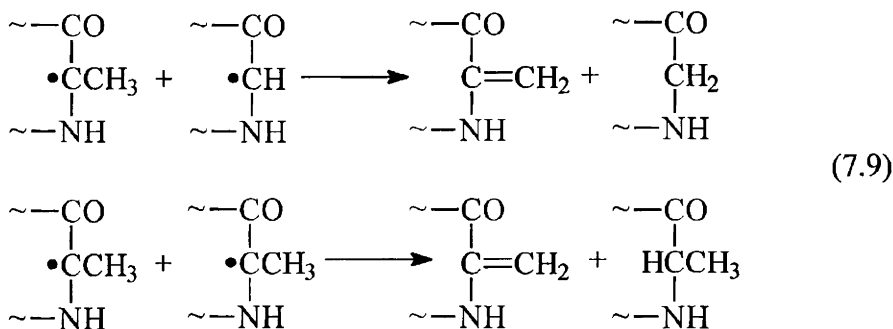


As temperature increases to 220 – 300 K, aromatic amino acid radicals R_{ar} (R₂, Table 7.2) disappear – the spectrum with $\Delta H \sim 10$ mT and doublet in the central part of the spectrum belonged to disulfide group anion-radicals. Hence, in the range of weak fields, additional components typical of sulfur-containing RS radical appear in the spectrum [23]. In the same temperature range, a five-component ESR band with $\Delta H \sim 9$ mT, the band of proline radicals, R₄, forming by the reaction (7a) appear in the spectrum.

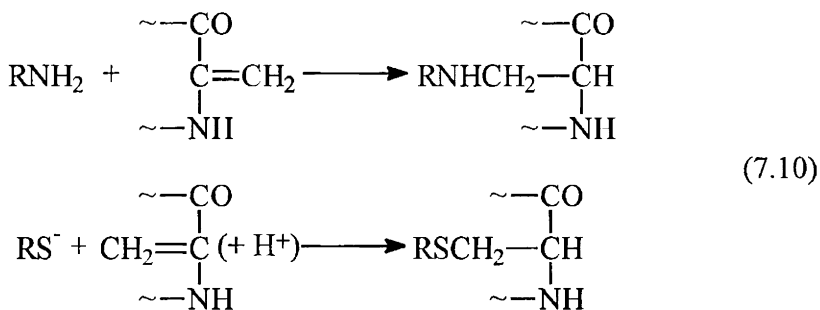
In the irradiated wool keratin, thyl RS radicals (R₇, Table 7.2), produced by the reaction (3) at C_α-H bond attack by H atoms, are the most heat-proof ones:



where R = H-R_{gly}; CH₃-R_{ala}. Spectral characteristics of R_{gly} and R_{ala} radicals (HFS and *g*-factor) indicate that the occurrence of unpaired electron at C_α is not accompanied by its delocalization to flat fragments of the neighbor peptide bonds. Obviously, their initial orientation in the macromolecule is preserved by rigid structure of the biopolymer. It is also obvious that in the radicals of this type free valence is shielded by amino acid radicals. These circumstances might explain the latest elimination of R_{gly} and R_{ala} radicals (total spectrum – the quartet with the component intensity ratio equal 1:7:7:1, Table 7.2) at thermal annealing of both dry preparations and frozen-up solutions in the absence of O₂ [26] – at the “highest” (for protein) temperatures. These radicals recombine, and dehydroalanine in the polypeptide molecule is formed:



As dehydroalanine units interact with amino groups, sulfhydryl groups or RS^\bullet ions, formed, for example, due to conversion of disulfide anion-radicals according to the reaction shown in Table 7.2, additional chemical bonds (crosslinks) of lanthionine or ornithialanine type may be formed in macromolecules of irradiated samples:



The crosslink formation in irradiated proteins is significantly affected by supermolecular structural organization of macromolecules. For example, at irradiation of collagen (which molecules are spiral-shaped and packed by three in strands, in turn, forming a structure shaped as α -spiral) in native preparations (containing up to 10% combined water) or water solutions additional chemical crosslink bonds between macromolecules are formed [30 - 35]. ESR measurement data [5, 10] allows for relating crosslink formation in collagen and gelatin to participation of macroradicals having unpaired electron in damaged Pro and HO-Pro, Phen and Tyr residues (Table 7.2). It is particularly remarkable that the highest yield of crosslinks is observed in the absence of O_2 (i.e. without participation of peroxide radicals in such a process, which is suggested in ref. [30]). The crosslink formation is significantly suppressed, if proteins are irradiated in the presence of carbohydrates, which are $\bullet\text{OH}$ radical

acceptors [2, 32, 35]. Beside the above-mentioned crosslinks, in the case of irradiation of other water-soluble proteins, the formation of crosslinks was detected, which might be explained by recombination of macroradicals with unpaired electron at Lys, Arg [36 – 38] and Cys [39] residues.

As deoxyribonucleoprotein (DNP), the representative of the so-called complex proteins – the natural complex of histone proteins and DNA, is irradiated, covalent bonds – the crosslinks of the protein–DNA type – between amino acid Lys (and Arg) and cytosine (modified by radiation in DNA composition) residues are formed [40]. The cytidyl-lysine crosslinks are formed not in the primary acts of cytidyl radical conversion (cytosine OH-adducts), but as a result of reamination reaction between final molecular product of cytidyl radical conversion (with saturated C₅–C₆ bond) and lysine amino acid residue: amino groups of these fragments are located nearby in the chromatin nucleosome (refer to Chapter 11 for details). One more example of the influence of DNP supermolecular structural organization on the protein–DNA crosslink formation is presented by the results of investigation [41], performed on phage particles in the media of different acidity. It is shown that at slight excess of the medium acidity above physiological pH level non-covalent protein–DNA crosslinks with participation of HC–DNA pairs and Gly and Asp residues are formed. As the medium pH decreases to 4, Schiff's base type protein–DNA crosslinks are formed due to the interaction between 2-deoxyribose carbonyl group (an open form in depurinated DNA sites) with lysine amino group in the protein. In the case of irradiation, such situation (local acidulation) may be realized in the presence of [•]OH radical modified 2-deoxyribose in the spur [42] containing aldehyde group or keto-group at C'1, C'2, and C'3 atoms (the so-called alkaline-labile sites [43]).

Thus, these two examples indicate participation of the final products of free radical conversions in the crosslink formation due to retaining functional groups of reacting fragments near one another by the structural organization of nucleosomes.

On the effect of denaturation of proteins

Denaturation of protein molecules is one of the manifestations of radiation chemistry specificity for these biopolymers, which means the break of secondary and tertiary supermolecular structure of proteins. Primarily, this is related to C(=O)...HN hydrogen bond break in α -spiral shaped areas inside the

molecule (desprialization) and in β -layers, formed by intermolecular hydrogen bonds. It is shown [44] that at irradiation of dry preparations or HSA aqueous solutions about 15 – 20 hydrogen bonds per one pair of ions formed in macromolecule are broken. The molecule desprialization effects (the changes in the secondary structure of protein) was comprehensively studied on the example of aqueous solutions of collagen irradiated in a wide range of concentrations [45, 46]. It is found that at irradiation of collagen solutions in doses up to 1 kGy, $\cdot\text{OH}$ radicals induce 90% desprialization of the initial level, whereas in the presence of O_2 this level reaches just 60%. The radiation-chemical yield of the process equals 0.007 and 0.004 molecules per 100 eV absorbed energy, respectively. In the presence of effective $\cdot\text{OH}$ radical acceptors, G (desprialization) is 5–10 fold reduced.

Contrary to thermal denaturation of proteins, radiolytic denaturation is the irreversible process. As is known [1], α -spiralized areas are formed by amino acid Ala, Glu, Gly, Leu, Lys, Met, and GIs residues in the fragments of polypeptides. The data on degradation and modification of these amino acid residues, obtained in the study of final molecular products of radiolysis [29, 33, 34], and the data (incomplete yet) on the unpaired electron localization site (on the origin of primary macroradicals, Table 7.2) at the same residues in the composition of irradiated proteins allow for a conclusion that the radiation irreversible denaturation of protein molecules results the formation and conversions of macroradicals and, finally, molecular products. Hence, generally, radicals possess unpaired electron either directly at the peptide chain (C_α or anion-macroradicals, Table 7.2) or C_β and C_γ carbon atoms in its branches.

Conversions of macroradicals and their heat resistance

Heat resistance of radicals in frozen-up aqueous protein solutions depends on the phase state of the system. As the protein solution is frozen up at 77 K, glassy-like solutions and samples can be formed, uniform by shape and representing polycrystalline mixtures of ice, protein and solid solution itself. The phase state of the aqueous protein system and the phase ratio in it depends on the amino acid protein composition, biopolymer concentration in the solution and the freezing up rate. The fact that at 77 K the current sample represents a glassy-like solution may be judged about by the following two signs:

1. Sample transparency;
2. Total radiation-chemical yield of free radicals, including \bar{e} , H^\bullet and $^\bullet OH$ reaching $G \sim 7$, which corresponds to complete involvement of water radiolysis products into the reaction [47].

At 77 K, in glassy-like protein solutions at thermal annealing or storage of samples in liquefied nitrogen, stabilized $^\bullet OH$, H^\bullet and \bar{e} may recombine with macroradicals and undamaged molecules. In polycrystalline unclassified samples, these processes proceed in microareas only, which represent the uniform phase.

Turning back to the analyzed examples of radical conversion in the aqueous protein systems in case of thermal annealing, the multistage type of these conversions should be noted. The comparison of results of radical thermal annealing in lysozyme, gelatin, serum albumin and thymus histone solutions [10, 48, 49] with data on changes in the phase composition of these aqueous protein systems [10, 50] indicates general coincidence of temperature ranges, in which radicals are formed or transformed and any structural change in the system are realized: arrangement of the water matrix due to redistribution of protons [51], softening of glasses and crystallization of glassy-like microregions formed from biopolymer-structured water and globular protein itself at cooling down to 77 K [50].

As a consequence of such changes, primarily, at heating the sample to 100 – 105 K $^\bullet OH$, H and stabilized on traps in frozen-up aqueous matrix are involved into the reaction first. In the case of glassy-like gelatin solutions, frozen up to 77 K, the existence of two types of biopolymer-structured water was observed. In the current aqueous protein system, these types form “soft” and “rigid” matrices for the radicals – the water radiolysis products – stabilized at 77 K [10]. Radicals stabilized in a “soft” matrix (\bar{e} and $^\bullet OH$) recombine at the liquefied nitrogen temperature.

As temperature increases to 120 and 150 – 155 K, concentration of radicals in gelatin solutions decreases: the processes of macroradical isomerism with cleavage of chemical bonds in the polypeptide chain (the breaks are formed) and recombination of radicals become possible. Hence, total concentration of radicals equals 50% of the initial one. It is admirable that such changes in ESR spectra of irradiated dry preparations of proteins are observed at temperatures exceeding the current range by 70 – 100 K (Table 7.2). It is obvious that in this case, water (bound and structured) serves as the plasticizer

in various microregions of macromolecule location promoting segmental movements in macromolecules at low temperatures. This conclusion may be confirmed by the results of RTL method, obtained for conformational mobility of macromolecules in collagen [52], the three spiral shaped protein. Four stages of collagen relaxation (4 temperature ranges) have been determined: 110 – 115 K, 155 K, 235 K and 320 – 325 K. Since water is evacuated from the samples (at 400 K), all typical luminescence peaks disappear, except the peak at 235 K. This allows for relating low-temperature maxima to the presence of several types of structured water molecules participating in formation of three spiral shaped structure of biopolymer [55].

ESR spectra of 10 – 20% gelatin solutions, heated up to 200 K, clearly demonstrate R_{gly} and R_{ala} radical components; at 220 – 225 K, the samples preserve these radicals in the total concentration about 20 – 25% of the initial one. As the sample is heated up to temperature, at which, as shown in the case humidified lysozyme, the bound water is cluster melted [50], macroradicals recombine and their concentration decreases to zero. As for dry protein preparations, temperature ranges of such preparations of the macroradicals are also shifted to higher temperatures (Table 7.2).

Analysis of the data on radical conversions in protein solutions and dry preparations does not allow for accepting a hypothesis [54] that C^\bullet radicals (R_{gly} and R_{ala}) disappear at the sample heating as a result of isomerization proceeding with H atom detachment from a neighboring imino group due to rehybridization of electron orbitals ($sp^3 \rightarrow sp^2 \rightarrow sp^3$). It is suggested that the latter radical reacts macroradicals. If it is true, the process of orbital rehybridization with respect to the temperature range of R_{gly} and R_{ala} radical existence is extended to the range between 77 and 225 – 230 K in frozen-up solutions. Moreover, acceptance of this hypothesis requires an assumption that molecular hydrogen is formed in recombination of H atoms. As follows from the experiment, the yield of hydrogen from dry gelatin does not exceed 2% of total gas yield (Table 7.1).

The relation to total yield of free radicals at low-temperature radiation ($G \sim 5$ [23]) allows estimation of $G(H)$ equal 0.1. This value is at least by an order of magnitude below the estimated level, determined with respect to amino acid composition of gelatin and the value of total radiation-chemical yields of R_{gly} and R_{ala} radicals.

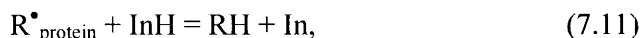
To conclude, let us note that the stage-wise considered conversions of protein radicals, initiated by structural changes in frozen-up solutions allow for explaining such effects of protein irradiation by deamination, the formation of

breaks and crosslinks in the polypeptide chains, and select the ways for controlling radical conversion processes, the radiation protection, in particular.

Radioprotection of protein molecules

At the initial stages of radiation damage of the protein, two mechanisms of the radiation protection by special radioprotector substances may be implemented, namely, the mechanisms of competition for water radiolysis products and free-radical reaction inhibition [2, 25].

The first way of radioprotection is presented by the results of investigations as follows (Table 7.1) [2, 32, 35, 46]. For example, in the case of gelatin solutions [2] as high concentrated as $1.5 \times 10^{-4} - 1.5 \times 10^{-3}$ mol/l and saccharose, the latter effectively competes with the protein for $\bullet\text{OH}$ radicals, and the yield of CO with saccharose concentration increase from 0.03 to 0.2 mol/l decreases by an order of magnitude e.g. in the presence of 0.2 mol/l saccharose the formation breaks in the polypeptide chain are suppressed by 80% and, as well, the process of C_α type radical formation. Radioprotection of the protein molecules by the second mechanism via transmission of unpaired electron from macroradicals, formed in the primary acts of radiolysis, to a substance – the inhibitor of free-radical reactions (the substitution) as follows:



may be illustrated by the radiolysis investigation data, obtained for dry protein preparation mixtures and substances-radioprotectors containing sulfhydryl groups [23]. As H atom is transferred from the substance-inhibitor to C_α radicals by the reaction (7.11), two products – stereoisomers – are formed. Hence, occurrence of one of these products means recovery of the initial structure of the macromolecule. As biologists put it differently, the initially damage of protein molecule is repaired, and the biological activity is restored. Hence, as a stereoisomer (epimeride) of this macromolecule fragment is formed (for example, when sulfhydryl group approaches the flat-shaped C_α radical from the other side), this means the change in conformation of the initial molecule. This may cause a loss of biological activity of the current protein molecule, although, in principle, the interaction between C_α radical and the inhibitor results in elimination of the free valence in the damaged

macromolecule, prevention of further degradation of biopolymer, and formation of breaks in the polymer chain.

Analyzing a possibility of realization of these two radioprotection mechanisms for substances-radioprotectors in relation to protein molecules note that such processes must proceed directly in the irradiated cell. For the substances competing for water radicals, aromatic and sulfur-containing amino acids, glutathione, thymine [25] and other compounds containing aromatic rings or sulfur-containing groups may be taken, present free in the cell or included in protein molecules. The protective action of radioprotectors with sulfhydryl groups at the cellular level proceeding by the competing mechanism for water radiolysis products is presented by the investigation results of biopolymer degradation in the cell, which is not a protein, but DNA: occurrence of breaks in irradiated DNA of cell L5178Y suspensions in the presence of mercaptoethanol (MET) in a wide range of concentrations in the cultural medium were studied (refer to Chapter 12). It has been found that as MET concentration in the suspension increases, DNA break yield gradually reduced and, starting from some intermediate concentration remained unchanged with the concentration increase (this illustrates the mechanism of indirect effect of radiation). Hence, the maximal radioprotection effect reached 86%.

The inhibitors of free-radical reactions may be the same compounds having sulfhydryl groups, spatially hindered phenols, etc., endogenous to the cell and manifesting properties of hydrogen atom donor. Radioprotection on proteins implemented by cysteine residues by the reactions (7.11) is confirmed by ESR data, obtained in the experiments of thermal annealing of proteins, evacuated and irradiated at 77 K [27]: in samples heated up to 280 - 360 K primary radicals annihilate forming RS-type radicals, the concentration of which increases with the sample temperature (Figure 7.2). To put it differently, in terms of radiation chemistry of polymers [55, 56], in the irradiated cell “external” and “internal” radioprotection mechanisms for protein molecules may be realized.

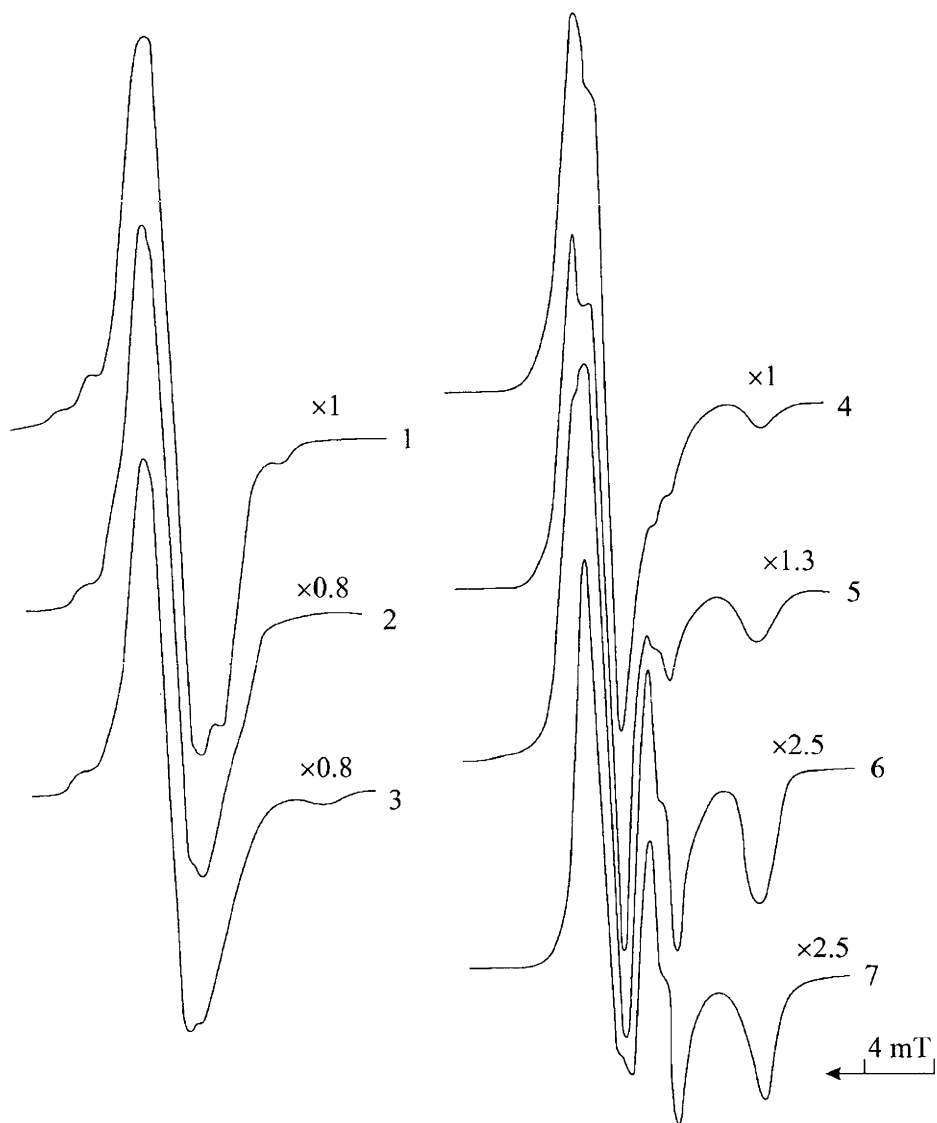
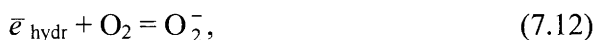


Figure 7.2. ESR spectra of wool fiber irradiated by 80 kGy dose at 77 K, measured at 77 K immediately after irradiation (1) and sample annealing during 10 min at 180 (2), 220 (3), 300 (4), 320 (5), 340 (6), and 360 k (7). Data were recorded at $P_{\text{UHF}} = 0.015$ mW and HF-modulation of 0.06 mT. Signal amplification is shown at the right of the spectrum

Also, in the irradiated cell, analogous processes are implemented with other chemical components in it – the above-mentioned nucleic acid, lipids, etc. All these experimental facts confirm the concept, proposed in 1950ies by N.M. Emanuel, on the application compounds-inhibitors of free-radical reactions as radioprotectors in the case of radiation pathology [57]. At present, such elementary processes were registered (directly or indirectly) in cells and tissues of animals, and the compounds possessing high antiradical activity are used in clinics.

7.3. OXYGEN EFFECT AT PROTEIN RADIOLYSIS

Primarily, the presence of molecular oxygen in the protein solution is observed at the initial stages of macroradical formation. Under these radiation conditions, even in air, hydrated electrons are generally captured by molecular oxygen:

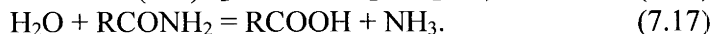
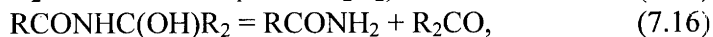
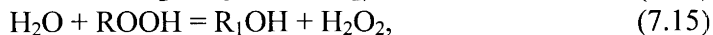
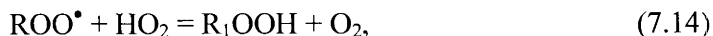


because oxygen concentration in the solution saturated with the air equal 3×10^{-4} mol/l, and its reactivity in relation to \bar{e}_{hydr} is high: $k = 2 \times 10^{10}$ l/mol·s. Thus, in the presence of oxygen in protein solutions in the concentration range between 5×10^{-5} – 5×10^{-4} mol/l the yield of primary anion-radicals is completely suppressed. This means “elimination” of macroradicals formed by the “channel” of participation in reactions of reduction component of radiolysis from all conversion stages of the protein degradation mechanism.

In the presence of molecular oxygen the mechanism of conversion of macroradicals synthesized by $\cdot\text{OH}$ interaction with protein molecules is also changed. For example, C radicals of the polypeptide chain react with O_2 forming peroxide radicals at irradiation of both dry protein preparations and its frozen-up aqueous solutions [49]:



Investigations performed on peptides [59, 60] allowed for a conclusion about proceeding of the following radical conversions in aqueous solutions containing oxygen:



Ammonia formation at irradiation of aqueous protein solutions in the presence of O_2 (deamination process) is one of the main processes of radiolytic degradation of said protein. In high concentration protein solutions, the yield of NH_3 reaches $G(\text{NH}_3) \sim 4$, which by the order of magnitude corresponds to complete consumption of oxidative products of water radiolysis [16].

Protein hydroperoxides represent unstable radiolysis products transforming due to various mechanisms. For example, as observed for peptide radiolysis, hydroperoxides having peroxide group at C atom are transformed as follows:



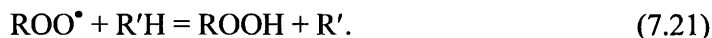
This process representing decarboxylation is one of the main processes of radiolytic conversion of polypeptides. The product formed by the reaction (7.18) is hydrolytically decomposed by peptide bond. As a consequence, amide and carboxylic groups are formed:



Beside the above-considered sequence of peroxide radical conversion, the reaction of their disproportionation termination is possible [60]:



The conversion of primary macroradicals in irradiated dry protein preparations proceeds in the presence of oxygen in accordance with the chain oxidation scheme [61] consisting of reactions (7.13) and (7.21):



Hence, hydroperoxides formed degrade to radicals and, therefore, initiating chain branching at room temperature:



Also, similar processes proceed in lyophilizates of irradiated protein solutions. These processes reason the protein oxidation degradation, observed in the post-radiation period of protein oxidative degradation in lyophilizates, irradiated in the presence of O_2 in ovum albumin solutions, also stored in the presence of O_2 at room temperature [62]. It is worthy of note that injection of a substance – free radical acceptor, into the solution of irradiated biopolymer significantly decreases the oxidation degradation yield of this biopolymer. As follows from the literature [63], the processes of oxidative degradation of polymers in lyophilizates of irradiated solutions proceeding in the presence of oxygen in the post-radiation period are typical of not only proteins, but also polysaccharides and, obviously, all systems, in which peroxides may be formed.

7.4. REACTIONS OF WATER RADICALS WITH SIDE BRANCHES OF POLYPEPTIDE CHAIN

According to reactivity of amino acids in relation to water radiolysis products, double bonds, aromatic groups of atoms and fragments with sulfur atoms possess increased reactivity, and namely these functional groups, being the sites for $\bullet\text{OH}$ and \bar{e}_{hydr} attacks, define radiolytic properties of any amino acid in the composition of the protein macromolecule [64, 65]. ESR spectra, recorded in the irradiated aqueous frozen-up protein solutions, demonstrated the above-mentioned types of primary macroradicals [5]. After heating the sample up, the chromatography method allowed for determining a change of amino acid residues in the protein composition, in which free valence is localized in accordance to ESR data, namely: phenylalanine, tyrosine, lysine, methionine, arginine, etc. [29].

Let us list the basic types of water radical reactions with amino acid residue fragments in the protein composition. They are:

for $\bullet\text{OH}$ radicals and hydrogen

- a) addition by double bonds ($\text{C}=\text{C}$, $\text{C}=\text{N}$) to aromatic cycles;
- b) H detachment at $\text{H}-\text{C}_\alpha$ bond attack with H_2O and H_2 formation;

Note that hydrogen reactivity is by an order of magnitude lower than $\bullet\text{OH}$ reactivity;

for \bar{e}_{hydr}

- a) addition by double bonds;
- b) addition to aromatic rings;
- c) capture by positively charged groups and groups having sulfur atoms.

The yield of the above-mentioned radical formation and conversion in branches depends on the protein amino acid composition, namely, the number of functional groups, attacked by water radicals, their location in the molecule (on the surface or inside the globule), and even on the origin of amino acid residues neighboring the one attacked by water radicals [18, 66 – 69].

The investigation results of radiation degradation of aromatic amino acid residues, obtained at irradiation of proteins in case of injecting various radicals from water (with respect to the origin of gas saturating the solution) allows for obtaining data on the directions of primary macroradicals. For example, in accordance with [33], as transiting from O_2 -saturated to N_2O -saturated irradiated collagen solutions, the yield of degraded tyrosine decreases from 0.17 to 0 that, of course, does not mean termination of tyrosine degradation. The analogous tendency is observed for HSA solution irradiation [37]. Under current conditions of collagen irradiation (at \bar{e}_{hydr} conversion to $\bullet\text{OH}$ in N_2O -saturated solutions) tyrosine subsidence is compensated by its accumulation in the process of phenylalanine by $\bullet\text{OH}$ radicals (via the stage of Phen adducts, $\bullet\text{OH}$ radical formation). The radiation-chemical yield of Phen degradation changes inconsiderably, but its values equal 0.38 and 0.52 indicate that tyrosine formation from Phen is not the single process of radiolytic modification of phenylalanine.

In the case histone solution irradiation at 77 K (reagents \bar{e} and H), phenylalanine concentration increases at the background of Tyr degradation, i.e. Tyr is reduced to Phen [29] and alanine concentration increases simultaneously.

Summing up all these data on the conversions of aromatic amino acid residues, a conclusion can be made that at Tyr interaction with H and \bar{e} ($+H^+$) H-adducts are formed – the radicals which conversions induce Tyr reduction to Phen and C1–C bond break with formation of alanine and phenol derivatives, similar to the case of phenylalanine and tyrosine solution irradiation [70].

On directional energy transfer in irradiated protein solutions and the role of structured water

The analysis of data on decomposition of amino acids in the composition of proteins at the liquid-phase irradiation indicates clear discrepancy between their damage degrees to the sequences of reactivities in relation radical products of water radiolysis: \bar{e}_{hydr} , $\cdot\text{OH}$ and $\text{H}\cdot$ [18, 33, 64 – 69]. In relation to \bar{e} and $\text{H}\cdot$, similar situation is observed for frozen-up solutions and dry preparations [29, 71]. One of the reasons for this discrepancy is location of amino acid residues in protein molecules and, therefore, the influence of neighbor amino acids on the conversion of primarily damaged one [18]. Another more important reason is impropriety of such estimation, because radiolysis processes proceeding in different systems are compared. For example, in one of these systems (diluted solutions of amino acids) \bar{e}_{hydr} is the reagent, whereas according to [15, 47] in another system representing essentially concentrated protein solution (basing on the sizes of macromolecules and globules formed by them, and the track spurs) pre-localized (mobile, dry) electron should play this role. Therefore, it would be more correct to compare damaging of amino acid residues in proteins with the reactivity of amino acids at irradiation of their highly concentrated solutions.

The low-temperature irradiation of frozen-up aqueous solutions and dry preparations of proteins gives an opportunity to register participation of electron (currently dry) under these conditions in reactions with various amino acid residues immediately by typical ESR spectra of the primary macroradicals – electron and H adducts (after anion-radical protonation). The fractional yields of primary macroradicals, calculated by these specific ESR spectra, allows for considering the damaging degree of one or another amino acid

residues in the protein composition reliable to a higher extent compared with the accumulation of final molecular products, because we are speaking about direct changes in accumulation of the primary radiolysis products, which are macroradicals, and no neighboring amino acids participate in the reactions. The data on ESR measurements, performed at irradiation of 10% gelatin and total histone thymus solutions, and dry wool keratin preparations [16, 21, 27], considerably different in the amino acid composition, performed at 77 K. Primary macroradicals were identified: R_{ps} (the radical with unpaired electron localized on the carbogroup peptide bond); R_{lys} (formed at electron attack on protonated NH_2 and NH groups of lysine and arginine); R_{ar} (protonated electron adducts of aromatic rings); R_{SS} ("cystine"). The fractional yields of these radicals and the relative damage level of the fragments were also determined (Tables 7.2 and 7.3). Comparing these data, note that sequence of fragments damaged by mobile electron is the same for all proteins:

$S-S > \text{peptide bonds} > \text{lysine} > \text{aromatic rings}.$

Hence, note also that each protein possesses self scale of relative damage degree of the mentioned fragments. It is worthy of note that in this sequence aromatic amino acids were ranked at the last place, whereas reactivity of the peptide bond carbogroup is higher than for positively charged amino and imino groups (lysine and arginine). Actually, the determined damaging hierarchy of amino acids is different from that determined by the individual reactivity of amino acids in relation to \bar{e}_{hydr} . One may suggest that the sequence of yields of amino acid radicals reflects just a contribution of molar content of corresponding amino acid residues (shown in brackets in Table 7.3). However, taking the peptide bond damaging in each protein for the unit, because the amount of these units in any protein is the highest, we get that the relative damage of lysine (and arginine) in gelatin composition is twice higher than in frozen-up histone solution. Meanwhile, molar content of these amino in gelatin is twice lower.

Table 7.3

The fractional yield of primary radicals (in %) in proteins at 77 K and relative damaging degree by electron of the main fragments at $G(R_{ap}) = 1$; shown in brackets are concentrations of fragments according to [71]

Irradiated system	G_R	Fractional yield of radicals, concentration of fragments, %					Fragment damaging degree			
		R_{ps}	R_{lys}	R_{ar}	R_{SS}	\bar{e}_{st}	S-S	Peptide bond	Lysine	Aromatic rings
Gelatin, 10% solution	3.1 ± 0.6	40 (100)	30 (13)	15 (2.5)	0	15	–	4	3	1
Thymus histone, 10% solution	0.5	65 (100)	27.5 (22.5)	7.5 (4.4)	0	0	–	9	4	1
Wool keratin	1.2 ± 0.1	25 (100)	> 10 (10)	7 (7)	40 (10)	0	4	3	1	1

These data allowed for a conclusion that the damaging degree of an amino acid residue, obtained at irradiation of frozen-up protein solution, mainly depends on the fact how homogeneous is the system formed by functional groups of amino acid residues with the solvent molecules e.g. how uniform their pseudo-microphase is and, therefore, how freely water radiolysis products access them. The conclusion is analogous to the case of liquid-phase irradiation of proteins [18].

The data under consideration indicate preferential damaging of amino acid residues, which form the uniform microphase with water molecules and hydrate layers in native proteins, induced by water radiolysis products, structured by biopolymer. NMR measurements of water molecule relaxation parameters have indicated a decrease in the amount of water molecules bound to macromolecules with increasing irradiation dose. Hence, the radiation denaturation of protein happens, completing at the dose about 1 kGy [72, 73]. It may be suggested that this dose level corresponds to complete radiation degradation of water structured by current protein-collagen (degradation of the structural organization of the hydrate protein layer). Taking into account the concentration of collagen solutions and other irradiation conditions (weight content – 0.1%, inert gas saturation, 0.5 mol/l *tert*-butyl alcohol concentration – $\cdot\text{OH}$ acceptor, only electrons are active), one may estimate the quantity of protein-bound water, which gives 15% for dry collagen. The value obtained correlates with the quantity of adsorbed water (total and structured) in collagen fibers, for instance, human tendons. It has been shown [34] that irradiation in low doses (5 – 25 Gy) decreases water concentration in these native preparations by 11% (by 4% for total and by 7% for structured water). Hence, in the case of collagen solutions the radiation-chemical degradation yield of structured water molecules due to \bar{e}_{hydr} participation (in the absence of oxygen) equals $G \sim 1$.

The value obtained correlate satisfactorily with the radiation-chemical yield of primary macroradicals – the electron adducts in irradiated glassy-like, frozen-up aqueous gelatin solutions [10] and denaturation yield (recorded by formation of insoluble fractions) at the liquid-phase irradiation of other proteins [22, 24].

The conversions of primary radicals of amino acid residues are affected by neighbor amino acid residues [18]. Therefore, a damage may migrate by their functional groups. Hence, the sequence of amino acid residue disposition and possible cluster type of interaction of their functional groups (both

hydrophobic and hydrophilic) in the peptide molecule should be taken into account.

All these effects must affect the composition and the ratio between yields of the final molecular products of protein molecule radiolysis and, certainly, define specificity of the radiolysis mechanism of one or another protein.

7.5. RADIOLYSIS FEATURES OF AQUEOUS SOLUTIONS OF PROTEID

Damaging of the active sites of enzymes

The typical feature of enzymes is their activity – the property reflecting the biological essence of these natural polymers and, therefore, the integrity of structure of these molecules. The studies of changes in the enzymatic activity of such proteins, irradiated in aqueous solutions, carried out with respect to the enzyme concentration and the origin of gas, with which the solution is saturated, are of special value, because under typical conditions of radiation-chemical investigations the scientists manage to get data on the effect on both primary structure of biopolymer and its supermolecular structural organization (the secondary, tertiary and quaternary structure of protein). For example, studies of papain aqueous solution radiolysis demonstrated the concentration dependence of the enzymatic activity change in solvents saturated by different gases: inert (nitrogen), nitrous oxide and oxygen (Table 7.4). It has been found that the enzyme activity decreases with papain irradiation. Two types of activity decrease (reversible and irreversible) were recorded. The yield of total activity loss shows low dependence on the origin of gas saturating the solution, to put it differently, on the damaging agent (\bar{e}_{hydr} , H, $\bullet\text{OH}$) reacting with the active site of the enzyme. This indicates that oxidative and reducing radicals react with this enzyme with similar efficiency.

Table 7.4

Radiation-chemical yield of papain activity loss at irradiation in aqueous solutions [74]

Gas saturating solution	Total activity loss	Irreversible activity	Reversible activity
N ₂	5.5 ± 0.5	4.0 ± 0.4	1.5 ± 0.9
O ₂	5.8 ± 0.2	3.0 ± 0.3	2.8 ± 0.5
N ₂ O	5.5 ± 0.5	1.8 ± 0.2	3.7 ± 0.7

The observed effect of reversible activity loss by the enzyme is induced by oxidation of sulfur-containing groups of cysteine residues. Papain radiolysis, the enzyme which active site includes a residue of cysteine, may be considered as a example of directional transfer of absorbed energy to this active site in the protein molecule. In this case, the effect of directional damage is coordinated with the ideas that the place of the primary localization of this damage in the protein molecule is determined, firstly, by high reactivity of sulfhydryl group in relation to both $\cdot\text{OH}$ and \bar{e}_{hydr} and, secondly, by obvious absence of steric hindrances at these particles access to the active site of the enzyme.

Radiolysis of hemoglobin aqueous solutions

The studies of low-temperature (77 K) radiolysis of 20% oxyhemoglobin (HbO₂) and methemoglobin (Hb⁺⁺) solutions indicated a remarkable feature of radiolytic behavior proteins containing heme. The latter in the composition of prosthetic groups of proteins demonstrate highly effective acceptor properties in relation to mobile electrons formed at low-temperature irradiation of aqueous solutions [75 – 77]. Analogous conclusion was made about acceptor properties of porphyrinic rings as the entire system to electron [78], where radiolysis of water-alcohol compared with concentrated solutions of some porphyrins and metalloporphyrins were studied. It has been found that the interaction between electron and metalloporphyrins reduces central Co(III) and Mn(III) ions, and the electron transfer rate depends on the origin of metal and porphyrin-ligand.

For HbO solution, it has been found that the electron entrapped by heme transits to the center of the porphyrin ring and, finally, is localized on distal hystidine forming an electron adduct on its imidazole cycle [77]. At

thermal annealing of HbO solutions in the temperature range of 77 – 105 K, these anion-radicals react with O₂, located in heme at Fe²⁺. Hence, peroxide radicals are formed.

Thus, in this system the reduction component of water radiolysis (electron) initiates proceeding of oxidative processes of macroradical conversion in the protein globule.

The considered examples of directional transfer of energy, absorbed by the solution (via water radical participation in the reactions), to definite protein fragments and further migration of a damage by macromolecule from primary to final localization place should be added by the data on serum albumin radiolysis in aqueous solutions [18, 67 – 69]. In the composition of albumin globules, three types of bonds (functional groups) differently accessible for attack by water radiolysis products and stabilizing albumins' structure were found. For example, in the case of HSA, tyrosine residues located on the globule surface and enclosing α -spiral-shaped areas are initially damaged [69]; water radicals (mostly $\cdot\text{OH}$) induce denaturation of bovine serum albumin macromolecules, hydrophilic areas of the polypeptide chain untwist, and albumin globule degrades [69].

7.6. CONCLUSION

The analysis of data from the literature on the radiolysis of aqueous solutions of proteins, obtained in recent 12 – 15 years, indicated some regularities specific for these systems. Essentially, in this Chapter we discussed only one of the questions among the problems of protein molecule radiolysis – the predominant role of free radicals in the radiation damaging of protein and their predominant role in this process. All radiolytic effects discussed may be interpreted as a result of macroradical conversions. Main ways of their conversions, sometimes down to formation of final products of protein radiolysis and manifestations of the final radiation effects for proteins were determined. These processes are:

- a) deamination of two types: lysine and arginine amino group detachment and amide groups at peptide bond break (“amide” ammonia releases);
- b) the formation of breaks in polypeptide chain: at attack of carbogroups of peptide bonds by mobile electrons (in dry proteins and frozen-up

- solutions) and \bar{e}_{hydr} , C–H bonds by $\cdot\text{OH}$ and $\text{H}\cdot$ radicals (H detachment reactions), at \bar{e}_{hydr} attack on disulfide bonds (S–S bond break);
- c) the change in macromolecule conformation at \bar{e}_{hydr} attack on peptide bond carbogroups in proline residues;
 - d) crosslink (additional covalent bonds) formation: as a result of macroradical recombination with localization of unpaired electron in polypeptide chain branches with the type C_α radicals of the proline unit, etc., at the interaction of sulfhydryl and amino groups in branches with dehydroalanine double bonds in the polypeptide chain, formed at irradiation;
 - e) the increase of hydrophobic group concentration in proteins – at degradation and detachment of polar groups of Lys, Arg and Asp residues.

A possibility of realization of two protective mechanisms of substances-radioprotectors possessing antiradical activity has been determined, namely: the competition for water radicals and inhibition of free-radical reactions. In this relation, let us note that oxidative degradation of proteins (and other biopolymers) lasts in the post-irradiation period in both solutions and their lyophilizates, irradiated and stored in the presence of oxygen (in air). The yield of these processes is significantly suppressed, if prior to irradiation any compounds – radical acceptors were added to solutions of biopolymers. These are the systems, in which both protective mechanisms are implemented.

Beside these more or less resolved questions, this Chapter touches upon such problem ones as, for example, the role of protein-structured water and its radiolysis:

- a) at primary stages of the protein radiation damage;
- b) in conversions occurring at irradiation of macroradicals.

One may suggest that in the closest period, beside the questions of maximal protection of irradiated proteins – the systems repairing radiation damages in the cell, the study of oligopeptide radiolysis mechanisms in the composition of lymphocyte receptors (responsible for immune functions of the organism), these investigation directions will be urgent for investigators.

REFERENCES

1. Filippovich Yu.B., *Biochemistry Foundations*, Moscow, Vysshaya Shkola, 1985, 504 p. (Rus)
2. *Radiation Chemistry of Major Food Components*, Eds. P.S. Elias and A.E. Cohen, Amsterdam, Elsevier Sci. Publ. Co., 1977.
3. Kayushkin L.P., Pulatova M.K., and Krivenko V.G., *Free Radicals and Their Conversions in Irradiated Proteins*, Moscow, Atomizdat, 1976, 272 p. (Rus)
4. Pulatova M.K., Rikhireva G.T., and Kuropteva Z.V., *Electron Spin Resonance in Molecular Radiobiology*, Moscow, Energoatomizdat, 1989, 232 p. (Rus)
5. Sharpatyi V.A., *Radiation Chemistry of Biopolymers*, Moscow, Energoizdat, 1981, 168 p. (Rus)
6. Il'yasova V.B., "Photosensitized formation of free radicals in amino acids and peptides", *Candidate Dissertation Thesis*, IBPh AS USSR, 1970. (Rus)
7. Stein G. and Tomkiewicz M., *Radiat. Res.*, 1970, vol. **43**(1), p. 25.
8. Gordy W., Ard W.B., and Shields H., *Proc. Nat. Acad. Sci. USA*, 1955, vol. **41**, p. 983.
9. Blyumenfeld L.A., Voevodsky V.V., and Semenov A.G., *The Application of Electron Spin Resonance in Chemistry*, Novosibirsk, Izd. SO AN SSSR, 1962, 187 p. (Rus)
10. Svanidze E.O., "The features of free radical conversion at radiolysis of frozen-up gelatin solutions", *Candidate Dissertation Thesis*, Moscow, ICP RAS, 1992, 189 p. (Rus)
11. Sharpatyi V.A., Aptekar' E.L., Zakatova N.V., and Pravednikov A.N., *Doklady AN SSSR*, 1964, vol. **155**(6), p. 626. (Rus)
12. Sharpatyi V.A. and Pravednikov A.N., *J. Polymer Sci. – C*, 1967, No. 16, p. 1599.
13. Bugaenko L.T. and Byakov V.M., *Doklady AN SSSR*, 1964, vol. **158**(1), p. 186. (Rus)
14. Pikaev A.K. and Kabakchi S.A., *Reactivity of Primary Products of Water Radiolysis*, Reference Book, Moscow, Energoatomizdat, 1982, 200 p. (Rus)
15. Byakov V.M. and Nichiporov F.G., *Intratrack Chemical Processes*, Moscow, Energoatomizdat, 1985, 152 p. (Rus)

16. Sharpatyi V.A. and Zakatova N.V., *Radiobiologia*, 1981, vol. **21**(1), p. 45. (Rus)
17. Sharpatyi V.A., *Khimia Vysokikh Energyi*, 1993, vol. **27**(1), p. 93. (Rus)
18. Vysotskaya N.A. and Rusakovskiy V.M., *Khimia Vysokikh Energyi*, 1991, vol. **25**(1), p. 32. (Rus)
19. Sharpatyi V.A. and Zakatova N.V., *Radiobiologia*, 1982, vol. **22**(5), p. 588. (Rus)
20. Sharpatyi V.A., *Proc. 5 Symp. Radiat. Chem.*, Budapest, 1982, p. 1021.
21. Zakatova, Svanidze E.O., and Sharpatyi V.A., *Radiobiologia*, 1983, vol. **23**(2), p. 227. (Rus)
22. Allen A.O., *Radiation Chemistry of Water and Water Solutions*, Ed. P.I. Dolin, Moscow, Gosatomizdat, 1963, 204 p. (Rus)
23. Henriksen Th., Sanner T., and Pihl A., *Radiat. Res.*, No. 2. P. 147.
24. Amiragova M.I., Duzhenkova N.A., Krushinskaya N.P., Mochalina A.S., Savich A.V., and Shal'nov M.I., *Primary Radiobiological Processes*, Moscow, Atomizdat, 1973, 336 p. (Rus)
25. Sapezhinsky I.I., *Biopolymers: Kinetics of Radiation and Photochemical Conversions*, Moscow, Nauka, 1988, 216 p. (Rus)
26. Milinchuk V.K., Klinshpont E.R., and Pshezhetsky S.Ya., *Macroradicals*, Moscow, Khimia, 1980, 264 p. (Rus)
27. Baeva N.N., Sadova S.F., and Sharpatyi V.A., *Khimia Vysokikh Energyi*, 1991, vol. **25**(4), p. 350. (Rus)
28. Sadova S.F., "Theoretical justification and development of wool material modification methods for the purpose of improving custom properties", *Doctor Dissertation Thesis*, Moscow, Textile Academy, 1991, 436 p. (Rus)
29. Zakatova N.V., Abramovich A.B., and Sharpatyi V.A., *Radiobiologia*, 1980, vol. **20**(6), p. 815. (Rus)
30. Labout J.J.M., *Int. J. Radiat. Biol.*, 1972, vol. **21**(5), p. 483.
31. Boguta G. and Danczewicz A.M., *Ibid*, 1983, vol. **43**(3), p. 249.
32. Lien Ye.-H., Stern R., Fu J.C.C., and Siegel R.C., *Science*, 1984, vol. **225**(4669), p. 1484.
33. Duzhenkova N.A. and Savich A.V., *Radiobiologia*, 1986, vol. **26**(5), p. 604. (Rus)
34. Nikolaeva S.S., Kondakova N.V., and Khoroshov Yu.A., *Radiobiologia*, 1988, vol. **28**(4), p. 483. (Rus)

35. Khenokh M.A. and Lapinskaya E.M., *Doklady AN SSSR*, 1955, vol. **102**(5), p. 993. (Rus)
36. Kondakova N.V., Ripa N.V., Kuznetsova N.V., and Amiragova M.I., *Khimia Vysokikh Energiy*, 1994, vol. **28**(6), p. 497. (Rus)
37. Kondakova N.V., Sakharova V.V., and Ripa N.V., *Radiobiologia*, 1988, vol. **28**(6), p. 748. (Rus)
38. Zakrzewski K., Klocenzak M., and Hay M., *Radiat. Res.*, 1973, vol. **53**(1), p. 124.
39. Schnessler H. and Schilling K., *Int. J. Radiat. Biol.*, 1984, vol. **45**(3), p. 267.
40. Zakatova N.V. and Sharpatyi V.A., *Radiobiologia*, 1984, vol. **24**(4), p. 499. (Rus)
41. Nasirov N.G., Sukhorukov B.I., Shabarchina L.I., and Petrov A.I., *Molekulyarnaya Biologia*, 1991, vol. **25**(4), p. 1024. (Rus)
42. Sharpatyi V.A., *Radiobiologia*, 1992, vol. **32**(2), p. 180. (Rus)
43. Teoule R., *Int. J. Radiat. Biol.*, 1987, vol. **51**(4), p. 573.
44. Kharchenko L.I. and Pavlovskaya T.E., *Radiobiologia*, 1973, vol. **13**(5), p. 669. (Rus)
45. Majewska M.R. and Danczewicz A.M., *Studia Biophysica*, Berlin, 1977, Bd. **63**(3), S. 189.
46. Duzhenkova N.A. and Klimova T.P., *Radiobiologia*, 1987, vol. **27**(5), p. 594. (Rus)
47. Bugaenko L.T., Byakov V.M., and Kabakchi S.A., *Khimia Vysokikh Energiy*, 1985, vol. **19**(4), p. 291. (Rus)
48. Devkin V.I. and Mikhailov A.I., *Biofizika*, 1978, vol. **23**(5), p. 775. (Rus)
49. Sharpatyi V.A., *Studia Biophysica*, Berlin, 1968, Bd. **8**(3), S. 187.
50. Barkalov I.M., Bol'shakov A.I., Gol'dansky V.I., and Krupyansky Yu.F., *Doklady RAN*, 1992, vol. **326**(6), p. 1083. (Rus)
51. Parsonidge N. And Savely L., *Dislocation in Crystals*, Ed. G.N. Zhizhin, Moscow, Mir, 1982, p. 436. (Rus)
52. Butlers P.I., *Mechanics of Composite Materials*, Riga, 1985, No. 6, p. 1124. (Rus)
53. Lazarev Yu.A., Grishnovsky B.A., Lobachev V.M., Pisarenko A.I., Khromova T.B., and Turkina T.V., *Molecular and Cellular Biophysics*, Moscow, Nauka, 1977, p. 73. (Rus)
54. L'vov K.M. and Iskakov A.A., *Biofizika*, 1993, vol. **38**(1), p. 7. (Rus)

55. Charlseby A., *Nuclear Radiation and Polymers*, Eds. Yu.S. Lazurkina and V.L. Karpova, Moscow, Izd. Inostr. Lit., 1962, 522 p. (Rus)
56. Ivanov V.S., *Radiation Chemistry of Polymers*, Leningrad, Khimia, 1988, 320 p. (Rus)
57. Emanuel N.M., "The role of free radicals in radiobiological processes", *Trudy MIOP*, vol. 7, Izd. AN SSSR, 1963, p. 63. (Rus)
58. Pikaev A.K., *Modern Radiation Chemistry. Radiolysis of Gases and Liquids*, vol. 2, Moscow, Nauka, 1986, 440 p. (Rus)
59. Garrisson W.M., *Chem. Rev.*, 1987, vol. 87, p. 381.
60. Sapezhinsky I.I., Silaev Yu.V., and Emanuel N.M., *Doklady AN SSSR*, 1963, vol. 151(3), p. 584. (Rus)
61. Sapezhinsky I.I. and Emanuel N.M., *Doklady AN SSSR*, 1965, vol. 165(4), p. 845. (Rus)
62. Bondarenko N.T. and Sharpatyi V.A., *Thes. Rep. I All-Union Radiobiological Congress*, vol. 1, Pishchino, 1989, p. 18. (Rus)
63. Bondarenko N.T., "Radiation conversions of dextrane", *Candidate Dissertation Thesis*, Moscow, ICP AS USSR, 1990. (Rus)
64. Braams R., *Radiat. Res.*, 1967, vol. 31(1), p. 8.
65. Devies J.V., Ebert M., and Shalek R.Y., *Int. J. Radiat. Biol.*, 1968, vol. 14(1), p. 19.
66. Vysotskaya N.A., Russakovsky V.M., and Kulish L.F., *Khimia Vysokikh Energiy*, 1987, vol. 21(5), p. 441. (Rus)
67. Vysotskaya N.A. and Russakovsky V.M., *Khimia Vysokikh Energiy*, 1989, vol. 23(3), p. 284. (Rus)
68. Vysotskaya N.A., Russakovsky V.M., and Kulish L.F., *Khimia Vysokikh Energiy*, 1989, vol. 23(4), p. 317. (Rus)
69. Vysotskaya N.A. and Russakovsky V.M., *Khimia Vysokikh Energiy*, 1989, vol. 23(6), p. 503. (Rus)
70. Brodskaya G.A., "Radiolysis of phenylalanine and tyrosine aqueous solutions", *Candidate Dissertation Thesis*, Tashkent, TGU, 1967, 151 p. (Rus)
71. Svanidze E.O. and Sharpatyi V.A., *Khimia Vysokikh Energiy*, 1992, vol. 26(6), p. 552. (Rus)
72. Babushkina T.A., Duzhenkova N.A., and Kaunov A.V., *Thes. Rep. VII All-Union Conference "Magnetic Resonance in Biology and Medicine"*, Chernogolovka, OICP AS USSR, 1989, p. 237. (Rus)

73. Babushkina T.A., Vasil'ev A.M., and Duzhenkova N.A., *Thes. Rep. VIII All-Union Conference "Magnetic Resonance in Biology and Medicine"*, Chernogolovka, OICP AS USSR, 1990, p. 46. (Rus)
74. Lynn K.R. and Louis D., *Int. J. Radiat. Biol.*, 1973, vol. **23**(5), p. 477.
75. Myshkin A.E. and Sharpatyi V.A., *Biofizika*, 1986, vol. **31**(4), p. 592. (Rus)
76. Myshkin A.E. and Sharpatyi V.A., *Biofizika*, 1986, vol. **31**(5), p. 752. (Rus)
77. Myshkin A.E. and Sharpatyi V.A., *Zh. Fiz. Khim.*, 1989, vol. **63**(4), p. 1030. (Rus)
78. Kovalenko N.I., Vrublevsky A.I., and Petryaev E.P., *Thes. Rep. II All-Union Conference on Theoretical and Applied Radiation Chemistry*, Moscow, NIITEKhim, 1990, p. 137. (Rus)

Chapter 8. Radiation chemistry of polysaccharides

Carbohydrates represent one of the classes of compounds composing cell structures and manifesting its viability. Plant tissues contain about 80% carbohydrates, whereas in animals this level does not exceed 2%. As fragments in the composition of nucleic acids and glycoproteids, carbohydrates represent the main “construction material” for these natural complexes, which are responsible for hereditary characters and immune functions in the organism affected by ionizing radiation. Hence, the study of the radiation degradation in such systems is induced by the purposes of their radioprotection. At preserving foods by radiation treatment (corn, flour, vegetables and fruits), control for concentration of toxic products of carbohydrate radiolysis in vegetables grown on radionuclide-contaminated soils, it is urgent for investigators to determine the origin of these toxicants and decrease their concentration in products to innocent for consumption.

The radiation processing of polysaccharide-containing agricultural and food industry wastes to the mass digestible by bacteria and animals determines the ways of increasing the yield of radiation-chemical processes. The fourth, medical, aspect of the problem is related to the application of radiation-modified natural and biologically synthesized polysaccharides as blood plasma substituents in medical practice. This supplies the deficiency in donor blood, reduces danger of possible introduction of viral or any other infection to recipients. Moreover, under emergency conditions, biological compatibility with the human organism gives an opportunity to render timely aid to victims with no respect to their blood type. Hence, such problems as radiation sterilization of medical forms of preparations and the storage time (reduction of possible post-irradiation degradation) should also be solved.

Thus, for reaching the target effect, the knowledge of the mechanisms of radiation degradation of polysaccharide (carbohydrate) containing systems defines the possibilities to control these processes [1].

Note that the investigations in the field of radiation chemistry of polysaccharides, carried out in Russia by the followers of Academicians N.N. Semenov, N.M. Emanuel and N.K. Kochetkov, formed grounds for the complex approach to solving the mentioned questions. It has been found that in irradiated polysaccharide-containing systems the main role in degradation of carbohydrates is devoted to free radicals: the yield of final molecular products

of radiolysis is comparable with the yield of radicals, generated by ionizing radiation [2 – 5].

8.1. STRUCTURE OF CARBOHYDRATES, POLYSACCHARIDES

Carbohydrates are compounds containing hydroxyl groups and carbonyl group (aldehyde or ketone) in the molecule structure. According to the presence of aldehyde or ketone group in the structure, carbohydrates (monosaccharides) are subdivided into aldoses and ketoses, which in the individual crystalline state represent cyclic hemiacetals of multiatomic aldehyde- or ketoalcohols, and in solvents are present in the equilibrium noncyclic forms.

Of monosaccharide molecules the presence of several cyclic forms – conformers, is typical. These conformers differ by from one another by location of various parts of the cycle. Contrary to isomerization, at mutual transitions of conformational forms the integrity of bonds between atoms is preserved. By analogy to cyclohexane molecule, conformations of the pyranose ring (the main structural unit of carbohydrates) in the six-membered carbohydrates are divided into C (“chair”) and B (“boat”) types.

Natural polysaccharides are polymers including glucoside (glucopyranose) ring as a monomeric unit, bound by glycoside bonds in positions 1 – 4, 1 – 6, and 1 – 3. In this sequence of monomeric units, in one unit hydrogen atom of hemiacetal hydroxyl is substituted by another monosaccharide residue, which, in turn, has hemiacetal hydroxyl hydrogen atom substituted by the third monosaccharide residue, etc. Firstly, various sorts of cellulose and starches, dextrans and other polysaccharides differ from one another by the ratio of glycoside bond types, branching degrees of macromolecules and, therefore, spatial structure.

Table 8.1 shows characteristics and properties of some natural polysaccharides (glucose superpolymers) having identical composition (monomeric unit is α -glucopyranose residue) differing by spatial location of monomeric units, the number of intramolecular and intermolecular hydrogen bonds – various starches, cellulose and dextrane, the latter produced by *Leuconostoc mesenteroides* bacteria. Clearly, the basic macromolecular properties of these natural polysaccharides are mostly defined by the ratio of

Table 8.1

Characteristics of some natural polysaccharides [3]

Polysaccharide	Structure		Macromolecular composition, %		Fraction molecular weight, dalton	Humidity, %
	Type of granules	Max particle size, μm	Amylopectine α -1,6-, α -1,4-	Amylose α -1,4-		
Corn (maize) starch	Laminar granules various shapes	25	77	23	32,000 – 160,000 (amylase) 250,000 – 500,000 (amylopectine)	13
Potato starch	Lens-shaped laminar granules	100	77	23	32,000 – 160,000 (amylase) 250,000 – 500,000 (amylopectine)	12
Waxy corn starch	Laminar-uniform granules	25	96	4	250,000 – 500,000	12
Amylopectin starch	Loose granules	> 100	96	4	>2,000,000	11
Dextrane	Torus-shaped granules	10	98 (α -1,6-)	2 (α -1,3-, α -1,4-)	250,000,000	11
Cotton cellulose	Micro fibrils			98.5 α -(β -1,4-)	200,000	4

quantities of various types of glycoside bonds in the volume and polymer chain branching (refer to various starches). Potato starch granules include branched amylopectin starch with α -1,4-glycoside bond (with “crystalline” zones sized 60 Å and less regulated, with abundant branching points) and linear polysaccharide amylose manifesting intense intra- and intermolecular interactions. The crystallinity index is 0.2 for potato starch and 0.7 – 0.8 for cellulose.

In native starch, linear amylose exists in two crystalline shapes: B-shape (hexagonal lattice: $a = b = 18.5$ Å, $c = 10.4$ Å) and A-shape (orthorhombic lattice: $a = 11.9$ Å, $b = 17.7$ Å, $c = 10.52$ Å; $\gamma = 120^\circ$). Both these conformations represent two-strand dextrorotatory spirals with 21 Å (6 glucose residues) with antiparallel packing of two strands in the crystalline cell. In the B-conformation, there is a hexagon-regulated channel, filled with water molecules. The elementary cell of B conformation contains 36 – 40 water molecules, a half of which is linked by hydrogen bonds to starch macromolecules, the rest of them are bound to one another. The A conformation cell contains 9 – 10 water molecules. The following transition was observed experimentally:



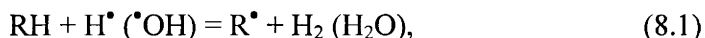
This dehydration of the crystalline structure happens at long-term thermal effect and simultaneous mechanical compression, elongation and shear stresses [6].

The radiation impact induces order degradation in granules – the process called homogenization or decrystallization of the sample, and decreasing “sensitivity” to water absorption [7]. The mechanical impact induces dehydration of the sample. This is the difference in the effects of mechanical and radiation impact on the sample of native potato starch.

In dextrane, monomeric units are bound by α -1,6- bond, and branching points are mostly located at C3 atoms. This polymer has no crystalline phase and is represented by irregular coils with high density in the center, abruptly reduced to periphery. Concluding the above-mentioned, it should be emphasized that differences in physical and chemical properties, and biological activity of these biopolymers is defined by both molecular and spatially-structural factors.

8.2. THE ROLE OF $\cdot\text{OH}$ AND ELECTRON IN CARBOHYDRATE DEGRADATION

Primary radiolytic processes proceeding in aqueous solutions of carbohydrates and polysaccharides are the following: formation of radicals in these systems due to C–H bond break at any carbon atom in the composition of oxymethylene unit or glycoside bond (in the case of di-, tri- and polysaccharides) at radical $\cdot\text{OH}$ attack on them. The relative yield of each of these radicals in biopolymer is defined by structural features of the macromolecule fragment. The main difference in radiolysis of aqueous solutions of mono- and disaccharides versus polysaccharides is due to the presence of molecules with open aldo- and keto-groups. As shown by direct ESR methods applied to investigations at radiolysis of aqueous frozen-up solutions of carbohydrates and polysaccharides, the reactions with dissolved substances mostly involve $\cdot\text{OH}$ (H_2O^+) and $\text{H}\cdot$ radicals [2 – 5, 8 – 10]:



where $\text{R}\cdot$ is radical formed by hydrogen detachment from any other oxymethylene unit in the monomeric cycle. The reaction rate constant for $\cdot\text{OH}$ radicals in aqueous solutions equals $\sim 10^9 \text{ M}^{-1}\text{s}^{-1}$, and for $\text{H}\cdot$ radicals $\sim 10^8 \text{ M}^{-1}\text{s}^{-1}$. The reactivity of \bar{e}_{hydr} particles in relation to carbohydrate molecules (mono- and disaccharides) is by 2 – 2.5 orders of magnitude lower compared with $\text{H}\cdot$ radicals.

Application of low-temperature irradiation technique to these systems allows for studying radiochemical properties of carbohydrates. For example, the study of photoemission of electrons in carbohydrate solutions, irradiated at 77 K, it has been found that \bar{e}_{st} dislodged by visible light from the traps are involved in the reactions with $\cdot\text{OH}$ radical, formed from water and dissolved carbohydrates ($\text{R}\cdot$):



Electron makes no contribution to the process of polysaccharide degradation, if the latter contain no aldehyde, keto- or carboxylic groups, but is

entrapped (stabilized) by carbohydrate molecule hydroxyls. As a result, the lifetime of such particle increases [10, 11], and it becomes able to participate in recombination of primary radicals (type (8.3) reactions). This is the reason that may explain formation of glucose stereoisomers (epimers) by C2 and C4 atoms, which are mannose and galactose, in irradiated glucose superpolymers – starches and cellulose [5]. Moreover, transferring of such “stabilized” electron from, for example, sugar fragment of a macromolecule to another, electrophilic fragment, apparently, to a nitrous base of nucleotide in DNA composition becomes possible [10, 11] (refer to Chapter 10). The radical yield from dissolved sugar increases with the amount of carbohydrates in aqueous (even frozen-up) solution, reaching for the highest concentrated ones the level $G = 4$ radicals/100 eV (Table 8.2).

Table 8.2

Radiation-chemical yield of radicals from glassy-like glucose solutions, irradiated at 77 K [12]

Matrix	Type of radicals	Glucose concentration, M				
		0	0.1	0.3	1	2.5
KOH, 10 M	\bar{e}_{st}	3.4	3.6	3.4	4.2	4.4
	O^-	3.4	2.5	1.8	–	0.7
	H^\bullet	0.1	0.1	0.1	0.03	0.01
	ΣR^\bullet , except for O^-	3.4	3.6	3.6	5.7	7.0
H_3PO_4 , 4.5 M	H^\bullet	0.8	0.7	0.4	0.2	0.1
	$R_{glucose}$	0	–	0.3	1.0	1.6
	ΣR^\bullet , except for H^\bullet	1.9	2.7	2.7	2.7	3.6

In the case of higher diluted solutions of carbohydrates (<1 M), we may also obtain these values $G(\Sigma R)$, if conditions promoting involvement of additional amount of $^\bullet OH$ (H_2O^+) radicals are created. Usually, these radical recombine in pairs, and proceeding of the reverse reactions (8.2) and (8.4):



As carbohydrate solutions irradiated in liquefied nitrogen are heated up (thermal annealing of irradiated samples), stabilized oxidative component of radiolysis, $^\bullet OH$ radical, enters into reactions with dissolved sugars. The yield in these transformations depends on the annealing temperature and carbohydrate

concentration in solutions. From 10% to 30% of $\cdot\text{OH}$ radicals, stabilized at 77 K may participate in reactions with dissolved sugars. Figure 8.1 shows changes in ESR spectrum of irradiated glassy-like glucose phosphate solution and variations in the concentration of radicals, formed from the solvent and glucose (conventional units) according to reaction 8.1 [13].

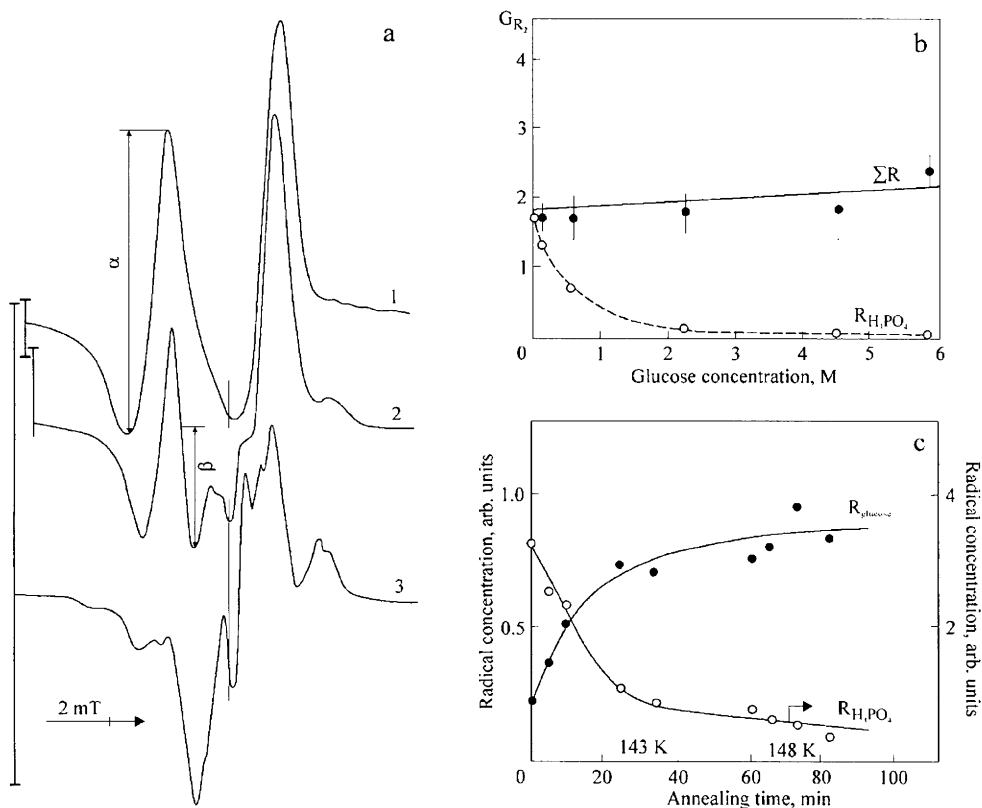


Figure 8.1. ESR spectra of 0.15 M glucose solution and 6 M H_3PO_4 irradiated (30 kGy) at 77 K. After irradiation termination the sample was heated up (a): 1 – 23 min at 98 K; 2 – 13 min at 143 K; 3 – 38 min at 173 K

The dependence of radical yield on glucose concentration in frozen-up phosphate solution (b)

The dependence of variation in radical concentration on the sample temperature (c)

Such antipathetic dependence of changes in concentrations of $\cdot\text{OH}$ radicals and carbohydrate was recorded in the experiment on thermal annealing of wet cellulose preparations, γ -irradiated at 77 K [8].

Contrary to polysaccharides with their monomeric cyclic units, some monosaccharide molecules are linear in the solution, i.e. having open aldehyde and keto-groups. Both aldehyde and keto-groups may capture electron and, thus, form anion-radicals. This type of processes representing formation and transformations of anion-radicals may make a significant contribution into the mechanism of carbohydrate transformation at irradiation of monosaccharides, but not polysaccharides, because in the latter case only the end unit of the macromolecule has open carbonyl (aldehyde or keto-, the so-called reducing, RA – the reducing agent) group.

As compared with total quantity of monomeric units, the contribution of end groups to the total process of radiolytic degradation of the biopolymer molecule is rather low.

In the case of polysaccharide irradiation, the basic radiolytic effects are the following:

- formation of breaks and crosslinks in macromolecules of mono- and disaccharides;
- formation of formation of new reducing and carboxylic groups, deoxy- and deoxyketo-units in the macromolecule composition.

Among the products of polysaccharide and their aqueous solution radiolysis, low-molecular compounds of the monomeric unit degradation were detected: CO , CO_2 , CH_4 , aldehydes, ketones, formic and other carboxylic acids, and alcohols [14]. The values of their radiochemical yields depend on the irradiation conditions (dose, dose rate, the origin of solution saturating gas, the presence of additives – radical acceptors, etc.). The formation of all these products of radiolysis is stipulated by transformation of primary radicals, which are macroradicals.

8.3. THE ORIGIN OF CARBOHYDRATE RADICALS

By type of occurrence in the system under discussion, it is desirable to divide radicals into primary and secondary ones. Primary radicals are formed at

radiolysis of aqueous solutions as a result of interactions between macromolecules and radicals $\bullet\text{OH}$, $\bullet\text{H}$ and \bar{e}_{hydr} , whereas at irradiation of dry polysaccharides due to break of C–H, C–OH and CO–H bonds hydroxyalkyl, alkyl and alkoxy radicals are formed. Total radical yield from polysaccharides equals $G(\text{radicals}) = 3 - 4$. Secondary radicals are mostly those formed at transformation of primary radicals by reactions of dehydration (allyl) and isomerization with C–O and C–C bond break (acyl, alkyl, etc.) [15 – 27] (for their structure and spectral characteristics, refer to materials below).

In polysaccharides, the places for attack by radicals $\bullet\text{OH}$ and $\bullet\text{H}$ may be all C–H bonds in the anhydride carbohydrate ring. Electrons mostly attack carbonyl groups (if they are present in the macromolecule, beside the end ones) with formation of anion-radicals.

In the primary acts of irradiation of dry carbohydrate preparations, the break of C–H, C–OH and CO–H bonds, induced by $\bullet\text{H}$ and $\bullet\text{OH}$ radicals, is confirmed by the structure of radical products, identified by ESR spectra, obtained at irradiation under low or room temperature (Table 8.3), as well as the composition of gas released during irradiation and the value of radiochemical yields of H_2 and H_2O (the products of $\bullet\text{H}$ and $\bullet\text{OH}$ radical interaction with the macromolecules by reaction (8.1)), comparable with the total yield of macroradicals. The latter may be illustrated by the ratio between yields of H_2 , HD and D_2 , recorded at irradiation of deuterated (–OD) glucose and dextrane (Table 8.4).

Comparing spectral data shown in Tables 8.3 and 8.5, identical origin of primary macroradicals formed at irradiation of glucose superpolymers under study, independently of the crystallinity degree (the phase composition) of the sample, which may be 100% amorphous (dextrane) or 70 – 80% crystalline (cellulose), should be noted.

The yield of primary radicals in irradiated polysaccharides depends on the origin of this polymer, more particularly, on the ratio between amorphous and crystalline microregions in the sample, and the content of adsorbed water in the sample, hence, for example, on the sample evacuation conditions (Table 8.6). Contrary to fractional yields, total yield of the radical formation is independent of the sample crystallinity degree.

Table 8.3

ESR spectrum characteristics for radicals, identified in evacuated potato starch preparation, irradiated at 77 K (decoded according to [17])

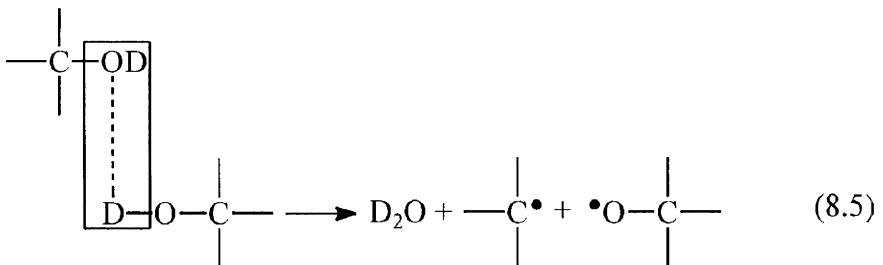
Radicals; apparent localization site for unpaired electron	HFS, g -factor	Band width, ΔH (mT)	Hyperfine interaction (HFI) constant, mT	Temperature range for radical registration, K; reactions, notes
R ₁ (C3, C5)	Triplet 2.003	6.6	3.0	77 – 313; R ₁ → R _A
R ₂ (C5, C2)	Triplet ~2.00	6.3	2.6 – 2.9	77 – 313; R ₂ → R _A
R ₃ (C2, C6)	Triplet border components	4.7	2.2	77 – 337; R ₃ → R _A
R ₄ (C4)	—//—	4.0	—	77 – 337
R ₅ (RO...H)	Doublet	1.5	0.9	77 – 200
R ₆ (C1)	Doublet	2.6	—	77 – 337; R ₆ → RC=O
R _A : -C(=O)-CH-	Doublet 2.0067	1.5	—	[R _A] increase in the range of 223 – 273; from R ₁ , R ₂ , R ₃
R-C=O	Singlet 2.0009	0.4	—	[R _A] increase in the range of 230 – 313; from R ₆
RO	Singlet 2.005	2	—	77 – 337

Table 8.4

The yield (G) of gaseous products of glucose radiolysis and related superpolymers [21]

Product	Nondeuterated glucose	Deuterated (OD) glucose	Poly-glucin	Dex-trane
H ₂	1.7	2.9 (H ₂ – 1.88; HD – 1.00; D ₂ – 0.02)	3	3
H ₂ O	0.15	2.4 (H ₂ O – 0.6; HDO - 1.3; D ₂ O - 0.5)	0.03	0.05
CO	0.05	–	0.5	0.05
CO ₂	0.01	0.1	0.09	
CH ₄	0.003	–	0.002	0.002
CH ₂ O	0.004	–	–	–

One of the main processes in the radiation degradation of polysaccharides is water release (dehydrogenation, see the next section for details). The yield of water increases with the radiation dose. As transiting from low-molecular carbohydrates to polysaccharides, the water yield decreases. As mentioned above, data in Table 8.4 confirm water release in dry carbohydrates mostly happen due to C–OH and C–H bond breaks. It is indicated [32] that water molecules are formed from hydroxyl groups of neighbor monosaccharide units of the polymer, which form the crystalline phase by hydrogen bonds. Using this hypothesis, one may explain a relatively high yield of heavy water (~20%) in γ -irradiated deuterated (–OD) glucose.



The conclusion about polymer crystallinity effect on the ratio of yields of various primary radicals is indirectly confirmed by the fact that the number of disordered (amorphous) microzones in the sample and the yield of alkoxy radicals RO[•] are bound by a proportional dependence. The yield of RO ... HC

Table 8.5

Free radicals formed due to cellulose photodegradation at room temperature, identified by RYDMR (reaction rate or yield detectable magnetic resonance) spectra [29]

Radical	Radical structure	Spectrum width, mT	Hyperfine interaction (HFI)			g-factor	Relative yield, %
			Number of components	Intensity ratio	HFI constant, MHz		
R ₁	C ₁	3	2	1:1	70.1	2.003	5
R ₂	C ₃	6	3	1:2:1	64.1	2.003	10
R ₃	CO	2	1	–	–	2.005	10
R ₄	O:C ₃ –CH–	2	2	1:1	42.1	2.004	15
R ₅	C ₄ H:C ₃ OH	4.5	2	1:1	112.2	2.003	5
R ₆	–C ₅ H–	8.5	5	1:4:6:4:1	56.1	2.003	15
R ₇	HCO	12 – 15*	2	1:1	322.5 – 392.5*	2.003	10
R ₈	RCO	0.4	1	–	–	2.001	2 – 5
RP	R ₃ ... R ₇	17 – 25*	4	1:1:1:1	126.3 – 196.3*	2.003	25
					42.1 – 70.1**		
R ₉	HC' ₄ <	4	3	1:2:1	45	2.003	~3
R ₁₀	C ₍₆₎ H ₂ –	6.7	4	1:3:3:1	64	2.004	~3
R ₁₁	C ₍₅₎ (CH ₃)<	6.6	5	1:4:6:4:1	48	2.003	~3
R ₁₂	CH ₃	7.5	4	1:3:3:1	70	2.003	~3

Notes: * – initial and final HFI values

** – initial and final HFI values for R₇ (in the structure of the radical pair, RP) with hydrogen atom of hydroxyl in the neighboring C₆H₂OH

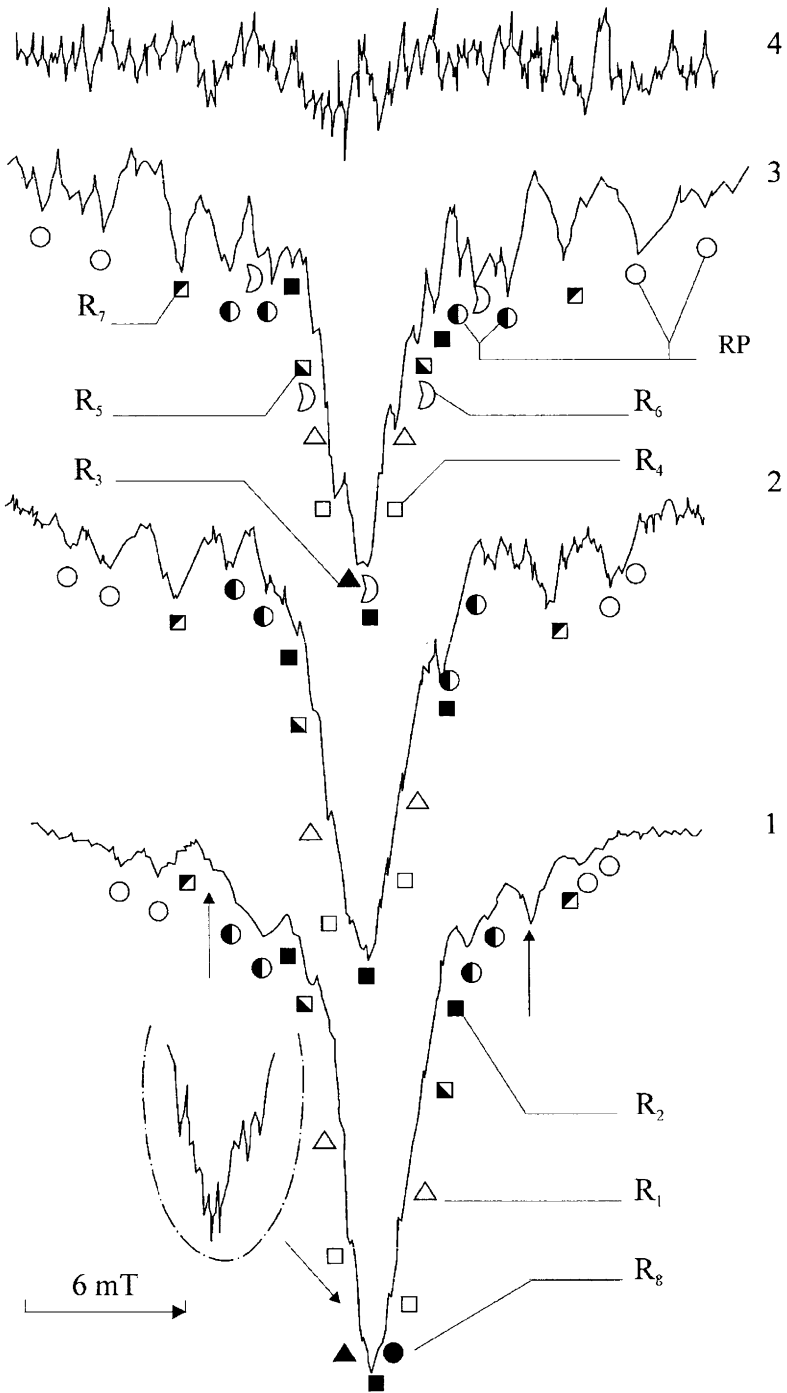


Figure 8.2. RYDMR spectra (1 – 3) typical of initial (1) and subsequent (2, 3) stages of photocatalytic degradation of cellulose containing a sensitizer, obtained at room temperature, at different exposure of the sample to UV-irradiation ($\lambda = 248.3$ nm) of constant intensity; the oval encloses the top of the spectrum 1, registered at lower constant time of recording. Curve 4 was recorded for cellulose sample containing no sensitizer at higher amplification than in cases of spectra 1 – 3

type and alkoxy radicals, bound by hydrogen bond to hydroxyls, becomes relatively high at transition to samples containing higher amount of oriented (crystalline) microzones (Table 8.6).

Table 8.6

Radiation-chemical yield of free radicals in glucose and its superpolymers, irradiated in vacuum [15]

Irradiated preparation	Irradiation temperature	Type of radical	$G(\text{radical})$	$G(\Sigma \text{ radicals})$
Undeuterated and deuterated (OD) glucose	77	RO ... H	~0.5	–
		R	2.5 – 3.0	3.4 – 2.8
	300	R _A	1.0 – 1.5	–
		RO ... H	0.5 – 1.0	3 – 4
Dextrane, polyglucin	77	RO + RO ... H	1	–
		R	2	3
Dextrane	300	R _A	0.5 – 0.7	–
		RO	1.5 – 2.0	2.8

At transition from one type of polysaccharide to another, the value of radiation-chemical yield of molecular hydrogen changes insignificantly (Table 8.7). It is worthy of note that H₂ is mostly formed at C–H and CO–H bond break, and over 60% of molecular hydrogen is released at C–H bond breaks only, whereas the rest 40% - at C–H and CO–H bond breaks. The yield of radicals in the latter process increases with transition from monosaccharide to polymers: $G(\text{RO ... H} + \text{RO})$ varies from 0.5 to 1 (Table 8.5).

8.4. PRIMARY MACRORADICAL TRANSFORMATIONS

The following reaction types are typical of the primary radicals irradiated of glucose superpolymers, occurring due to C–H and C–OH bond breaks: dehydration (β - and α -elimination of H_2O), isomerization with C–C and C–O bond splitting, rearrangement of C–H bonds in anhydroglucose cycle (AGC), and hydrolytic splitting of β -bonds in carbon-centered glycoside radicals (irradiation in the presence of water).

Dehydration of the primary free radicals in carbohydrates is indicated by the experimental results obtained for water-free glucose and superpolymer samples (starches and dextrane), irradiated at room temperature [18]. The same samples were subjected to ESR studies for formation and accumulation of the primary and secondary radicals, and to mass-spectroscopy for the composition of the radiolysis gaseous products. The identical analytical shape of the dose dependencies of secondary allyl radicals and water accumulation was determined [18, 21]. It has been found that after absorption of 30 – 50 kGy dose by the sample, further irradiation causes a sharp increase of water release rate, and bands typical of allyl radicals, centered at $g = 2.007$ (Figure 8.3), begin dominating in ESR spectra [18]. At the background of primary radical bands with uneven number of components, centered at $g = 2.003$, their presence in the total ESR spectrum causes its asymmetry, which increases with the irradiation dose. Analogous changes in the spectra, testifying about occurrence of allyl-type radicals in the sample, are also observed at heating up carbohydrates (starches, in particular), irradiated at low temperature [10].

The ESR spectra of allyl radicals with the mentioned g -factor (for the liquid phase, $g = 2.004$) show a doublet and quadruplet HFS relating to the number of protons in the radical, which interact with unpaired electron [3].

Radicals of the allyl type were also detected at irradiation of multiatomic alcohols, mono-, di- and polysaccharides in the absence of O_2 [33]; at thermal annealing of “dry” sodium alginate [19] and cellulose [20] preparations, irradiated at 77 K.

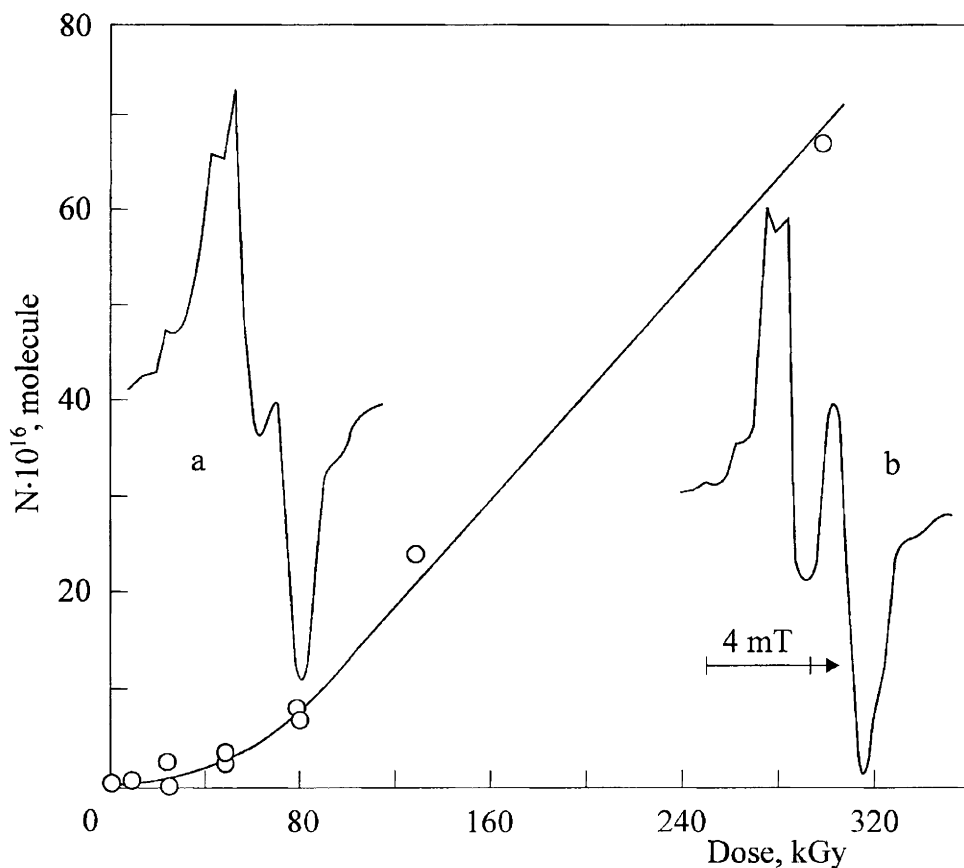


Figure 8.3. Accumulation of water, released at radiolysis of glucose preparations; ESR spectra for glucose irradiated by 35 (a) and 300 kGy (b) doses ($T = 300$ K)

The mechanism of carbohydrate primary radical dehydration is disclosed at the analysis of the investigation results of isotope composition of water molecules (light, heavy and mixed), dose dependencies of their accumulation and the values of the radiation-chemical yield at radiolysis of deuterated glucose samples, in which H atoms were substituted by deuterium in hydroxyls only (Table 8.4) [18]. The noteworthy feature of deuterated glucose radiolysis at room temperature is the difference in dose dependencies of accumulation of three types of water molecules: mixed water (HDO) shows

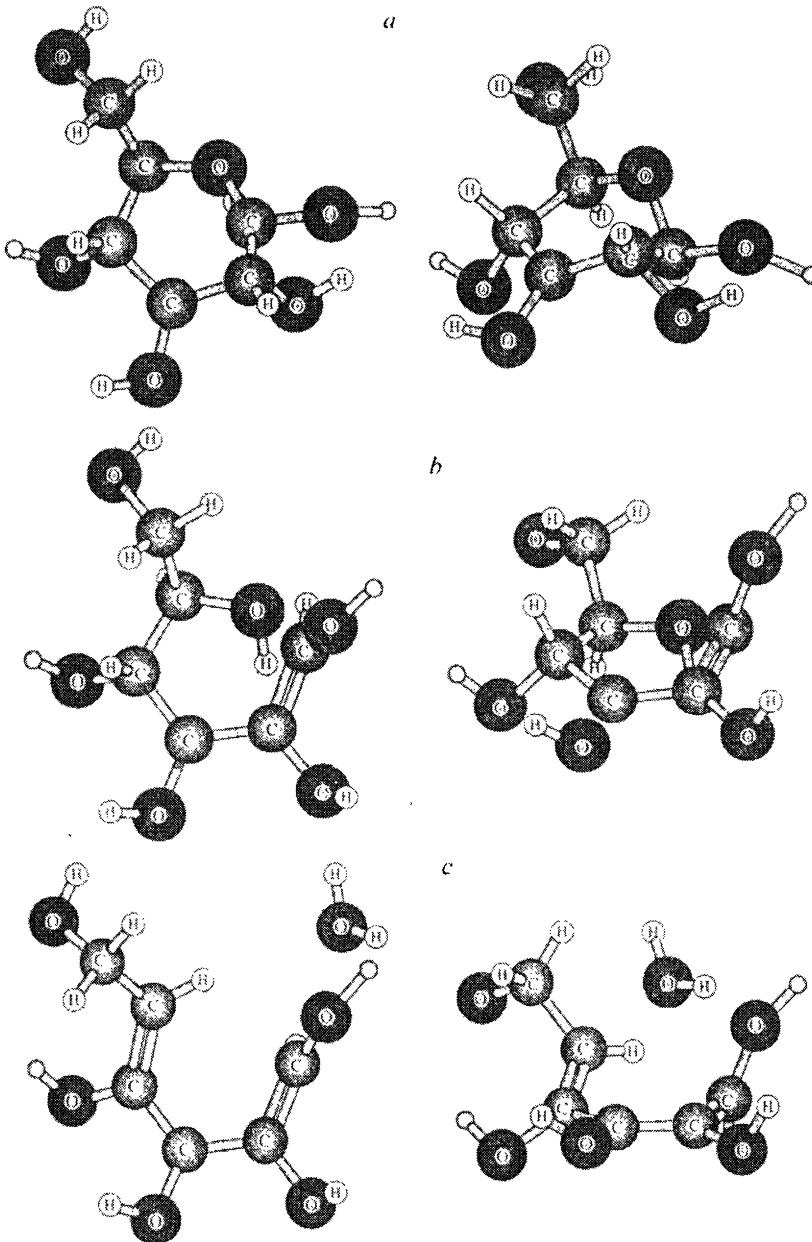
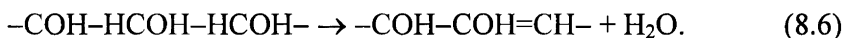


Figure 8.4. Three-dimensional molecular models of $\cdot\text{C}_3$ in the anhydroglucose cycle (two projections): alkyl (a), allyl (b) and dienyl (c) radicals

linear dependence, light water (H₂O) demonstrates quadratic accumulation curve and heavy water (D₂O) – the shape typical of the curve with “saturation plateau”.

The formation of mixed water (HDO) in this system is explained by β -elimination of water molecules (reaction (8.6)) proceeding spontaneously at room temperature in carbohydrates [21]:



Its yield equals 55% of total water yield (Table 8.4). In this case, linearity of the dose dependence directly testifies about spontaneous dehydration of the primary radical (β -elimination of water) at room temperature, because the primary radical formation under the effect of irradiation is the limiting stage for this process. In case of glucose irradiation, such “source” of water may be represented by primary hydroxyalkyl radicals with unpaired electron at each of six carbon atoms. In the case of polysaccharide with glycoside C1–O–C4 bonds, hydroxyalkyl radicals $\cdot\text{C1}$, $\cdot\text{C4}$ and $\cdot\text{C5}$, as well as alkyl radicals might participate in β -elimination of water.

The occurrence of light water indicates that, firstly, only atoms of hydrogen added to carbon atoms participate in H₂O molecule formation and, secondly, its “origin” is related transformations of primary not alkyl radicals ($\cdot\text{OH}$ detachment radicals), but hydroxyalkyl radicals ($\cdot\text{H}$ detachment radicals). Moreover, note that oxygen atom participating in light water molecule formation is never related to hydroxyls. At light water formation, oxygen atoms are originated by O5 oxygen of the cycle, and two hydrogen atoms are used, which occur at C–H bond break at the second and the fourth carbon atoms. This logic of reasoning causes a conclusion that light water formation at radiolysis of deuterated (–OD) glucose (or a polymer) is induced by transformations of the primary hydroxyalkyl radical $\cdot\text{C3}$ by the mechanism of β -elimination of two (seemingly) water molecules as follows: firstly, H atom is detached from C2 and C1–O5 is broken, and a “half” of light water molecule is formed (Figure 8.4); hence, H–C4 and C5–O5 are broken, which gives the “entire” water molecule. (In principle, an alternative sequence of β -C–H and γ -C–OH bonds’ break in the primary radical is possible: first, H–C4 and C5–O5 break, and then H–C2 and C1–O5 bonds, respectively). Thus, dehydration of the primary radical $\cdot\text{C3}$ induces production of a radical with conjugated double bonds in AGC – the dienyl radical.

The mentioned sequence of elementary transformation acts (the mechanism) of primary radical $\cdot\text{C3}$ with formation of dienyl radical $\cdot\text{C3}$ within cellulose AGC was confirmed by computer modeling: the program used allowed for analyzing the run and direction of water molecule elimination with respect to the most profitable energetic way [24]. As shown by computer analysis, the first alternative of the sequence of elementary β -elimination acts (H–C2 and C1–O5, and then H–C4 and C5–O5 bond break) is energetically more profitable. In dienyl radical $\cdot\text{C3}$, formed in AGC, unpaired electron is delocalized in the conjugation system, which, beside p-orbital at atom C3, includes two π -bonds (C1=C2 and C4=C5). Most likely, due to delocalization of unpaired electron, ESR spectrum of such radical should represent a single, apparently, slightly split band, whereas for polycrystalline sample [25] the spectrum represents an extended singlet.

In experiments performed on cellulose samples, irradiated at liquefied nitrogen temperature and then heated up, spectra with a doublet ($a = 1.2$ mT) HFS for allyl radicals (at room temperature) were registered, which at $T = 400 - 420$ K was substituted by a singlet (which might be ascribed to dienyl radical – unpaired electron is delocalized by the system of conjugated π -bonds).

Finally, the conclusion about the “two-stage” mechanism of a single molecule of light water release in this system is confirmed by a quadratic dependence of this water type accumulation on the irradiation dose [18].

It may be suggested that heavy water formation in this glucose preparation indicates the realization of α -elimination of water (reaction (8.7)), so that the initial part of the dose dependence tends to the S-shape.

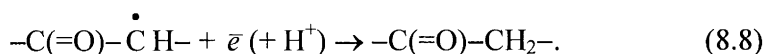


The “teething” induction period might be explained by the initial absence of acid in the sample and its consecutive occurrence as the radiolysis product during irradiation at room temperature. After absorption of 150 – 160 kGy by the sample, an abrupt decrease of the curve tangent (by ~ 10 times) might testify about limiting the dehydration process by reached stationary concentration of acids in the sample. For the initial dose range, the yield of D_2O gives 20% of total water release.

The type of radical dehydration (β - or α -elimination of H_2O) with allyl radical formation proceeding in both frozen and liquid solutions are stipulated by the medium acidity: β -elimination dominates in neutral solutions, whereas α -elimination dominated in acidic ones. At further irradiation of carbohydrates,

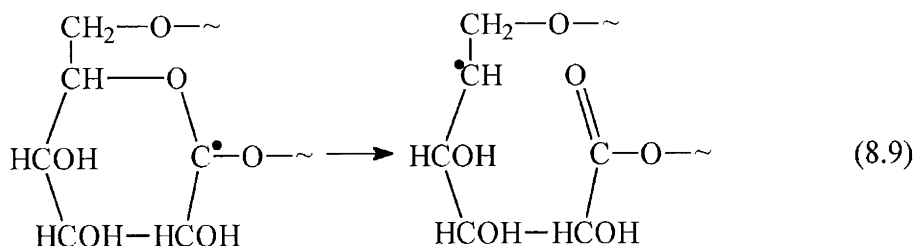
allyl-type radicals may also lose water [4]. As a result, a system of conjugated bonds is formed in sugar or polysaccharide molecules. This is the reason for coloring of irradiated samples (yellow or brown, if the number of conjugated bonds exceeds 3 – 4), which is observed at relatively high irradiation doses [20].

Recombination of allyl radicals may be the reason for the occurrence of deoxyketo-groups in the composition of irradiated polysaccharides:



The content of deoxyketo-groups in irradiated carbohydrates is the estimating parameter for the yield of allyl radicals, which in case of radiolysis of monosaccharides equals 30 – 50% of total yield of initial degradation compounds, whereas in polysaccharides this quantity reaches 10% only [23].

Isomerization of primary radicals with C–O and C–C bond breaks in polysaccharide AGC. Radical C1 isomerization with C5–O5 bond break was observed at thermal annealing of frozen-up aqueous solutions of polyglucin and dextrane, irradiated in liquefied nitrogen, due to typical ESR spectrum shape: during heating the sample from 77 to 115 K the doublet of C1 radical is eliminated with simultaneous occurrence and increase of quintet components. Hence, total concentration of radicals in the samples was constant. Such changes in the spectrum may be explained by formation of a radical, in which unpaired electron interacts with four equivalent protons. The unique position of this electron in the polymer AGC is localization at C5 atom – HC5 (reaction (8.9)) [16].



The alternative way of radical C1 transformation is isomerization with C2–C3 bond break in AGC. This is indicated by formation of secondary acyl radicals in starches (Table 8.3) and one of the final molecular products of their

transformation, which is carbon oxide. The yield of acyl radicals and $G(\text{CO})$ depend on the structural features of irradiated polysaccharides (Table 8.6).

The alternative ways of primary radical C1 transformations are clearly observed at the comparison of CO (formed from C2) and CH_2O (formed from C6) yields in irradiated waxy and corn starches (Table 8.7). These glucose superpolymers demonstrate high content of amylopectin and amylose e.g. the ratio between glycoside C1–C4 and C1–C6 bonds (Table 8.1).

Table 8.7

The yield (G) of polysaccharide degradation products at irradiation of their dry preparations in the presence of O_2 ($T = 300 \text{ K}$) [8, 17]

Radiolysis product	Glucose	Amylose	Corn starch	Potato starch	Waxy starch
H_2	4.1	3.4	3.5	4.5 [8]	4.8
CO	0.01	0.2	1.4	1.5 [8]	2.3
CH_2O (primary)	0.004	–	0.04	0.05	0.03
–CHO	0	–	6	–	9
CH_2O (secondary)	–	–	8.7	–	5.5

Analysis of the data obtained [17] allowed for a conclusion that the processes of formation of these products are, generally, mutually exclusive e.g. stipulated by transformations of the same radical-precursor, namely, primary radical with unpaired electron at C1 atom in the glycoside C1–O–C4 bond.

$$\frac{G_{\text{corn starch}}(\text{CH}_2\text{O})}{G_{\text{waxy starch}}(\text{CH}_2\text{O})} = \frac{G_{\text{waxy starch}}(\text{CO})}{G_{\text{corn starch}}(\text{CO})} = 1.6.$$

Since formaldehyde molecule must be formed by free (non-participants of glycoside C1–C6 bonds) groups of atoms – $\text{C}_6\text{H}_2\text{OH}$, with respect to ESR measurement results one may conclude that among starches this type of degradation (radical $\bullet\text{C1}$ transformation with formaldehyde formation by C6) is mostly typical of linear fragments of amylopectin macromolecule and the whole amylose molecule. Therefore, radical $\bullet\text{C1}$ transformations must include alternative stages: isomerization with C5–O5 bond break in AGC and further CH_2O formation or isomerization with C2–C3 bond break and further CO formation (from C2) [3, 15] (Figure 8.5).

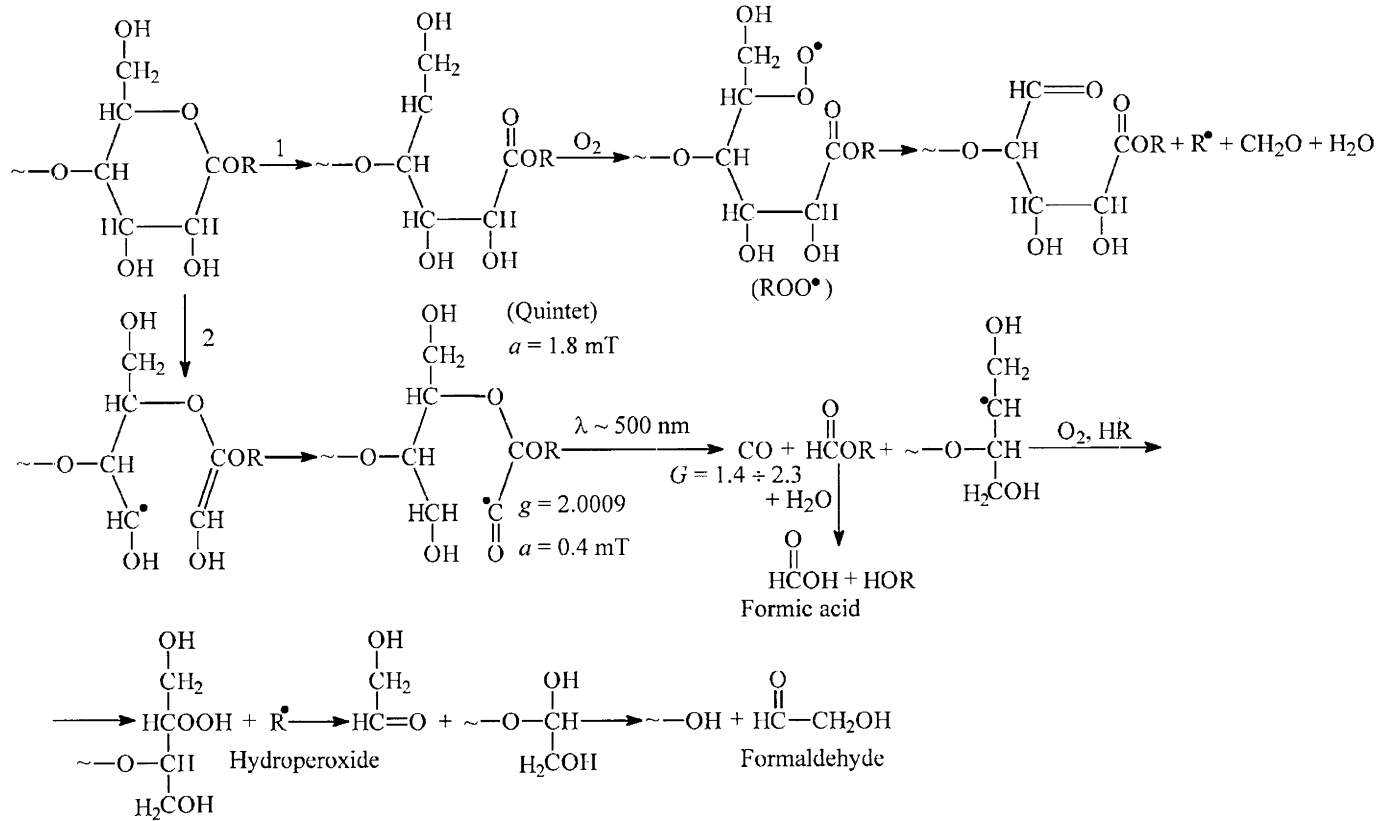


Figure 8.5. The mechanism of $^{\bullet}\text{C1}$ radical conversions via the first and the second ways for the starches of various types [23]

Corn starch contains amylose in the quantity 5 – 6 times higher than in waxy starch, and at transition from waxy to corn starch formaldehyde yield increases by 60% only. Hence, one may conclude that in accordance with the current sequence of elementary acts of radical $\cdot\text{C1}$ transformations formaldehyde is formed from linear fragments of amylopectin.

A possibility of primary radical $\cdot\text{C1}$ transformations by these two ways was demonstrated [27] in the experiments, performed on irradiated samples of crystalline water-free α -D-glucose. It is shown that secondary radicals $\cdot\text{C5}$ and $\cdot\text{C3}$, relatively unstable at room temperature and formed at primary radical $\cdot\text{C1}$ isomerization, induce formation carboxyl groups by the chain mechanism in a solid (radical $\cdot\text{C5}$) and carbon oxide (radical $\cdot\text{C3}$), which is shown in Figure 8.5. The first of these reactions produces carboxylic acids with the yield $G(\text{COOH}) \sim 20$.

In polysaccharides, the isomerization in AGC of primary radicals with C–C and C–O bond break is most strongly proved by the structure of final molecular products formed at radiolysis of starches (potato and wheat) – carboxylic and dicarboxylic acids, and tribasic citric acid [34]. Molecules of these acids contain from one to five carbon atoms in the linear chain that reflects C–C bond breaks in AGC, whereas for dicarboxylic and citric acids they reflect radical $\cdot\text{C1}$ isomerization proceeding with C–O bond break. The formation dicarboxylic acids is induced by primary hydroxyalkyl radical $\cdot\text{C1}$ transformations [35 – 37]. One of carboxylic groups is formed with participation C1 atom (radical $\cdot\text{C1}$ isomerization with C5–O5 bond break) and the second as a result of transformations of peroxide radicals (isomerization of peroxide radicals with O–O and C–C bond breaks), formed by any atoms. The direction of this process (Figure 8.5) depends on the fact if $\cdot\text{C1}$ radicals occur in AGC, at the branching sites in amylopectin macromolecules of in the structure of linear amylose.

In the first case, radical $\cdot\text{C1}$ isomerization with C5–O5 bond break in AGC and the occurrence of radical $>\overset{\cdot}{\text{C}}\text{5}$ (reaction (8.8)) and then at the interaction with oxygen – peroxide radical $>\text{HC5OO}\cdot$, the transformation of which induces formation of tartaric and fumaric acids (refer to Figure 8.11, see Section 8.5 for details).

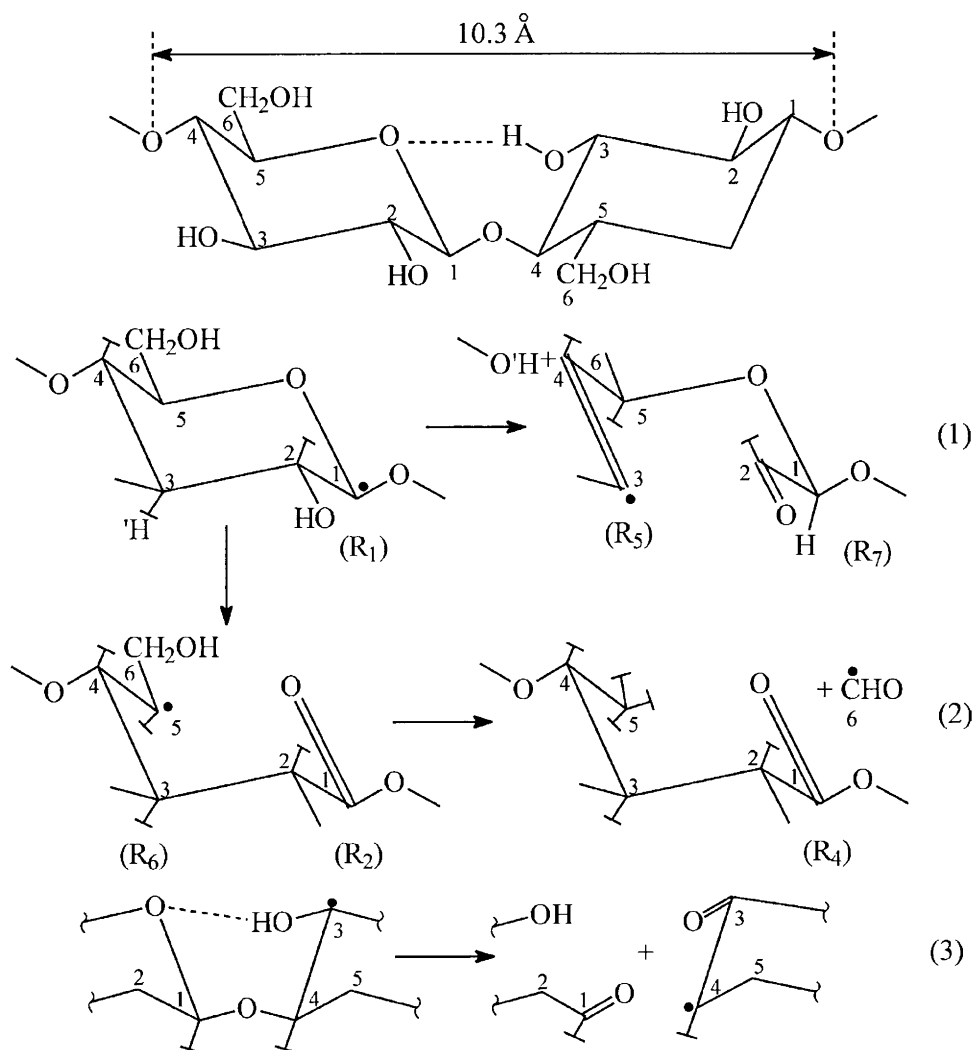


Figure 8.6. The conversion stages of R_1^\bullet and R_2^\bullet radicals in irradiated cellulose (for characteristics, see Table 8.5)

The RYDMR measurements carried out on cellulose at room temperature confirmed the results of experiments on low-temperature γ -irradiation with further thermal and photo annealing of other glucose superpolymers – dextrane, polyglycine, starches (both dry and frozen-up

aqueous solutions) – the regularity of alternative ways of radical $\bullet\text{C1}$ isomerization with C5–O5 or C2–C3 bond splitting in AGC [29 – 31]. This method allowed for observation of radical transformations both as individual particles and in the composition of radical pairs and, therefore, with the help of a radical-companion to search for the behavior of a radical-partner in the composition of the current radical pair (distant by 5.8 – 6.2 Å for cellulose). This gave an opportunity to determine that the formation of the primary hydroxyalkyl radical $\bullet\text{C1}$ at cellulose irradiation is accompanied by formation of another type of radical – alkyl HC1 – due to C1–O bond break in the glycoside C1–O–C'4 [30]. This radical detected in the composition of the radical pair is also isomerized with C5–O5 bond break, and the spin-spin interaction of the formed radical >HC5 with its companion alkoxy radical R3 (Table 8.5) allowed for detecting migration of unpaired electron from C5 to C6 (refer to rearrangement of C–H chemical bonds below) with formation of formyl radical $\text{H}\overset{\bullet}{\text{C}}\text{O}$ by C6.

The RYDMR method registers two types of $\text{H}\overset{\bullet}{\text{C}}\text{O}$ radicals. At relatively long-term UV influence on the sample, mainly, $\text{H}\overset{\bullet}{\text{C}}\text{O}$ radical spectrum with HFI constant increased by 17% compared with the first spectrum of detected (Figure 8.2). Both spectra possess additional sub-splitting in doublet bands. It may be suggested that in these radicals unpaired electron interacts with different neighboring protons (see Section 8.6 for details).

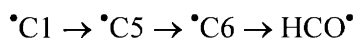
Transformations of the primary hydroxyalkyl radical $\bullet\text{C1}$ in cellulose by the second route (isomerization with C2–C3 bond break) is accompanied by vinyl radical formation with unpaired electron transfer to C3 and consecutive break of C'1–O'1–C4H< glycoside bond in the polymeric chain due to β -elimination of water (reaction 1, Figure 8.6).

This result differs from that observed at radiolysis of starches (Figure 8.5). Obviously, the occurrence of O'1–C4 bond break is stipulated specificity of the monomeric unit of cellulose (cellobiose residue): there is a hydrogen bond $\text{–C3–OH}\dots\text{O'5}<$ between two AGC. This hydrogen bond between hydroxyl at C3 atom and oxygen in the ring of neighboring residue adhere additional rigidity to this fragment of the macromolecule, compared with starches, which is obviously manifested in the break formation (stress removal). It is worthy of note that in cellulose the process proceeds at room temperature [30].

To the greater extent, such specificity of the cellulose structure affected the transformation of hydroxyalkyl end radical $\cdot\text{C3}$ (reaction 3, Figure 8.6). The analysis of RYDMR spectra allowed for a suggestion that due to structural rigidity of the mentioned fragment of the polymer radical $\cdot\text{C3}$ conversions (Table 8.5) is implemented by the mechanism of specific α -elimination of water molecule. Hence, from the first AGC deoxyaldehydes with two and four carbon atoms are formed, whereas from the neighboring AGC a molecule of glucose instead of water molecule is released and, as a result, a break occurs in the polymeric chain.

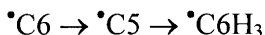
Using RYDMR spectroscopy method in cellulose at room temperature, the third type of radical $\cdot\text{C1}$ isomerization was detected: isomerization with C1-O-C' glycoside bond break, O-C'4 β -bond break and unpaired electron transfer to neighbor AGC with formation of C'4 alkyl radical. As a resulting this reaction, in the first AGC lactone is formed, and the neighbor AGC degrades with formation of low-molecular products. Hence, in macromolecule glycoside bond is broken.

The third type of radical transformations represents rearrangement of chemical bonds C-H and O-H . Actually, in irradiated samples of polysaccharides this process is induced by the radiation effect on the radicals. According to estimation results, in different polymers, polysaccharides, in particular, seeming activation energy of the radiation effect on the radicals and their annihilation may vary in the range of 0.3 (for alcohol radicals) – 0.6 kcal/mol (for peroxide radicals in polytetrafluoroethylene) [38, p. 347]. The changes in spectra observed by RYDMR method in cellulose, UV-irradiated at room temperature, are explained by radical conversions by stages



with formyl radical (and, consecutively, formaldehyde) formation. In this sequence of radical conversions, C-H bonds are rearranged at C6 (C6-H bond breaks) and C5 (C5-H bond is formed) atoms, and in hydroxyalkyl radical $\cdot\text{C6}$ formed O-H bond breaks in hydroxyl-group, and C5-H and C6=O bonds are formed. The bond C5-C6 is broken simultaneously, and as a result formyl radical is formed. According to estimation, duration of the formyl radical formation is $(8 - 10) \times 10^{-8}$ s or shorter [29].

Another example of rearrangement of chemical bonds in the radical is the sequence of elementary acts of conversions of primary alkyl radical $\cdot\text{C6}$:



(the interaction between methyl radical and C–H bond forms methane). This sequence of primary alkyl radical $\cdot\text{C6}$ conversions was also determined for cellulose and lasted during 10^{-7} s.

The fourth type of primary radical of polysaccharides conversions is represented by hydrolytic splitting (hydrolysis) of β -bonds in carbon-centered glycoside radicals. As for cellulose, this relates toradicals with unpaired electron at C1 and C4 atoms; in PS and AS, beside C1 and C4, atom C6 (in the branching point of amylopectin) participate, whereas in D – C1 and C6 atoms. For radiolysis of aqueous hyaluronic acid, it has been shown that in glycoside macroradical (C1–O–C3) with unpaired electron at C1 atom β -bond is hydrolyzed with formation of hydroxyalkyl radical $\cdot\text{C1}$ in the first AGC and N-acetylglucosamine derivative of the second AGC [37, 38]. As estimated, for the liquid phase [39, 40] the rate constant of β -bond radiolysis in glycoside radical is by 4 orders of magnitude higher than analogous value for usual glycoside bond in polysaccharides.

Table 8.8

Composition of gaseous products from linen fabric treated by low-temperature plasma (80 mA, 5 min 295 K) in nitrogen or in air; the error in gas release rate determination (maximal values) is $\pm 25\%$ at the level of confidence equal 0.9 [41]

Products	I^*		P^{**} , Pa		Number of molecules, 10^{16}	
	nitrogen	air	nitrogen	air	nitrogen	air
H ₂	0.77	0.84	6.4	7.8	1.3	1.6
H ₂ O	0	1.1	0	7.2	0	1.5
CO ₂	0.3	2.3	5.7	12.5	1.2	2.5
CO	0	0.02	0	0.1	0	0.02
–O ₂	0.12***	1.8	0.8	12	0.15	2.4

Notes: * The intensity of molecular peak in the mass-spectrum

** Partial pressure of gaseous products

*** Traces of oxygen in used nitrogen

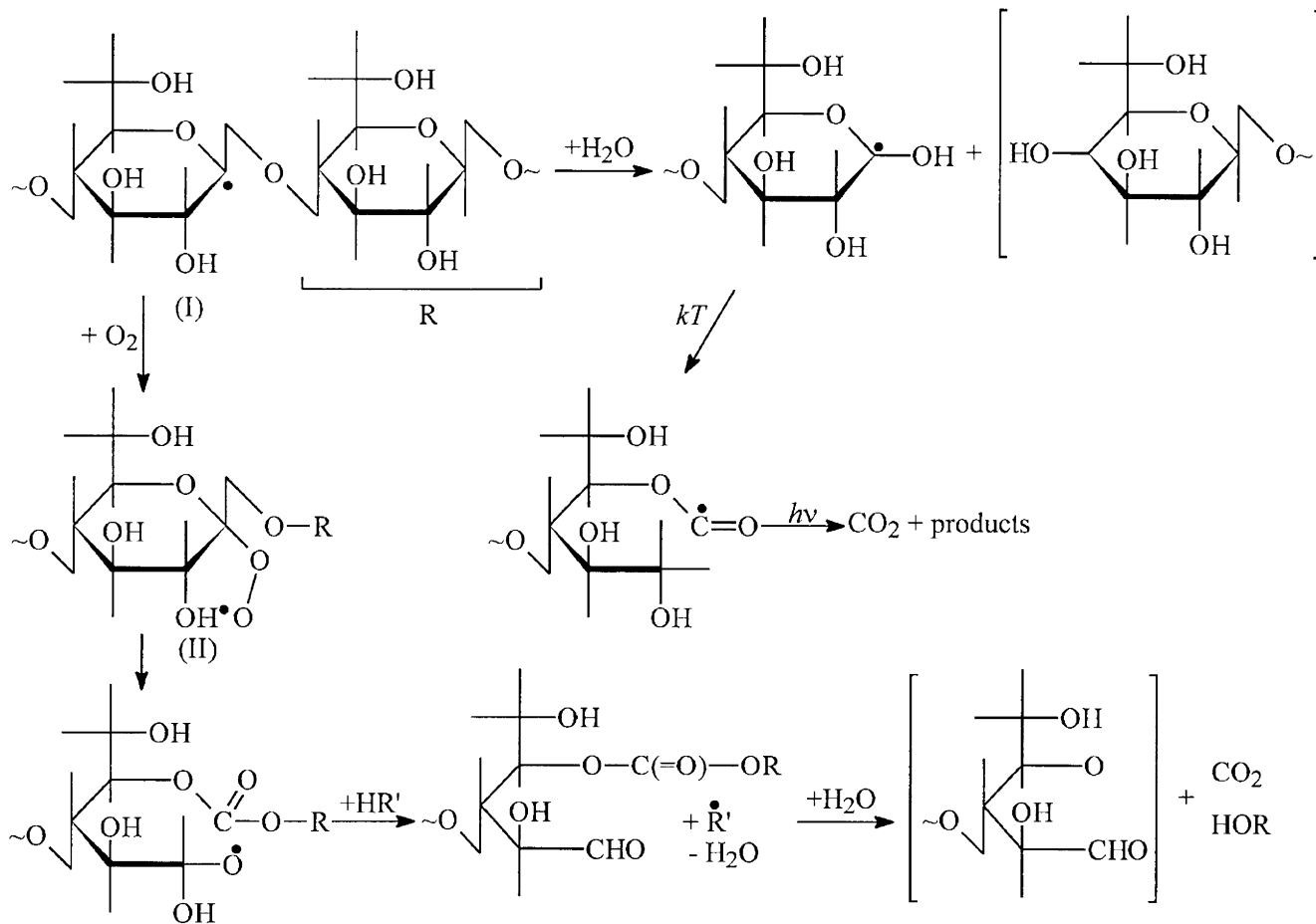


Figure 8.7. Radical $\cdot\text{C1}$ conversions in cellulose and starch: vicinal bond hydrolysis, break formation in macromolecule and CO_2

Let us illustrate a possibility hydrolytic splitting of the glycoside bond in the carbon-centered radical on the example of linen fiber (consisting by 90% from cellulose) degradation, induced by low-temperature plasma (acting agents: electron, ions, excited gas plasma molecules, etc.). Linen fiber (cellulose) degradation by plasmolysis mostly proceeds by the free-radical mechanism [41]. Table 8.8 shows the composition of gaseous products of linen fabric treated by low-temperature plasma in nitrogen and in air (mass-spectrometric measurements). Clearly, in the absence of oxygen (“nitrogen plasma”) no water is released in the sample, but is consumed in the reaction. Analogous situation of water consumption in polysaccharide is also observed at γ -irradiation of potato starch – in the dose range from 10 to 30 kGy, at transition from irradiation in air to evacuated samples the water consumption twice increases [42].

In the case of linen fiber treatment by “air plasma”, water is released and similar to carbon dioxide is accumulated in the sample with relatively high yield (Table 8.8). Hence, values of the yield of carbon dioxide and molecular oxygen consumption by the sample are comparable. It follows from these data that:

- a) water formed during radiation degradation of cellulose (and starch) is absorbed by the sample e.g. consumed in the reaction with radicals;
- b) water and molecular oxygen absorption by irradiated sample and carbon dioxide formation are processes related to proceeding of alternative conversions of the same primary radical, which is identified as $\cdot\text{C1}$ radical (Figure 8.7).

As analyzed in the review [14], the role of free radicals in the radiation degradation of starches indicates a dependence of starch degradation on the initial humidity of the sample and a significant increase of it with time, as well as of radicals stabilized at room temperature in the post-irradiation period (water is consumed in reactions with radicals). The rate of water consumption by the irradiated sample depends on the origin (structure) of starch: in amylose corn starch humidity decreased by an order of magnitude in 50 days, whereas in potato starch – by two times during 100 days.

The effect of carbon-centered glycoside radical hydrolysis was discussed [4, 43] at the study of methane formation mechanism in irradiated polysaccharides (see Section 8.6 for details).

8.5. OXYGEN EFFECT

The presence of O₂ in the irradiated system affects the accumulation of molecular products of polysaccharide radiolysis, formed in both primary acts of their degradation (H₂ and H₂O) and the products, which formation is stipulated by deep degradation of pyranose cycle (Table 8.9).

Table 8.9

The yield of radiolysis products from glucose superpolymers (polyglucosin and dextrane), irradiated at room temperature [32]

Radiolysis products	Polyglucosin		Dextrane (evacuated)
	evacuated	with O ₂	
H ₂	3	2	3
CO	0.5	2.9	0.05
CO ₂	0.09	0.96	0.01
H ₂ O	0.03	0.15	0.05
Malone dialdehyde	0.08	0.06	0.05
Deoxy-compounds	0.08	0.05	0.04
Carboxylic groups	5.4	8	4

The oxygen effect is explained by proceeding of two basic processes: the competition between molecular oxygen and the macromolecule for hydrogen and \bar{e}_{hydr} , and its interaction with macroradicals formed. The reactions of macroradicals with O₂ form peroxide radicals of two types, possessing different ESR spectra with respect to dormancy of peroxide group rotation around C–O bond e.g. with respect to the place of peroxide group localization in the damaged monomeric unit. In the case of dry polysaccharide irradiation in the presence of O₂, RO₂ formation is the main process [36, 37]:



This is testified by the equality of total radical accumulation and molecular oxygen consumption by the irradiated sample:

$$G(\Sigma R^*) = G(-O_2) = 3.2.$$

The molecular oxygen reacts with both primary and secondary radicals with respect to the fact, if primary radical conversions, discussed in the previous Section, manage to proceed (degradation, isomerization or hydrolysis) until they are reached by diffusing O₂ [1, 8, 32]. For example, this is confirmed by the composition of dicarboxylic acids in irradiated starches (Table 8.10).

Table 8.10

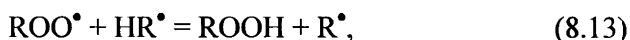
The yield (weight part) of dicarboxylic acids formed in corn and potato starches, irradiated in air by 500 kGy dose, $T = 300$ K [35]

Acid	Yield
Tartaric	42.4
Citric	33.5
Malic	16.4
Succinic	4.6
Malonic	1.8
Fumaric	1.3

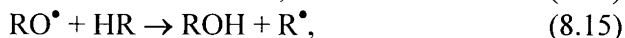
The formation of dicarboxylic acid is the result of inclusion of an additional oxygen atom into the monomeric unit, because a “procurement” for the “first” carboxylic group is C1OO[•] fragment. To put differently, occurrence of the second group in AGC is related to the occurrence of peroxide radical in the presence of O₂ and its conversions. In the dose range of 40 – 500 kGy the probability of the recurrent radiation damage of the same monomeric unit is extremely low, and it may be concluded that radiation-induced free-radical chain processes proceed in starches by the reactions (8.1), (8.11) and (8.12):



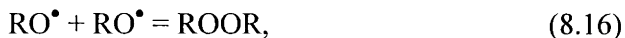
Chain propagation reactions are (8.10) and (8.13):



and chain branching reactions (8.1), (8.14) and (8.15):



Recombination of radicals formed by the reaction (8.14) causes the chain termination. Hence, the following products – peroxide and hydroperoxide – are formed:



Obviously, the reactions (8.13) and (8.15) in the samples of native starch are possible only between neighbor H and O atoms (in C–O, C–OO and H–C bonds) with a monomeric unit or in two units of neighbor chains due to their segmental mobility. Hydroperoxide decomposition by the reaction (8.14) is accelerated by γ -irradiation. Beside the processes (8.1), (8.13), (8.15), in polysaccharides irradiation may also induce peroxide macroradical conversion via isomerization with C–C and O–O bond breaks.

Identical macromolecular compositions of corn and potato starches (77% of branched amylopectin and 23% of linear amylose, Table 8.1) and “identical” dominant doublet HFS of ESR for both starches, irradiated at 77 K, allowed for a conclusion about the highest yield of primary radicals $\bullet\text{C1}$ from these samples. Obviously, consecutive conversions of $\bullet\text{C1}$ radicals are induced by the stress in AGC fragment (of radical) of C'4–O1–C1–(–O5–)–C2–C3 atoms, occurred during re-hybridization of orbitals and retained by both (left and right) parts of the macroradicals. By isomerization of radical $\bullet\text{C1}$ proceeding with C5–O5 bond break and radical $\bullet\text{HC5}$ formation this stress in the damaged AGC (radical) may be removed.

This conclusion is confirmed by relatively high total yield of the final products of radical $\bullet\text{C5}$ conversion – malic, tartaric, malonic and fumaric acids (70%, refer to Figures in Section 8.6). In radicals $\bullet\text{HC5}$ formed, water is β -eliminated (by C4–C3 bond) of C–H bond at the 4th and the 5th carbon atoms is rearranged with H atom transfer from C4 to C5. The interaction between radicals $\bullet\text{HC5}$ and O_2 produce peroxide radicals, the conversions of which are accompanied by either malic and fumaric acids (fumaric acid is formed after additional rearrangement of chemical bonds, peroxides by C5 atom) or tartaric and malonic (peroxides by C4 atoms, refer to Figures 8.12 and 8.13 [37]) acid formation.

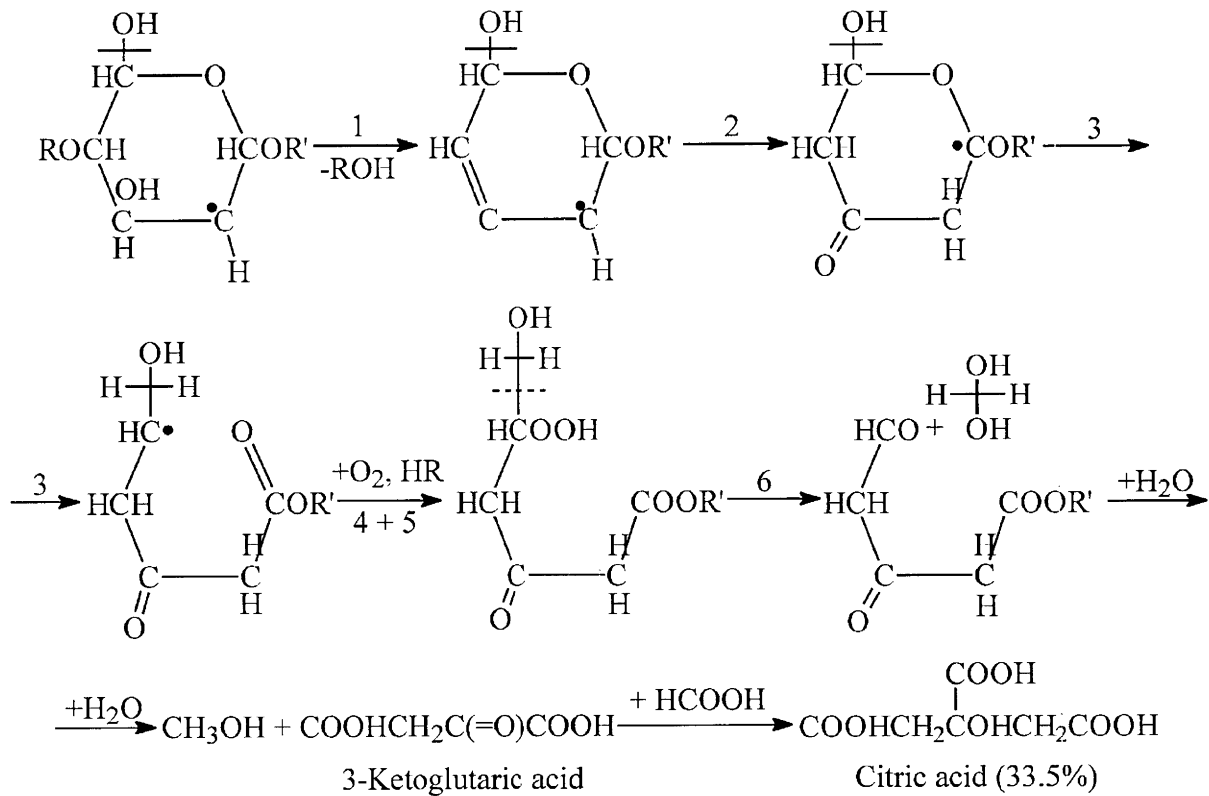


Figure 8.8. The mechanism of citric acid formation in irradiated starches

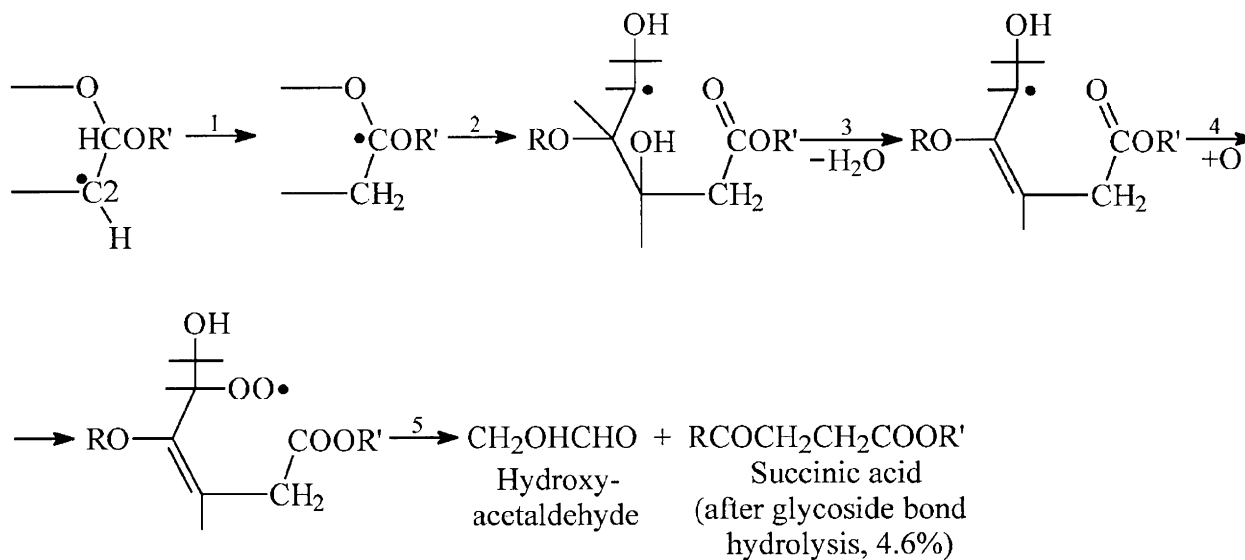


Figure 8.9. The mechanism of succinic acid formation in irradiated starches

Further transformations of the radical $\bullet\text{C4}$ formed in the monomeric unit, modified by radiation, may proceed by two routes: with peroxide radical formation either directly (tartaric acid) or after β -elimination of water (by C3–C2 bond, malonic acid). Comparing the yields of tartaric and malonic acids and suggesting being identical the consecutive stages of peroxide radical conversions up to final products, it may be estimated by how many times the rate of malonic acid release, compared with tartaric acid, due to water release from radical $\bullet\text{C4}$: 42.4:1.8 ~ 20.

For citric acid, three stages of the primary alkyl radical $\bullet\text{C2}$ (the initial detachment of $\bullet\text{OH}$ from C2) are prior to the peroxide radical formation:

- β -elimination of water (an allyl radical C2–C3=C4 is formed);
- migration of H atom from C1 to C2 atom;
- isomerization of the radical $\bullet\text{C1}$ with radical $\bullet\text{HC5}$ formation; at its interaction with O_2 peroxide radical is formed.

Conversion of the latter radical is accompanied by C5–C6 bond break, consecutive formation of two aldehyde groups (one of which is formaldehyde), and then by reaction of their disproportioning (the Cannizzaro reaction) – the formation of methanol and 3-ketoglutaric acid. In the interaction with butyric acid (which is also the product of starch radiolysis) citric acid is formed [37] (Figure 8.8).

In the mechanism of succinic acid formation, prior to the stage of peroxide radical formation by the same C5 atom, three stages of the primary alkyl radical $\bullet\text{C2}$ proceed (Figure 8.9). Contrary to the previous case, instead of the primary alkyl radical $\bullet\text{C2}$, here water molecule is eliminated by $\bullet\text{HC5}$ radical: H is detached from C4, and OH group – from C3. In this case, no glycoside bond break is observed. The break of macromolecule in this point is possible only as a result of consecutive hydrolytic splitting of the glycoside bond.

Current schemes demonstrating transformations of primary radicals $\bullet\text{C1}$ and $\bullet\text{C2}$ up to formation of corresponding carboxylic acids are composed with respect to the fact that according to ref. [4] at room temperature isomerization (bond break) and dehydration in solid polysaccharides (starches) proceed at high rates (with the activation energies ranging within 35 – 42 kJ/mol), and the rate of O_2 interaction is by an order of magnitude higher compared with the rate of radical interaction.

The formation of aldehyde and carboxylic groups in the polymer composition is one of the basic processes of radiolytic modification of carbohydrates. Their yield significantly increases (similar to the yield of carbon oxide – the product of aldehyde group transformation) at transition from irradiation of evacuated samples to irradiation in the presence of O₂.

Both these functional groups in irradiated starches are formed as a result of transformations of the same precursor, peroxide radical [1]. The increase of yields (by the same value, Δ*G* = 2.5) of carbon oxide and carboxylic groups –COOH also relates to peroxide radical transformations, for example, in irradiated polyglucin at transition from vacuum to O₂ (Table 8.9 [32]). These peroxide radicals are formed by the reaction (8.10) at oxygenation of allyl type radicals [1]:

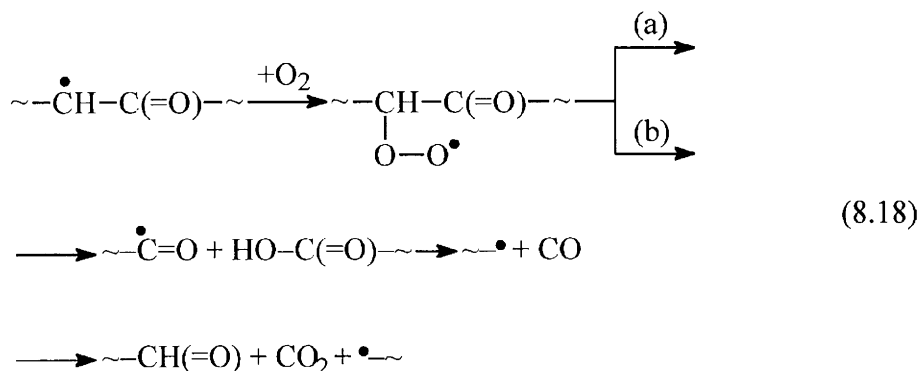


Table 8.9 shows that the yield of CO in the presence of O₂ is an order of magnitude higher compared with irradiation in vacuum. This is the reason that the sequence of reactions by (8.18b) route involves any carbon atom in the glucopyranose ring, whereas in evacuated samples a possibility of CO₂ (or carboxylic group) formation is realized specifically by means of [•]C1 radical (with initially attached two oxygen atoms). Oxygenation of allyl radicals gives up to 50% of total yield of the polymer degradation process.

8.6. FORMATION MECHANISMS FOR LOW-MOLECULAR PRODUCTS

Radiation degradation of polysaccharides proceeds by two routes: modification of macromolecules (occurrence of carboxylic, aldehyde, keto- and deoxyketo-groups) and formation of low-molecular products (with the number of carbon atoms from one to six – carboxylic acids, aldehydes, ketones, sugars, alcohols, esters), including gases (hydrogen, carbon oxide and dioxide). The radiation-chemical yields for the sum of products formed by each of these two directions are comparable.

Schemes of the formation mechanisms for molecular products of radiolysis, starches, for example, are of a hypothetical character due to their yielding from the results of radiolysis investigations, performed for model systems – mono- and disaccharides.

Formic acid and carbon oxide

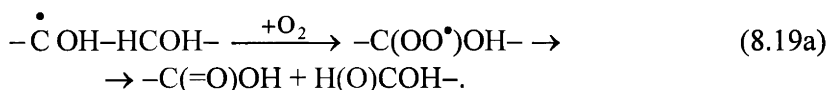
Impropriety of transferring such data to radiolysis of polymers is obvious due to dropping differences in the structural organization of glucose and glucose superpolymer and, therefore, in the specificity of radiolysis of these two systems: separate molecules and macromolecules with the well-developed supermolecular structure. For example, it is assumed that carbon oxide in irradiated glucose is formed by its elimination from hydroxyalkyl radical $\cdot\text{C1}$ after hydrogen transfer from hydroxyl at C1 to O5 and C1–C2 bond break [45]. Hence, oxidation of the end radical $\cdot\text{C2}$, formed in this case, produces pentacarbon sugar – arabinose. However, the material balance by the yield of end products of glucose radiolysis is not observed: $G(\text{CO}) = 0.05$ [18], whereas arabinose yield is 5 times higher [45]. In polysaccharides with glycoside C1–O–C4 bonds (starches, cellulose) such process may not proceed, because C1 atom has no free hydroxyl. In various types of starch, with respect to concentration of linear macromolecules (amylose) and branchings (amylopectin), $G(\text{CO})$ value varies from 0.2 (amylose) to 2.3 (waxy starch containing 96% of amylopectin) [17, 46]. In this case, only traces of arabinose are detected [46].

After analyzing the data on accumulation of two basic low-molecular products of starch radiolysis – formic acid (with the yield $G = 2.5 - 3$ [47 – 49]

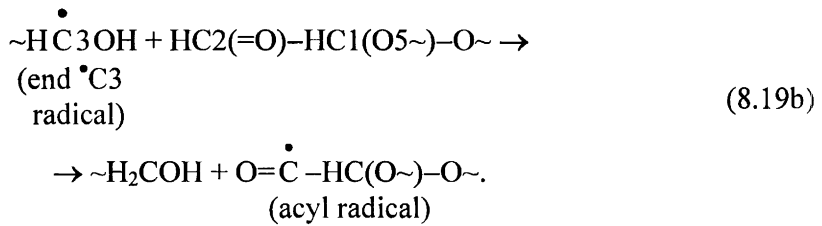
that gives 80% of total yield of carboxylic acids [48]) and carbon oxide (with G up to 2.3), let us present a scheme for the sequence of the elementary acts (the mechanism) of their transformation.

As comparing yields of the main degradation processes of native starch preparations, of special urgency is the indication that total yield of HCOOH and CO ($G \sim 4$) [16, 47 – 49] is by more than an order of magnitude higher than the yield of breaks in polymeric molecules ($G \sim 0.3$ for the initial dose range [50]). Here data of the experiments, performed under identical conditions, are present. Formally, it is obtained that one act of break occurrence in a macromolecule is accompanied by “processing” up to 12 carbon atoms into CO and HCOOH. For this purpose, they should be taken from, at least, two neighboring monomeric units of macromolecule – anhydroglucose cycles (AGC).

The yield of breaks in the irradiated starch is independent on the sample irradiation conditions, i.e. either it proceeds in the presence of oxygen or the sample is evacuated [49]. The yield of HCOOH is 1.5 – 3-fold higher at starch irradiation in the presence of O_2 , with respect to the type of starch [48]. In the absence of O_2 , potential source of formic acid in AGC is O5–C1–O1 fragment, because C1 atom is bound to two oxygen atoms. At irradiation in the presence of oxygen any of the rest carbon atoms may participate in HCOOH molecule formation. This process includes stages of peroxide radical formation from the primary radicals (since the material balance is observed: $G(\Sigma R^\bullet) = G(-O_2) = 3$ [18]) and peroxide radical isomerism with C–C bond break in AGC and O–O bond break in peroxide radical, which proceed according to the sequence of reactions as follows [35]:



The process of carbon oxide molecule formation in polysaccharides irradiated in the absence of O_2 includes stages of C2–C3 bond break in AGC and acyl radical (CO precursor) formation at the interaction of already formed end hydroxyalkyl radical $^\bullet C3$ and aldehyde group by C2 atom according to the reaction (8.19b) [35]:



In evacuated samples of cellulose exposed to mechanical or UV influence (in the presence of sensitizer) at room temperature C2–C3 bond break with the end radical $\overset{\bullet}{\text{C}}\text{3}$ formation resulting isomerization of the primary radical $\overset{\bullet}{\text{C}}\text{1}$ was detected using RYDMR method [29, 31]. Acyl radicals (with unpaired electron at C2 atom) are identified by ESR spectra (a narrow band with $g = 2.0009$, which disappears at sample irradiation by light with $\lambda_{\text{max}} \sim 500 \text{ nm}$) in evacuated samples of dextrane [16], potato starch [17] and frozen-up glucose solution [13], irradiated at 77 K. The measurements were performed after annealing of the samples at temperatures approaching room temperature. At irradiation of glucose superpolymers in the presence of O_2 , H atom may also be detached from aldehyde group by peroxide radicals [1]. Therefore, the yield of CO in the presence of O_2 increases compared with evacuated samples (in the case of polyglucin – low-molecular dextrane – at transition to irradiation in the presence of O_2 $G(\text{CO})$ increases from 0.5 to 2.9 [32]). As the samples are affected by radiation or heated up, allyl radicals are converted with CO release and corresponding end radical formation. The energy of C–C bond break in allyl radical in the polymer composition does not exceed 10 kcal/mol [38].

For instance, note that the mechanisms of formic acid and carbon oxide formation at irradiation of native corn starch preparations at room temperature in the presence of oxygen must include their relative yield as the reference value:

$$\frac{G(\text{HCOOH})}{G(\text{CO})} = \frac{2.5[5]}{1.4[3]} = 1.78.$$

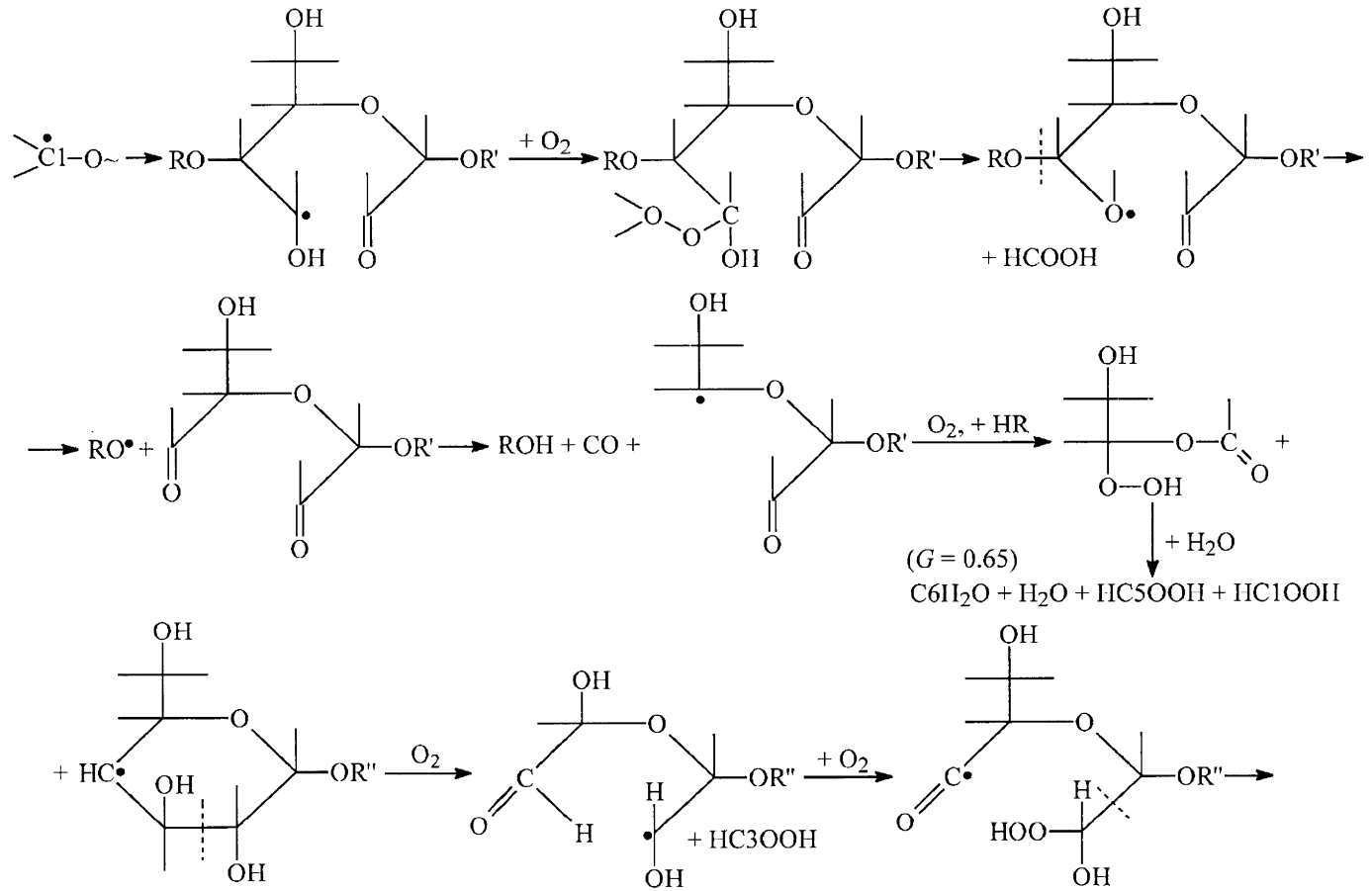


Figure 8.10. The mechanisms of formic acid and carbon oxide formation in irradiated starch and cellulose

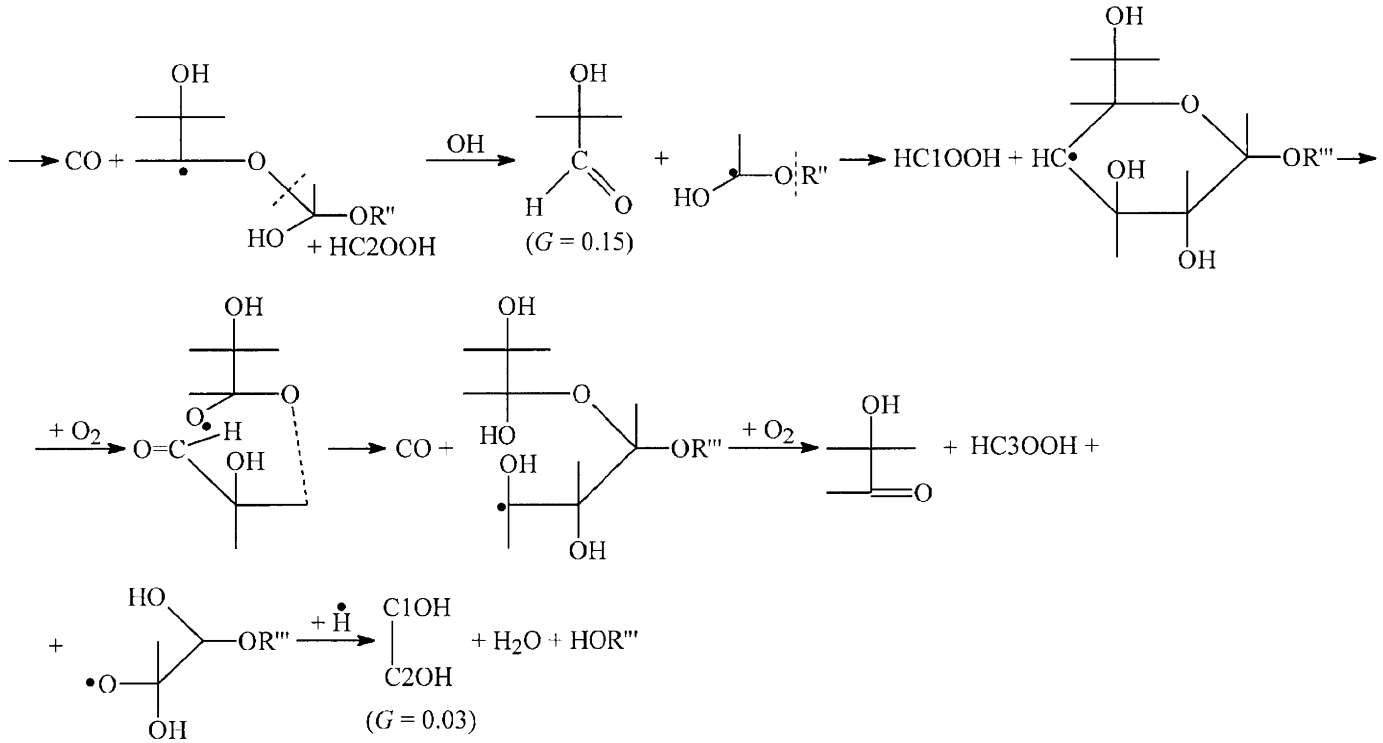


Figure 8.10 (continued)

This means that the process of processing into HCOOH and CO molecules requires minimal number of carbon atoms: 7 for the first product and 4 for the second product ($7/4 = 1.75$) or 8 and 4 ($8/4 = 2$), respectively, i.e. 11 ($7 + 4$) or 12 ($8 + 4$) carbon atoms are involved. Hence, it should be taken into account that the source of HCOOH molecules is represented by peroxide radicals, whereas CO release from acyl radicals, in turn, formed from aldehyde groups. Describing radiolytic effects in corn starch, the use of data on the properties of these radicals provided limitation by “degradation” of three AGC (Figure 8.10) [50].

Beside HCOOH and CO accumulation, the diagram indicates formation of formaldehyde (the first AGC degradation), glycol aldehyde (the second and the third AGC degradation) and glyoxal (the third AGC degradation) [47]. Note that for the first AGC the requirements to radiolysis product balance are observed: the yield of two CO equals

$$G = \frac{1.4}{4} \times 2 = 0.7$$

that coincides with the yield of formaldehyde ($G = 0.65$), observed in the experiment. The yields of glycol aldehyde ($G = 0.15$) and glyoxal ($G = 0.03$) are several times lower than it follows from balance considerations for the yield of two CO molecules at degradation of the second and the third AGC (for glycol aldehyde) and one CO molecule at degradation of the third AGC (for glyoxal). All these facts may be explained as follows: in the presence of carboxylic acids and other radiolysis products these aldehydes are unstable and degrade (participate in redox reactions) and/or polymerize. As detected [51], during initial 4 days after irradiation, the concentration of glycol aldehyde in irradiated corn starch (containing 13% of water, at 298 K, irradiated by 20 kGy dose in the presence of oxygen) two-fold decreases. As accumulating in irradiated starches, HCOOH and CO may enter chemical reaction, which is indicated by bell-shaped curves of dose dependencies for accumulation of these products [38, 48].

It should be noted that the diagram in Figure 8.10 shows free-radical processes of formic acid and carbon oxide accumulation in irradiated starches and cellulose. For dextrane or polyglucin, which are glucose superpolymers with α -C1-O-C6 glycoside bonds and, consequently, free hydroxyls by C4 atom, a possibility of primary radical \cdot C1 isomerization with C5-O5 [16] bond break [16] and conversions of peroxide radicals formed (in the presence of

oxygen) should be taken into account. These reactions may also produce formic acid, aldehydes – acyl radical precursors and, consequently, carbon oxide [17].

Formaldehyde

It is one of the basic products of native polysaccharide radiolysis, which maximal radiation-chemical yield (G) equals 5 – 10 molecules per 100 eV of absorbed energy with respect to the origin of polysaccharide, sample irradiation and analysis conditions (Table 8.7: humidity, irradiation in the presence of oxygen or in inert atmosphere, analysis duration for CH_2O since irradiation impact removal). In the case of cellulose irradiation, similar yield of xylose is observed: $G(\text{xylose}) = 10.1 \pm 2.0$ [8]. As follows from coincidence in symmetry of xylose and glucose molecules (the carbon backbone C1–C2–C3–C4–C5 fragment), xylose in polysaccharide is formed as a result of C6 atom removal from glucoside residue; hence, formaldehyde is formed from this C6 atom. With respect to all above-mentioned about the reactions of primary radicals of carbohydrates, it may be concluded that xylose is synthesized by isomerization of primary hydroxyalkyl radical $\bullet\text{C}_6$ with C5–C6 bond break in the glucose residue and O–H bond break in hydroxyl at C6 atom, accompanied by H atom transition from C6 to C5:

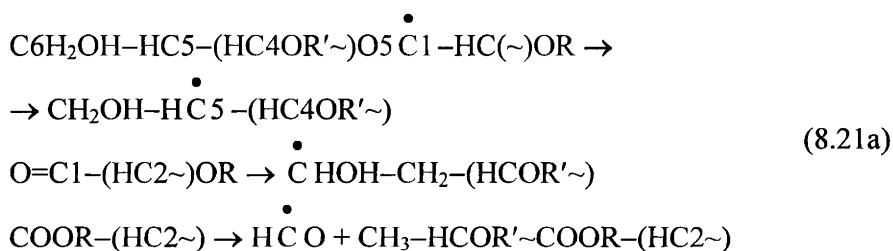


Hence, the yield of formyl radical formed by C6 atom according to the diagram (8.20) might be equal xylose yield. The yields of CH_2O , recorded in experiments on irradiated glucose (starches) superpolymers, are always below $G \sim 10$. Most likely, this may be related to proceeding of formyl radical reactions directly in the solid phase (for example, recombination – glyoxal formation, and CH_2O reactions with ketones, oxidation, polymerization, etc. reactions) or during preparing the irradiated sample to analysis on formaldehyde at contact with water, including extraction of the radiolysis products for analysis [52].

However, another reason for reaction (8.1) product yield decrease, observed at transition from irradiated cellulose to starch, is also possible. For example, for corn starch the yields are the following: $G(\text{xylose}) \sim 0.04$,

$G(\text{formaldehyde}) \sim 0.65$ [47]. Taking into account similar time condition of analysis of the radiolysis products, such difference in formaldehyde and xylose yields is, most likely, related to the existence of several formation mechanisms of these products. It is obvious that as transiting from cellulose to starches, the ratio of primary radical yields and the fractional contribution of their conversions with xylose and formaldehyde formation are changed. First of all, this may be caused by variation of the crystalline phase content in irradiated samples (the crystallinity index equals 0.7 – 0.8 for cellulose and 0.2 – 0.25 for starch), if it is considered that in the crystalline phase monomolecular decomposition of primary radicals (currently, radicals with unpaired electron at C6 atom) are predominant – radical isomerization with C5–C6 bond break.

Beside the scheme present on hydroxyalkyl radical $\cdot\text{C6}$ conversion proceeding in the absence of oxygen, another possibility of formyl radical formation (and, consequently, formaldehyde) by means of the primary radical $\cdot\text{C1}$ conversion sequence is obvious (8.21a):



In this case, the sequence of elementary acts of radical $\cdot\text{C1}$ conversions is the following: isomerization with C5–O5 bond break and unpaired electron transfer to C5 (AGC is disclosed by the reaction (8.9)), rearrangement of C–H chemical bonds at C6 and C5 atoms in the formed radical $\cdot\text{C5}$, and then radical $\cdot\text{C6}$ is isomerized with C5–C6 bond break. Hence, beside formyl radical, 5-deoxyxylic acid is formed.

Among the polysaccharide radiolysis products, the compounds of this type were chromatographically detected [23]. The scheme (8.21a) helps in explaining why at transition from cellulose to starches the ratios of yields change from $G(\text{xylose}) > G(\text{formaldehyde})$ to $G(\text{xylose}) < G(\text{formaldehyde})$: xylose is not formed. For more details of this mechanism, see below.

Beside this sequence of elementary acts of radical $\cdot\text{C1}$ conversions with formyl radical or formaldehyde formation by the reaction (8.21a), the

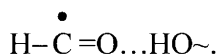
mechanism of these products formation at polysaccharide irradiation in the presence of molecular oxygen should also be considered. This sequence possesses the same first stage – radical $\bullet\text{C1}$ isomerization with C5–O5 bond break in AGC by the reaction (8.9). The subsequent stages, proceeding in the presence of molecular oxygen, are the following: peroxide radical formation by C5 atom and its conversion with C5–C6 and O–O bonds break. An aldehyde group is formed by C5 atom, whereas formaldehyde is formed by C6 atom. At the irradiation of aerated starches the yield of CH_2O is twice higher than for the inert atmosphere [52].

The conclusions about a possibility of the formyl radical formation as a result of primary $\bullet\text{C6}$ and $\bullet\text{C1}$ radical conversions are confirmed by RYDMR measurements of free radical conversions in cellulose at room temperature, initiated by UV-irradiation [29]. The initial stage of photocatalytic degradation of cellulose indicates a typical anisotropic doublet spectrum of the formyl σ -radical with ~ 12.5 mT splitting. As the time of UV exposure of the sample increases, the intensity of components of this doublet (I) decreases and, simultaneously, another, more intensive doublet of the formyl radical with 13.6 mT splitting (II) occurs in the RYDMR spectrum. As suggested, the difference in the hyperfine (HF) splitting in formyl radical is related to two conformations of it, “bent” and “linear ones [53, p. 201]. Both doublets (I and II) possess an additional splitting. In the doublet I, in the range of intense fields, the triplet HFC with the central band of twice higher intensity compared with the intensity of the border bands (1:2:1) and the HFC constant equal 0.2 mT (spectrum 1, Figure 8.2) is clearly observed. For the doublet II, the bands are split into 5 components (≤ 0.2 mT) showing the ratio of intensity, also close to a binomial 1:4:6:4:1 (spectrum 2, Figure 8.2). As the time of sample exposure to UV irradiation is extended, the intensity of the doublet II lines is much more extended, and at this background the presence of bands of the initial doublet I becomes hardly observable (spectrum 3, Figure 8.2).

Analysis of the data allowed for a conclusion about the formation of two kinds of formyl radicals ($\text{HCO}\bullet\text{-I}$ and $\text{HCO}\bullet\text{-II}$) in irradiated cellulose, occurring at UV-irradiation of the sample longer than in the first case.

Additional splitting of the doublet lines with the constants about 0.2 mT indicates that unpaired electron at the radical $\text{HCO}\bullet$ interacts with protons of the surrounding. In the case I, it is interaction with two equivalent protons. These protons might be two protons of C5 atom in xylose molecule (reaction (8.17)) or (the second alternative) one proton belongs to xylose 5-deoxy-group and the second proton – to hydroxymethylene unit hydroxyl of the neighbor

glucose residue (in the elementary cellulose cell), bound by a hydrogen bond to formyl radical formed:

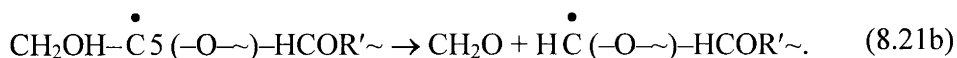


Sub-splitting to quintet of HCO^{\bullet} -II doublet in the spectrum indicates the interaction with unpaired electron with four equivalent protons. It may be suggested that three of these four protons belong to methyl group formed during C-H and O-H chemical bonds rearrangement in the radical $^{\bullet}\text{C}_6$ with hydrogen transition from hydroxyl at C6 to C5 in alkyl radical $^{\bullet}\text{C}_5$ (process (8.3), Section 8.4). Hence, similar to the radical $^{\bullet}\text{CHO}$ -I (the second alternative), the fourth proton may belong to hydroxyl at C6 of the hydroxymethylene unit of the neighbor glucose residue.

According to the estimation, the rearrangement of chemical bonds in the alkyl radical $^{\bullet}\text{C}_5$ takes $(8 - 10) \times 10^{-8}$ s [31]. Taking into account sub-splitting of the formyl radical doublet (into triplet or quintet), it may be noted that 5-deoxy-group formation in the glucose residue takes the same or shorter time.

According to the estimation [29], the yield of formyl radical (II) in cellulose, irradiated at room temperature, does not exceed 10% of total quantity of radicals, detected in the sample. Hence it appears that formaldehyde formation by this route of free-radical degradation of cellulose must not also exceed 10% of total yield of cellulose degradation products.

The third route of formaldehyde formation relates to the primary hydroxyalkyl radical $^{\bullet}\text{C}_5$ conversions by the isomerization reaction with C5-C6 bond break and hydrogen transition from hydroxyl C6 to C5 (reaction (8.21b)):



Resulting recombination of a radical with unpaired electron at C5 atom, formed in this case, D-xylose is synthesized. Basing on the above-mentioned experimental fact for starch radiolysis that

$$G(\text{xylose}) < G(\text{formaldehyde}),$$

it may be concluded that the primary radical $\cdot\text{C5}$ conversion with formation of formaldehyde by C6 atom and D-xylose might be the predominant process.

One more alternative of the radical $\cdot\text{C5}$ conversion by the reaction (8.21b), namely, not its recombination but isomerization with C5–O5 bond break and AGC disclosure with an oxo-group (or deoxy-group) formation by C5. In the first case, unpaired electron is transmitted from C5 to C1. The possibility of such process indicates results of experiments with irradiated crystalline preparations (monocrystals and crushed crystals) of xylose, arabinose and disaccharides (saccharose, lactose) [54]. As determined in these experiments, the fineness factor of crystals does not affect the yield of primary $\cdot\text{C5}$ radicals, but has an effect on the yield of molecular products of radiolysis – carbonyl compounds and oxy-acids: the yield of carbonyl compounds ($>\text{C5}=\text{O}$, $\cdot\text{C5}$ radical isomerization with C5–O5 bond break and unpaired electron transmission to C1 atom) in monocrystals of monosaccharides and saccharose is 1.5 – 3 times higher than in powders.

For polysaccharides irradiated in the absence of oxygen, the process of radical $\cdot\text{C5}$ isomerization under discussion with consequent recombination of $\cdot\text{C1}$ radical must yield in L-xylose formation. Among radiolysis products, xylose L-isomer recognition may finally confirm a conclusion about the existence of this sequence of elementary acts of the primary $\cdot\text{C5}$ radical conversion.

Fractional yields of D-xylose and formaldehyde, formed by the above-considered routes, are determined by the yields of radicals $\cdot\text{C6}$ and $\cdot\text{C5}$, are not determined yet.

The above-mentioned mechanism of formaldehyde formation in polysaccharides, irradiated in the presence of molecular oxygen, may be related to both conversions of C6–C5–OO \cdot peroxide radical caused by radiation and spontaneous into hydroxyl and alkoxy radicals, formed from the peroxide radical by reaction of hydroperoxide molecule substitution. Hence, alkoxy radical formed in this act may appear the precursor of formaldehyde after C5–C6 bond break in it.

Implementation of the first alternative related to the mechanism of peroxide radical annihilation by irradiation [38] is possible in the current system: for example, in the case of irradiation of native potato starch in the presence of molecular oxygen, the dose dependence of formaldehyde accumulation curve has a shape typical of saturation curves (in the studied dose range of 0 – 30 kGy the saturation plateau was observed at 6 – 8 kGy, with the

dose rate equal 67 kGy/h and $T = 300$ K [52]). According to the estimation made in the suggestion that in the presence of molecular oxygen in starch CH_2O is formed only via peroxide radicals, and the rate constant of radical annihilation by radiation at $T = 300$ K is $k = 0.36 \text{ kGy}^{-1}$. This value is by an order of magnitude, approximately, higher than the analogous value for the radiation annihilation of peroxide radicals in polytetrafluoroethylene (completely eliminated at the dose exceeding 60 kGy, $T = 300$ K [38]). Hence it appears that in the case of starches irradiation by 30 kGy dose at the dose rate equal 67 kGy/h, the process of peroxide radical treatment by radiation, including formaldehyde as the final product, lasts about 1 h. By the moment of extracting products of radiolysis from irradiated starch (by water extraction) not only formaldehyde formation from peroxide radicals in the solid phase will be finished, but CH_2O molecules in the starch solution or suspension may enter the above-mentioned reactions (the yields of formaldehyde detected in starches are $G \sim 1$ or lower [47, 52]).

Implementation of the second “peroxide” alternative and the contribution of such a process into total yield of formaldehyde in the irradiated polysaccharides may be estimated with respect to the results of accumulation of peroxides and free radicals in the postradiational period on the example lyophilizates of starches (amylose, amylopectin), dextrane, and ovalbumin solutions irradiated at room temperature [32]. Immediately after lyophilization of irradiated solutions of the above listed biopolymers, ESR investigations detected no radicals in these samples. Only peroxides were detected (H_2O_2 , ROOH, ROOR), which total concentration equaled $\sim 2 \times 10^{-4}$ mol/l. A day or two after, lyophilizates stored in the oxygen atmosphere at room temperature obtained radicals (two types of peroxide and alkoxy ones), which concentration increased with time increasing by an order of magnitude after 200 days of storage. The shape of the accumulation curve for free radicals in the lyophilizates is similar to the peroxide accumulation curve in the same solutions. Similarity of these curves indicates peroxides as the source of radicals. Hence their initial total concentration has not exceeded the corresponding concentration of peroxides in the solution (2×10^{-4} mol/l). Transiting to native starch samples with respect to all above circumstances (6% lyophilizate solutions; not all peroxides are sufficient for consideration, but just a one third part of them – hydroperoxides by C6 atom only at 30 kGy dose) and the sample storage time before analysis equal ~ 1.5 h, note that the concentration of radicals formed due to spontaneous degradation of peroxides during 1.5 h after irradiation termination does not exceed 1.5×10^{-7} mol/g.

Hence it appears that the yield of formaldehyde in the process most sufficient for us does not exceed $G = 0.05$.

Thus, the above-considered reactions of formaldehyde formation in irradiated polysaccharides by the free-radical mechanisms indicate that the main contributors into this process are primary $\cdot\text{C1}$, $\cdot\text{C5}$ and $\cdot\text{C6}$ radical conversions. The two-fold increase of CH_2O yield, observed at the starches irradiation in the oxygen atmosphere, is mainly caused by radiation-induced $\text{C5-C6-OO}\cdot$ peroxide radical conversions.

Methane

Among gaseous products of dewatered polysaccharides radiolysis (starches: potato (PS) and amylopectin (AS); cellulose (C); dextrane (D)), irradiated in the absence of oxygen at room temperature, methane was also detected. As native PS, AS and C preparations are irradiated, no methane is formed; at D irradiation methane is formed, but its yield is lower as compared with the water-free form [43]. Figure 8.11 presents curves of methane accumulation in polysaccharides with respect to the dose of irradiation [43, 55]. In this family of curves two areas may be outlined – for relatively low and relatively high doses. Obviously, in all polymers the initial yield of CH_4 is low. As the dose increases, the methane yield increases simultaneously, and the curves show two plateau (in the initial (low) dose range and at high doses) or demonstrate a tendency “to enter” a plateau (for AS and PS). Hence, the difference in stationary concentrations of CH_4 (corresponded to the plateau at both low and high doses) is the highest between D and other three polysaccharides (6 – 20 times), whereas between PS, AS and C it falls within the range of 2 – 3 times.

The step-like shape of dose curves indicates two sources of methane in these irradiated systems. Already at low doses, one of these sources produces CH_4 (let us call it conditionally “primary”). Hence, relatively low, compared with other polymers, quantity of methane is accumulated in D; at PS irradiation the highest yield of methane is observed in the initial dose range (Figure 8.11, Table 8.11).

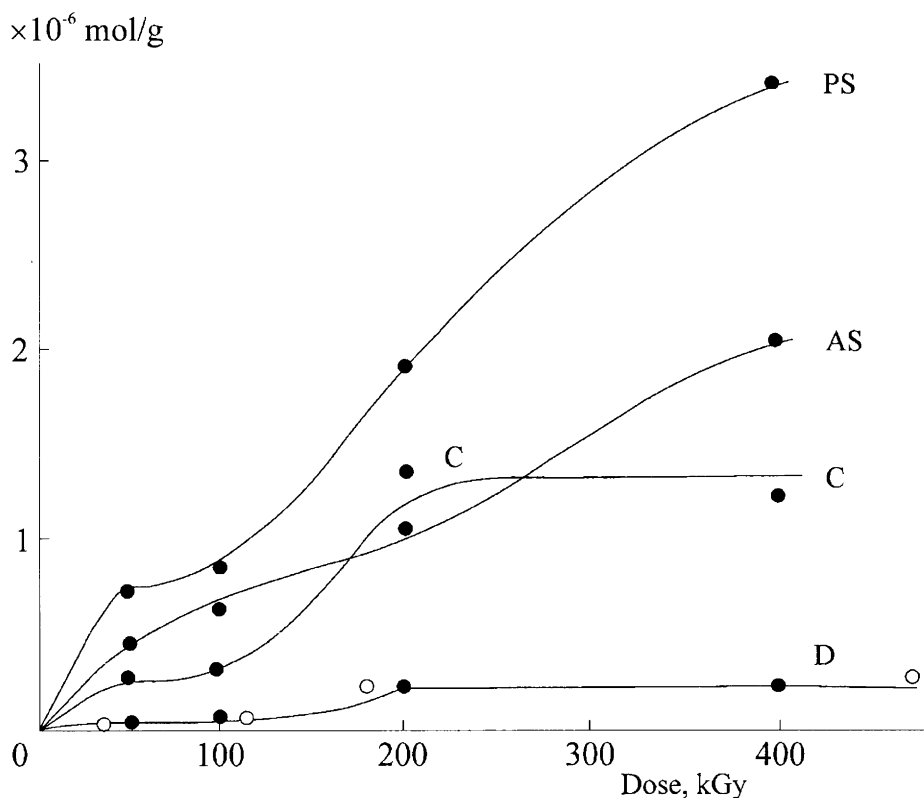


Figure 8.11. Accumulation of methane in water-free samples of potato (PS) and amylopectin (AP) starches, cellulose (C), and dextrane (D) samples, γ -irradiated at room temperature; o – methane accumulation in the native dextrane. The mass-spectrometry data, molecular CH_4^+ ion peak intensity was determined by the intensity of a fragment CH_3^+ ion ($m/e = 15$), the statistic data error is 4 – 6%

Table 8.11 presents radiation-chemical yields of methane $G(\text{CH}_4)$, calculated by initial sections of curves (formally, by initial points of the dose dependencies).

It is obvious that another source of methane (“secondary” methane) is represented by any product of macromolecule radiolysis, accumulated during irradiation of the sample and degraded by radiation or due to relative instability

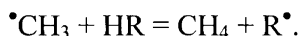
at room temperature: for each polysaccharide, stationary concentration of methane is reached at appropriate doses (the second plateau on the curves). Generally, the radiation degradation of polysaccharides proceeds by the free-radical mechanism [1, 43]. It might be suggested that one of free macroradicals is the immediate source of the secondary methane.

Table 8.11

Radiation-chemical yields of methane in water-free polysaccharides, γ -irradiated under vacuum at room temperature [55]

Sample	$G(\text{methane})$
Potato starch	0.14
Amylopectin starch	0.08
Cellulose	0.04
Dextrane	0.008

The following suggestion also seems natural: methyl radical must be immediate precursor of methane. This radical possesses mobility in irradiated polymers even at low temperatures and, moving in the matrix, may enter the reactions with immovable fragment of a macromolecule:



So far as concerns the place of origin of the primary CH_4 in AGC, the precedence should be devoted to the atom C6. Thus atom is bound to the greatest number of hydrogen atoms (two of them). As a consequence, to form the methyl radical from hydroxymethylene group by C6 atom, a hydroxyl should be removed from it, one H atom should be added to it, and C5–C6 bond should be broken. Of course, all the above-mentioned should be related to free (non-involved into glycoside bonds) hydroxymethylene $\text{C}_6\text{H}_2\text{OH}$ groups of polysaccharides only. Therefore, it is no wonder that at transition from irradiation of starches and cellulose (polysaccharides with glycoside C1–O–C4 bonds) to dextrane (glucose superpolymer possessing α -C1–O–C6 glycoside bonds) the yield of the primary methane ($G \sim 0.008$, Table 8.11) is 5 – 10 times lower.

It may be suggested that in the irradiated polysaccharide this primary methane is formed as a result of alkyl radical $\cdot\text{C}_6$ conversion ($\cdot\text{OH}$ detachment radical; in hydroxymethylene units C–OH bond breaks at radiolysis of dry

carbohydrates only [1]) with methyl radical formation according to Figure 8.12.

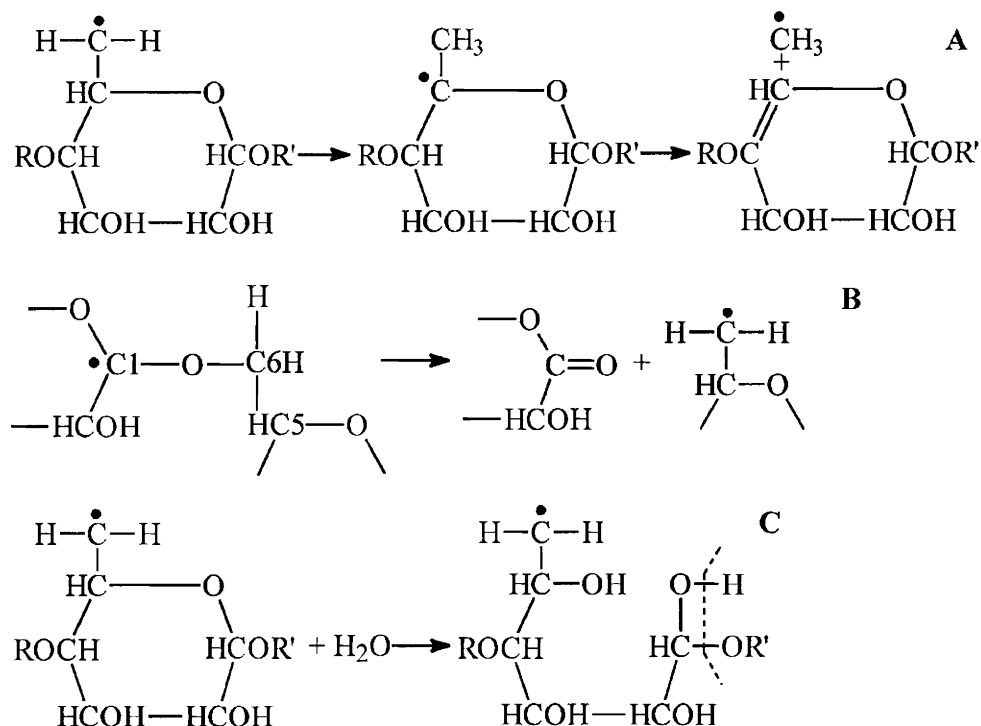


Figure 8.12. The mechanisms of $\cdot\text{C6}$ and $\cdot\text{C1}$ radical transformations with methyl radical formation in irradiated dry polysaccharides

The first and the second stages of the process A represent rearrangement of chemical bonds C-H at the 5th, 6th and 4th carbon atoms, and the act of methyl radical detachment by alkyl radical with double C4=C5 bond formation in AGC. The scheme is composed with respect to the investigation results on isomerization of the so-called end and middle alkyl radicals of the polymer with formation of methyl radical in γ -irradiated polyethylene [53, p. 226].

As suggested, the secondary methane formation is related to C1 glycoside radical (C1-O-C6) conversion, occurred at atom H detachment from C1 atom in the primary act or as a result of H-C1 bond attack by H atoms or $\cdot\text{OH}$ radicals. This is the circumstance, which may explain methane formation

in both water-free and native D samples. Among primary radicals, the hydroxyalkyl radical $\bullet\text{C1}$ is mainly detected in native polysaccharides at room temperature. The first stage of this radical conversion includes β -bond break with lactone formation from the initial AGC and unpaired electron transfer from C1 to C6 of the neighbor AGC, proceeding in accordance with Figure 8.12B [55]. Further conversion of alkyl radical $\bullet\text{C6}$ proceeds according to the scheme in Figure 8.12A.

An additional reason for the benefit of the scheme in Figure 8.12 is the already mentioned fact of the water-induced methane formation inhibition in irradiated native polysaccharides by the reaction in Figure 8.12B (hydrolytic splitting of the β -bond). Therefore, the plateau at the dose curves (at reaching stationary concentrations) of methane formation by irradiation of water-free samples (Figure 8.11) might be explained by accumulation of water in irradiated samples due to dehydration of free radicals formed [43]. If it is assumed that the outcome of the methane accumulation dose curves to the second plateau is related to the rate of β -bond hydrolytic splitting in glycoside radicals of polysaccharides (the lower the plateau is, the higher the inhibition rate of methane formation is), then the relative efficiency of H_2O interaction with glycoside radicals in polysaccharides is as follows:

$$\text{D:C:AS:PS} = 1:0.8:0.5:0.15.$$

For the purpose of checking the suggested mechanism of methane formation, the sequences of elementary acts of radicals $\bullet\text{C1}$ and $\bullet\text{C6}$ conversions, demonstrated in Figure 8.12, were modeled by analogy to ref. [24], according to the program allowing the analysis of proceeding and the route of primary $\bullet\text{C1}$ and $\bullet\text{C6}$ radical conversions with rearrangement of C–H bonds and C–O and C–C bonds dissociation in the AGC composition with respect to selection of the most energetically profitable route. The computer modeling of primary $\bullet\text{C1}$ and $\bullet\text{C6}$ radical conversion are equivalently reflected by routes (2) and (3) (Figure 8.12) [55, 56].

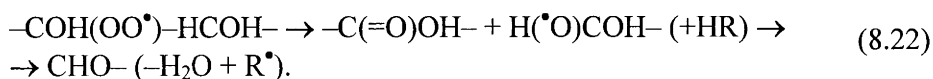
The use of a highly sensitive technique of nano-layer magnetic resonance spectroscopy (RYDMR) for the study of the origin and free radical conversions in cellulose at room temperature, occurring UV-irradiation of the sample in the presence of a sensitizer, confirmed the sequence of elementary acts of radical conversions, presented in the Figure 8.12A [31], and estimate times of their occurrence in the surface layer of the sample: the first and the

second stages of the process presented in Figure 8.12A last $(5 - 8) \times 10^{-8}$ s, and the stage of methyl radical formation takes about 10^{-7} s.

Mono- and dicarboxylic, citric and quinic acids

Among radiolysis products of native potato and corn starch preparations (12% humidity, γ -irradiation by 40 – 1,000 kGy dose in air at room temperature), citric, dicarboxylic (succinic, malic, fumaric, tartaric, malonic), pyruvic and glyoxylic acids were detected [34, 47]. All these acids are members in the set of eleven carboxylic acids of the so-called glyoxylate Krebs cycle – one of the metabolism components, the assembly of biochemical processes providing vital activity of the organism. Therefore, inclusion of such compounds, derived by radiation modification from polysaccharide-containing waste of food industry and agriculture, into cattle forage would also promote increased digestibility of the forage and solution of the problem of this waste type utilization with the help of a simple γ -irradiation technology [1].

These acids were recorded at irradiation of native starches, but not their solutions. Since the radiation degradation of macromolecules proceeds by the free-radical mechanisms, in solid samples primary radicals must convert by monomolecular degradation reactions. The above-listed acids are compounds containing 2 – 5 carbon atoms. This indicates that the stage of final molecular product formation must be preceded by C–C bond break in polysaccharide AGC. Such process in starches, γ -irradiated in the presence of molecular oxygen, is realized as a result of formation and conversions of peroxide radicals [1]. These radicals are formed due to primary alkyl and hydroxyalkyl radicals with molecular oxygen. In the first case, C–C bond break is accompanied by occurrence of two aldehyde groups in AGC; in the second case, it is accompanied by formation of one carboxylic and one aldehyde group by the reaction (8.22) below [1, 35]:



The process of C–C bond break in AGC also happens due to conversions of oxygenated (peroxide) secondary (allyl) radicals by the reaction (8.18a) [1].

The formation of carboxylic acids with unsaturated bonds and deoxy-groups indicates that, at least, one of the stages in the multistage conversions of appropriate primary radicals represents dehydration of a radical according to the mechanism of H_2O β -elimination with allyl radical formation [1].

Thus, the composition (structure) of carboxylic acids indicates that during their formation in starch AGC dehydration, oxygenation and radical conversions with C–C chemical bond break may also proceed. In some cases of polysaccharide, low-temperature irradiation and subsequent annealing of the samples, some stages of the primary free radical conversions were recorded by the ESR method [1].

For cellulose tested at room temperature, the RYDMR method allowed for detecting the basic sequences of elementary acts of primary radical conversions up to formation of the radicals-precursors of the final molecular products. This gives an opportunity to compare results of the RYDMR spectrum analysis, implemented on irradiated cellulose, with the mechanisms of carboxylic acid formation in other polysaccharides.

Among the mechanisms of carboxylic acids under consideration, the most "huge" mechanism seems to be formation of the tribasic citric acid [37]. The final stage of this acid formation is the reaction of nucleophilic addition of formic acid to carbonyl group of keto-dicarboxylic acid (both these acids represent starch radiolysis products). In the carbonyl group, the electrophilicity of C and O atoms is different: the π -bond is partly polarized, and α -proton from HCOOH in the acidic medium is one of the main products of starch radiolysis (the yield of which reaches 80% of total initial yield of the acids [48]). The bell-like shape of the dose dependence of this acid accumulation indicates the participation of starch in reactions with other products of radiolysis.

Let us analyze a possibility of this process realization according to the free-radical mechanism, basing on the above data on reactions typical of irradiated polysaccharides and suggesting that in citric and dicarboxylic acid molecules one of carboxylic groups is formed from $-O_5-C_1(-O'1)-$ fragment.

The molecule of citric acid contains two deoxy-groups (the second and the fourth carbon atoms). The most probable process providing their formation in the molecule (with respect to conversions within AGC of only one radical) is conversion of the primary radical $\cdot C_2$, hydroxyl detachment radical from the second carbon atom according to the mechanism of H_2O β -elimination, namely, H atom detachments from the third carbon atom and OR from the fourth carbon atom (allyl radical is formed) with subsequent H atom transfer

from hydroxyl at C3 atom to C4 atom (the phenomenon of tautomerism); by C3 atom a keto-group is formed (Figure 8.8).

Time of occurrence of detachment radicals $\bullet\text{OH}$ in AGC is $(3 - 7) \times 10^{-9}$ s. The radical dehydration with allyl radical formation in AGC lasts about $(1 - 3) \times 10^{-8}$ s [31]. As shown by computerized modeling, migration of the double bond $\text{C3}=\text{C4} \rightarrow \text{C3}=\text{O3}$ (due to tautomerism) may be accompanied by H-C1 and H-C2 bond rearrangement (H atom transfer from C1 to C2 and unpaired electron migration from C2 to C1). This process in AGC of irradiated cellulose lasts about $(8 - 10) \times 10^{-8}$ s. Allyl radical $\bullet\text{C5}$, formed in this case at the interaction with molecular oxygen ($k \sim 2 \times 10^{10}$ l/mol·s), produces peroxide radical and hydroperoxide group by C5 atom.

Peroxide C5 conversion in the irradiated starch includes rearrangement with the break of chemical bonds C5-C6 in AGC and O-O in the peroxide group. As a result, an aldehyde group -C5HO and hydrated molecule of formaldehyde by C6 in AGC are formed. The latter represents an ideal "procurement" as a reagent-companion for the aldehyde group -C5HO in the Cannizzaro reaction. This process (disproportioning) induces occurrence of methanol (the yield¹⁾ of methanol in corn starch is $G \sim 0.1$ at the dose about 10 kGy [47]) and 3-ketoglutaric acid. As mentioned above, the interaction of 3-ketoglutaric acid with formic acid produces citric acids (with the yield up to 33.5% of total yield of multibasic acids [33]).

Thus conversion of the primary alkyl radical $\bullet\text{C2}$ up to formation of citric acid molecule consists of 6 stages (a sequence of 6 elementary acts). Duration of these stages of the free-radical process (without consideration of non-radical reactions duration - the Cannizzaro reaction and nucleophilic addition at the interaction between 3-ketoglutaric and formic acids) falls within the range of $(3 - 7) \times 10^{-9} - 10^{-8}$ s. Note that at the sample irradiation the latest, sixth stage may represent conversion of not peroxide itself, but peroxide precursor - peroxide radical $\bullet\text{C5}$ [22]. This note also concerns the schemes 4 and 5.

The alternative conversion of the primary radical $\bullet\text{C2}$ relates to succinic acid formation and includes 5 stages. The sequence of elementary acts is the following: rearrangement of bonds H-C1 \rightarrow H-C2 (unpaired electron transits to C1), radical $\bullet\text{C1}$ isomerization with C5-O5 bond break and alkyl radical $\bullet\text{C5}$ formation, β -elimination of H_2O (from C4-C3), radical $\bullet\text{C5}$ oxygenation and hydroperoxide group formation by C5, hydroperoxide (or peroxide radical $\bullet\text{C5}$) conversion with C4-C5 bond break in AGC and O-O bond break in peroxide

group and, finally, succinic acid and glycol aldehyde formation (after hydrolysis of two glycoside bonds in AGC). The yield of succinic acid equals 4.6% of total yield of multibasic acids [35].

The comparison of citric and succinic acid yields indicate that the differences in them may be stipulated by the effect of the following factors: a stress in the AGC fragment C1–C2–C3–C4 appearing due to a change in configuration of chemical bonds at unpaired electron occurrence at C2 and “retaining” the macroradical structure by right and left halves of the initial polymeric molecule, the quantity and sequence of radical $\cdot\text{C}2$ conversions, radical reaction durations (β -elimination of water, H–C1 and H–C2 bond rearrangement, isomerization with C–C and C–O bond break).

Among these factors, obviously, the first is the most valuable. The stress occurred in the above-mentioned AGC fragment and, obviously, the structure of this monomeric unit define the route of radical $\cdot\text{C}2$ conversion – the reaction of water β -elimination type by C3–C4 then leading to citric acid, or C1–H and C2–H bond rearrangement leading to succinic acid (V). In the case of citric acid, rearrangement of the above-mentioned chemical bonds under the effect of ionizing radiation happens in the allyl type radical and requires lower energy than in the case of succinic acid, for which rearrangement proceeds in the alkyl radical. The difference in optical absorption spectra of such radicals equals ~ 1.8 eV [53]. The second factor, which is the difference in the structure of the initial radicals eliminating ROH and H₂O and the energy performance of this process, may also affect the relative yield of citric and succinic acids. In the first case, a break occurs in the macromolecule (the stress in the radiation-modified AGC is removed). In the second case, water molecule is released, and C5–C4=C3 fragment in AGC obtains flattened configuration of σ -bonds. Quantitative estimation of the relative validity of each of these factors requires additional investigations.

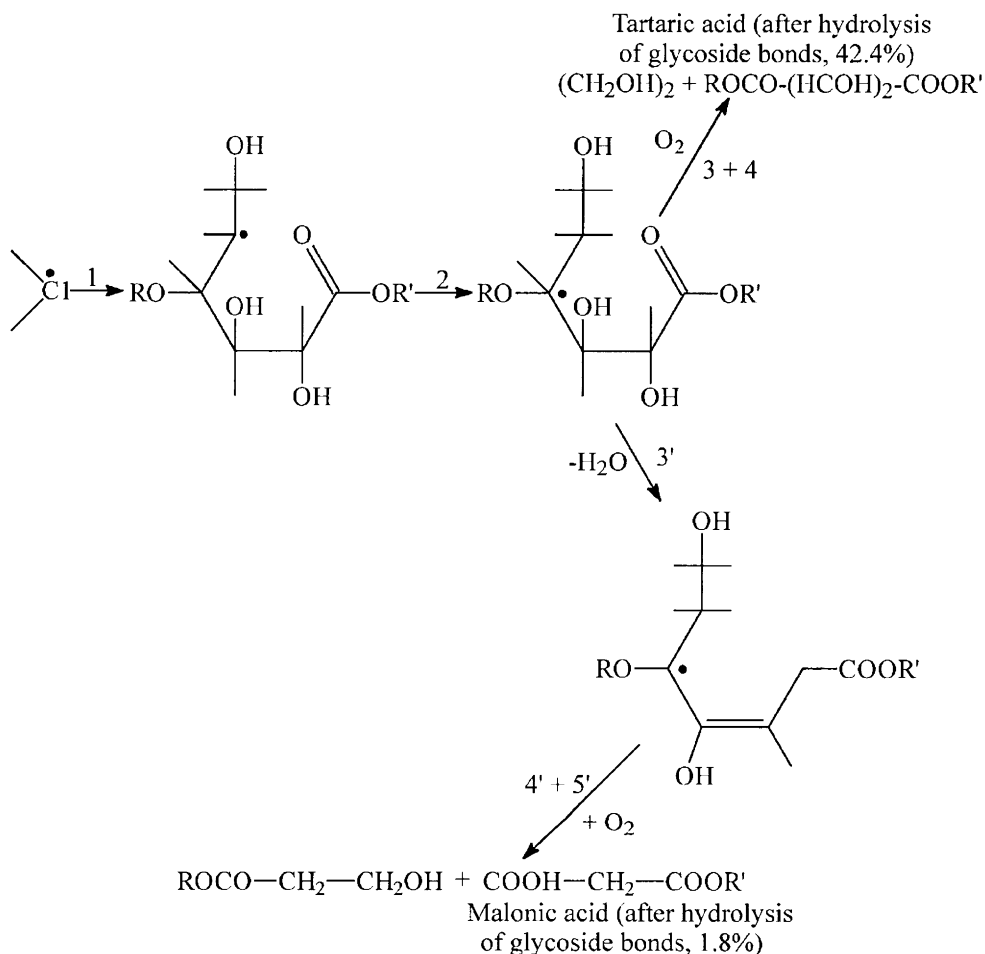


Figure 8.13. The mechanism of malonic acid in the irradiated starches

If the differences in the mechanisms of radical $\cdot\text{C}2$ conversions by two routes affect upon the time of molecule formation for each of two mentioned carboxylic acids (speaking about radical conversions but not about non-radical reactions), these times must not exceed the error range in the estimation of times of the elementary acts of reactions between radicals [31]. Hereof, the differences in the yields of citric and succinic acids are most likely related to conditions of non-radical reactions proceeding.

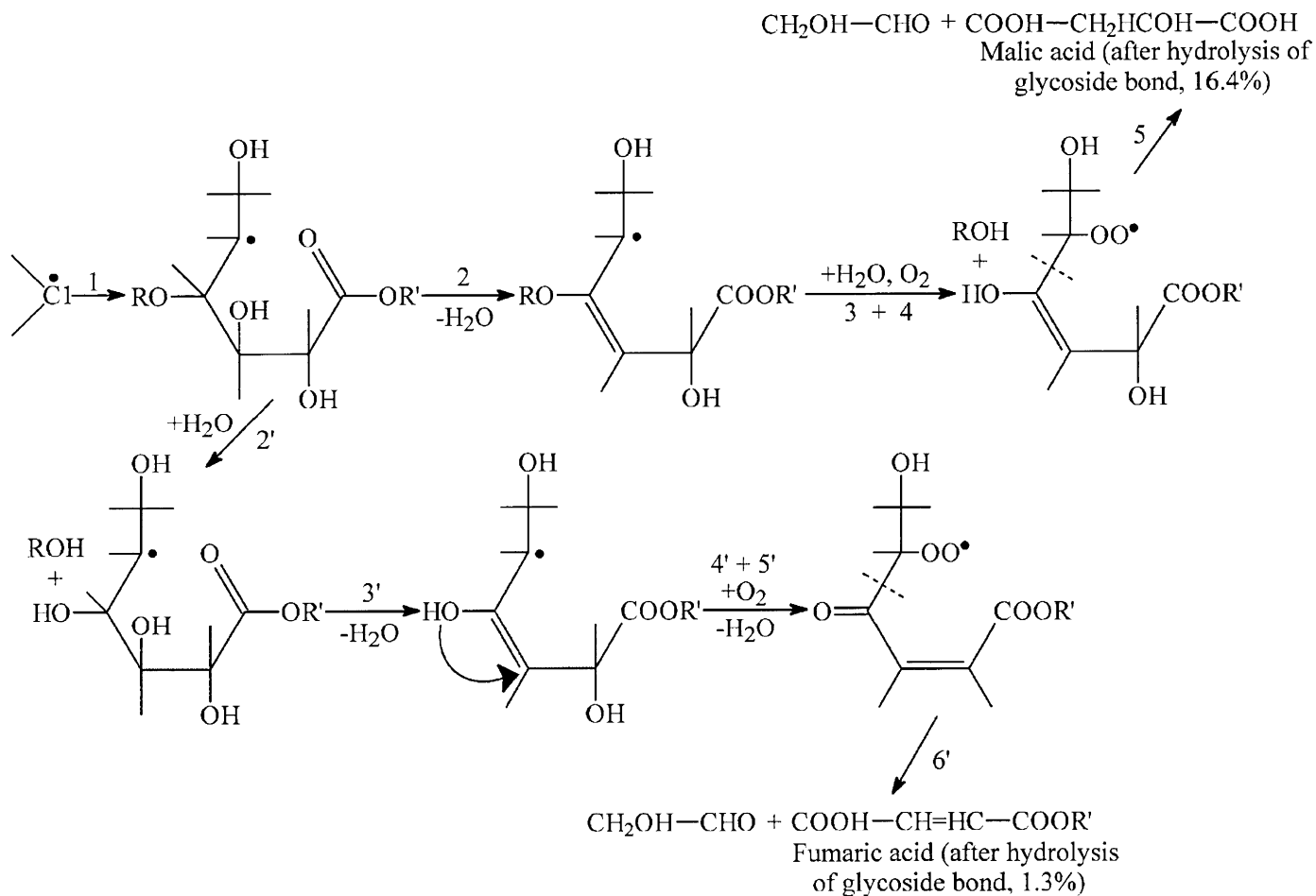


Figure 8.14. The mechanism of fumaric acid formation in irradiated starches

The ratio of citric and succinic acids yields is 7:1 [35]. Since the yield of glycol aldehyde is $G = 0.15$, at the observation of the material balance conditions by the products, in accordance with Figure 8.9, the equality of the yields of glycol aldehyde and succinic acid is determined. Therefore, the citric acid yield should be:

$$G = 7 \times 0.15 - 1.05.$$

The formation of malic, fumaric, tartaric and malonic acids is related to conversions of the primary hydroxyalkyl radical $\bullet\text{C1}$, the initial elementary act of which represents isomerization with C5–O5 bond break – the disclosure of AGC and formation of a “procurement” for one (or two) carboxylic group –C1OOH. For alkyl radical $\bullet\text{C5}$ formed in this case, two routes of conversions are observed:

- 1) conversions related directly to the radical $\bullet\text{C5}$ – dehydration (β -elimination of water – H atom detachment from C4 and OH detachment from C3 – the route to malic acid formation) or β -bond hydrolysis and consequent β -elimination of water (the route to fumaric acid formation, Figure 8.13);
- 2) chemical bond H–C4 and H–C5 rearrangement (H atom transfer from C5 to C4 and unpaired electron transfer to C4, which is the route to tartaric and malonic acid formation, Figure 8.14).

The formation of malic acid includes 4 stages of the primary radical $\bullet\text{C1}$ conversions, whereas fumaric acid is formed in six stages (Figure 8.14). Most likely, the shorter number of stages is the reason for more than an order of magnitude difference in the yields of these acids: 16.4% (for malic acid) and 1.3% (for fumaric acid) [35]. The attention should be paid to the dehydration act (proceeding by C2–C3 bond, after H atom transfer from hydroxyl at C4 to C3 due to tautomerism phenomenon, stage 4') of allyl radical $\bullet\text{C5}$ formed. As a result, the carbon backbone C4–C3–C2–C1 of disclosed AGC possesses a conjugation chain of double bonds. This process is energetically more profitable for a radical rather than for dehydration of an acid molecule (which requires heating to 383 K).

According to estimation, the sequence of radical $\bullet\text{C1}$ conversion with malic acid formation (except non-radical reactions) proceeds during time

within the range of $(3 - 7) \times 10^{-9} - \sim 10^{-7}$ s, whereas the time of fumaric acid formation is 3 – 5 times longer [29].

The general stages in the sequences of radical $\cdot\text{C1}$ conversions with tartaric and malonic acid formation (scheme (5)) are the following: isomerization with C5–O5 bond break and H–C4 and H–C5 bond rearrangement (H atom transfer from C4 to C5 atom and, correspondingly, unpaired electron transfer from C5 to C4 atom). Obviously, the latter stage is realized due to action of the “structural” factor: $\text{sp}^3 \rightarrow \text{sp}^2$ transition at C4 atom removes stress in C4–C3–C2–C1 fragment in alkyl radical $\cdot\text{C5}$ of disclosed AGC. This is the factor affecting the yield of tartaric acid (which is the highest – 42.4% [35]). For tartaric acid formation, the sequence consists of 4 stages; for malonic acid – it is 5 stages (Figure 8.14). The yield of tartaric acid is 25 times higher than for malonic acid [35], which is due to additional stage – β -elimination of water in malonic acid.

The formation mechanisms of the above-mentioned monobasic (pyrotartaric and glyoxylic) acid formation in starches are related to conversions of the primary radicals, formed by H atom detachment from C4 and C2, respectively, and include the following stages. For pyroracemic acid, four stages are observed:

- 1) C5–O5 β -bond hydrolysis;
- 2) β -elimination of water (H atom detachment from C5 atom and OH-group detachment from C6 atom);
- 3) the interaction of occurring allyl radical with molecular oxygen;
- 4) hydroperoxide formation by C5 atom, which degradation with C3–C4 bond break leads to pyroracemic acid formation with the yield $G \sim 0.01$.

For glyoxylic acid, four stages are observed:

- 1) C1–O5 β -bond hydrolysis;
- 2) peroxide radical and hydroperoxide formation by C2;
- 3) hydroperoxide degradation with C2–C3 bond break;
- 4) glyoxylic acid ($G \sim 0.03$) and erythrose ($G \sim 0.01$) formation.

The alternative process of C4OOH hydroperoxide (or its precursor – peroxide radical) degradation with C4–C5 bond break is accompanied by

acetic acid formation ($G \sim 0.03$). According to the estimation results, all these processes proceed at a time shorter than 10^{-7} s.

As one of the intermediate stages of the radical conversions, all the above-considered mechanisms of carboxylic acid formation include oxidation – oxygenation of one radical or another with formation of peroxide radical and then peroxide. The exception in the sequence of the mechanisms of carboxylic acid formation is the **free-radical mechanism of quinic acid synthesis**.

Quinic Acid (QA) was detected only at irradiation of waxy corn starch (WCS). Its yield equals 0.7 wt.% of total quantity of carboxylic acids (low-molecular ones, including formic and acetic acids giving 89% yield, and high-molecular acids giving 11% yield; see Table 8.12) [57].

Table 8.12

Composition and yield (wt.%) of carboxylic acids in the irradiated waxy corn starch [57]

Acid	Yield
Tartaric	37
Citric	28
Malic	12.5
Succinic	4.1
Fumaric	0.3
Quinic	0.7
Glucuronic	0.9
Formic + acetic	4
High-molecular	10.9

According to the estimation results (at 0.9kGy dose), the radiation-chemical yield of quinic acid equals $G(\text{QA}) \sim 0.02$ per 100 eV of absorbed energy. This relatively low yield and the fact of QA detection exclusively in the irradiated starch containing 96% amylopectin (α -glycoside bonds $1 \rightarrow 4$ and α -1 $\rightarrow 6$ per every 20 monomeric units) allowed for a suggestion that QA molecules are synthesized only during modification of anhydroglucose cycle (AGC) with two types of glycoside bonds – in the branching points of amylopectin. Obviously, due to low concentration of amylopectin in natural starches (from 15 to 25 wt.%) no QA synthesis at their irradiation was observed.

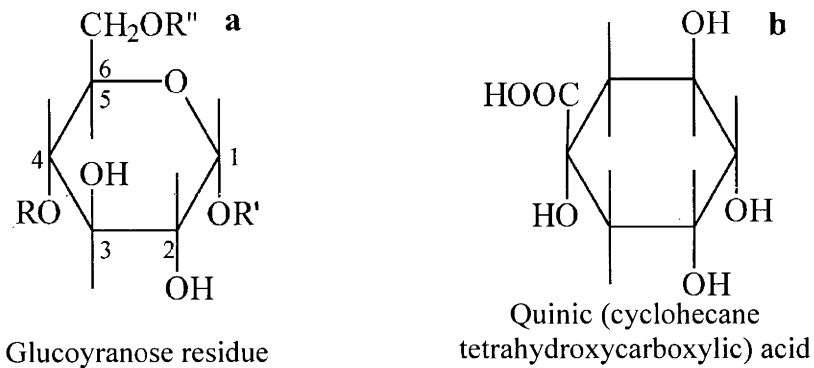


Figure 8.15. Structural formulae glucose and quinic acid residues

The comparison of the structural formulae of α -D-glucoyranose (a) and quinic (cyclohexane tetrahydroxycarboxylic) acid (b) in Figure 8.15 unambiguously indicates that at “radiation construction” of QA molecule (b) from AGC (a), the following conversions happen in AGC: Oxygen atom is detached from the cycle, deoxy-groups by atoms C3 and C5 are formed, and carboxylic group occurs at C4 atom. The final stage is formation of chemical bond C1–C6 and, as a result, a cyclohexane ring is formed.

The data obtained [24, 29, 35] indicate a possibility of the “radiation construction” of the QA molecule in the framework of the free-radical mechanism. As is known, the elimination of semi-acetal oxygen from AGC in cellulose (β -glycoside 1 \rightarrow 4 bond) is induced by the primary alkyl radical \cdot C3 conversions (OH detachment) [29]. Figure 8.16 presents a scheme according to the data from [27]. It shows the totality of elementary acts (the mechanism) of radical \cdot C3 conversions. At the first stage of this multistage process, a dienyl radical $C1=C2-C3=C4-C5$ and H_2O molecule are formed. (from H atoms detached from C2 and C4 atoms and O5 atom, the mechanism of β -elimination of water), stages 1 – 3 (Figure 8.16).

In the dienyl radical atoms C1, C2, C3 and C4 are located in the same plane, from which the atom C5 is displaced by 0.7 \AA [24]. Obviously, similar to the cellulose AGC, the presence of glycoside bonds in WCS (R–O–C4, C1–O–R', and C6–O–R'' bonds in the branching points) induces a stress of the dienyl radical structure. As a consequence, the modified AGC of WCS may also demonstrate rearrangement of chemical C–H bonds at C6 and C5 atoms

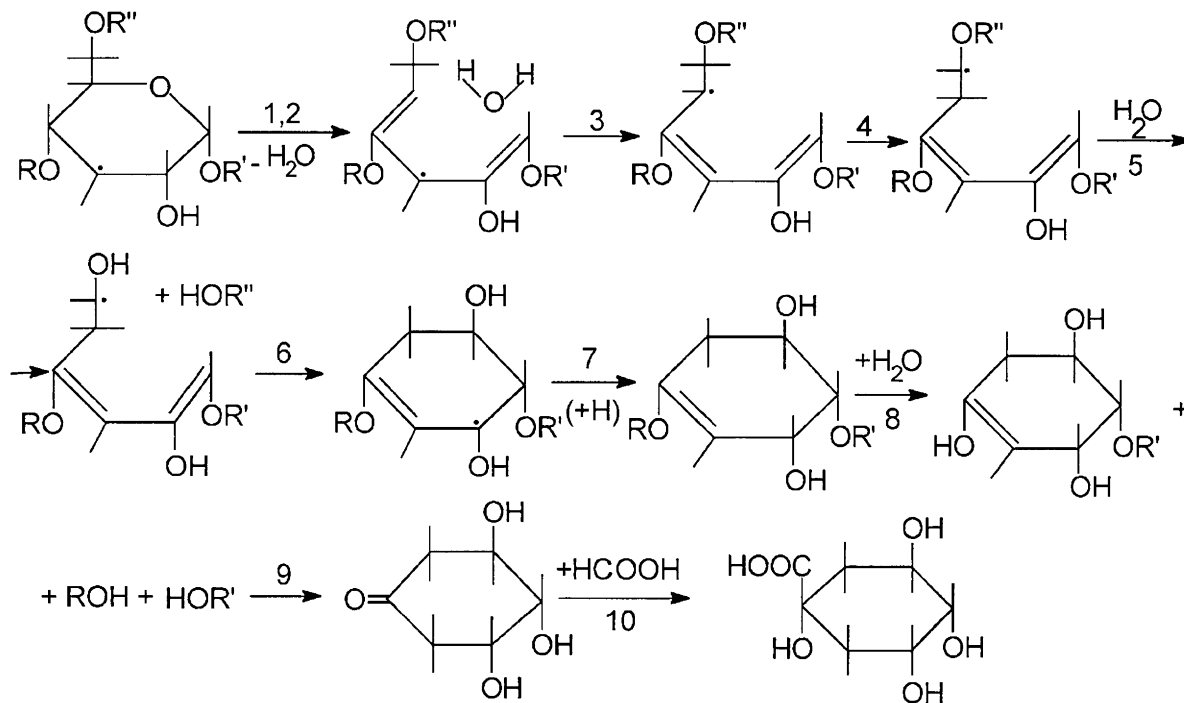
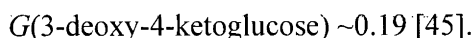


Figure 8.16. The mechanism of quinic acid formation in amylopectin starch

with H atom transition from C6 to C5 atom and, respectively, unpaired electron transition from C5 to C6 atom [24]. As a result of β -bond hydrolysis in $\bullet\text{C}_6\text{H}-\text{O}-\text{R}'$ radical (β -break of a vicinal bond [58]) with a suggested formation of water molecule, previously observed at the same place, an end hydroxyalkyl radical $\bullet\text{C}_6\text{H}-\text{OH}$ [41] (Figure 8.16, stages 4 and 5) occurs. As this radical attacks the C1C2 bond by C1 atom, a chemical C6–C1 bond is formed, and the ring is locked. As alkyl radical $\bullet\text{C}_2$ formed by the addition reaction of radical $\bullet\text{C}_6\text{HOH}$ by double bond, is reduced, a cyclohexane-3,4 ring in amylopectin molecule (by the place of the previous branching point) is formed (stages 6 and 7).

As the irradiated sample contacts water, hydrolysis of glycoside C1–O–R' and R–O–C4 bonds in modified amylopectin AGC and hydroxyl-group tautomerism by C4 atom at double C3=C4 in the final product of WCS radiolysis, a keto-group by C4 and deoxy-group by C3 atom are formed (stage 9). The formation of compounds of this type was detected at γ -irradiation of crystalline D-glucose:



The interaction of keto-group with formic acid (stage 10) produces quinic acid. The analogous process (the reaction of nucleophilic addition) also proceeds for citric acid formation – at the interaction of the precursor (3-ketoglutaric acid) with HCOOH (Figure 8.10) [35].

Time ranges, obtained by RYDMR technique, and the sequences of basic radical types conversion in cellulose exposed to photo influence [31] allowed for estimation (in the first approximation) of conversion times of analogous radicals in radiation-modified AGC of WCS. Hence, it is suggested that due to the presence of three glycoside bonds in AGC (the branching point of amylopectin) the primary $\bullet\text{C}_3$ radical conversions proceed similar to AGC of cellulose crystallite.

It seemed to be of interest to compare times of formation of radicals in the polymer and the rate constants of their reactions in the multistage sequence of elementary acts of the primary $\bullet\text{C}_3$ radical conversions up to QA formation and, therefore, determine the limiting stage.

At dehydration of the primary radical in cellulose, the allyl type radicals (and water molecules) are formed during $(1 - 3) \times 10^{-8}$ s [31]. The time of double bond rearrangement in dienyl radical (stage 4) is comparable with duration of the consequent rearrangement of chemical C–H bonds at C6 and

C5 atoms, which is $(5 - 8) \times 10^{-8}$ s [31]. To estimate time for hydrolytic splitting (β -break) of the glycoside bond in the radical $\cdot\text{C6H-R''}$ with the end alkyl $\cdot\text{C6HOH}$ radical formation, the following experimental data were used. The rate constant of saccharose inversion ($k = 4.2 \times 10^{-4}$ l/mol·s) was accepted for as the basic value and, taking into account the fact that carbon-centered carbohydrate radicals at the glycoside bond possesses $k(g)$ four orders of magnitude higher than in the case of usual glycoside bond [59], for the radical $\cdot\text{C6HO-R''}$ we obtain the constant of β -bond hydrolysis equal $k(g) \sim 4.2$. Therefore, for these radicals the time of β -bond hydrolytic splitting may be estimated under the suggestion that their concentration in irradiated WCS is 10^{-4} M^{-1} , $t = 60 \text{ min}$.

According to the data obtained [60], for the liquid phase, the rate constant of alkyl radical addition by double bond is rather high: 10^5 l/mol·s. In this case, when C6–C1 chemical bond is formed at the cycle of six carbon atoms locking, the rate constant of the reaction is higher and the process duration may be comparable with the time of rotary vibrations of macromolecule units of the polyethylene type in a liquid solution equaling 10^{-8} s. Thus the limiting stage in formation of the cyclohexene ring proceeding due to primary $\cdot\text{C3}$ radical conversion (Figure 8.16) may be represented by the above-mentioned stage of hydrolytic β -bond in the radical $\cdot\text{C6HO-R''}$.

Therefore, for the purpose of active effect on the yield of quinic acid in the free-radical process of this sequence, “dry” e.g. native WCS samples must be irradiated in the absence of oxygen.

As the first condition is observed, the possibility of the primary peroxide radicals, $\text{C5OO}\cdot$, in particular, is observed, and the radical $\cdot\text{C2}$ recombination is provided (stage 7, Figure 8.16). As shown in the scheme mentioned, the formation of radical $\text{C5OO}\cdot$ and rearrangement of C6–H and C5–H bonds are competing processes. The conversions of $\text{C5OO}\cdot$ radical are accompanied by C5–C6 bond break with aldehyde group formation by C5 atom and formaldehyde molecule formation by C6 atom. For starches irradiated in the presence of molecular oxygen, $G(\text{CH}_2\text{O}) \sim 0.7$; disproportioning of the aldehyde group C5HO and CH_2O leads to formation of carboxylic (by C5 atom) and alcohol (methanol – by C6 atom) [35].

The irradiation of water-free native WCS preparations (the second condition of irradiation) excludes premature hydrolytic splitting of the glycoside bond R–O–C4, which might impede rearrangement of C6–H and

C5-H bonds and, hence, the end hydroxyalkyl $\cdot\text{C}_6\text{HOH}$ radical formation (stage 5, Figure 8.16).

Table 8.13

The decrease of water content and increase of gaseous products at γ -irradiation of native and evacuated polysaccharides at room temperature [61]

Polysaccharide humidity, %	Native samples, O ₂			Water-free samples			
	G(H ₂ O)	G(H ₂)	G(CO ₂)	G(H ₂ O)	G(H ₂)	G(CO ₂)	G(CO)
Potato starch, 13	6.7 (100)	14.3	0.6	0.1	0.5	0.2	0.5
Amylopectin starch, 11	7.6 (175)	3.5	0.7	0.3	1.5	0.1	1.8
Dextrane, 11	4.9 (135)	6.8	0.9	0.4	1.3	1.0	0.5
Cellulose, 4	25 (115)	1.9	1.1	0.6	1.2	1.0	0.3

The following experimental fact is noteworthy: the relative QA yield in WCS, irradiated in the presence of molecular oxygen, is 40 times lower compared with the yield of citric acid (Tables 8.10 and 8.13). The multistage part of both processes is practically identical (7 and 6 staged, respectively) and includes identical basic stages of radical conversions. To be more correct, their sequence is different and includes different primary radicals – $\cdot\text{C}_3$ and $\cdot\text{C}_2$, respectively (compare schemes in Figures 8.10 and 8.16) [35]. To the authors' point of view, such difference in the yields of acids is defined by two factors. Firstly, citric acid is formed at modification of all AGC, whereas QA is formed from AGC branching points ($\sim 100/20 = 5$), and the dominating factor (8) represents the formation and conversion of the peroxide radical by C5 atom (is defined by molecular oxygen access to radical $\cdot\text{C}_5$).

As follows from the above-mentioned, in the absence of molecular oxygen both oxygenation of any radical in the multistage process of the primary alkyl radical $\cdot\text{C}_3$ conversion and the possibility of hydroxyl-alkyl radical $\cdot\text{C}_2$ recombination (stage 7, Figure 8.16). Taking into account the fact that quinic acid is detected only at the irradiation of waxy corn starch aerated

native preparation and accumulated in the sample with relatively low yield (Table 8.13), it may be assumed that this product is formed in AGC only – the branching points of amylopectin (in amylopectin it is present after every 20 monomeric units), and O₂ access to free radicals in this modified AGC is hindered.

To conclude this Section, let us note that:

- 1) The schemes of free-radical mechanisms shown for carboxylic acid formation in starches (polysaccharides) exposed to radiation are stereotype – they include the above-mentioned reactions as the stages of the radical conversions. The main difference in the formation mechanisms of each dicarboxylic acid – this is the order in sequences of such stages, which is obviously stipulated by lower or higher stress of AGC, modified by irradiation. The comparison of acid synthesis durations (falling within the range of $7 \times 10^{-9} - 10^{-7}$ s) and the values of their radiation-chemical yields (from the hundredth parts to units) shows that dehydration and β -bond hydrolysis proceeding in primary radicals during conversions increases time of reactions and reduces the yield of acids;
- 2) The formation of acids is mostly related to the conversions of primary hydroxyalkyl and alkyl radicals of $\cdot\text{C}1$, $\cdot\text{C}2$ and $\cdot\text{C}4$ type.

8.7. THE ROLE OF ADSORBED WATER IN FORMATION AND CONVERSIONS OF MACRORADICALS; RADIOLYSIS OF THE STRUCTURED STARCH–WATER SYSTEM

The investigators of radiolysis of polysaccharides are meeting extremely high variability of parameters characterizing degradation processes, even at operations with the same type of polymers. This is stipulated by unequal content of water, adsorbed by the polymer, which radiolysis defines the degradation of macromolecules [43, 61].

To clear it up, let us consider two sets of experiments. In the first set performed in the sealed ampoules in the air atmosphere the samples with natural humidity were irradiated (the so-called native, dry preparations), which were potato and amylopectin starches (PS, W – humidity 13 wt.%;

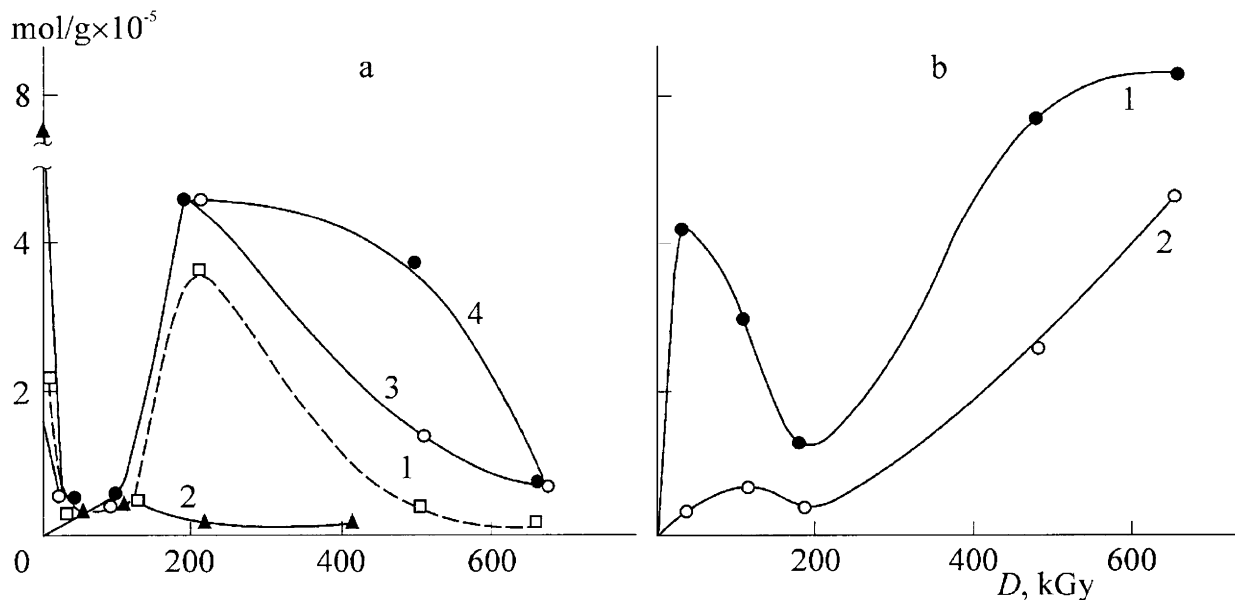


Figure 8.17. *a* is the adsorbed water content in γ -irradiated potato starch (PS), dextrane (D) and cellulose (C) samples with respect to irradiation dose; 1 – native PS samples with 13% humidity; 2 – water-free samples; 3 – D with 11% humidity; 4 – C with 4% humidity, according to mass-spectrometric measurements

b is the accumulation of H_2 (1) and CO_2 (2) in native PS samples, γ -irradiated at room temperature and in the presence of molecular oxygen, in sealed ampoules with respect to the irradiation dose

The abscissa axis presents the irradiation dose, kGy; the axis of ordinates presents: *a* – the water content in the samples, $(\text{mol/g}) \times 10^{-5}$; *b* – the released gas quantity, $(\text{mol/g}) \times 10^{-5}$

AS – humidity 11%), dextrane and cellulose (D – humidity 11%; C, cotton – humidity 4%). The second set of experiments samples, preliminarily dried and then evacuated, were irradiated. In the irradiated samples, the mass-spectroscopic method was used for the study of gaseous product accumulation and H₂O and O₂ absorption (native preparations).

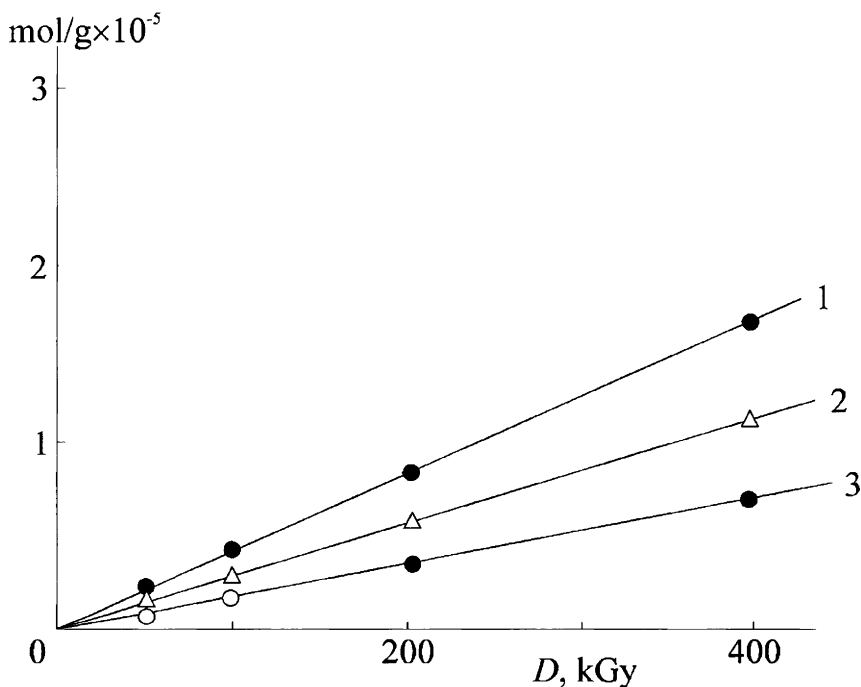


Figure 8.18. The rate of H₂ (1), CO (2) and CO₂ (3) accumulation in water-free PS samples, irradiated at room temperature, with respect to the irradiation dose

By the abscissa axis – the irradiation dose, kGy; by the axis of ordinates – the quantity of gas released, (mol/g) × 10⁻⁵

Figure 8.17 shows dependencies of the water content on the irradiation dose in native and evacuated PS samples (curves 1 and 2). The analogous dose dependencies are also recorded at AS, D and C irradiation. As for evacuated samples, the dose dependencies of gaseous products' accumulation approach the linear shape (Figure 8.18). At irradiation of native samples by doses ranged within 0.01 – 0.8 MGy, bimodal curves of H₂ and CO₂ with respect to the dose

with the first maximum in the range of 0.03 – 0.1 MGy and the second in the range of 0.5 – 0.6 MGy were recorded. The curves for water content change in these samples on the irradiation dose are antipathetic to H₂ and CO₂ accumulation curves.

From these data it may be concluded that in native polysaccharides γ -radiation induces two processes. One of them proceeds with water absorption (the descending branches of the dose curves). The second process is accompanied by water release (the ascending branches of the same curves). As water is accumulated in the sample, it begins being absorbed. Water absorption in the irradiated polysaccharide is stipulated by the interaction between water molecules and macroradicals formed, whence the water release is related to dehydration of primary radicals in polysaccharides.

Figure 8.17 shows that independently of the polysaccharide type and its crystallinity degree, water is absorbed by macroradicals in the samples practically to the zero humidity (mass-spectrometric measurements). Except for AS, it happens in the initial, always the same dose range. Therefore, it is natural to suggest that in the case of native polysaccharide radiolysis the macroradicals formed enter uniform reactions and mainly interact with water molecules from the hydrate layer of the polymer. Hence, at transition from starches and dextrane to cellulose the rate of water absorption increases by 3 – 4 times. Obviously, such difference may be caused by a transition to more regulated (crystalline) structure of the sample that predefines the interaction of a radical crystallite with water from the monohydrate layer in the damaged AGC – in this reaction in said AGC the stress occurred is removed.

So far as concerns water molecules eliminated by primary macroradicals, they react with both previously formed primary radicals and the radicals representing products of the primary radical conversions. It is worth of the note that independently on the crystallinity degree of the polymer (PS, D and C; Figure 8.17) and the dose range, in which the water content in samples increases (0.05 – 0.2 MGy) and the maximal yield of water ($\sim 4 \times 10^{-5}$ mol/Gy) are equal, except native AS samples. In this case, water is accumulated in the dose range 2.5 times broader, and the maximal value of water eliminated by the radicals is twice higher compared with other polysaccharides.

The shape of the dose curves for “burning off” water, eliminated by the radicals in these samples, is also worthy of the note. If in PS and D this process is initiated at ~ 0.2 MGy dose, an abrupt decrease of AS and crystalline C sample humidity is initiated at ~ 0.5 MGy, and at 0.65 MGy sample humidity

Figure 8.19. The change of radicals in aerated γ -irradiated ($T = 300$ K) samples of polysaccharides of natural humidity 4 days after irradiation: 1 – dextrane; 2 – potato starch; 3 – cellulose (cotton, lint, 7% humidity, 3 days after contact with water); 4 – cellulose (paper, 2.3% humidity); 5 – waxy corn starch ; 6 – corn powder (commercial preparation, 12 – 15% humidity)

became lower than 10% of its maximum. Therefore, it may be suggested that in PS and D both eliminated water molecules and radicals reacting with them are mainly located at the same place – the place of their formation, and water molecules may react with the radicals, which are the products of primary radical conversions. In AS and C, such potential reagents (H_2O and macroradicals) are accumulated and stabilized in hardly accessible places for one another (apparently, in different microareas, incompatible by the structure). This is testified by the extreme shape of the dose dependencies of macroradical accumulation in the dose range within 0.02 – 4 MGy for starches [56, 57] and cellulose [58] (Figure 8.19): hydrolysis reactions and subsequent recombination of radicals require relatively high concentrations of the reagents (much higher doses exceeding 0.5 – 0.6 MGy).

The study of the dose dependence of humidity of irradiated native samples, measured by a derivatograph e.g. under conditions of complete elimination of adsorbed water from the samples by their heating up to 400 K, shows the analogous dose dependence of the water content change in all studied polysaccharides, similar to mass-spectrometric measurements.

The values of radiation-chemical yields of water absorbed, molecular oxygen and accumulation of gaseous radiolysis products of these polysaccharides (Figures 8.17 and 8.18), estimated by the initial sections of the curves (Figure 8.17, curves 1, 3 and 4), are shown in Table 8.13, where in the second column (in brackets) the values of the radiation-chemical change of water content in the samples, estimated by the data of derivatographic changes, are present.

These values reflect the total part of water molecules, adsorbed by the polymer, $G(\text{derivat.})$ both subject to radiolysis, $G(\text{mass-spectr.})$ and possibly involved at the sample heating up to 400 K in the reaction with the polymer radiolysis products or hydrolysis of glycoside bonds of the polymer.

For the initial dose range (0 – 0.05 MGy), the values of molecular hydrogen accumulation in the native polymers vary from 1.9 (for C) to 14.3 (for PS), and in evacuated ones from 0.5 (for PS) to 1.5 (for AS). Herefrom, in

the initial dose range the accumulation of molecular hydrogen in the native compounds is stipulated by radiolysis of water, adsorbed by polymers.

The inverse property of the water content and H₂ accumulation curves for polysaccharides in the whole dose range indicates that molecular oxygen is formed both due to radiolysis of water absorbed by polysaccharide and water synthesized during macroradical dehydration (at dose 0.2 MGy or higher, see maxima 1 and 2 on the curve 1, Figure 8.17). Identical shape of H₂ and CO₂ accumulation dose dependencies indicates participation of the same radical precursor – [•]H atom, the water radiolysis products – in formation of both molecular products.

It is worthy of note that recalculation of H₂ yield in cellulose, $G = 1.9$), per amorphous phase (27%), in which the most quantity of water, leads to the same yield ($G \sim 7$), obtained for fully amorphous dextrane ($G = 6.8$, Table 8.13). Radiation-chemical yields of O₂ absorption in these polymers show the similar ratio. These experimental facts allowed for a conclusion that this route of radiation degradation of the polysaccharide–water system is related to water radiolysis in the amorphous (with irregular structure) phase of polysaccharide.

Also, the radiation degradation of polysaccharides proceeds in the crystalline phase, which is proved experimentally [63, 64]. It has been found that as exposed to radiation impact, starch is amorphized (the crystalline phase volume decreases and the amorphous phase volume increases) and loses its water binding ability. This ability is caused by the presence of hydrogen bonds between hydroxyls of macromolecules and water molecules that forms a monohydrate layer. In macromolecules of irradiated polymer OH-groups participating with water molecules in hydrate cover formation, due to primary macroradical formation and conversions, are replaced by new non-polar functional groups (keto-groups, for example; see the next Section for details). The occurrence of non-polar groups in a macromolecule breaks the system of hydrogen bonds in the monohydrate layer that affects the hydrogen binding ability of the polymer [1, 7].

Also, crystallites are amorphized as irradiated in an air-dry (with 70 – 80% crystallinity) cotton cellulose (containing 7 wt.% of water). This phenomenon was recorded for 1 – 2 MGy dose [63]. The irradiated cellulose also demonstrated degradation of the system of inter- and intramolecular hydrogen bonds. It has also been found that the yield of OH-groups free from hydrogen bonds increases with the irradiation dose [63, 64].

The above experimental data allow for an unambiguous conclusion that, basically, radiolytic degradation of polysaccharides proceeds in the interfacial

region between amorphous and crystalline phases of the polysaccharide–water system.

The product of radical $\cdot\text{OH}$ recombination ($\cdot\text{H}$ “antipode”) is H_2O_2 . In irradiated native PS this compound, similar to molecular hydrogen, is accumulated only in the initial dose range due to radiolysis of water, adsorbed by the polymer. As dose increase, the yield of H_2O_2 (similar to the yield of H_2) decreases [65]. It may be suggested that H_2 and H_2O_2 accumulation decrease in PS (and other polysaccharides) with the dose increase is the consequence of the interactions between molecular products of water radiolysis and its radicals proceeding as follows:



All these data (plus high yields of water “degradation” at relatively low amounts of it in the irradiated system falling within the range of 13 – 14%, Table 8.14) allow for a paradoxical conclusion that the radiation degradation of native (“dry”) polysaccharides is determined by the radiolysis of water molecules from hydrate layers of polymers structured by these polymers and, therefore, participation of $\cdot\text{H}$ and $\cdot\text{OH}$ radicals in these reactions.

Equilibrium humidity starch radiolysis

Some investigations on radiolysis of native polysaccharides and other biopolymers (proteins, DNA) demonstrate an effect on the degradation of water macromolecules, structured by a biopolymer (the hydrate layer of the polymer) [61, 66 – 68]. Biopolymer degradation is initiated by the radiolysis of water molecules in the polymer hydrate layer. To estimate the contribution of water radiolysis into the degradation of potato starch (PS), for example, let us compare the results of tests on γ -irradiation of native PS preparations not only with different water content, but also possessing different structures of the PS–water system. Let us consider radiolysis of native PS preparations possessing the equilibrium humidity (from 5 to 45%) and PS gels (jellies) 69 – 72]. To put it differently, we are speaking about radiolytic degradation of PS in these systems, possessing identical chemical composition (PS + water), but having different concentrations of water structured by starch.

As mentioned above, as native PS samples are irradiated at room temperature, water proves itself in three ways: it is radiolized ($\bullet\text{OH}$ and $\bullet\text{H}$ radicals are formed, which then react with macromolecules), is involved into the reactions with the primary radicals with H detachment from C1, C4 and C6 by glycoside bonds (in these radicals O–C β -bonds are hydrolyzed) and, finally, it is released and accumulated in the sample during dehydration of radicals formed from the polymer. As a consequence of these processes proceeding, the dose dependence of H_2O content in the samples irradiated at room temperature is of the extreme type, having a minimum in the dose range between 0.03 and 0.1 MGy (Figure 8.17). In this dose range water content in the sample does not exceed 10% of the initial (the initial humidity of PS is 13%) and 5% of the maximal quantity, reached at 0.2 MGy. Therefore, it has been concluded that in this dose range the “opposite” processes with water participation (water radiolysis + its consumption for β -bond hydrolysis in carbon-centered $\bullet\text{C1}$, $\bullet\text{C2}$ and $\bullet\text{C6}$ radicals and water synthesis during dehydration of radicals) are almost compensated. If under these conditions the PS–water samples of the same composition (87% PS and 13% water) possessing different structures (solution and gel, for example) are irradiated, any changes in the yields of either PS radiolysis products or water release (at transition from solution to gel) may be ascribed to the action of a structural factor (because primary processes of ionizing radiation energy absorption in the systems possessing the same structure are suggested to be identical).

Let us compare data on RA and water accumulation in the native starch samples of identical humidity but different synthesis technique [61, 70]. In other works [55] a usual commercial PS of “pure” brand with 13% humidity was used. Some authors [70] primarily humidified PS samples in a desiccator above water until the equilibrium humidity of 44.4% was obtained. Then in dessicators with sulfuric acid of different concentration the samples obtained the required equilibrium humidity exposed at room temperature in darkness during 4 – 5 months. Such method of sample preparation provided a gradual hydration of all three hydroxyls in the monomer unit of PS (water structuring) with the humidity increase (W) in the samples: one hydroxyl at $W = 12\%$, two hydroxyls at $W = 19\%$ and three hydroxyls at $W = 25\%$. As follows from the

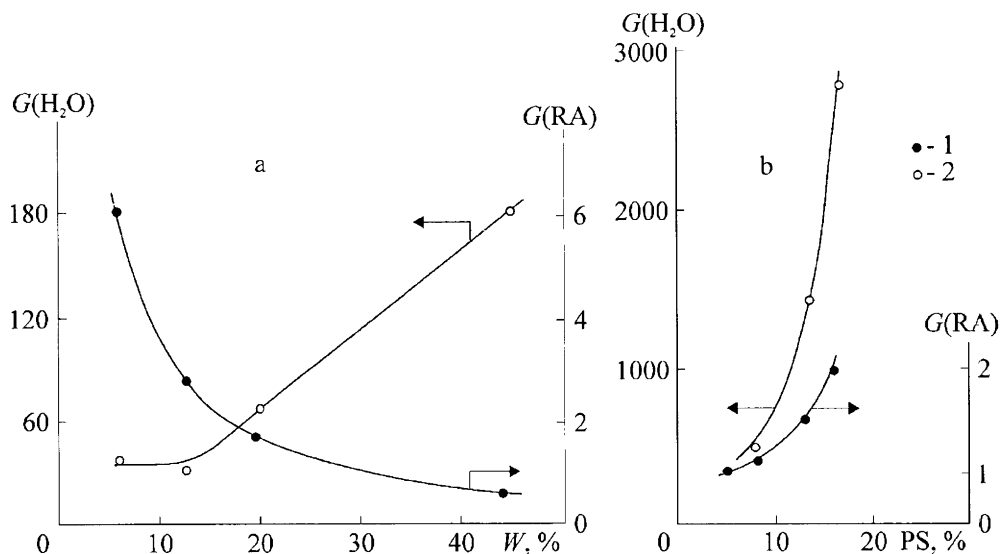


Figure 8.20. Radiation degradation of PS at room temperature – native preparations of the equilibrium humidity (a, 44 kGy γ -irradiation dose) and their jellies (b, 33 kGy irradiation dose) with respect to their wetness degree:

- 1 – the yield of reducing agents (RA) (PS depolymerization);
- 2 – the yield of water [60]

data [60] shown in Figure 8.20, the yields of RA and water in PS with 13% humidity depends on the sample preparation conditions. For common native PS $G(\text{RA}) = 6.5$, and for the samples with equilibrium humidity $G(\text{RA}) = 2.5$. The yield of water equals $G(\text{H}_2\text{O}) = 0.5$ in the dose range of 30 – 100 kGy (if the opposite water processes are compensated) and $G(\text{H}_2\text{O}) = 32$ for the cases one and two, respectively. As transiting from PS samples of the equilibrium humidity the increase of $G(\text{H}_2\text{O})$ is most likely induced by the decreasing contribution of one of two components into the resulting process of water accumulation: it is reduction of the part of H_2O molecules involved into hydrolytic splitting of glycoside bonds in macroradicals. It is obvious that under conditions of PS equilibrium humidity the greater part of water molecules is included into the regular structure of intermolecular bonds of macromolecules [71, p. 132].

This conclusion may be also confirmed by the shape of the water yield $G(\text{H}_2\text{O})$ concentration curve depending on PS humidity (Figure 8.20, curve 2):

for PS samples with low humidity (5 – 13%) the curve has a plateau; for the samples with $W = 20 - 44.4\%$, $G(\text{H}_2\text{O})$ gradually increases from 70 to 180 per 100 eV of absorbed energy. Such shape of the concentration dependence demonstrates the presence in a native starch (in proteins, for example [66, 68]) of microareas possessing at least two types of structural organization of water.

The tests of PS of the equilibrium humidity indicate the presence of two types of intermolecular hydrogen bonds in these systems [72]: type 1 represents 2 hydrogen bonds between hydroxyls of neighbor macromolecules; type 2 represents hydrogen bonds (1 in each chain) in the sequence “PS hydroxyl...H₂O...PS hydroxyl”. In a water-free starch hydroxyls of macromolecules are bound by type 1 hydrogen bonds only. As the starch is humidified, hydroxyls in its molecules are hydrated and starting from 25% equilibrium humidity (when all 3 hydroxyls in the molecule are hydrated) only type 2 hydrogen bonds are present in the sample.

The following feature of native PS radiolysis is worthy of the note: as humidity of samples increases from 5 to 44.4%, RA yield (RA accumulation in irradiated PS testifies about its depolymerization, reaction (8.18) decreases by an order of magnitude, approximately. Similar situation of polysaccharide depolymerization suppression is observed at the irradiation of humidified cellulose (C) samples: the yield of C depolymerization reduces by 15%, approximately, with the humidity increase from 1 to 70% [73, p. 276].

The above-considered examples of $G(\text{H}_2\text{O})$ and $G(\text{RA})$ concentration dependencies on water concentration in PS samples indicate a paradoxical situation:

- 1) an original mechanism of direct radiation effect on “PS aqueous solution” in relation to water – H₂O is released almost proportionally to its concentration in the irradiated system;
- 2) water represents a kind of radioprotector in relation to degrading polymer [66].

The discrepancies with the common ideas on radiolysis may be solved under the suggestion that this PS–water system (having low water quantity, up to 25% humidity) represents the entire single-phase system and radiolysis processes proceeding in it mostly involve the polymer and water from its hydrate layer e.g. water structured by polymer hydroxyls. Therefore, the role of water as the original radioprotector may be explained as follows: the

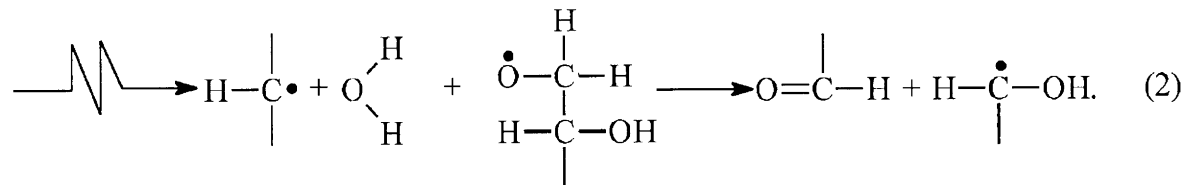
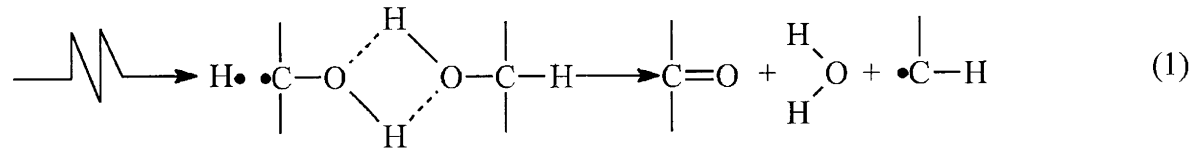
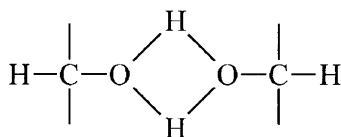


Figure 8.21. The formation mechanisms of H and OH detachment primary radicals in starch–starch and starch–water structured systems

occurrence of a water molecule at the polymer hydroxyl instead of hydroxyl of the neighboring molecule (the substitution of type 1 hydrogen bonds by type 2) must affect both the rate of primary macroradical conversions and the mechanisms of these conversions. Since in PS hydroxyls are located at the second, the third and the sixth carbon atom, the above-said should also be related to primary radicals: hydroxyalkyl (H atom detachment), alkyl hydroxyl detachment), and alkoxy radicals at carbon atoms listed above. At transition from water-free to humidified starch samples, changes in the mechanisms of primary radical formation are also obvious.

Unusually high yields of molecular hydrogen (14.3 [61]) and water (32; Figure 8.20, curve 2) in 13% humidity PS (corresponds to hydration of 1.3 hydroxyl units per PS monomer unit) with respect to the interaction between the polymer and H atoms and $\bullet\text{OH}$ radicals formed (reaction (8.1)) indicate that these processes proceed directly in the place of radicals $\bullet\text{H}$ and $\bullet\text{OH}$ occurrence in the hydrate layer of the polymer. The explanation of the water yield, twice exceeding $G(\text{H}_2)$ in this case, requires involvement of an additional route of its formation in the primary acts of PS radiolysis. This route is fully realized in the case of water-free samples (hydroxyls of neighbor macromolecules are bound by type 1 hydrogen bonds as, for example, in cellulose crystallites, by C6 atoms).

Figure 8.21 shows primary stages of water molecules and free radicals formation in irradiated structures systems – polysaccharides. In water-free starches the system of intermolecular H-bonds is the following:



Both hydrogen atoms are bound to oxygen atoms by hydrogen bonds (oxymethylene units of 2 macromolecules form something like a “procurement” of a water molecule). High yield of water molecules compared with the yields of alkyl and alkoxy radicals in such structured system may be explained by proceeding of reactions 1 and 2 (Figure 8.21). According to these reactions, the yields of primary radicals (pairs of radicals) must equal the value of H_2O molecule yield, which, in turn, must twice exceed $G(\text{H}_2)$. All this is observed in the present case. Moreover, the equation

$$G(\text{H}_2\text{O}) = G(\sum >\text{C}=\text{O}),$$

where $\sum >\text{C}=\text{O}$ is the sum of carbonyl groups (keto-groups by C2 and C3 carbon atoms and aldehyde groups by C6 atom). Unfortunately, there no reliable data yet in the literature on the yield of keto-groups and aldehyde groups for completely dried irradiated PS. For C, $G(\sum >\text{C}=\text{O}) = 58$ [73]. This value is at least comparable with that required for PS according to the equations (2) and (3), Figure 8.21.

So far as concerns the initial yields of corresponding primary radicals and alkoxy radicals, the data in the literature present for PS, C and other polysaccharides at room temperature are highly overestimated. This may be explained by instability of paramagnetic particles in the presence of water formed in the primary acts of radiolysis (reactions (2) and (3), Figure 8.21) – their recombination and, as well, in the ESR-measurements at room temperature relatively high doses of ionizing radiation were always used, which promoted radical recombination under the radiation effect [38].

The RYDMR method [29, 31] was used for testing evacuated C at room temperature, exposed to UV-irradiation (in the presence of a sensitizer). In these tests, a full set of radicals typical of irradiated polysaccharides was detected and their predominant formation in pairs was determined [29]. The HFS of the radical spectra, registered by common classical ESR method under stationary conditions of irradiation at room temperature, is significantly simplified. This testifies about the presence of lower number of the types of radicals in the sample compared with RYDMR method. Such data indicate that by the moment of radical ESR-registration beginning under stationary conditions in irradiated C at room temperature the processes of radical pair formed recombination are globally finished and, therefore, their yields are underestimated.

The final confirmation of the suggested scheme of native PS radiolysis requires additional experiments determining fractional yields of the primary radicals in the reactions (2) and (3), Figure 8.21.

Radiolysis of starch gels (jellies)

As PS gels with different water content (prepared by PS heating with water up to gelatinization point and then cooled down to room temperature) are irradiated, the “solidified” aqueous starch solutions, which differ from the

previously considered PS solutions by higher developed regular system of water molecules (bound by hydrogen bonds and forming together with PS macromolecules the cell walls, the edges of the a three-dimensional structure), demonstrated the following features of radiolysis [69, 70].

- 1) As the water content increases by 10% (from 84 to 95%), the yield of PS, $G(\text{RA})$, decreases by twice (Figure 8.20b);
- 2) In this case, free water (squeezeable liquid) is released in the sample, which yield for maximal PS concentration used (16%) reaches $G(\text{H}_2\text{O}) = 2,800$ [74]. This equals 20% release of water, absorbed by PS, from the gel volume.

In the case of starch gel γ -irradiation, the dominating role of polymer-structured water radiolysis may be illustrated as follows. The formation of a single macroradical (by H detachment from hydroxymethylene unit at the attack of H-C bond by water radical) is accompanied by the change of configuration of C-C and C-OH chemical bonds remained in the radical (tetragonal sp^3 conversion to flat sp^2). This leads to breaks of hydrogen bonds between AGC hydroxyls and water molecules participating in the formation of three-dimensional lattice edges. This act is accompanied by releasing up to 500 molecules of water from a single cell (squeezing liquid) [74].

In γ -irradiated native cellulose the analogous process also takes place: The fraction of OH-groups in the polymer, free or weakly involved into intermolecular hydrogen bonds with water molecules from the hydrate layer covering the surfaces of intermolecular cavities in this polymer, increases with the dose [64]. Analysis of the data allowed for determining a correlation between PS depolymerization and degradation of its gels and suggesting the following interpretation of the experimental results. The initiating process for the gel degradation may be presented by the primary radical formation, detachment radical $\cdot\text{H}$ or $\cdot\text{OH}$ from oxymethylene unit in AGC (Figure 8.21, reactions (1) and (2)).

At any such act hydrogen bonds linking PS macromolecules to chain bridges from water molecules break. Therefore, one of the components in the three-dimensional structure of cells in the gel is destroyed. If even a single "edge" of the cell is destroyed, water molecules existing in these cells leave them. Among alternatives, the following may be suggested. Firstly, at irradiation hydrophobic groups (keto-groups, aldehyde and carboxylic groups) occur in the composition of macromolecules, which may lead to a change in

the polymer swelling degree and affect the quantity of water retained in the cells [75, Chapter II]. Secondly, beside depolymerization of macromolecules, at PS irradiation intermolecular crosslinks are formed. As the frequency of crosslinks increases, the possibility of formation of freely fold coils from the fragments of macromolecules, which represent edges of the cell, is reduced. This is displayed in reduction of the polymer swelling degree and, therefore, in release of great quantity of squeezing liquid [76].

The latest suggestion may be indirectly confirmed by two facts as follows:

- 1) The increase of elastic strength of irradiated gels with their humidity [76];
- 2) Radiation syneresis is accompanied by gel cracking. Small are formed in the case of more humid gels, whereas large and deep cracks are observed for jellies of lower humidity [69].

Finally, a choice between these hypotheses is possible after implementation of additional investigations.

Thus, the analysis of the above results allows for a conclusion the PS degradation in gels is significantly defined of radiolysis of PE and its hydrate cover. Radiation decomposition of H_2O in hydrate layer of the polymer (polymer-structured water) proceeds with the yield 3 times higher (reaction (8.1)), approximately, than the radiolytic yield of water molecules ($G(-H_2O) \sim 4$), registered in the case of irradiation of aqueous dilutes solutions of low-molecular substances. The same yield is observed for the radiolysis of water located in the three-dimensional lattice of the jelly. As the cells are destroyed (or the swelling degree of the polymer changes due to formation of crosslinks or hydrophobic groups in its composition), water is released from them (squeezing liquid). Therefore, $G(H_2O)$ becomes extremely high.

8.8. POST-RADIATION EFFECTS IN POLYSACCHARIDES

The degradation processes in polysaccharides, irradiated in the presence of oxygen, is also continued after radiation removal. These reactions in the presence of oxygen proceed in both native preparations and aqueous solutions.

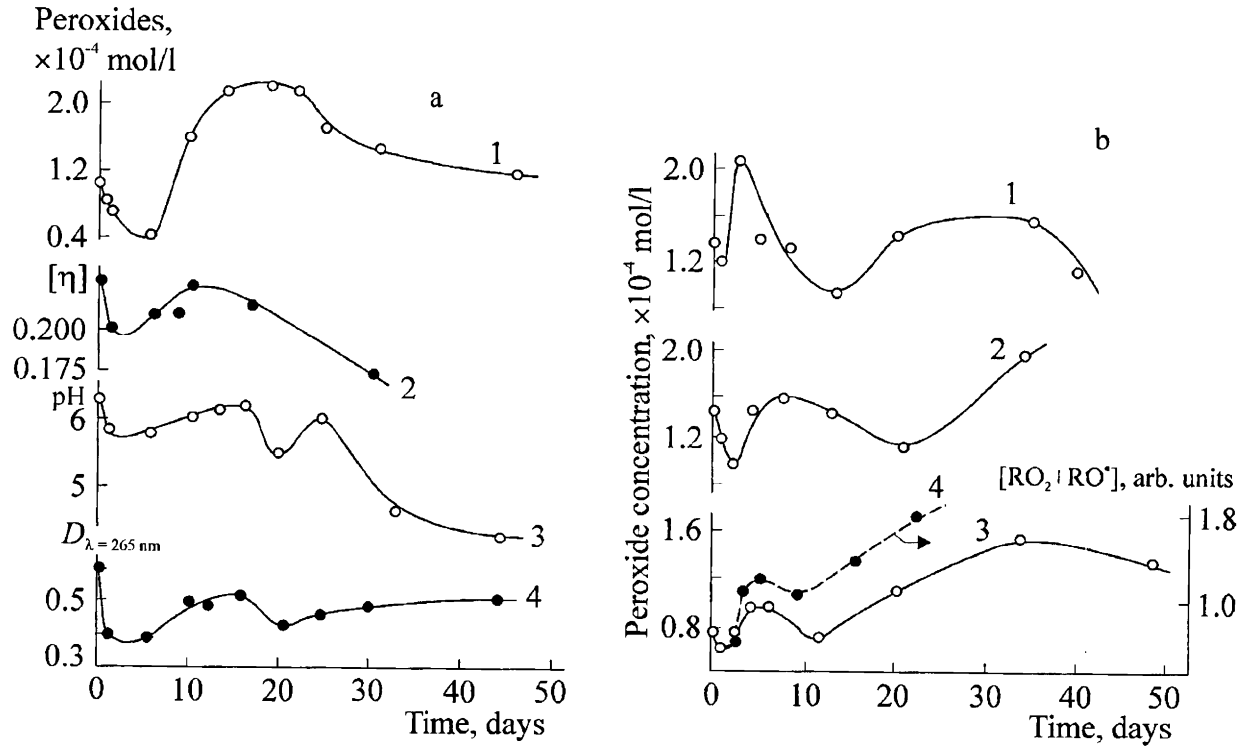


Figure 8.22. *a.* Radiation aftereffect in dextrane solutions in the absence of the air exchange: the changes of 1 – total concentrations of peroxide compounds; 2 – characteristic viscosity of the solution; 3 – solution pH; 4 – optical density of UV-absorption of the solution 6% solutions of dextrane with initial pH ~ 9 ; 35 kGy radiation dose
b. Post-radiation formation of peroxide compounds (total) during storage of solutions in the air (1 – 3) and free radicals (4) in lyophilizates; the irradiation dose: 1 – 50; 2 – 200; 3 and 4 – 150 kGv

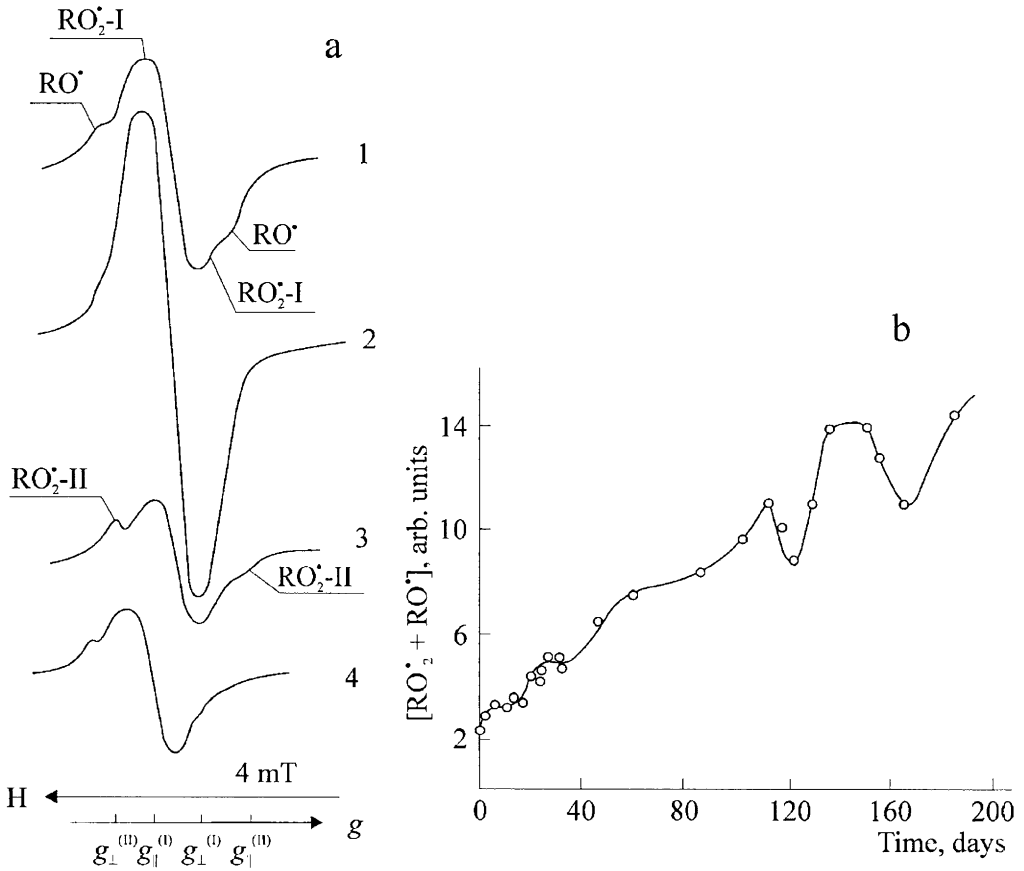


Figure 8.23. *a.* ESR spectra (and their analysis) for lyophilizate of irradiated 6% solution of dextrane (pH 7, 30 kGy dose) during storage in the air:

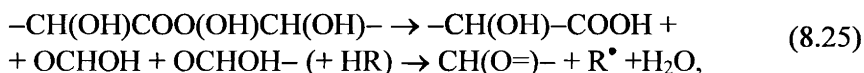
1 – 0.5 h; 2 – 4 days; 3 – 60 days; 4 – 7.5 months. Before been lyophilized, the solution was stored at room temperature during 1 month with regular air exchange (during sampling), after lyophilic drying – 14 days without air exchange. Spectra were registered at $T \sim 300$ K, $P_{UHF} \sim 0.5$ mW; HF modulation amplitude ~ 0.4 mT

b. The change of total radical concentration in the lyophilizate depending of the storage time in the air (initial solution pH 8.5; 80 kGy irradiation dose; aftereffects in the solution – 5 days)

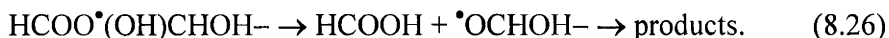
For example, in irradiated dextrane solutions, stored in the air at room temperature, peroxide compounds (H_2O_2 , ROOH, ROOR) are accumulated and degrade, breaks and intermolecular crosslinks are formed in polymeric chains, carbonyl and carboxylic groups are formed in the polymer structure, low-molecular aldehydes, ketones and acids are formed, too [32, 77]. The accumulation of peroxides and acids in solutions follows the extreme time dependencies (Figure 8.22a, b); the storage time dependencies of solution pH demonstrate the basic tendency of the solution acidity increase. The injection of compounds – free radical acceptors into the solution significantly decreases the yield of peroxides. In lyophilizates (polysaccharide solutions, lyophilized after irradiation) the following free radicals are detected: alkoxy and peroxide of two types (for the first type – unpaired electron is localized on the end monomeric unit, for the second type – unpaired electron is localized on the “middle” unit, with the anisotropy parameter equal $g_{\parallel} - g_{\perp} = 0.01$; Figure 8.22b, curve 4; Figure 8.23a). Their concentration in the samples increases with the time of storage in the oxygen (or air) atmosphere (Figure 8.23b) [77].

All these facts are explained so that in irradiated solutions of dextrane (and in starch) radical-chain processes of the polymer oxidative degradation proceed, initiated by degradation of peroxides via formation of free radicals by the reaction (8.14), and their consecutive conversions in the presence of oxygen are described by the reactions (8.1), (8.10a), (8.15) – (8.17).

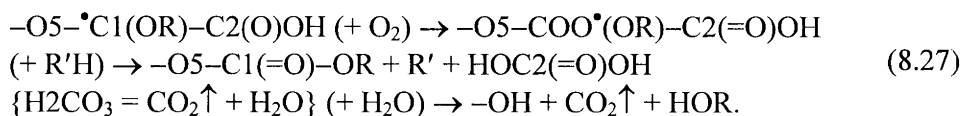
Hence, the occurrence of carboxylic and carbonyl groups in the polymer composition relate to radical conversions of the RO_2 -II type:



whereas by radical conversions of RO_2 -I type (Figure 8.23a), formic acid is obtained (reaction (8.26)):



Periodic variation in solution pH, observed in the tests, may be explained by conversions of peroxide radicals, which occur in already modified carboxylic groups of monomeric units according to the scheme, composed with respect to the above reactions:



Carbon dioxide release from dissolved lyophilizate should be accompanied by increasing pH of the medium. Beside formation of carboxylic groups, this process provides regularity in the solution pH variations.



On the example of the above-discussed systems we have tried to show basic routes of free radical conversions, basing on the comparison of the data on the origin and dynamics of accumulation of native polysaccharides and their molecular (final) products of radiolysis. Turning back to the problem of controlling radiolytic processes, let us outline two basic directions in creating conditions of polysaccharide irradiation for the purpose of radioprotection (for example, at food canning – to provide preservation of their organoleptic properties after radiation treatment) or stimulation of polysaccharide degradation (decreasing molecular mass in order to increase digestibility of cellulose-containing forage by the cattle). In the first case, compounds – radical acceptors should be used (the inhibitors of free-radical reactions or antioxidants, if irradiation happens in the presence of molecular oxygen, and oxidative processes with participation of peroxides are initiated [78]). Hence, reacting with alkoxy ($\text{RO}\overset{\bullet}{\text{C}}$) and peroxide ($\text{ROO}\overset{\bullet}{\text{C}}$) radicals, InH suppress such oxidative degradation processes of macromolecules (refer to Chapter 13). In some works [79, 80] on the example of sephadex (cross-linked dextrane) in the presence of InH with sulfhydryl group direct ESR measurements demonstrated a possibility of radical substituting ($\text{R} + \text{HSR}' = \text{RH} + \text{SR}'$) proceeding. Thus, elimination of unpaired electron not at all means repair (reduction of the initial structure) of damaged sugar unit [10], and may be the reason for stereoisomers (epimers) formation [81] (Chapter 10). It has been found [82] that at irradiation of deaerated aqueous frozen-up ribose solution its stereoisomers are formed. Figure 8.24 shows the scheme for formation of such stereoisomers. The solutions were irradiated at 195 K. Under these conditions, ribose hydroxyalkyl radicals and electron \bar{e}_{st} stabilized on the matrix traps were registered. As

affected by visible light, electrons left the traps and recombined with radicals, and their concentration decreased.

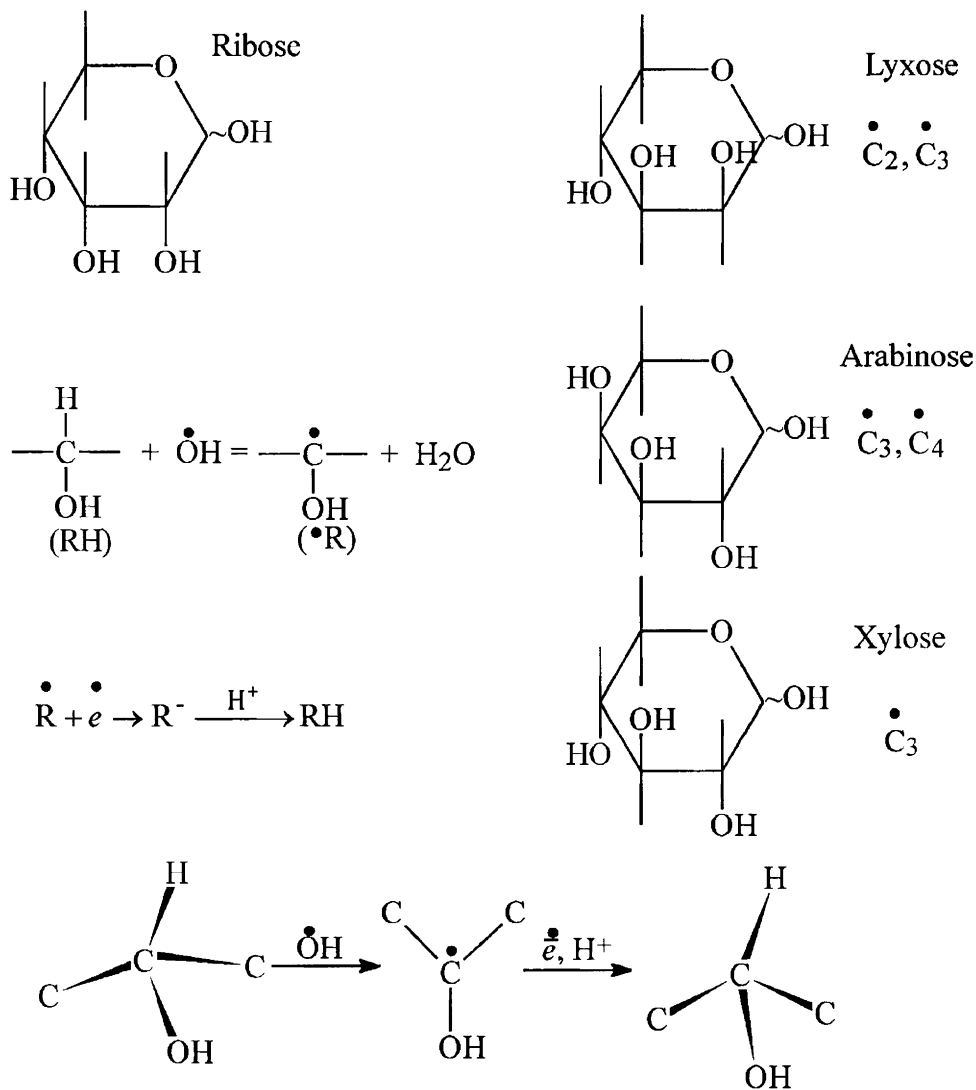


Figure 8.24. The scheme of glucose stereoisomers (epimers) formation

After defrosting the samples obtained, the products shown in the Figure 8.24 were chromatographically detected in the solution. The process of sugar

epimers formation was registered at thymidine irradiation under the same conditions [83]. The formation of glucose epimers – mannose (by C2) and galactose (by C4), is also observed at the irradiation of polycrystalline cellulose and starch samples in the absence of oxygen [1]. As follows from these data, the radiation conversion of carbon atom configuration is also possible for polymers, which include carbohydrate chains. Their realization must cause a change of the initial macromolecule conformation. For example, in the case of DNA, the formation of 2-deoxyribose residue epimers must be accompanied by the change of spatial orientation of a nitrous base and, therefore, represents a potential possibility of occurrence of gene mutations (transversions and transitions) [11, 84, 85] (Chapter 10) in this site of DNA.

For the purpose of stimulating degradation of polysaccharides (the second case), humidified preparations or aqueous solutions should be irradiated in the presence of molecular oxygen (processes (8.3), (8.4), (8.9)) and substances – radiosensibilizers. For instance, due to electron “conversion” to OH-group in solutions saturated by nitrous oxide the “initial” yield of oxidative degradation of carbohydrates two-fold increases: OH-group interacts and electron does not react with oxymethylene units in carbohydrate molecule. Nitrate-ion and chloroacetic acid should be belonged to radiosensibilizers: at their interaction with electron oxidant radicals are forms [5, 10], which then may participate in reactions with carbohydrate molecules. At the irradiation of solutions of carbohydrates and the mentioned compounds or even their mechanical mixtures (more or less homogeneous), the yield of oxidative degradation of carbohydrates is much higher compared with radiolysis of individual compounds [3, 5].

Speaking about stimulation of polysaccharide degradation by the free-radical mechanism, new approaches to resolving this task should also be outlined. It is shown that degradation of α -diol type compounds (monomer units of polysaccharides have such structural units) is implemented by means of primary radical fragmentation by the coordinated mechanism with simultaneous break of two bonds, vicinal in relation to localization of unpaired electron, via pentatomic cyclic transition state of the reagent [58, 86, 87]. In this case, injection of additives forming such pentatomic cycles (the intermediate complexes) into aqueous solutions helps in increasing yields of the mentioned processes. For example, the injection of dextrane and borax and Cu(II) salts laminarin, forming pentatomic complexes from hydroxylic groups of polymers, into aqueous solutions increases the yield of these polymers degradation by 2 – 2.5 times [87].

To conclude this Chapter, note that currently radiation chemistry of polysaccharides is the branch of chemistry of biopolymers, the most developed concerning the investigations of the free-radical mechanism of their radiation degradation. The facts as determination of initial sites of damage localization (unpaired electron) in the irradiated polymer (determination of origin of primary macroradicals) and the basic types of development of these damages (primary free radical conversions) are self-explanatory.

REFERENCES

1. Sharpatyi V.A., *Chim. Fiz.*, 1995, vol. **14**(10), p. 113. (Rus)
2. Emanuel N.M., Sharpatyi V.A., Najimiddinova M.T., *et al.*, *Doklady AN SSSR*, 1967, vol. **177**(5), p. 1142. (Rus)
3. Sharpatyi V.A., *Radiation Chemistry of Biopolymers*, Moscow, Energoizdat, 1981, 168 p. (Rus)
4. Abagyan G.V., 'Free-radical processes at various physical impacts on solid carbohydrates and DNA', *Doctor Dissertation Thesis*, Moscow, N.N. Semenov Institute of Chemical Physics, AS USSR, 1988. (Rus)
5. Fedorova G.A., 'Radiation-chemical modification of starch', *Candidate Dissertation Thesis*, Moscow, N.N. Semenov Institute of Chemical Physics, AS USSR, 1988. (Rus)
6. Karpov V.G. and Yur'ev V.P., *Khranenie i Pererabotka Sel'khozsyrya*, 1998, No. 10, p. 27. (Rus)
7. Ciesla K. and Eliasson A.-Ch., *Radiat. Phys. Chem.*, 2002. vol. **64**, p. 137.
8. Ershov B.G., *Uspekhi Khimii*, 1998, vol. **67**(4), p. 353. (Rus)
9. Sharpatyi V.A., Najimiddinova M.T., Korotchenko K.A., and Kovalev Yu.I., *Doklady AN SSSR*, 1968, vol. **181**(3), p. 655. (Rus)
10. Sharpatyi V.A., 'Primary mechanisms of the radiation damage of biologically sufficient biomacromolecules: DNA, proteins, DNP, polysaccharides', *Doctor Dissertation Thesis*, Moscow, N.N. Semenov Institute of Chemical Physics, AS USSR, 1972. (Rus)
11. Sharpatyi V.A., *Radiobiologia*, 1992, vol. **32**(2), pp. 180 - 193. (Rus)
12. Sharpatyi V.A., Pristupa A.I., Prikhid'ko I.I., and Sultankhojaeva M.N., *Izv. AN SSSR, Ser. Khim.*, 1970, No. 3, pp. 702 – 705. (Rus)

13. Sharpatyi V.A. and Sultankhojaeva M.N., *Izv. AN SSSR, Ser. Khim.*, 1969, No. 5, pp. 1183 - 1185. (Rus)
14. Tomasik P. and Zaranyika M.F., In Coll.: *Advances in Carbohydrate Chemistry and Biochemistry*, Ed. D. Horton, 1995, vol. **51**, pp. 243 - 317.
15. Gol'din S.I., Markevich S.V., and Sharpatyi V.A., *Doklady AN SSSR*, 1971, vol. **201**(1), pp. 133 - 136. (Rus)
16. Sharpatyi V.A. and Gol'din S.I., *Izv. AN SSSR, Ser. Khim.*, 1971, No. 6, p. 1367. (Rus)
17. Korotchenko K.A., Nadjafova M.A., and Sharpatyi V.A., *Radiobiologia*, 1978, vol. **18**(5), pp. 661 - 666. (Rus)
18. Gol'din S.I., Ivko A.A., Bondarenko N.T., *et al.*, *Doklady AN SSSR*, 1976, vol. **228**(2), p. 389. (Rus)
19. Sharpatyi V.A., *Radiobiologia*, 1983, vol. **23**(1), p. 69. (Rus)
20. Filonenko Yu.A., 'Free radicals in radiation-chemical and chemical conversions of wood components', *Candidate Dissertation Thesis*, Moscow, N.N. Semenov Institute of Chemical Physics, RAS, 1993. (Rus)
21. Ivko A.A., Gol'din S.I., Bondarenko N.T., *et al.*, *Izv. AN SSSR, Ser. Khim.*, 1977, No. 1, pp. 88 - 91. (Rus)
22. Korotchenko K.A., Nadjafova M.A., and Sharpatyi V.A., *Izv. Vuzov. Pishchevaya Tekhnologiya*, 1982, No. 1, pp. 76 - 80. (Rus)
23. Kochetkov N.K., Kudryashov L.I., and Chlenov M.A., *Radiation Chemistry of Carbohydrates*, Moscow, Nauka, 1978, 288 p. (Rus)
24. Sharpatyi V.A., Shapilov A.A., and Pintelin S.N., *Khim. Fiz.*, 2001, vol. **20**(12), p. 19. (Rus)
25. Kuzina S.I., 'Free radicals in photo, radiation and cryochemistry of synthetic and natural polymers', *Doctor Dissertation Thesis*, A.V. Topchiev INPS, RAS, 1998. (Rus)
26. Pintelin S.N., Shapilov A.A., and Sharpatyi V.A., In Coll.: "Aging of Polymers, Polymer Blends and Polymer Composites", vol. **2**, Ed. G.E. Zaikov, A.L. Buchachenko, and V.B. Ivanov, Nova Science Publishers, Inc. NY, 2002, p. 205.
27. Abagyan G.V. and Apresyan A.S., *Khimiya Vysokikh Energiy*, 2002, vol. **36**(4), p. 263. (Rus)
28. Pristupa A.I., Lesin V.I., and Krasotkina I.A., *Chem. Phys. Lett.*, 1991, vol. **180**(6), p. 569. (Rus)

29. Pristupa A.I. and Sharpatyi V.A., *Doklady AN*, 1998, vol. **359**(1), p. 58. (Rus)
30. Pristupa A.I. and Sharpatyi V.A., *Doklady AN*, 1997, vol. **352**(3), p. 358. (Rus)
31. Pristupa A.I. and Sharpatyi V.A., *Doklady RAN*, 2002, vol. **387**(5), p. 643. (Rus)
32. Bondarenko N.T., 'Radiation conversions of dextrane', *Candidate Dissertation Thesis*, Moscow, N.N. Semenov Institute of Chemical Physics, AS USSR, 1989. (Rus)
33. Gol'din S.I. and Markevich S.V., *Izv. AN BelSSR, Ser. Khim.*, 1970, No. 6, p. 47. (Rus)
34. Korotchenko K.A., Stanimirovich S.G., and Stanimirovich D.L., *Prikl. Biokhim. Mikrobiol.*, 1968, vol. **4**(6), p. 727. (Rus)
35. Korotchenko K.A. and Sharpatyi V.A., *Khimia Vysokikh Energiy*, 1993, vol. **27**(4), p. 50. (Rus)
36. Korotchenko K.A., Shapilov A.A., and Sharpatyi V.A., *Thes. Rep. I Intern. Conf. "Starch and Starch-containing Sources – Structure, Properties and New Technologies"*, Oct. 30 – Nov. 1, 2001, Moscow, p. 97. (Rus)
37. Korotchenko K.A., Pristupa A.I., and Sharpatyi V.A., *Khimia Vysokikh Energiy*, 2004, vol. **38**(2), p. 107. (Rus)
38. Pshezhetsky S.Ya., Kotov A.G., Milinchuk V.K., Roginsky V.A., and Tupikov V.I., *ESR of Free Radicals in Radiation Chemistry*, Moscow, Khimia, 1972, 480 p. (Rus)
39. Deeble D.J., Bothe E., Schuchmann H.-P. *et al.*, *Z. Naturforsch.*, 1990, Bd. **45**(9/10), S. 1031.
40. Von Sonntag C., *Adv. Carbohydr. Chem. Biochem.*, 1980, vol. **31**(1), p. 7.
41. Kvach N.M., Kuvaldina E.V., Sadova S.F., and Sharpatyi V.A., *Doklady RAN*, 1996, vol. **349**(1), p. 60. (Rus)
42. Ciesla K., *Zeszyty Naukowe PL-Inzynieria Wlokiennicza i Ochrona Srodowiska*, 1993, vol. **16**(20), p. 343.
43. Fedorova G.A., Ivko A.A., Bondarenko N.T., and Sharpatyi V.A., *Khimia Vysokikh Energiy*, 1992, vol. **26**(6), p. 493. (Rus)
44. Gol'din S.I., Bondarenko N.T., Ivko A.A., *et al.*, *Izv. AN BelSSR, Ser. Khim.*, 1976, No. 1, p. 131. (Rus)
45. Dizdaroglu M., Henneberg D., Neuwald K., Schomburg G., and von Sonntag C., *Z. Naturforsch.*, 1977, vol. **32b**, S. 213.

46. Ershov B.G. and Isakov O.V., *Izv. AN SSSR, Ser. Khim.*, 1987, No. 11, p. 2337. (Rus)
47. Mucchielli A., 'Evolution toxicologique des produits formes au cours de l'irradiation gamma de l'amidon. Influence sur la croissance et le me-tabolisme bacteriens', *These de Doctorat d'Etat es Sciences*, Universite des Sciences et Techniques de Lille, 1975.
48. Raffi J., Frejaville C., Dauphin J. F., Dauberte B., d'Urbal M., and Saint-Lebe L., *Starch/Starke*, 1981, Bd. **33**(7), S. 235.
49. Fedorova G.A., Bondarenko N.T., Berlin S.M., Volkovich S.V., and Sharpatyi V.A., *Khimia Vysokikh Energiy*, 1992, vol. **26**(5), p. 423. (Rus)
50. Sharpatyi V.A., *Khimia Vysokikh Energiy*, 2003, vol. **37**(6), p. 369. (Rus)
51. Hamidi E. and Dauphin J.F., *Starch/Starke*, 1976, vol. **28**(10), S. 333.
52. Raffi J., Angel J.P., Dauberte B., d'Urbal M., and Saint-Lebe L., *Starch/Starke*, 1981. Bd. **33**(6), S. 188.
53. Milinchuk V.K., Klinkshpont E.R., and Pshezhetsky S.Ya., *Macroradicals*, Moscow, Khimia, 1980, 264 p. (Rus)
54. Kavetsky V.G. and Yudin I.V., *Khimia Vysokikh Energiy*, 1991, vol. **25**(5), p. 476. (Rus)
55. Sharpatyi V.A., *Khim. Fiz.*, 2003, vol. **22**(6), p. 23. (Rus)
56. Pintelin S.N., Shapilov A.A., and Sharpatyi V.A., *Thes. Rep. I Moscow Intern. Conf. "Starch and Starch-containing Sources – Structure, Properties and New Technologies"*, Oct. 30 – Nov. 1, 2001, Moscow, p. 68. (Rus)
57. Korotchenko K.A. and Sharpatyi V.A., *Izv. Vuzov. Pishchevaya Tekhnologia*, 1983, No. 2, p. 45. (Rus)
58. Petryaev E.P. and Shadyro O.I., *Radiation Chemistry of Bifunctional Organic Compounds*, Minsk, Izd Universitetskoe, 1986, 166 p. (Rus)
59. Von Sonntag C., *Adv. Carbohydr. Chem. Biochem.*, 1980, vol. **37**(1), p. 7.
60. Denisov E.T., *Rate Constants of Homolytic Liquid-phase Reactions*, Moscow, Nauka, 1971, 712 p. (Rus)
61. Fedorova G.A., Ivko A.A., Bondarenko N.T., and Sharpatyi V.A., *Doklady AN SSSR*, 1987, vol. **297**(4), p. 902. (Rus)
62. Korotchenko K.A. and Sharpatyi V.A., *Khimia Vysokikh Energiy*, 2004, vol. **38**(4), p. 265. (Rus)

63. Kovalev G.V. and Bugaenko L.T., *Khimia Vysokikh Energiy*, 2003, vol. **37**(4), p. 247. (Rus)
64. Klimentov A.S., Fedorov L.A., Kotel'nikova N.E., Petropavlovsky G.A., Volkova L.A., and Ershov B.G., *Zh. Prikl. Khimii*, 1981, vol. **54**(3), p. 686. (Rus)
65. Raffi J., Angel J.P., Dauberte B., and Saint-Lebe I., *Starch/Starke*, 1981. Bd. **33**(8), S. 269 - 271.
66. Svanidze E.O., 'The features of free radicals at radiolysis of frozen-up gelatin solutions', *Candidate Dissertation Thesis*, Moscow, N.N. Semenov Institute of Chemical Physics, RAS, 1992, 143 p. (Rus)
67. Sevilla V.D., La Vere Th., Becker D., Wang W., Swarts S. and Wheeler K.T., In Coll.: *Radiat. Res. 1895 - 1995. Congress Proc.*, vol. **2**. Congress Lectures, Ed. U. Hagen, D. Harder, H. Jung, and C. Streffer, Wurburg: Universitatsdruckerei H. Sturtz AG., 1995, pp. 262 - 265.
68. Babushkina T.A., Duzhenkova N.A. and Kaunov A.V., *Thes. Rep. VII All-Union Conference "Magnetic Resonance in Biology and Medicine"*, May 1989, Zvenigorod, pp. 237 - 238. (Rus)
69. Oreshko V.F. and Korotchenko K.A., *Izv. Vuzov. Pishchevaya Tekhnologia*, 1959, No. 4, p. 51. (Rus)
70. Oreshko V.F. and Korotchenko K.A., *Izv. Vuzov. Pishchevaya Tekhnologia*, 1959, No. 5, p. 29. (Rus)
71. Lipatov S.M., *Superpolymer Compounds (Lyophilic Colloids)*, Tashkent, Izd. AN BSSR, 1943, 160 p. (Rus)
72. Oreshko V.F. and Korotchenko K.A., *Izv. Vuzov. Pishchevaya Tekhnologia*, 1962, No. 4, p. 25. (Rus)
73. Arthur J., In Coll.: *Cellulose and Derivatives*, Ed. N. Bickles and L. Segal, vol. **2**, Moscow, Mir, 1974, p. 256. (Rus)
74. Korotchenko K.A. and Sharpatyi V.A., *Radiats. Biol. Radioekol.*, 2000, vol. **40**(2), p. 133. (Rus)
75. Papkov S.P., *Jelly-like State of Polymers*, Moscow, Khimia, 1974, 256 p. (Rus)
76. Korotchenko K.A., *Izv. Vuzov. Pishchevaya Tekhnologia*, 1962, No. 4, p. 29 - 31. (Rus)
77. bondarenko N.T. and Sharpatyi V.A., *Doklady AN SSSR*, 1989, vol. **304**(5), p. 1158. (Rus)
78. Emanuel N.M., *Biofizika*, 1984, vol. **29**(4), p. 706. (Rus)
79. Sanner T., Henrriksen Th., and Phil A., *Radiat. Res.*, 1967, vol. **32**(3), p. 463.

80. Phil A., Henrirsen Th., and Sanner T., *Radiat. Res.*, 1968, vol. **35**(2), p. 235.
81. Sharpatyi V.A., *Radiats. Biol. Radioekol.*, 1999, vol. **39**(1), p. 156. (Rus)
82. Kochetkov N.K., Kudryashov L.I., Clenov M.A., *et al.*, *Doklady AN SSSR*, 1968, vol. **183**(2), p. 376. (Rus)
83. 83. Sharpatyi V.A., Cadet J., and Teoule R., *Int. J. Radiat. Biol.*, 1978, vol. **33**(5), p. 419.
84. Kuzurman P.A. and Sharpatyi V.A., In Coll.: *Bioantioxidant – Proc. Intern. Symp. “Medicine and Health Protection. Medical Instruments and Pharmacy”*, Sent. 16 – 19, 1997, Tyumen’, Izd. Tyumen State University, p. 105. (Rus)
85. Kuzurman P.A. and Sharpatyi V.A., *Radiats. Biol. Radioekol.*, 1998, vol. **38**(2), p. 147. (Rus)
86. Petryaev E.P., Shadyro O.I., Kovalenko N.I., and Boltromeyuk V.V., *Izv. AN BelSSR, Ser. Khim.*, 1984, No. 3, p. 80. (Rus)
87. Edimecheva I.P., ‘Radiation initiated degradation and dextrane modification in aqueous solutions’, *Candidate Dissertation Thesis*, Moscow, MSU, 1989. (Rus)

Chapter 9. The radiolysis method for glycoproteids

9.1. STRUCTURE AND PROPERTIES OF GLYCOPROTEIDS

Organic compounds including protein and non-protein fragments (the latter represent a prosthetic group) are called the conjugate proteins or proteids. Glycoproteids are biopolymers consisting of a protein and a carbohydrate fragments. Muconic compounds are belonged to these substances – the polymers including proteins, polysaccharides and lipids, linked by covalent and ionic bonds. Mucoproteids composed of proteins (the predominant component of the natural complex) and carbohydrates (oligo- or polysaccharides) are the components of mucous linings of the animal organs, blood and milk; mucopolysaccharides are the components of connective tissues, liver and lungs. Among glycoproteids are immunoglobulins (A, E, D, G, M), Ig, produced by B-lymphocytes and plasmatic cells. Ig function as antibodies, which protect the organism from dangers of intervention of the aliensubstances – antigens. The structure of immunoglobulins is based on a dimer consisting of two light (L) and two heavy (H) polypeptide chains, to which oligosaccharide fragments are bound. IgM have five such fragments consisting of mannose and N-acetylglucosamine residues. The structures of IgA, IgE and IgD also include fucose, galactose and N-acetylneuraminic acid. Some immunoglobulins are freely disposed in the blood serum (IgE), intestinal and bronchial secretion, pituitary membrane (IgA) and so on; Ig(G, A, M, D and E) are found in the membrane (the surface) of B-lymphocytes.

The above-listed compounds are responsible for many functions of the cells and the organs of animals, affected by irradiation. For example, it is known that one of the consequences of an animal and a man irradiation is disturbance of the immune functions of the organism. At the molecular level, this might be explained by radiolytic modification of oligosaccharide units of glycoproteids, which form receptors. In the cell membranes, receptors (antibodies) extend to the environment and participate in the recognition of various substances-antigens. A change in the conformation of glycoprotein fragment induced by radiation modification prevents its (antibody's) contact with the antigen – the immunity is disturbed.

There are scanty works in the literature devoted to the investigations of the radiation effect on glycoproteids. In this Chapter we discuss radiolysis of one of the glycoproteids, the so-called total blood substance (TBS) and compounds modeling some fragments of this natural complex. The composition of this TBS complex (Figure 9.1) is studied well. TBS determines species differences in animals and a man, and participates in immunization phenomena. TBS extracted from gastric mucous cover protects stomach walls from proteolytic action of the enzyme. TBS extracted from pig's gastric mucous cover is a high-molecular compound (MM = 300,000 – 400,000) with the polypeptide chain of the TBS complex (15 wt.%) including 400 – 450 amino acid residues [1]. More than a half of these residues are oxyamino acids (serine and threonine) and proline, added by an insignificant quantity of aromatic amino acid residues. The polypeptide backbone has branches of carbohydrate chains, which contain from three to twenty monomer units, representing N-acetyl-substituted residues of glucosamine and galactosamine, linked to one another by glycoside bonds. Carbohydrate chains are bound to the peptide backbone by threonine and serine amino acid residues (mostly O-glycoside bonds), particularly, by locations of hydroxyl groups in these amino acids. Figure 9.1 shows a fragment of TBS complex, artificially composed of identified units so that it includes all determined types of bonds.

The irradiation of aqueous solutions of glycoproteids causes degradation of these biopolymers. TBS is depolymerized: the solution viscosity decreases (Table 9.1), molecular composition of the biopolymer (the quantity of neutral sugars and amino sugars) (Table 9.2), and the quantity of amino acids (Table 9.3) change.

Table 9.1

The change of glycoprotein solution viscosity (0.1%, F1 fraction) induced by irradiation [2]

Irradiation dose, Gy	Relative viscosity
0	1.43
5	1.39
100	1.12
1,000	1.07

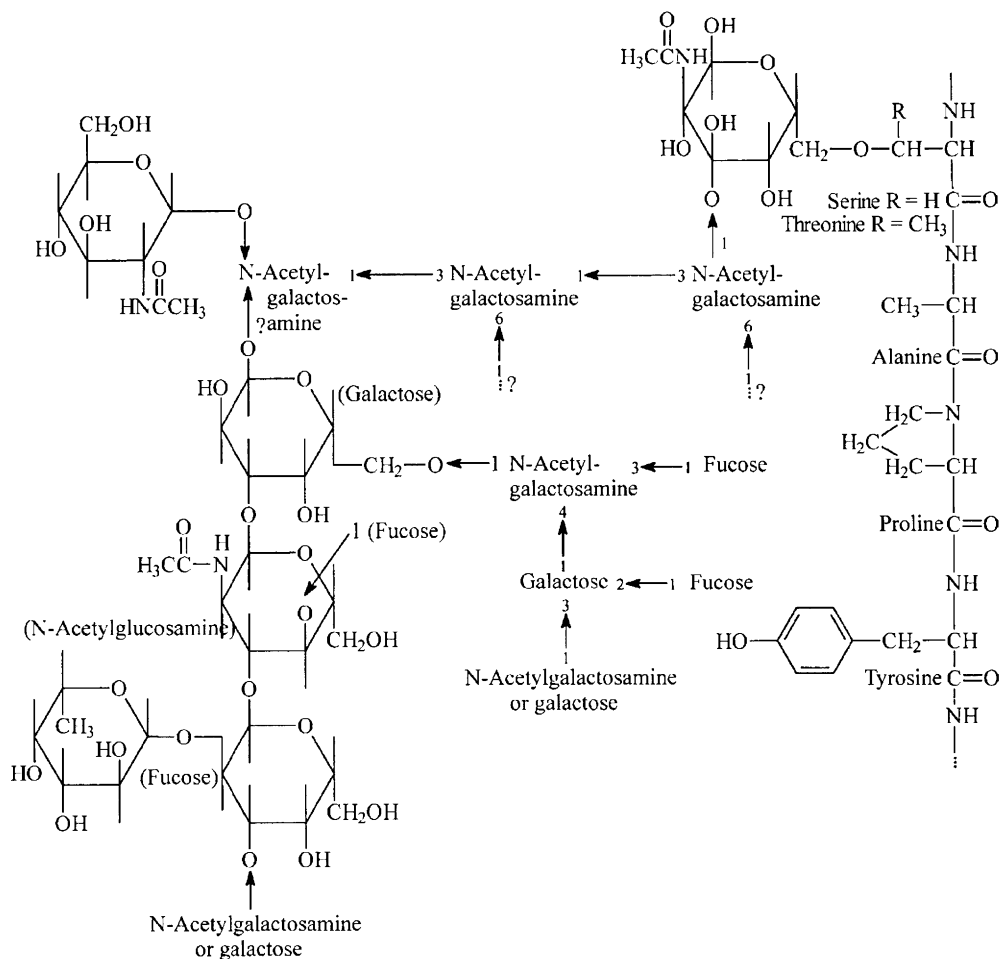


Figure 9.1. The structure of glycoprotein (a hypothetical fragment) according to the data of biochemical analysis methods [1]

Table 9.2

The change of neutral and N-acetyl-substituted amino sugar composition (%) in glycoprotein (F1 fraction) at irradiation of its 0.1% solution [2]

Irradiation dose, Gy	Hexose	Fucose	N-Ac-glucosamine	N-Ac-galactosamine
0	21.6	8.3	24.19	13.85
1,000	18.6	6.4	21.82	13.16

Table 9.3

The change in amino acid composition (%) of glycoproteid (F1 fraction) at irradiation of its 0.1% aqueous solution by 1 kGy dose [2]

Amino acid	Non-irradiated solution	Irradiated solution
Serine	1.94	1.84
Threonine	3.59	3.20
Proline	2.59	2.07
Glycine	0.34	0.36
Alanine	0.80	0.73
Valine	0.54	0.50
Leucine	0.38	0.38
Isoleucine	0.15	0.13
Asparaginic acid	0.22	0.26
Glutamic acid	0.71	0.76
Tyrosine	Traces	Traces
Phenylalanine	Traces	Traces

The yield of biopolymer radiation-induced degradation registered in the irradiated aqueous solution depends on the origin of saturation gas. For example, at transition from the solutions saturated with Ar to the ones saturated with N₂O the yield of radiolysis products, which absorb in the range of 260 – 360 nm, increases twice, approximately. Analogous results were obtained for other glycoproteids – acidic amino polysaccharides: heparin, keratan sulfate and chondroitin-4-sulfate [3 – 5]. These data indicate the predominant responsibility of [•]OH radicals for degradation of said polymers in solutions.

9.2. RADIOLYTIC PROPERTIES OF GLYCOPROTEID COMPONENTS

To make head of the radiolysis mechanism of a glycoproteid complex, let us consider radiolytic properties of compounds in its fragments: protein, amino sugars and their N-acetyl-substituted derivatives, oligo- and polysaccharides. It might be suggested that all listed components of the TBS complex generally define its radiation-chemical properties. As analyzing radiolytic properties of some TBS complex components, let us manage to

estimate the most probable sites in the glycoprotein molecule to be attacked by primary radicals of water, analyze properties of macroradicals formed (and possible routes of their conversions) and relate the final effects of irradiation on the glycoprotein molecules in aqueous solutions to primary stages of radiolysis.

Polypeptide radiolysis

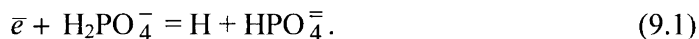
The mechanisms of primary radical formation and conversions in a polypeptide, which is a protein molecule, are already discussed in detail (refer to Chapter 7). The mechanism of amino acid radiolysis was also discussed and a conclusion was made about water radical attack sites in amino acid residues in the protein molecule. With respect to the amino acid composition of TBS protein fragment composition, one may state *a priori* that the electron attack sites (at irradiation of solutions in the absence of oxygen) are carbonyl groups of peptide bonds, end protonated amino groups of lysine, arginine, C=O double bonds of carboxylic and carboamide groups of asparaginic and glutamic amino acids, if these groups does not participate in formation of any internal bonds of the TBS complex. Radicals $\cdot\text{OH}$ and $\cdot\text{H}$ (in the absence of molecular oxygen in the solution) attack H-C $_{\alpha}$ bond of the polypeptide chain in the protein fragment (Chapter 7). The second ranked sites for water radical attack must be tyrosine and phenylalanine aromatic rings, which quantity in TBS is rather low. This conclusion is based on the ESR data [6] identifying radical H-adduct of phenyl ring among free radicals in the irradiated phenyl- β -D-glucopyranoside.

The TBS complex composition also includes amino sugar, N-acetyl-substituted amino sugars and neutral sugars.

Glucosamine radiolysis

The typical feature of glucosamine radiolytic properties in aqueous solutions, which differs it from radiolysis of neutral carbohydrates, is its interaction with hydrated electron. The rate constant of glucosamine reaction with the electron equals 4.2×10^8 l/mol·s, which is comparable with the rate constant of $\cdot\text{OH}$ reaction with carbohydrates. The electron participation in reactions with glucosamine may be proved by the results of atoms H yield change in phosphate glassy-like solutions of glucosamine of various

concentrations, irradiated at 77 K. In this case, atomic hydrogen is formed by the reaction as follows:



The observed decrease of atomic hydrogen accumulation with increasing glucosamine concentration in the solution (Table 9.4) reflects proceeding of the following competing process:



Table 9.4

The yield of radicals G in frozen-up solutions of glucosamine (GA) [7 – 9]

GA concentration, M	$G(\Sigma R^\bullet)$	$G(\text{O}^-)$	$G(\Sigma R^\bullet)$	$G(\text{H}^-)$	$G(\Sigma R^\bullet)$	$G(\bullet\text{OH})$
	10 M KOH		5 M NaH_2PO_4		H_2O	
0	3.8 ± 1.3	2	1.9	0.7	0.7	0.7
0.11	–	1.5	–	–	–	–
0.55	–	–	2.5	0.05	–	–
1.10	3.5 ± 0.2	0.45	2.2	0.03	1.6 ± 0.3	0.8

The influence of γ -irradiation on frozen-up aqueous solutions of glucosamine produces radicals from it via reactions with electrons and $\bullet\text{OH}$ (O^- in alkaline medium and H_2O^+ in acidic medium) and $\bullet\text{H}$ radicals. Data from Tables 9.4 and 9.5, as well as test results on photoannealing of electron and tests, in which isothermal conversions of paramagnetic particles, stabilized at 77 K (the tunneling effect for \bar{e} and $\bullet\text{H}$), show that in both cases, the rates of \bar{e} and $\bullet\text{H}$ recombination processes (proceeding by the reactions $\bar{e} + \bar{e} = e^-$, $\bar{e} + \text{O}^- = \text{O}^-$ and $\text{H}^\bullet + \bullet\text{H} = \text{H}_2$) are significantly reduced in the presence of glucosamine in this matrix due to reactions (9.2) and (9.3):

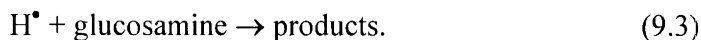


Table 9.5

The change (Δ) of total concentration of radicals and O^- ($\times 10^{18} \text{ g}^{-1}$) in glucosamine (GA) alkaline solution at photoannealing of electrons by $\lambda > 540 \text{ nm}$ [7 – 9]

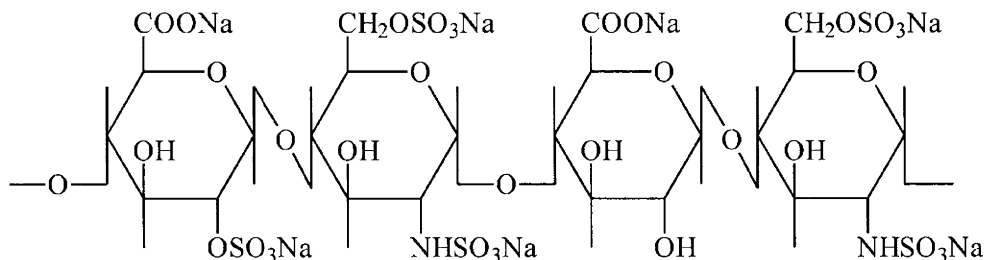
Dose, kGy	ΣR^\bullet	ΔR^\bullet , %	O^-	ΔO^- , %	ΣR^\bullet	ΔR^\bullet , %	O^-	ΔO^- , %	ΣR^\bullet	ΔR^\bullet , %	O^-	ΔO^- , %
	10 M KOH, without GA				10 M KOH + 0.27 M GA				10 M KOH + 1.1 M GA			
5	0.7*	93	0.4	75	1.2	87	0.2	50	1	70	0.3	50
	0.08**		0.1		0.16		0.1		0.3		0.15	
10	1.6	90	0.8	81	1.3	90	0.3	67	2.0	80	0.2	50
	0.15		0.15		0.16		0.1		0.4		0.1	

Notes: * Before photoannealing.

** After photoannealing.

Heparin radiolysis

Heparin is a heteropolysaccharide with MM $\sim 10,000$, which macromolecule contains repeating tetrameric units of sulphated disaccharide aminoglucose residues, linked by α -1-4- bonds. Tetrameric unit contains two glucosamine residues with two types of sulfate groups:

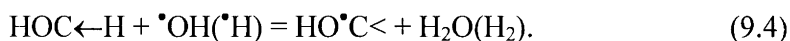


Heparin is of interest for us as a polymer simulating structural fragment of a glycoprotein without polypeptide chains. Heparin is degraded by radicals $\cdot\text{OH}$ and $\cdot\text{H}$ (similar to polysaccharides), and electron. The sites for electron attack are N-sulfate (substituted amino) groups. As a result, macromolecule desulfation is initiated. At low-temperature irradiation primary radicals of H detachment from C1 and C4 atoms are formed with the highest yield (conversions of these radicals are discussed in Chapter 8). The main result of irradiation is formation of breaks in macromolecules (by glycoside bonds) [10].

9.3. FORMATION AND CONVERSIONS OF RADICALS IN GLYCOPROTEID COMPONENTS

Glucosamine radicals

The influence of radicals $\cdot\text{OH}$ and $\cdot\text{H}$ on glucosamine molecule induces C-H bond break in anhydrocarbohydrate cycle with formation of radicals by the reaction:



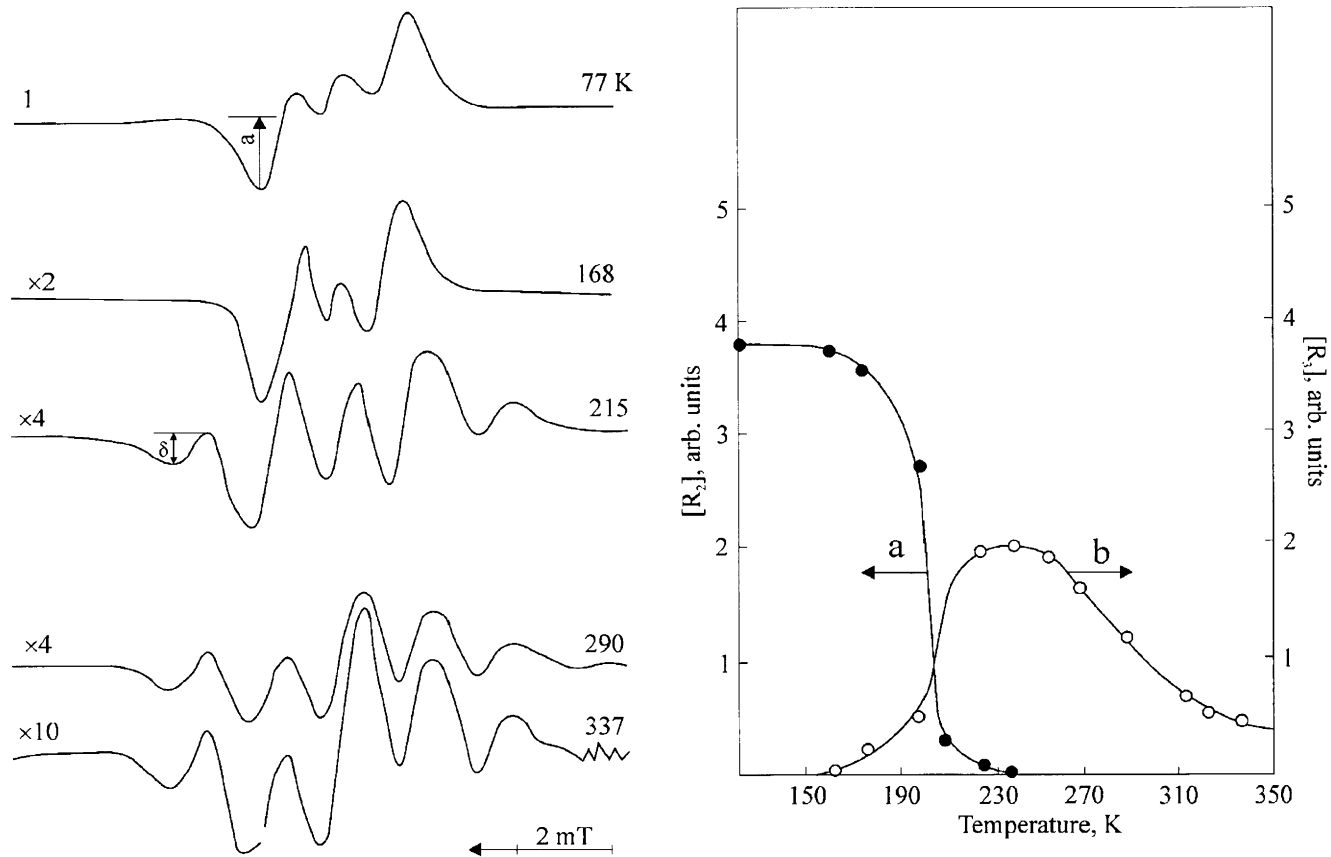


Figure 9.2. ESR spectra registered at different temperatures and the change in concentration of radicals in glucosamine chloride polycrystalline evacuated preparation, irradiated at 77 K [9]

Hence, similar to the case of neutral monosaccharides, H atoms may be detached from all carbon atoms. In the glycoprotein molecule, glucosamine and galactosamine residues are ring shaped. Let us consider the structure of radicals formed at radiolysis of glucosamine and its derivatives (ring shaped): glucosamine chloride (GA·HCl) and N-acetyl-substituted glucosamine (N-Ac-GA).

At low-temperature irradiation of GA·HCl radicals are detected; hence, the predominant yield is observed for radicals, the ESR spectrum of which represents a doublet band with $\Delta H \sim 2.6$ mT (Figure 9.2). After heating the sample up to 170 K, an additional wide (~ 8 mT) band with five equidistant components is observed. The ratio of intensities of these components with respect to their resolution approaches a binomial e.g. a quintet. The change in intensities of the doublet "a" and the quintet "b", which reflects variation in concentrations of corresponding types of radicals, follows the inverse dependence, hence, total concentration of radicals in this intermediate temperature range remains constant within the measuring error. Thus, it should be concluded that at the sample heating the radical conversion $R_a^\bullet \rightarrow R_b^\bullet$.

As regards the structure of GA molecule and ESR bands characteristics, it may be concluded that in this case R_a^\bullet radical is isomerized with C5-O5 bond break, because C5 atom is the only site in the radical, where unpaired electron may interact with four equivalent protons (with splitting on each of them is ~ 2 mT). The radical R_a^\bullet conversion proceeds according to the scheme, analogous to the reaction (8.9), Chapter 8.

Radicals in irradiated N-acetylglucosamine (N-Ac-GA) and their conversions

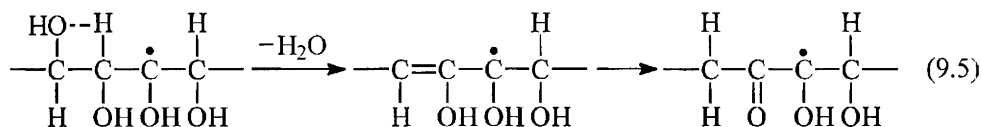
HFS of the irradiated N-Ac-GA spectrum differs from that of the above-discussed GA base and GA·HCl spectrum. This is stipulated by occurrence of a substituent in the N-position and formation of radicals from this group at irradiation, which will be discussed below. Note that the character of conversions in primary radicals formed in the anhydroglucose ring and the yield of corresponding reactions of radical conversions is changed compared with GA base and GA·HCl. The reason is the origin of the substituent, which interlocks the amino group. The allyl radical formation of R_a^\bullet type is the

Table 9.6

Characteristics of ESR spectra and radicals recognized in glucosamine chloride (GA·HCl) and N-acyl-substituted glucosamine (N-Ac-GA) preparations, irradiated at 77 K [9]

Radical	HFS	ΔH_{tot} , mT (max)	ΔH_{split} , mT	<i>g</i> -factor	Suggested structure of the radical	Temperature range, K
R ₁	1	0.6	–	2.002	GA–	77 – 215
R ₂ (a)	1:1	3.9	2.6	2.003	C ₁ [•]	77 – 290
R ₃ (b)	1:4:6:4:1	9.0	2.0	2.003	–C ₍₄₎ HOH, –C ₍₅₎ [•] H–C ₍₆₎ H ₂ OH	215 – 337
R ₄	1:1	4.2	–	2.003	–C [•] (OH), except C ₁ [•]	77 – 150
R _A	1:1	1.55	1.25	2.007	–C [•] (=O)–CH–	95 – 180
R ₅	1:2:1	6.7	–	2.003	2H _β or 1H _α and 1H _β	77 – 130
R ₆	?	4.5	–	2.003	?	77 – 150
R ₇	1:1	3.0	2.0	2.003	1H	77 – 180

typical feature of radical conversion in irradiated N-Ac-GA at thermal annealing. ESR spectrum parameters for R_a^\bullet radical are stipulated by delocalization of unpaired electron by the fragment including a carbonyl group, the double bond of which is conjugated with p-orbital of unpaired electron, and the difference of the factor $g = 2.007$ from that for free electron is explained by a significant part of the orbital component. Table 9.6 shows parameters of identified radicals. As follows from the data on thermal annealing, the formation of type R_a^\bullet radicals is related to conversion of the primary radicals of R_4^\bullet type by the reaction with water molecule release and H_2O β -elimination (9.5).

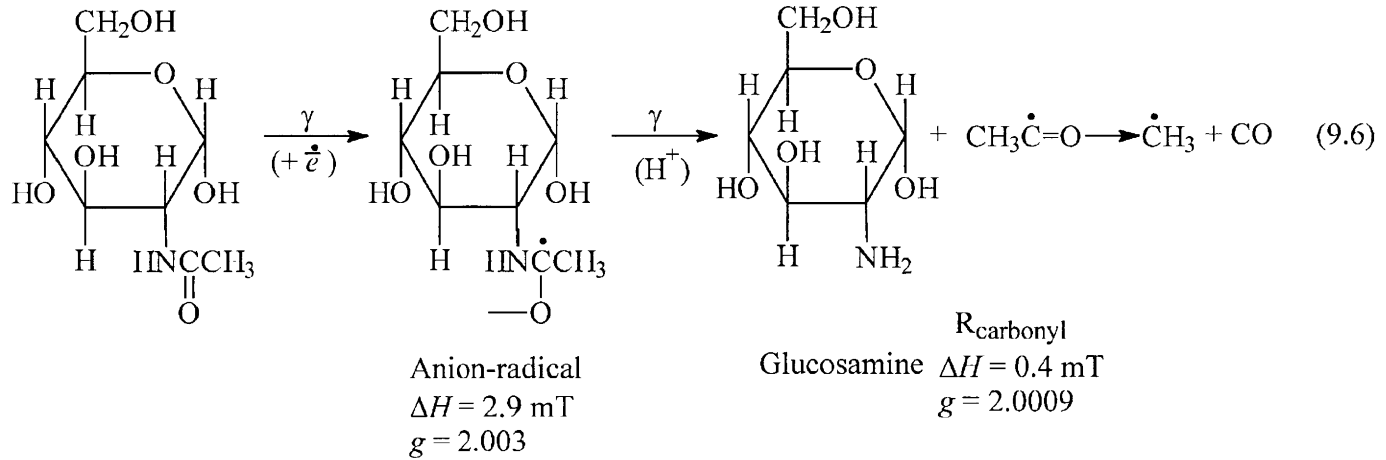


Acetamide radiolysis

Acetamide is a compound modeling the side fragment of N-acetylglucosamide. The analysis of ESR spectra of irradiated acetamide showed that anion-radical formation (doublet 1:1, $\Delta H \sim 2.9$ mT, $g = 2.003$) at the electron attack on $>C=O$ bond is one of the main processes of radiolysis of this compound. As impacted by γ -radiation, anion-radical decays with formation of an acyl radical ($\Delta H = 0.4$ mT, $g = 2.0009$). The scheme of radical formation and conversions with participation of electron in the reactions with N-acetyl-substituted group in amino sugars with respect to the data on acetamide radiolysis may be presented as follows [9] (see the scheme (9.6)).

This process must proceed at higher rate in the presence of water, because hydration of the anion-radical gains energy up to 3 eV.

Thus, the electron participation in reactions is reduced to damaging of N-acetyl-substituted amino groups in the carbohydrate fragment of glycoprotein. Finally, a sequence of conversions of radicals formed in this unit must be accompanied by carbon oxide and methane release, and amino group formation at carbohydrate units. So far as concerns radiolysis of aqueous



solutions, all these processes must proceed in the absence of molecular oxygen, because oxygen intercepts the electron and, therefore, O_2^- radicals (or HO_2^\bullet with respect to the medium pH) participate in the reactions.

Chitosan radiolysis

Chitosan is a glucosamine superpolymer ($MM = 10,000 - 70,000$) demonstrating radioprotector properties: its intravenous injection to mice, dosed 20 mg/kg, 15 – 30 min prior to irradiation by 8 Gy (minimal absolutely lethal) dose increases survivability of animals to 73% [11]. Chitosan is produced from chitin – the natural analogue of cellulose, consisting of N-acetyl- β -D-glucosamine residues, linked by β -1,4-glycoside bonds – by enzymatic deacetylation (full or partial) or treatment by concentrated alkaline [12].

Similar to polysaccharides (Chapter 8), primary radicals in irradiated dry chitosan preparations are H and OH detachment radicals from carbon atoms. Irradiation of aqueous solutions produces H detachment radicals only (formed at water $^\bullet OH$ radical attack on C–H bonds in the monomeric units). Contrary to neutral amino sugars, the ring shaped ones react with electron at a rate comparable to that for $^\bullet OH$ radical [13].

Basic processes of chitosan degradation are the following [14]: deamination ($G \sim 3$), break formation in the polymer chain ($G = 4.2 \pm 0.3$), molecular hydrogen ($G = 1.3$) and carbon dioxide ($G = 1.5$) release. ESR spectra of chitosan and chitin (Figure 9.3 [15]), irradiated at low temperature, recognized the radicals of H detachment from C1 (1:1, $a = 3.0$ mT – splitting) and C4 (1:2:1, $a \sim 2.6$ mT) atoms and the radical of amino group detachment from C2 atom (doublet 1:1, $a \sim 2$ mT; triplet 1:2:1, $a \sim 3.8$ mT). As irradiated chitin is heated up to $T \sim 200$ K, $^\bullet C1$ and $^\bullet C4$ concentrations decrease (significantly for the latter) and $GluNHC^\bullet(OH)CH_3$ radical is detected (1:3:3:1, $a \sim 1.4$ mT), where Glu is a fragment of the polymeric chain. Total yield of radicals at 77 K is 3.0 for chitosan and 2.3 for chitin. Irradiation of chitosan at $T = 300$ K accumulates carboxylic ($G \sim 0.6$) and carbonyl groups in it, the yield of reducing groups being equal 25 ± 2 (determined by copper index) [15].

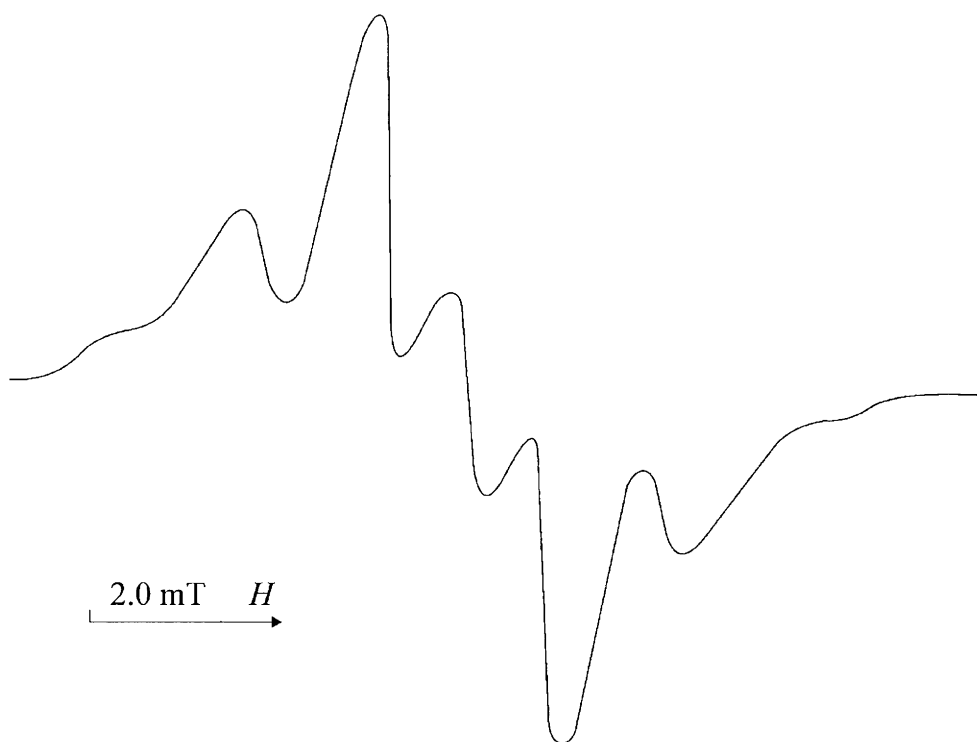


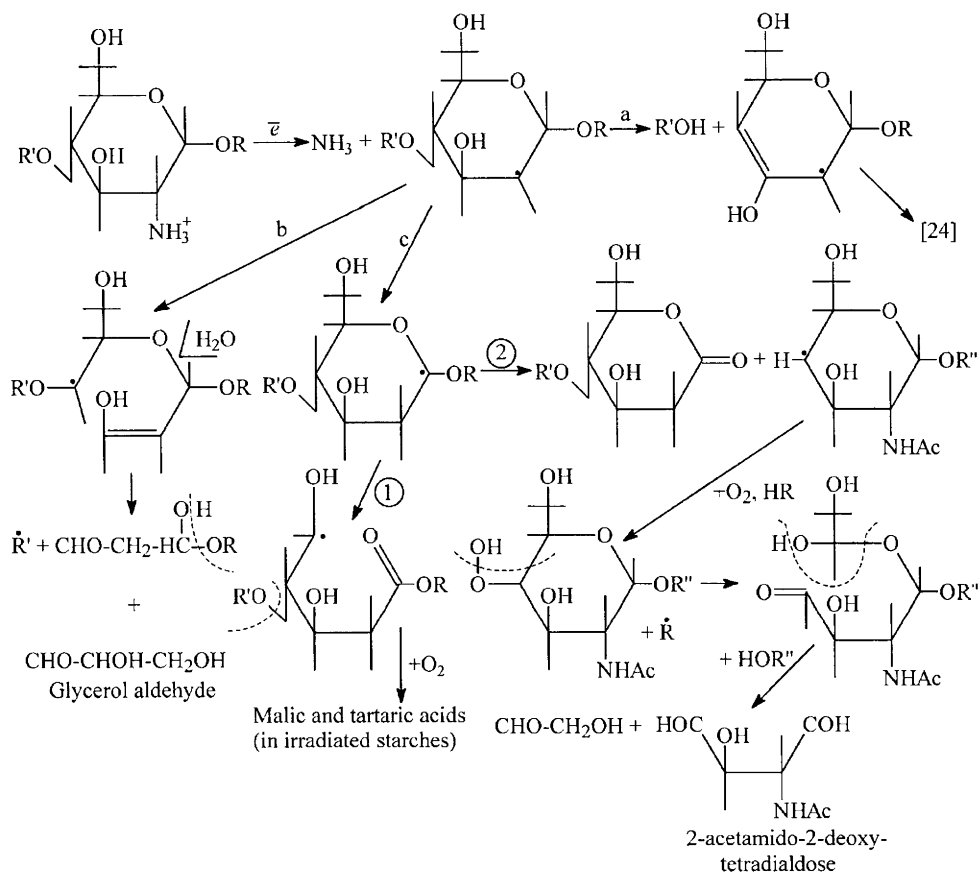
Figure 9.3. ESR spectrum of evacuated chitosan, γ -irradiated at 77 K [15]

Chitosan deamination results the interaction of glucosamine residue amino group with electron [13]. As it captures the electron, C2–N bond breaks, ammonia is released and alkyl radical $\cdot\text{C}2$ is formed. Analogous process was detected in proteins irradiated at low temperature – deamination of lysine amino acid residues (Chapter 7). According to estimation, the concentration of alkyl radicals of amino group detachment $\cdot\text{C}2$ in the sample at 77 K is 20 – 25% of total quantity of radicals or higher.

For $\cdot\text{C}2$ radical, three alternatives of conversions exist [16]:

- a) by type of β -elimination of water (H detachment from C3 and OR – from C4). Hence, a break occurs in the polymeric chain, and in the monomeric unit deoxy(C4)- and keto(C3)-groups are formed;
- b) isomerization with C3–C4 bond break, double C2=C3 bond and radical with unpaired electron at C4 formation;

c) rearrangement of chemical H–C bonds at C1 and C2 with unpaired electron transfer to C1 and then radical \cdot C1 conversion (Scheme 9.1):



Scheme 9.1

Scheme 9.1 and subsequent ones show compounds, recognized at radiolysis of glucosamine and/or N-acetylglucosamine aqueous solutions [13].

The possibility of a) alternative implementation is proved by detection of citric and succinic acids among starch radiolysis products. These acids have the above-mentioned functional groups at C3 and C4 atoms (Chapter 8). The sequence of elementary acts of this process was already discussed in detail [17].

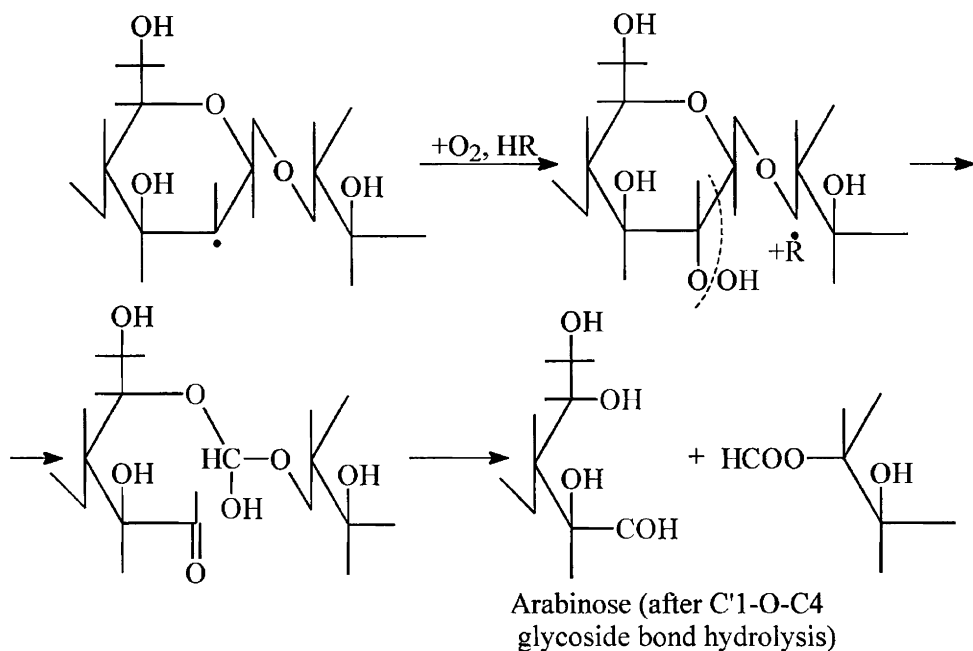
Radical $\cdot\text{C}2$ conversions by the route b) are confirmed by the results of glucosamine radiolysis in solutions, for which glyceraldehyde with the yield $G = 1.3$ in 0.05 M solution was detected [13].

The first stage of radical $\cdot\text{C}2$ conversions by the route c) – the rearrangement of H–C bonds at C1 and C2 atoms in the ring – is similar to the process proceeding in cellulose [16]. Radicals $\cdot\text{C}1$ may convert by two routes: $\cdot\text{C}1$ isomerization with C5–O5 bond break and unpaired electron transfer to C5. This process is registered by the ESR method at low-temperature irradiation of glucosamine [18]. The subsequent stages of radicals $\cdot\text{C}5$ conversions, for example, in dry starches irradiated in the presence of oxygen produce malic and tartaric acids [17] (Chapter 8).

Another possible route for $\cdot\text{C}1$ conversions is isomerization with $\cdot\text{C}1\text{--O}1\text{--C}'4$ glucoside bond break, keto-group formation by C1 and unpaired electron transfer to C'4 of the neighbor monomeric unit. Radical $\cdot\text{C}'4$ conversions, for example, in the presence of oxygen may cause accumulation of type 2-amido-2-deoxytetradialdose (from glucosamine residue) and 2-acetamido-2-deoxytetradialdose (from N-acetyl-substituted glucosamine residue) compounds. The latter product was detected at irradiation of N-actyl-2-glucosamine aqueous solutions, saturated with nitrous oxide in the presence of O_2 . The yield reached 0.5 (0.01 M solution) [13].

In radicals with unpaired electron at carbon of $\cdot\text{C}1\text{--O}1\text{--C}'4$ in the presence of water, $\text{O}1\text{--C}'4$ β -bond may be hydrolyzed [11]. In this case, hydroxyl groups occur at C1 atom of the current bond and at C'4 atom in the neighbor monomeric unit. At H transition from hydroxyl C1OH to O5, by C1 atom an acyl radical is formed eliminating CO, which formation is chitosan was detected [15].

If at chitosan irradiation in the presence of molecular oxygen the deamination act is accompanied by peroxide radical $\text{C}2\text{OO}\cdot$ and then peroxide by C2 atom formation, after dissociation of the latter with O–O and C1–C2 bond break (as it happens in irradiated starches [9] an aldehyde group at C2 atom is formed. Resulting the rearrangement of chemical bonds at C1 (Scheme 9.2), arabinose may be synthesized.



Scheme 9.2

If beside glucosamine residues chitosan sample includes N-acetyl- β -D-glucosamine residues (incompletely deacetylated), a possibility of electron capture by carbonyl group in acetyl with anion-radical formation should be taken into account. This process is observed for the above-considered acetamide, proteins and peptides, irradiated at low temperature: electron attacks carbonyl group of the polypeptide bond. Anion-radicals recognized at 77 K in irradiated proteins (low resolved doublet with ~ 1.5 mT splitting) are protonated at sample heating up to 190 – 200 K (at the interaction with water molecules, which obtain mobility due to structural changes in the matrix). A neutral radical is formed – H-adduct with the ESR parameters similar to the initial anion-radical (low resolved doublet R_{pb} , Chapter 7).

As indicated [3], ESR spectrum parameters and $\text{GluNHC}^*(\text{OH})\text{CH}_3$ radical registration conditions for chitin, first irradiated at 77 K and then annealed at 200 K (methyl group rotates), allow for a conclusion that the radical is formed from the primary anion-radical of acetyl. Subsequent hydrolysis of N–C bond in the radical induces formation of amino group in anhydroglucose ring and acetic acid molecule with identical yields [14].

The mechanisms of chitosan radiation degradation demonstrate participation of macroradicals, formed due to electron attack. The main result of such influence is polymer deamination. This process is accompanied by breaks in the polymer chain: by glycoside bonds or as a result of monomeric unit decomposition. Hence, taking into account the yield of breaks in the chitosan macromolecule and the yield of deamination, it may be assumed that the latter value and, correspondingly, the electron participation in the polymer degradation give over 2/3 part of the effect (71%). The rest 29% (~30%) of the primary macroradical degradation are given by H atom detachment.

The mechanisms of chitosan primary radical conversions are presented basing on the studies of dry polysaccharide radiolysis. As aqueous liquid solutions of chitosan are irradiated, the electron (\bar{e}_{hydr}) eliminates amino group, therefore, these mechanisms are also suitable for explaining conversions of alkyl $\cdot\text{C}2$ radical.

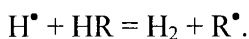
The radiation chemistry studies of glucosamine and N-acetylglucosamine were performed for 0.01 – 0.1 M aqueous solutions, i.e. in conditions of complete involvement of water radicals into reactions with dissolved substances (the indirect effect of radiation is maximal) [13]. Electrons attack N–C2 fragment, and $\cdot\text{OH}$ radicals – H–C bonds at each of 6 carbon atoms, and H detachment radicals are formed. The latter fact in these systems is confirmed by the composition of recognized radiolysis products in the absence of molecular oxygen: they are compounds containing keto- (or aldehyde) group at each carbon atom. The formation mechanisms of these compounds have been already considered [13]: the first stage of hydroxyalkyl radical conversion is oxidation (H transfer from hydroxyl to any reagent). Using the yields of corresponding radiolysis products of N-acetyl-substituted glucosamine in aqueous solutions [5], the contribution of each H detachment radical to the monomeric unit degradation may be roughly estimated (Table 9.7). Relatively low yield of an oxo-product by C1 may be explained by radical $\cdot\text{C}1$ participation in various processes (see Schemes 9.1 – 9.3). For instance, one of them produces arabinose in irradiated solutions of these monomers (about the mechanism see below).

Table 9.7

The yields of ketones and aldehydes – some products of N-acetylglucosamine radiation modification in aqueous solutions (0.01 – 0.1 M), saturated with N₂O [13]

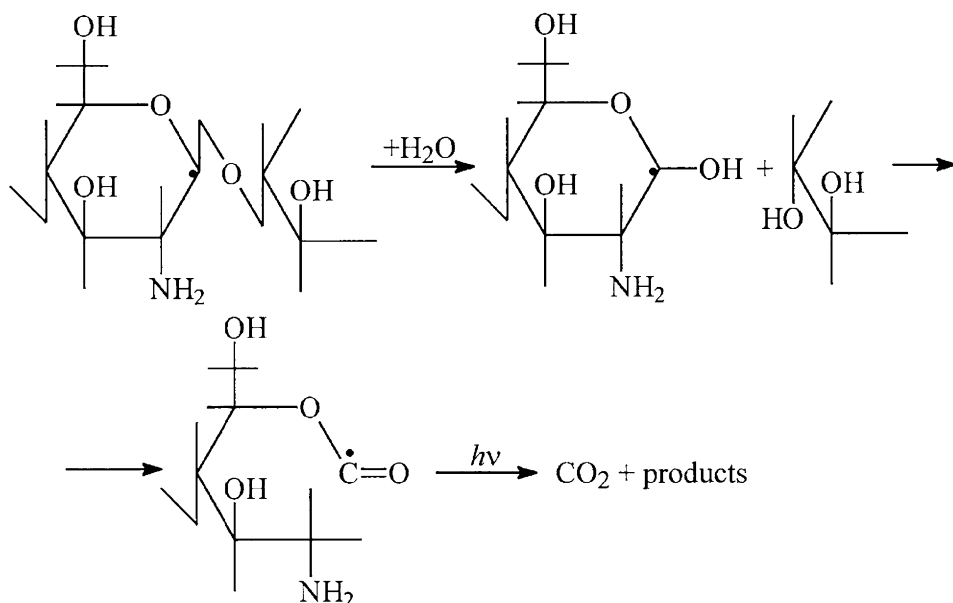
H detachment radical	Molecular product	G(product)
•C1	2-acetamido-2-deoxygluconolactone	0.15
•C2	1-acetamido-1,3-dideoxypent-2-ulose	0.1
•C3	1-acetamido-1-deoxypent-2-ulose	
•C4	2-acetamido-2,3-dideoxyhexos-4-ulose	0.35
•C5	2-acetamido-2-deoxyhexos-5-ulose	0.4
•C6	2-acetamido-2-deoxyhexodialdose	0.5

In the case of dry chitosan irradiation, the yield of molecular hydrogen $G = 1.3$ may be used as the basic value for the estimation of H detachment radicals contribution into degradation of this polymer, if we accept that H₂ in polysaccharides is formed by the reaction



Then the part of H detachment radicals into chitosan degradation equals $1.3/4.2 \sim 0.3$, which means $\sim 30\%$ – the value deduced before by the difference between total degradation process yield and the contribution of electrons into this process, which promote deamination of the polymer. Direct measurements of the radical concentration in chitosan at low temperature gave $G = 3.0$ [14]. This value exceeds the estimation, but is lower than it would be required under a suggestion that one radical produces one break in the polymer chain.

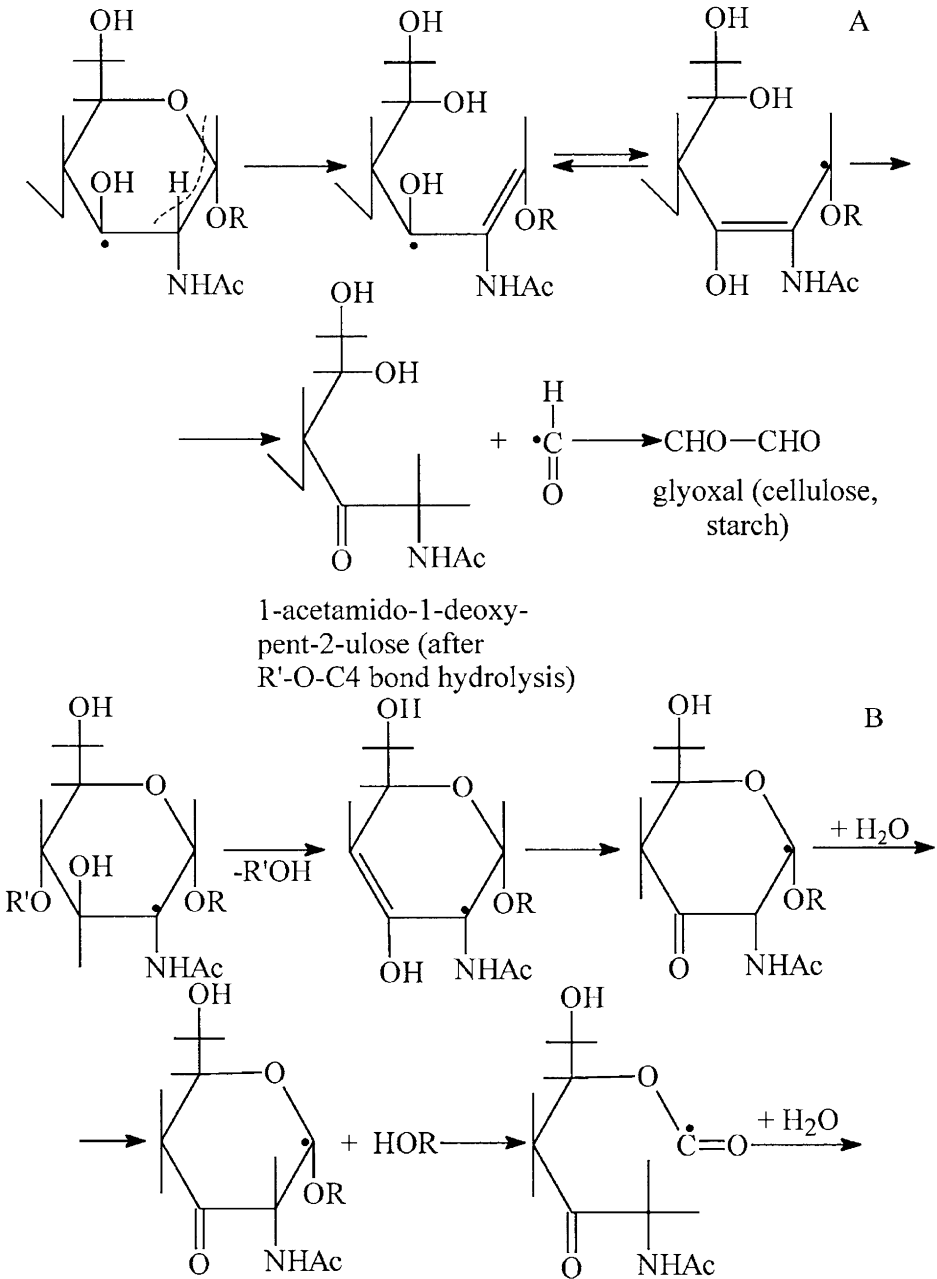
Basing on the radiolytic effects of carbohydrates (Chapter 8), note that CO₂ formation in irradiated chitosan (and chitin), glucosamine keto- and deoxyketo-derivatives – in solutions of chitosan, glucosamine and N-acetylglucosamine, is related to H detachment primary radical conversions. The mechanism of CO₂ formation in the absence of O₂ (this means by C1, because only this atom is bound to two oxygen atoms) is shown in Scheme 9.3 [19].



Scheme 9.3

Arabinose synthesis is also related to conversions of H detachment radical from C1 in the presence of O₂. The mechanism of this process in glucosamine and N-acetyl-substituted glucosamine solutions is considered [13]: after O1–C'4 β-bond hydrolysis in [•]C1 and H transition to O5 acyl radical C1 eliminates CO, and for N-acetyl-substituted glucosamine the end radical [•]C2HNHAc is formed. As it interacts with water, acetamide is detached and the end hydroxyl radical is formed, oxidation of which (H removal from hydroxyl) produces arabinose (Scheme 9.3; *G*(arabinose) = 2.1).

The formation of N-acetylglucosamine keto- and deoxyketosugars [13] with respect to data on cellulose and starches [17] represent a multistage H detachment primary radical conversion. For example, [•]C3 radical conversions include the stages as follows: β-elimination of water with cyclic O atom participation [20], rearrangement of bonds in the allyl type radical, its isomerization with C1–C2 and O–H bond break in hydroxyl at C1, and formyl radical detachment (Scheme 9.4a). Then the formyl radical is dimerized forming glyoxal, detected at cellulose and starch irradiation.



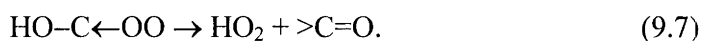
Scheme 9.4

chitosan (~8 carbonyl groups per 1 radical). Degradation of neighbor monomeric rings has no effect on the number of breaks in the polymer.

- b) Chitosan degradation is induced by participation of electron, $\bullet\text{OH}$ and $\bullet\text{H}$ radicals [21], superoxide and alkyl radicals [22]. This means that at irradiation of aqueous solutions chitosan effectively captures all components of water radiolysis. Taking into account the linear polymer structure, the presence of two hydroxyl and one amino groups in the monomeric unit (as it has been shown for the starch, for its water structuring), note that the same properties are typical of chitosan. Apparently, the ability of polymer to structure water (gel formation) and, consequently, “distant” capturing of water radicals by it [24] is provided by its high efficiency as a radioprotector: as it is injected to the animal organism prior to the radiation impact [11] (radioprotection based on competition for water radicals, manifestation of indirect radiation effect).

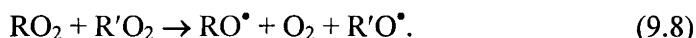
Oxygen effect

Damaging of TBS complex carbohydrate fragment by $\bullet\text{H}$ radicals (in dry preparations) of $\bullet\text{OH}$ radicals (in aqueous solutions) proceeds via attack of these radicals on C–H bonds in anhydroglucose ring and alkyl radical formation. As mentioned above, in the case of dry preparations, further conversion of such radicals is mostly defined by the origin of a substituent interlocking amino group, whereas in the case of deaerated aqueous solutions it depends on the ratio of the reaction rates of primary radical disproportioning or their isomerization. In the presence of molecular oxygen in solution, peroxide radicals must be formed. Hence, the yield of carbohydrate unit radiolytic degradation increases. The main type of peroxide radical conversion of the liquid-phase radiolysis is the following:



As follows from the data obtained [21], according to this scheme conversions of peroxide radicals by C2, C3 and C6 atoms in the monomeric unit of glucosamine oligomers (irradiation at pH 3) proceeds. Proceeding of this process may also be confirmed by radiolytic oxidation of manna sugar for mannose in aqueous solution [24].

At radiolysis of compounds with glycoside bonds, peroxide radicals derived from primary radicals with unpaired electron localization on carbon atoms, involved in glycoside bonds, or on C5 atoms enter the reaction as follows:



9.4. RADIOLYSIS OF GLYCOPROTEID AND RADICAL CONVERSIONS

As TBS aqueous solutions are irradiated, the molecular mass of the polymer decreases and monosugars (fucose and galactose) are extracted. Among products of TBS carbohydrate fragment degradation, malonic aldehyde (MA) or its analogues, deoxysugars (DS), and deoxyketosugars (DKS) were detected. The yield of these products depends on the origin of gas saturating the irradiated solution (Table 9.8). For example, the yield of MA is two-fold increased at substituting the inert gas by nitrous oxide.

Table 9.8

Relative yield of carbohydrate fragment degradation products at irradiation of 0.1% TBS solution (5 kGy dose) [25]

Solution saturating gas	MA	DS	DKS
N ₂	0.041	0.237	0.190
N ₂ O	0.070	0.297	0.210
O ₂	0.012	0.195	0.110

This indicates the dominating role of $^\bullet\text{OH}$ radicals in formation of the current product. Table 9.6 shows that the presence of molecular oxygen in the solution significantly affects the yield of the radiolysis products under consideration. Carbohydrate fragment of the polymer is the main site for the water radical attack. However, amino acid residues of the protein fragment are also decayed by radiation (see Table 9.3). The preferable sites for $^\bullet\text{OH}$ attack in TBS are C–H bonds in oxymethylene units of carbohydrate TBS fragment and

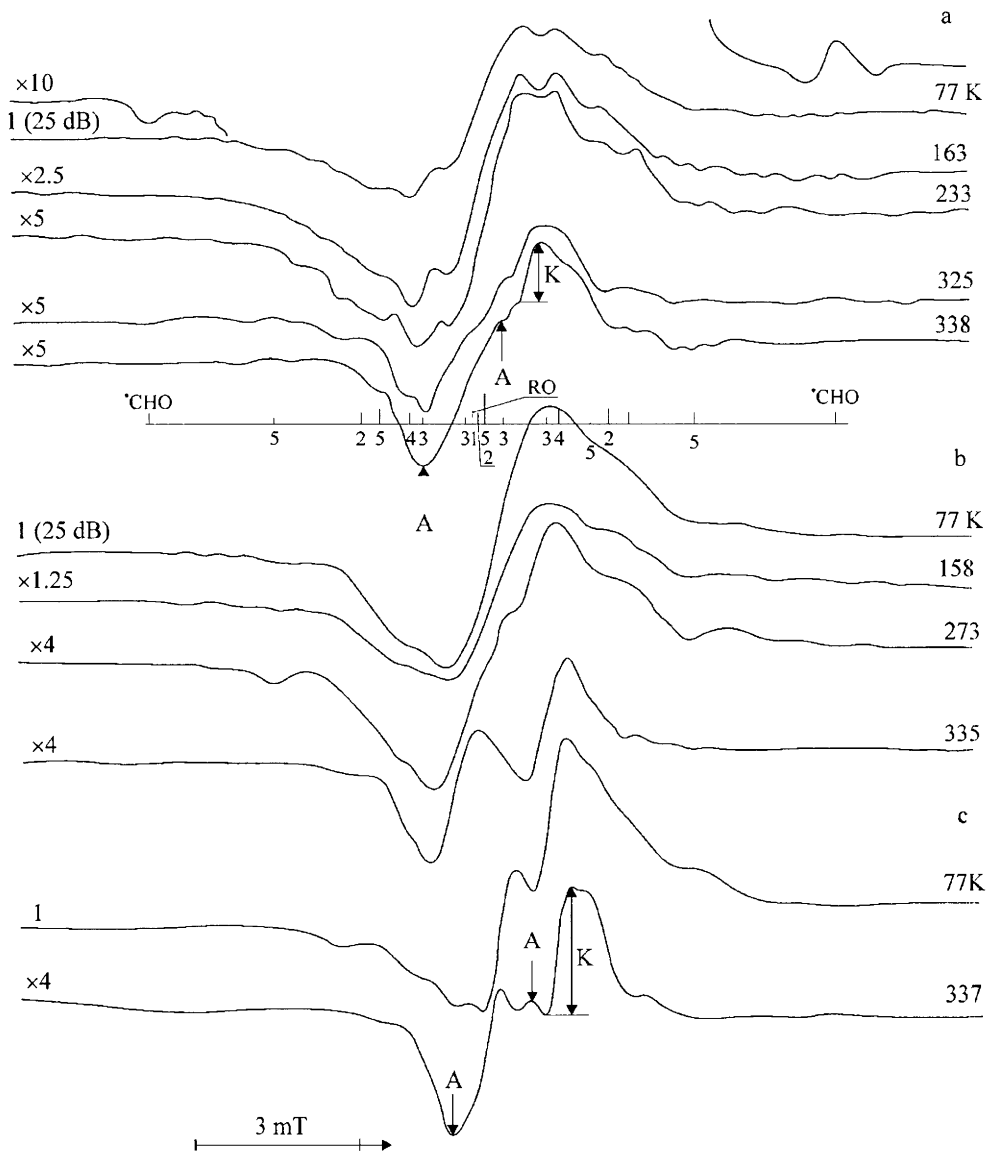


Figure 9.4. ESR spectra of evacuated TBS preparations from (a) pig stomach mucous cover, (b) histone protein and (c) potato starch, irradiated at 77 K and recorded at different temperatures. See [9] for details

Table 9.9

Characteristics of ESR spectra and radicals recognized in evacuated glycoprotein preparation, irradiated at 77 K [24]

Radical	HFS	ΔH_{tot} , ΔH_{split} , mT	<i>g</i> -factor	Suggested radical structure	Radical formation and conversion reaction
R ₁	Singlet	0.8	2.004	C ₁ [•]	Registration range 77 – 340 K R ₁ [*] → R _k , R ₁ → R ₅ , R ₁ → R _A
R ₂	Triplet 1:2:1	5.0 4.5	2.003	C ₄ [•] C ₅	77 – 340 K; R ₂ → R ₄ ; C ₅ [•] → R _A
R ₃	Doublet of doublets 1:1:1:1	2.5 1.5 0.8	2.003	C ₆ [•]	77 – 273 K; RC ₍₆₎ [•] HOH → RH + CHO [•]
RO [•]	Singlet	2	2.005	RO [•]	77 – 273 K H detachment from OH group with C–C bond break and by reaction with RH
C [•] HO	Asymm. doublet 1:1	12.5	2.001	RC ₍₆₎ [•] HO	Very low, at 30 kGy dose, 77 K C [•] HO → CH ₂ O

Table 9.9 (continued)

R_A	Asymm. doublet 1:1	1.4 1	2.007		Formed from R_1, R_3
R_k	Singlet	0.4	2.0009		Formed from $R_1, 242 - 340 \text{ K};$ $R_1 \rightarrow R_k \rightarrow \text{CO}$
R_4	Triplet 1:2:1	$3.0 \rightarrow 2.7$	2.003		Formed from $R_2;$ $280 - 340 \text{ K}$
R_5	Quintet 1:4:6:4:1	8 2	2.003	$-\text{HC}_{(4)}\text{OHHC}_{(5)}\cdot$ $\text{CH}_2\text{-O-}$	Formed from $R_1; 77 - 276 \text{ K};$ concentration increase at 240 K

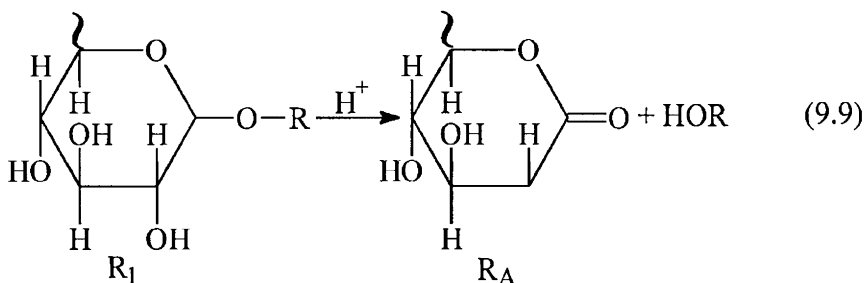
Note: R^* is a radical, the valence in which is localized in the neutral sugar unit rather than amino sugar.

C–H bonds in the polypeptide chain of the protein fragment (refer to Chapter 7). The role of hydrated electron is reduced to attacking acetyl groups of N-acetyl-substituted glucose- and galactosamine chains of the complex. As mentioned above, some amount of electrons is consumed for damaging protonated amino- and other groups in branches of the polypeptide chain, tyrosine aromatic rings.

ESR spectra of glycoprotein irradiated at 77 K represent an overlapping of ESR bands of several radicals (Figure 9.4).

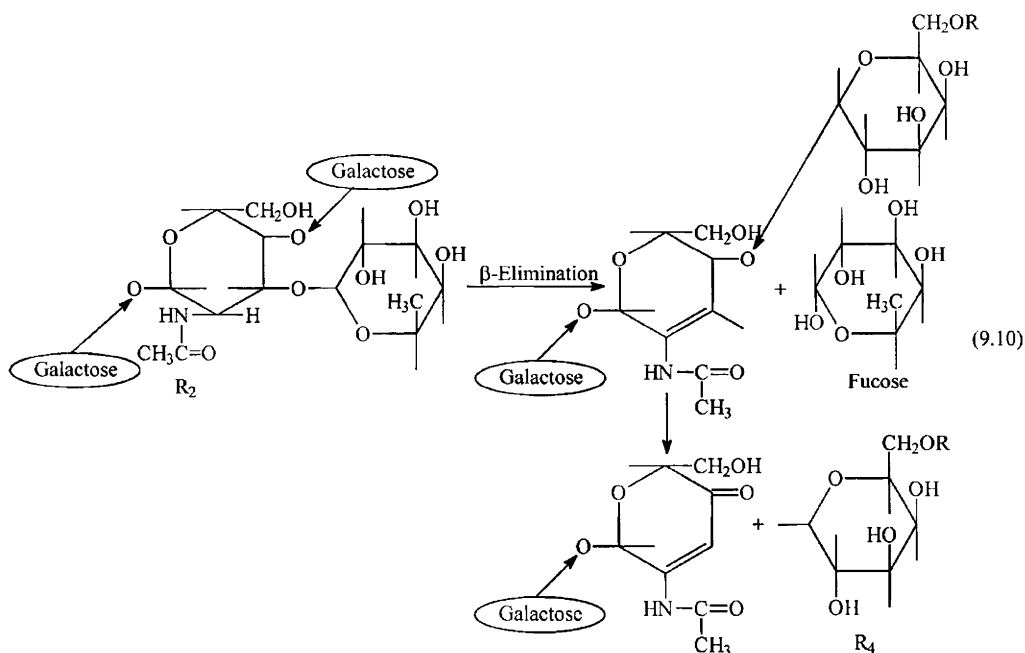
As irradiated sample is gradually heated up, the spectrum shape changes. The analysis of ESR spectra performed allowed for recognizing several types of radicals, formed at radiolysis of glycoprotein, divided into primary and secondary ones (Table 9.9).

The changes in ESR spectra, observed at annealing of the samples are the result of primary radical conversions. Comparing the data on radiological properties of glycoprotein and its models, discussed in this Chapter, a conclusion can be made about basic reaction types of formation and conversions of radicals in this natural compound. Radicals $\cdot\text{OH}$ and $\cdot\text{H}$ induce breaks of $\text{C}_n\text{--H}$, where $n = 1 - 6$, in the carbohydrate fragment of biopolymer and, therefore, radicals are formed. Type $\cdot\text{C1}$ radical conversions depend on the monomeric unit of this radical formation: in the neutral sugar or amino sugar unit. The comparison of the data on radiolysis of model compounds [25] indicates that in the second case isomerization of $\cdot\text{C1}$ radicals with C5--O5 bond break and further conversions of $\text{H}\cdot\text{C5}$ radical formed dominates. If $\cdot\text{C1}$ occurs in a unit of neutral sugar, its isomerization may cause either C5--O5 bond break or changes involving C1 and C2 atoms. Apparently, the first case is realized, when this monomeric unit of neutral sugar is bound to neighbor glycoside C6--O--C1 bond. So far as concerns the second route of $\cdot\text{C1}$ radical conversions, the most probable is proceeding of α -elimination of water, intensified in the acid medium:



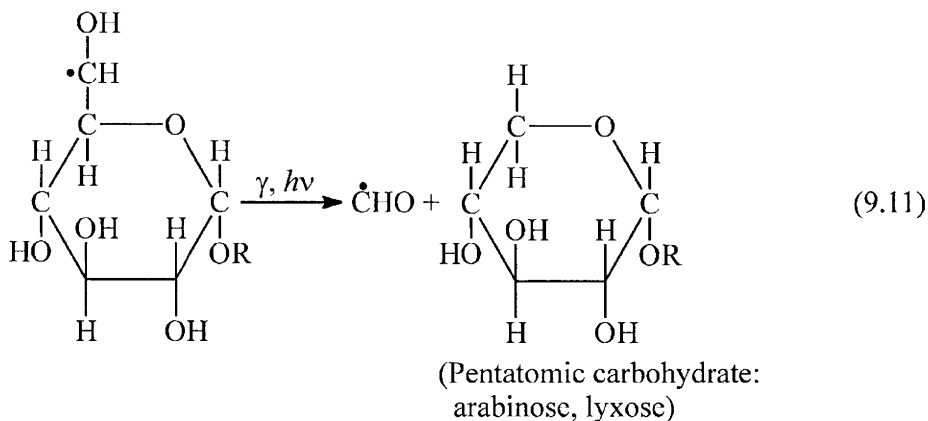
The radicals of $H^{\bullet}C2<$ (RA) type, formed by the reaction (9.9), may interact with other radicals, forming deoxy-sugar groups. The formation of the allyl type radicals is proved by direct registration of ESR bands of irradiated glycoprotein with the following parameters: $\Delta H = 1.4$ mT and $g = 2.0067$ (Figure 9.3). Another confirmation is the detection of 2-deoxygluconic acid among radiolysis products of glucose aqueous solutions. The yield of 2-deoxygluconic acid is 1, i.e. the value equals a half of total yield of the detected radiolysis products of glucose aqueous solutions.

Since radicals in the sugar fragment of the polymer are formed due to H atom detachment from any C atom in the anhydrocarbohydrate cycle, the formation of detected monosugars, fucose, for example, might be explained by type $\bullet R2$ radical conversion, presented by the formula (9.10) below:

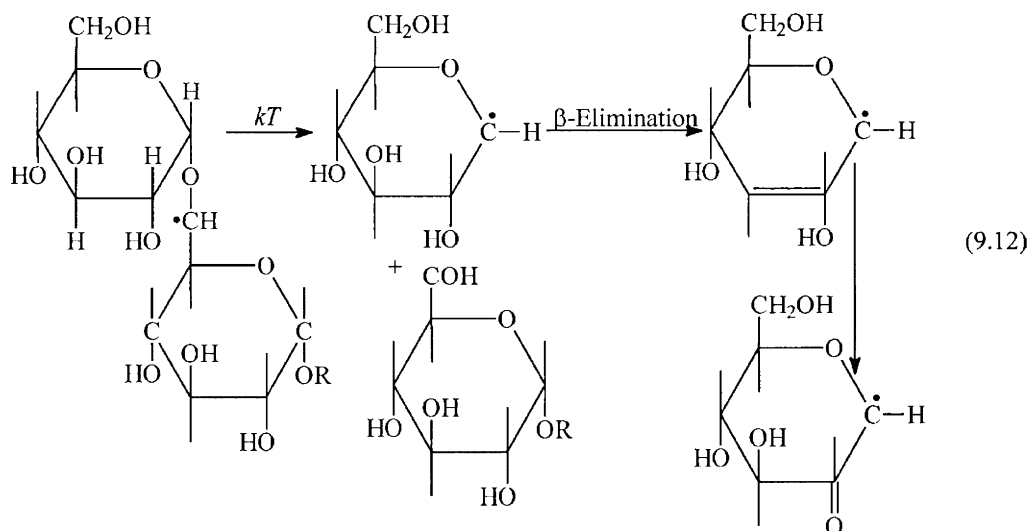


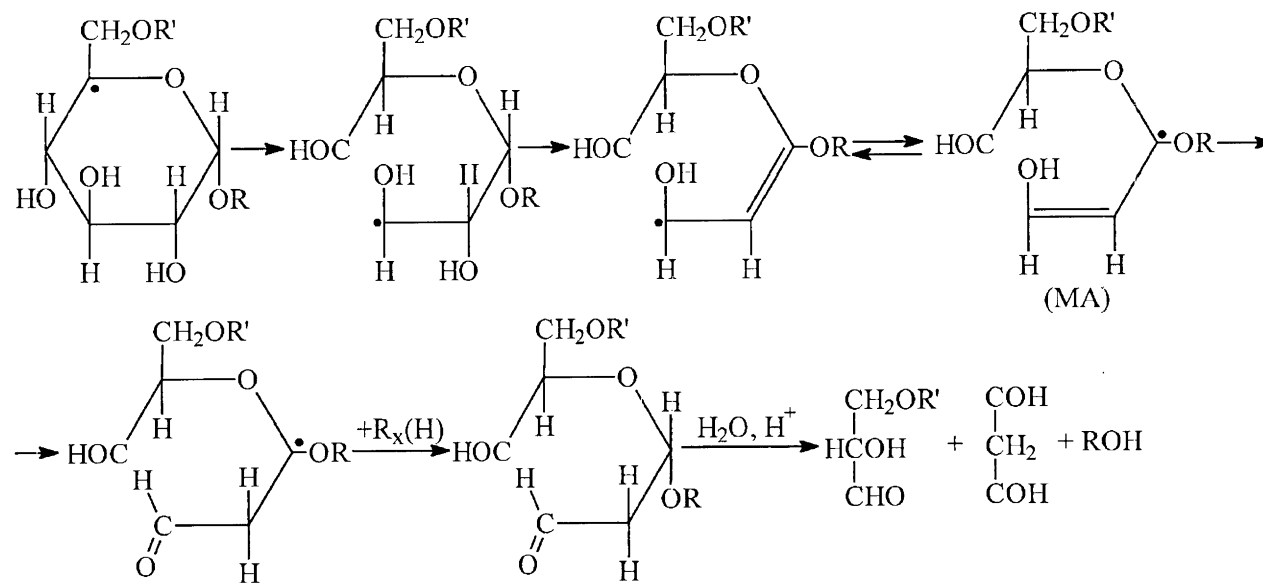
It may be suggested that conversions of analogous radicals (β -elimination of water) in other units of the damaged TBS fragment induce the polymeric chain degradation. Type $\bullet C6$ radical conversions may be performed by two routes in relation to either this carbon atom is located in the free end group or $\bullet C6$ is included in the glycoside bond. It may be suggested that

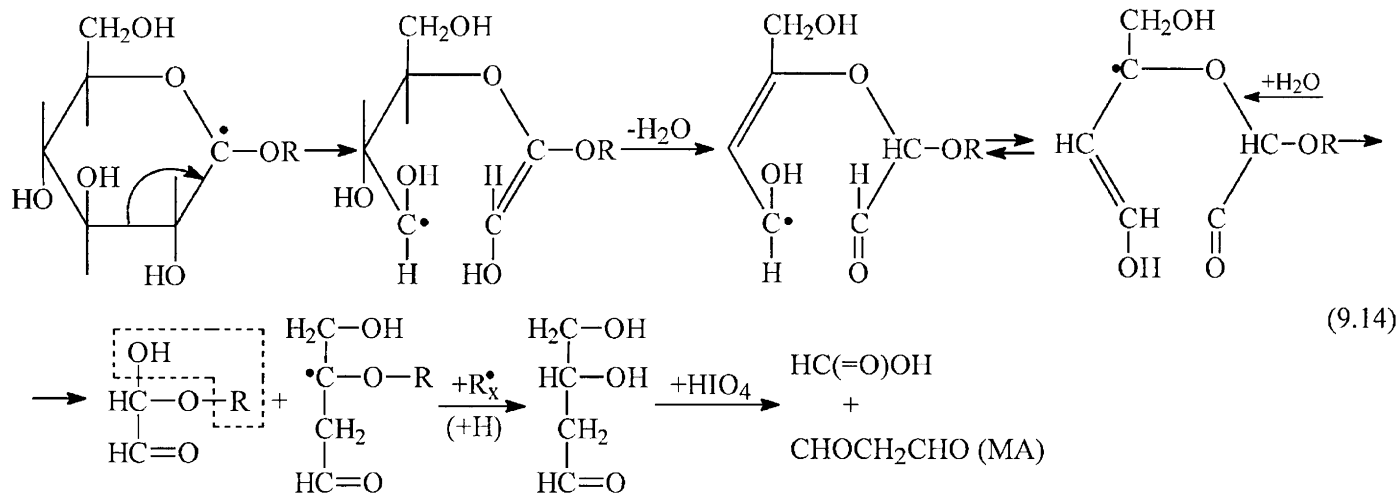
formation of the formyl radical, detected at relatively high irradiation doses, happens owing to the radiation effect:

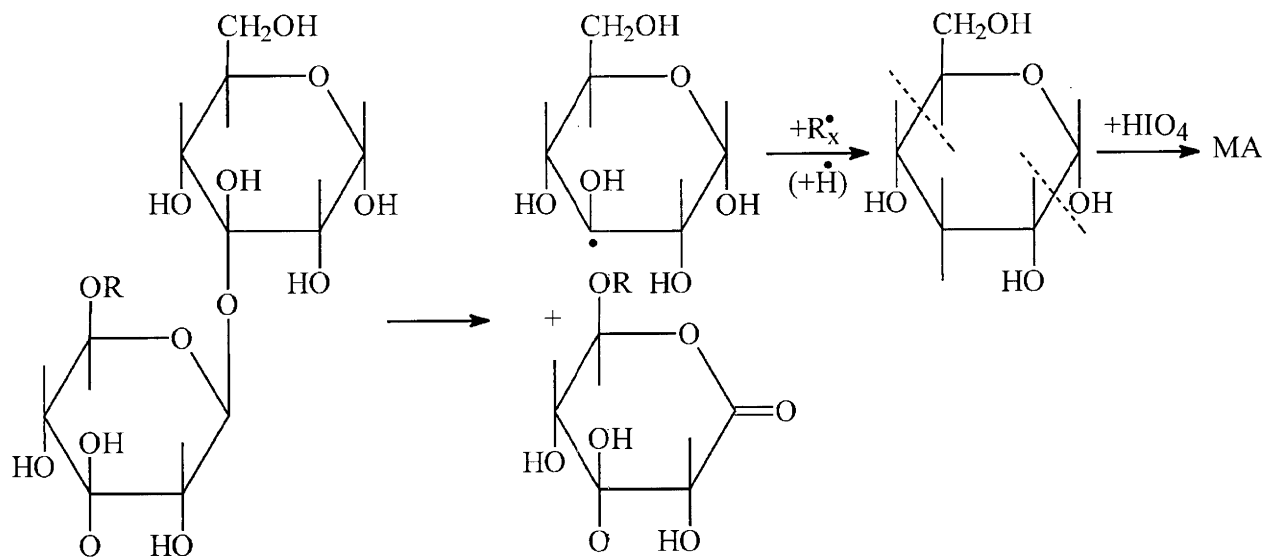


Carbohydrates with the number of carbon atoms lower by one were detected in the tests on model systems (disaccharides). Hence, in the second case, according to ESR data, it may be suggested that $\cdot\text{C}_6$ is converted with allyl radical formation, which contains a keto-group:



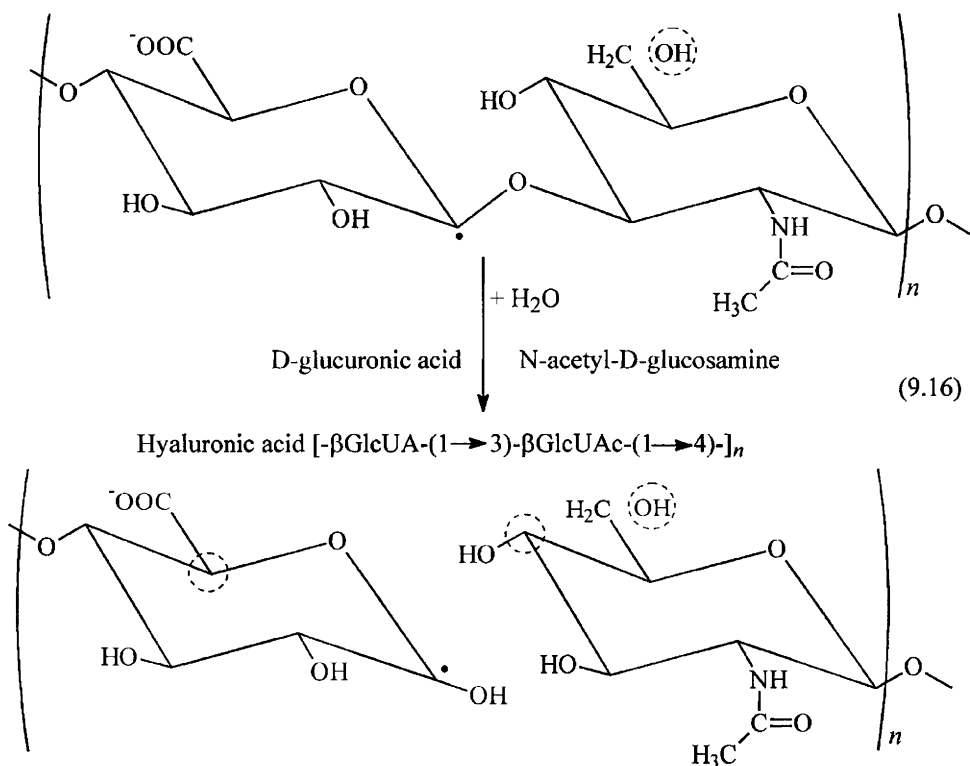






It may be suggested that malonic aldehyde (MA) and deoxysugars, registered among radiolysis products, are formed due to radical $^{\bullet}\text{C5}$ or, for example, $^{\bullet}\text{C1}$ conversions (see diagrams (9.13) – (9.15)).

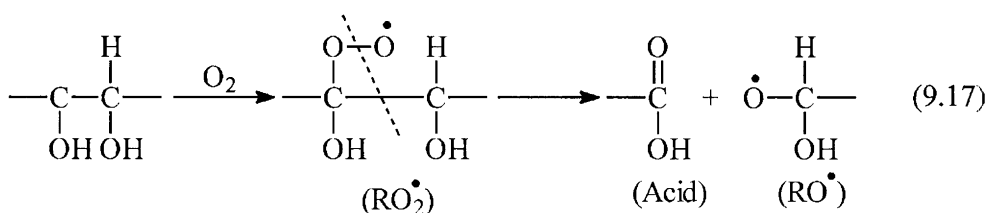
For type $^{\bullet}\text{C1}$ radicals in aqueous solutions, the reaction of hydrolytic splitting of $\beta\text{-O-C4}$ bond (in the glycoside bond) is possible. This process was detected for radiolysis of gilauronic acid [13] (reaction (9.16), a \rightarrow b). Reaction (9.16) is the main process of radiolytic depolymerization of oligo- and polysaccharides in aqueous solutions [26 – 29].



It may be suggested that such process as C3–OP bond hydrolysis is also realized in the case of DNA solution irradiation, which is one of the reasons for forming breaks in DNA strands at the cell irradiation (Chapter 10).

The schemes of radical conversions in the irradiated glycoprotein, discussed in this Section and including formation of some detected final products, must be added by the case of glycoprotein irradiation in the presence

of molecular oxygen. However, the multistage sequence of the radical conversions may not be presented in full yet. It may be just stated that the mentioned sequence includes stages of peroxide radical formation and C–C bond break, neighbor to the peroxide group [30], for example, by the following reaction:



The scheme (9.17) explains formation of carboxylic and aldehyde groups with equal yield (1:1) at irradiation, for example, of potato starch in the presence of oxygen (Chapter 8) [31, 32].

Finally, the following conclusions should be made. Firstly, free radicals play the dominating role in radiolytic degradation of glycoprotein aqueous solutions. Secondly, these radicals are formed at a damage of carbohydrate fragment of the biopolymer. Similar to radiolysis of polysaccharides, the reason for observed radiation effects (reduction of the biopolymer biomass, formation of monosaccharides and other low-molecular products) is conversions of primary alkyl macroradicals proceeding by the following reactions:

- 1) dehydration (α - or β -elimination of water) or analogous process with hydroxyl group formation at the end of the carbohydrate unit;
- 2) isomerization with C–C and C–O bond break in anhydrocarbohydrate units;
- 3) formation of peroxide radicals at polymer irradiation in the presence of molecular oxygen, the conversion of which change the radical degradation mechanisms: C–C bond breaking processes dominate over dehydration of radicals.

For radiolysis of glucosamine superpolymer aqueous solution specific is electron interaction with amino group, which is accompanied by deamination by $^\bullet\text{C}2$ and formation of the corresponding radical. Its subsequent conversions

are analogous to conversions of radical $\cdot\text{C}_2\text{H}$ (OH detachment radical) in carbohydrates (Chapter 8).

REFERENCES

1. Kochetkov N.K., Derevitskaya V.A., and Arbatsky N.P., *Europ. J. Biochem.*, 1976, vol. **67**(1), p. 129.
2. Palavicini G., Getta G., Sinigaglia F., Badiello R., and Tamba M., *Int. J. Radiat. Biol.*, 1976, vol. **30**(3), p. 287.
3. 3. Baugh P.J., Morgan R.E., Kershaw K., and Phillips G.O., *Radiat. Res.*, 1971, vol. **45**, p. 455.
4. 4. Jooyahdeh F., Moore J.S., Morgan R.E., and Phillips G.O., *Radiat. Res.*, 1971, vol. **45**, p. 455.
5. Moore J.S., Phillips G.O., and Phys D., *Int. J. Radiat. Biol.*, 1973, vol. **23**(1), p. 113.
6. Moore J.S. and Phillips G.O., *Carbohydrate Res.*, 1971, vol. **16**(1), p. 79.
7. Nadjafova M.A., Sharpatyi V.A., and Emanuel N.M., *Doklady AN SSSR*, 1972, vol. **220**(1), p. 128. (Rus)
8. Sharpatyi V.A. and Nadjafova M.A., *Izv. AN SSSR, Ser, Khim.*, 1972, No. 11, p. 2564. (Rus)
9. Nadjafova M.A., 'Physicochemical study of radicals formed at gamma-irradiation of glucosamine, its derivatives and glycoprotein', *Candidate Dissertation Thesis*, Baku, S.M. Kirov Azerbaijan State University, 1979, 157 p. (Rus)
10. Kudryavtsev V.N., Grushevskaya L.N., Yurik T.K., and Kabanov V.Yu., *Khimia Vysokikh Energyi*, 1993, vol. **27**(1), p. 41. (Rus)
11. Il'in L.A., Andrianova I.E., and Glushkov V.A., *Radiats. Biol. Radioekol.*, 2004, vol. **44**(2), p. 176. (Rus)
12. Stepanenko B.N., *Chemistry and Biochemistry of Carbohydrates (Polysaccharides)*, Moscow, Vysshaya Shkola, 1978, 256 p. (Rus)
13. Kochetkov N.K., Kudryashov L.I., and Chlenov M.A., *Radiation Chemistry of Carbohydrates*, Moscow, Nauka, 1978, 288 p. (Rus)
14. Ershov B.G., *Uspekhi Khimii*, 1998, vol. **67**(4), p. 353. (Rus)
15. Ershov B.G., Isakova O.V., Rogozhin S.V., Gamza-zade A.I., and Leonova E.Yu., *Doklady AN SSSR*, 1987, vol. **295**(5), p.1152. (Rus)

16. Pristupa A.I. and Sharpatyi V.A., *Doklady RAN*, 2002, vol. **387**(5), p. 643. (Rus)
17. Korotchenko K.A., Pristupa A.I., and Sharpatyi V.A., *Khimia Vysokikh Energyi*, 2004, vol. **38**(2), p. 107. (Rus)
18. Nadjafova M.A. and Sharpatyi V.A., *Doklady AN Azerb.SSR*, 1977, vol. **33**(8), p. 41. (Rus)
19. Kvach N.M., Kuvaldina E.V., Sadova S.F., and Sharpatyi V.A., *Doklady RAN*, 1996, vol. **349**(1), p. 60. (Rus)
20. Sharpatyi V.A., Shapilov A.A., and Pintelin S.N., *Khim. Fiz.*, 2001, vol. **20**(12), p. 19. (Rus)
21. Ulansky P. and von Sonntag C., *J. Chem. Soc., Perkin Trans.*, 2000, vol. **2**, p. 2022.
22. Pyo-Jam Park, Jae-Young Je, and Se-Kwon Kim, *Carbohydrate Polymers*, 2004, vol. **55**, p. 17.
23. Korotchenko K.A. and Sharpatyi V.A., *Radiats. Biol. Radioekol.*, 2000, vol. **40**(2), p. 133. (Rus)
24. Phillips G.O., *J. Chem. Soc.*, 1963, p. 273.
25. Yarovaya S.M., Nadjafova M.A., and Sharpatyi V.A., *Radiobiologia*, 1981, vol. **21**(5), p. 716. (Rus)
26. Deeble D.J., Bothe E., Schuchmann H.-P., Parsons B.J., Phillips G.O., and von Sonntag C., *Z. Naturforsch.*, 1990, vol. **45c**(9/10). S. 1031.
27. Parsons B.J., Phillips G.O., Thomas B., Wedlock D.J., and Clarke-Sturman A.J., *Int. J. Biol. Macromol.*, 1985, vol. **7**, p. 187.
28. Moore J.S., Phillips G.O., and Phys D., *Int. J. Radiat. Biol.*, 1973, vol. **23**(2), p. 113.
29. von Sonntag C., *Adv. Carbohydr. Chem. Biochem.*, 1980, vol. **37**(2), p. 7.
30. Milinchuk V.K., Klinshpont E.R., and Pshezhetsky S.Ya., *Macroradicals*, Moscow, Khimia, 1980, p. 216. (Rus)
31. Korotchenko K.A. and Sharpatyi V.A., *Khimia Vysokikh Energyi*, 1993, vol. **27**(4), p. 50 – 55. (Rus)
32. Petrov P.T., Fedorova G.A., and Markevich S.V., *Vesti AN BSSR, Ser. Fiz.-Energ.*, 1980, No. 3, p. 84 – 88. (Rus)

Chapter 10. Radiation chemistry of DNA aqueous solutions

It is common knowledge that the decisive role in development of radiobiological reactions causing cell death, occurrence of gene and chromosomal mutations is belonged to the unique cell structure called DNA – unique because it is responsible for hereditary information storage and transmission.

10.1. DNA STRUCTURE

DNA is a double-stranded macromolecule, each strand of which represents a sequence of monomeric units – four nucleotides (in relation to the number of nitrogen bases), linked to one another by phosphoroether C'3–OPO–C'5 bonds. The nucleotide includes residues of phosphoric acid, 2-deoxy-D-ribose (β -furanose form) and nitrogen base, bound to a “sugar” fragment (2-deoxyribose) by C'1–N-glycoside bond. A single-chain polynucleotide (a strand) with the self system of chemical bonds forms the so-called primary structure of DNA. Both DNA strands are linked to one another by hydrogen bonds (the secondary structure), in which atoms O...H...N (of oxo- and nitro-groups) of complementary nitrogen bases are involved: thymine-adenine (two hydrogen bonds) and cytosine-guanine (three hydrogen bonds). According to some conditions (wetness degree, ionic strength of the environment) DNA, preserving the general shape of polydeoxyribonucleotide bispiral structure, exists in variously modified conformations (over 10 forms, among which A, B and C crystalline forms, were studied by the X-ray diffraction analysis), between which intertransitions are performed. Each of conformation structures in the cell is responsible for a definite function. Biologically, the A-form is the most adequate for transcription process (information transmission from DNA to RNA), B-form – for replication processes (extension of the information volume), and C-form – for DNA packing in the structure of chromatin supermolecular structure (information storage).

A-DNA is a spiral with 25.6 Å step and 11 nucleotide pairs per a spiral turn; for B-DNA the step is 33.8 Å at 20 Å diameter, and each turn contains 10

nucleotide pairs, a gap between nucleotides is 3.38 Å; for C-DNA the number of nucleotide pairs per turn is 9.1 with a gap between nucleotides equal 3.32 Å.

DNA molecules possess two conformations, linear and circular shaped, existing in coiled and supercoiled states. In chromatin and chromosomes DNA is present in the supercoiled state, and several levels of supercoiling are realized. Such supermolecular structural organization of biopolymer is belonged to the tertiary structure of DNA.

Molecular mass of DNA depends on the tissue origin and varies from units to hundred million Daltons.

10.2. RADIOLOGICAL EFFECTS

The effect of ionizing radiation on DNA in aqueous solution induces two basic processes: dissociation (modification) of nitrogen bases and degradation of the sugar-phosphate DNA backbone – formation of breaks in the macromolecule chains, single-strand (SB) and double-strand (DB) breaks. The occurrence of chemically modified bases in the DNA composition may be the reason for formation of point mutations. SB are repaired by enzymatic systems of the cell, whereas DB in DNA are lethal for cells; single-strand breaks, unrepaired by the enzymes may also produce additional DB. The number of SB in DNA increases linearly with the irradiation dose, and the number DB – proportional to the irradiation dose square [1]. The DB/SB ratio depends on the molecular mass of DNA and damaging degree of the polymer.

Both processes (decay of bases and degradation of DNA sugar-phosphate backbone) change the basic biological function of DNA – the transcribing ability [1 – 3].

At irradiation of aqueous solutions of DNA, water radiolysis products, which are radicals $\cdot\text{OH}$, $\cdot\text{H}$ and \bar{e}_{hydr} , attack all components of the monomeric unit – the nucleotide. The reactivity of $\cdot\text{OH}$ radicals in relation to nucleotide fragments is reflected by the following sequence:

base:2-deoxyriboseyl:phosphoric acid residue ~ 1,000:100:1.

In relation to H atoms, the reactivity of these fragments is about an order of magnitude lower, than for $\cdot\text{OH}$ radicals. Analogous sequence of hydrated

electron reactivity looks as follows: 10(5):10:1. The main routes of DNA free radical formation and conversions are shown in Scheme 10.1.

Primary base radicals are formed as a result of $\cdot\text{OH}$, $\cdot\text{H}$ and \bar{e} addition by double bonds of nitrogen bases (A) with formation of radicals-base adducts – the intermediates, macroradicals, then involved in reduction and oxidation reactions:



Preferable site for $\cdot\text{OH}$ and $\cdot\text{H}$ attack in pyrimidines are C6 and C5 atoms, and C8 atom in purines (OH- and H-adducts of pyrimidines and purines are formed). The electron in pyrimidines attacks C6 atom and electron adducts of pyrimidines are formed. As they are protonated (at the interaction of anion-radical with water molecule) H-adducts of pyrimidines are formed:



Table 10.1

Concentration of radicals (radical/g) in alkaline solutions (10 M KOH) of thymine, irradiated at 77 K [4]

Thymine concentration, M	In prepared samples		[O ⁻], 10 ¹⁷		[TH] ^{••} , 10 ¹⁷ (after thermal annealing) ^{••}
	[T [•]], 10 ¹⁷	[R], 10 ¹⁷	Before bleaching of \bar{e}_{st}	After bleaching of \bar{e}_{st}	
0 (15)*	0	–	11 ± 0.4	3.6 ± 0.4	0
0 (130)	0	–	27 ± 5	25 ± 0.4	0
0.01 (15)	1 ± 0.4	3.2 ± 0.4	9.7 ± 1	7.0 ± 0.7	0.34 ± 0.14 (20)
0.03 (15)	2.6 ± 0.4	6.7 ± 0.4	12 ± 2	5.1 ± 0.6	3.3 ± 0.4 (115)
0.03 (130)	2.7 ± 0.4	29 ± 0.4	27 ± 5	25 ± 0.4	3.5 ± 0.2 (70)

Notes: * Shown in brackets: in the first column – irradiation dose (Gy), in the last column – duration (min) of sample exposure to 158 K;

^{••} [TH]^{••}, in the samples before and after bleaching of \bar{e}_{st} equals $(2.5 \pm 1.2) \times 10^{16}$.

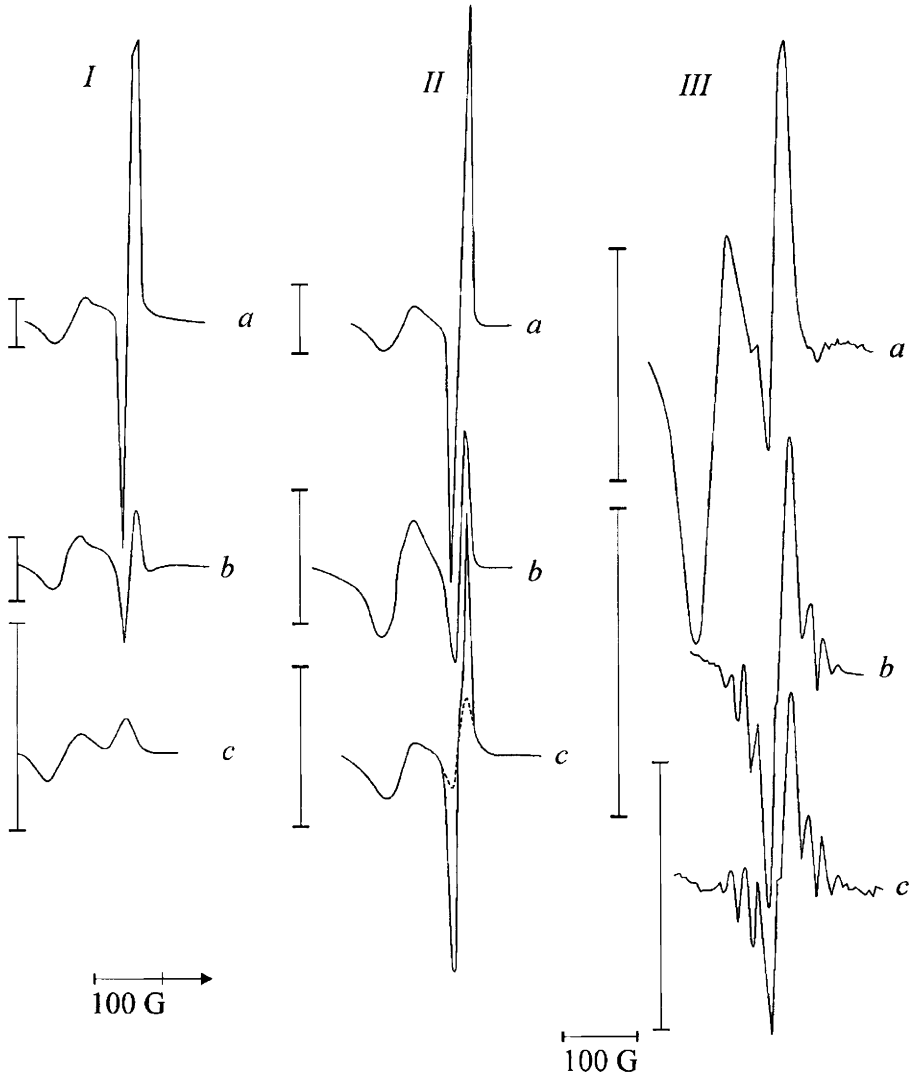


Figure 10.1. ESR spectra of irradiated solutions: 10 M KOH (I), thymine (0.03 M, dashed line – 0.01 M) in 10 M KOH (II, III), recorded at different UHF intensity levels: (*a* – P_{\min} , *b* – P_{\max} , *c* – P_{\min}), after irradiation by visible light (I, II: $P_{\max} - P_{\min} = 20$ dB); I and II – before thermal annealing, irradiation dose is 1.5 Mrad, III – after thermal annealing of the radicals during 30 min (*a*), 70 min (*b*), 100 (*c*) at 158 K, P_{\min} at 13 Mrad dose

Table 10.2

Computerized analysis of anisotropic ESR spectra of nitrogen bases, irradiated in frozen-up aqueous solutions [6]

Radical-adduct	$g_{\perp} - g_{\parallel}$	Δ_{\perp}	Δ_{\parallel}	d_{iso}	d'_{iso}	d''_{iso}	d_{\perp}	d_{\parallel}	d'_{\perp}	d'_{\parallel}	a^{N}_{\perp}	a^{N}_{\parallel}
TH	0.00417	8.38	5.98	21.15	21.55	21.55	17.80	17.41	56.53	55.87	–	–
TOH	0.00001	7.00	6.00	21.70	–	–	16.65	15.75	19.75	17.50	26.50	14.65
GH	0.00345	5.60	8.21	36.00	36.00	–	3.14	4.22	–	–	0.10	25.47
GOH	0.00206	6.00	9.00	32.80	3.45	–	–	–	–	–	0.83	23.00
AH	0.00026	8.14	10.46	38.27	40.17	–	0.04	11.41	–	–	0.19	15.85
AOH	0.00100	8.70	11.63	29.94	3.14	–	1.20	10.40	–	–	3.20	18.70
UOH	0.00005	11.50	11.00	–	–	–	1.50	18.80	13.80	20.00	–	–
COH	0.00019	9.00	8.65	–	–	–	0.03	18.50	10.20	23.50	1.40	21.70

A conclusion about reactions (10.1), (10.2) proceeding is illustrated by the data of ESR measurements of alkaline solutions (10 M KOH) of thymine, performed at low temperature (77 K). Thymine anion-radicals, formed under the effect of γ -irradiation at 77 K, are stable in this glassy-like matrix up to $T \sim 158$ K [4]. If the sample is exposed to this temperature during 1.5 h, gradual recombination of thymine anion-radicals may be observed (the doublet intensity decreases) and TH type radicals are accumulated (octet component intensity increases, Figure 10.1). In this case, total concentration of T^- and \bullet TH radicals remains constant (Table 10.1). With respect to the fact that in this solution (0.03 M T^- + 10 M KOH) concentration of protons approach zero, and water molecules are mobile in this matrix at 160 – 170 K, it may be concluded that the observed conversion of the radicals (within the measurement accuracy at 100% yield) is stipulated by the reaction (10.2). At irradiation of DNA preparations in acidic medium anion-radicals are mostly protonated by the following reaction:



To obtain data on the structure of primary radicals of bases, ESR spectra of individual bases and DNA, irradiated in glassy-like (alkaline and phosphate) matrices at 77 K and then annealed at $T = 180$ K, were analyzed.

It is found that ESR signals observed at 77 K are provided by paramagnetic particles, formed at the interaction of bases with \bar{e} , \bullet H, and \bullet OH (H_2O^+). The reactivity of bases in relation to the products (the totality of products) of water radiolysis at 77 K is reflected by the following sequence – G:T:A:C = 3.5:2.2:2:1 [5]. At irradiation of DNA solutions under the same conditions, radicals are formed from all four bases, and their fractional yield corresponds to the above-mentioned sequence. Computerized analysis of the spectra recorded at γ -irradiation of polycrystalline and glassy-like nucleotide solutions and nitrogen bases, implemented by the program of anisotropic ESR spectrum reconstruction in the variation search mode, coincides with the experimental spectra (Figure 10.2) [6]. ESR spectrum parameters shown in Table 10.2 allowed for determination of unpaired electron site at each H- and OH-adduct in nitrogen bases.

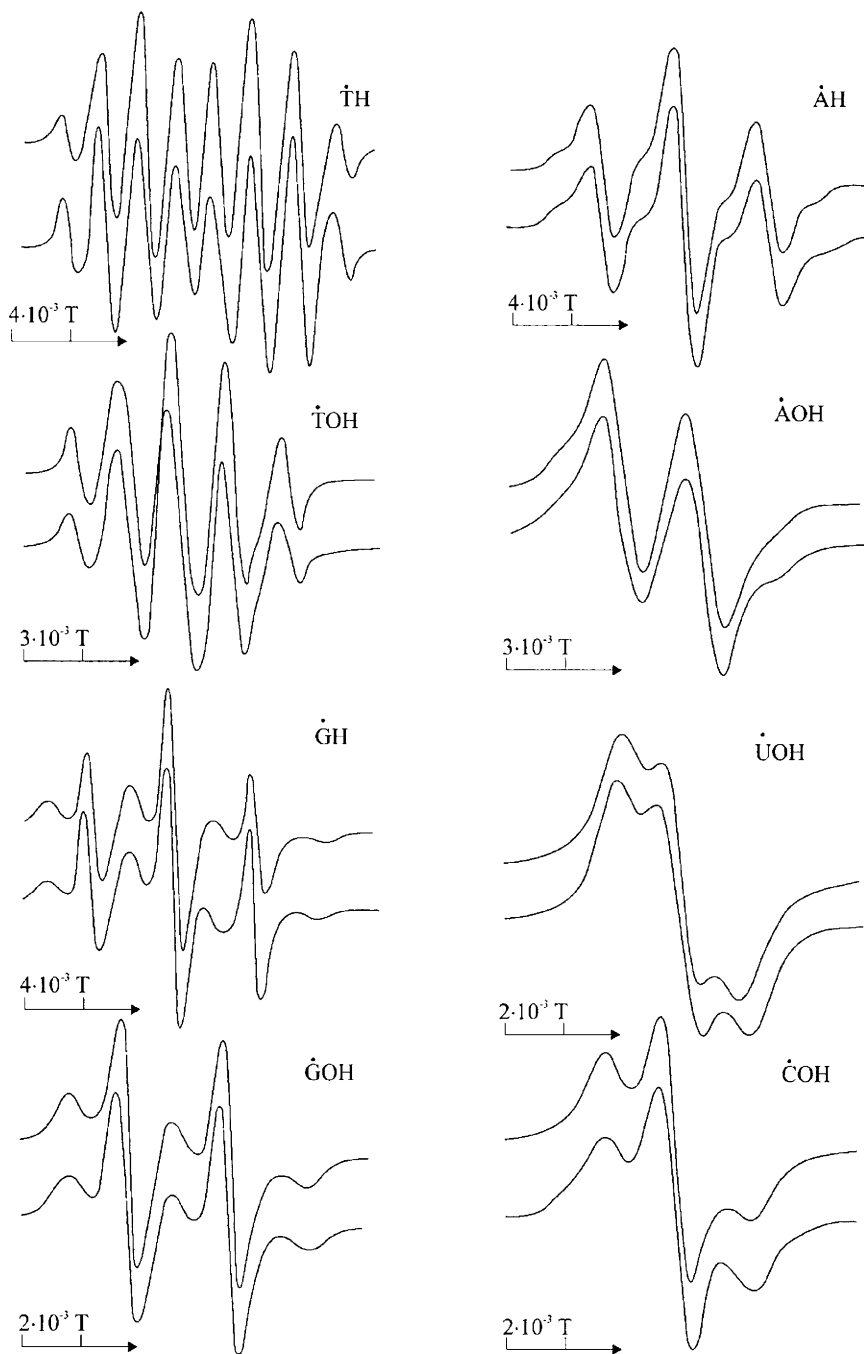


Figure 10.2. ESR spectra (theoretical at the top and experimental at the bottom) for radical H- and OH-adducts of nucleotides (thymine, adenine, guanine) and nitrogen bases (cytosine, uracyl), formed at γ -irradiation of their frozen-up aqueous solutions (1 Mrad dose, $T = 77$ K) and subsequent annealing of the samples up to 1170 – 180 K

From these data follows, for example, that for guanine, $\bullet\text{OH}$ only effectively attacks C8 atom in the imidazole cycle, and unpaired electron in OH-adduct of guanine is delocalized by the fragment, in which it may interact with one nitrogen and two hydrogen atoms. Hence, hyperfine interaction (HFI) constant with one hydrogen atom (at C8 atom) is comparable with that for N7, whereas for the second H atom (in hydroxyl at C8) this value is an order of magnitude lower.

10.3. MACRORADICAL CONVERSIONS

The conversions of nitrogen base radicals induces formation of glycols and peroxides (in the presence of molecular oxygen, refer to Section 10.4), pyrimidines, base derivatives with saturated bonds, deep degradation products and base deamination products in the DNA structure [7].

Using radiochromatography methods at irradiation of aqueous DNA solutions in the absence of oxygen, macromolecules with modified thymine bases, the compounds with saturated C5–C6 bonds were recognized: 5,6-dihydrothymine, cis- and trans-5,6-dihydroxy-5,6-dihydrothymine, 5-hydroxy-5,6-dihydrothymine [8]. Such composition of DNA radiolysis products allows for a conclusion that in the case of pyrimidine bases, $\bullet\text{OH}$ and \bar{e} ($+ \text{H}^+$) formed at radical attack on C5 and C6 atoms enter disproportionation (oxidation and reduction) reactions with free radicals of various origin.

As mentioned above, $\bullet\text{OH}$, $\bullet\text{H}$ and \bar{e} , formed at the radical attack on pyrimidine C5 and C6 atoms, convert and initiate deamination of bases. Table 10.3 shows data on this process (by ammonia release) under the effect of $\bullet\text{OH}$ and \bar{e}_{hydr} in aqueous solutions of DNA and thymine [9]. In the presence of \bar{e}_{hydr} acceptors (nitrous oxide or cadmium ions) only $\bullet\text{OH}$ radicals were

involved in reactions with DNA and thymine. These data show that both $\cdot\text{OH}$ and \bar{e} initiate this process with the same efficiency.

Table 10.3

The yield of deamination in DNA and thymine solutions under different irradiation conditions, pH 7.0 [9]

Irradiated solution concentration	Ar	N ₂ O	Ar, Cd ²⁺	O ₂
	$\cdot\text{OH}$, \bar{e}_{hydr}	2HO \cdot	$\cdot\text{OH}$	$\cdot\text{OH}$, O ₂ ⁻
3.3×10 ⁻³ M by DNA nucleotide	1.35 ± 0.2	1.3 ± 0.3	0.7 ± 0.2	2.25 ± 0.25
0.01 M thymine	0.28 ± 0.04	0.16 ± 0.02	0.18 ± 0.02	0.40 ± 0.05

As known from the data of biological investigations, in neutral aqueous solutions of base-modified nucleotides containing saturated bonds C'1–N bond is hydrolyzed forming hydroxyl group C'1OH (or aldehyde >C'1=O group) in 2-deoxyribose and detachment of the base derivative with saturated bonds. As the base derivatives with saturated bonds occur in the irradiated DNA, C'–N bond is hydrolyzed, and such modified base is detached from the sugar-phosphate backbone (reaction (10.5)). A residue of 2-deoxyribose, free from the base (apurine or apyrimidine sites), the acyclic tautomeric form of which includes the aldehyde group, occurs in DNA. In the alkaline (and acidic) medium, at this site of the macromolecules phosphoether bonds break (see below for details). The main routes of nitrogen base radical are also considered [7].

Macroradicals of DNA sugar fragment and their conversions

The detachment of H atom from C'–H bonds in 2-deoxyribose at the attack of $\cdot\text{OH}$ radicals represents the main process of 2-deoxyribose radicals, H atom detachment radicals, and alkyl radicals R = C'_n (n = 1 – 5):



The fractional yields of the radicals in the DNA composition is not yet determined experimentally, but as indicated by the data on radiolysis of crystalline carbohydrates are different and depend on the structural features of

2-deoxyribosyl in nucleotide and the origin of heteroatom of the substituent group (O or N) in the methylene unit. The reaction (10.4) reflects primary elementary act of 2-deoxyribosyl modification in DNA by neutral $\cdot\text{OH}$ radicals. The studies of carbohydrate solution radiolysis allows for a conclusion that in the case of humidified DNA, not only $\cdot\text{OH}$ may react with 2-deoxyribosyl, but also its precursor – the charged particle H_2O^+ [10]. In this case, a cation-radical of 2-deoxyribosyl is formed, which deprotonation at the interaction with water leads to formation of a neutral alkyl radical $\text{R}\cdot$ of the origin similar to that formed in the reaction (10.4).

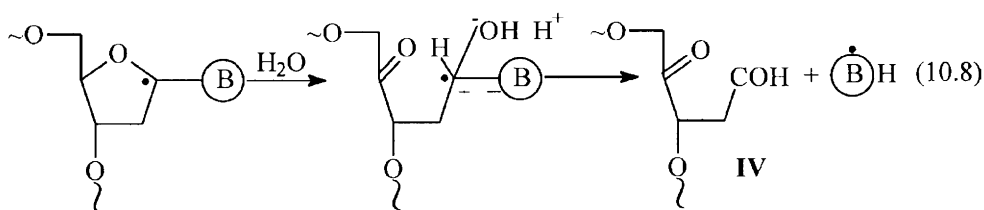
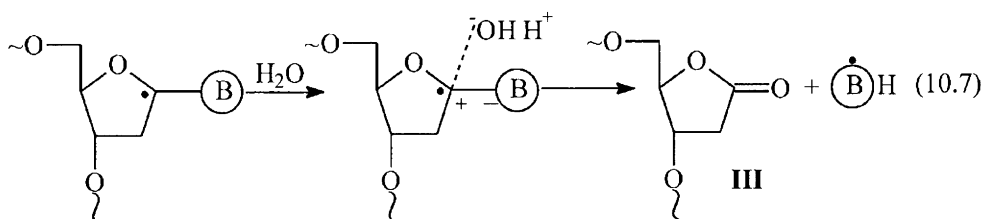
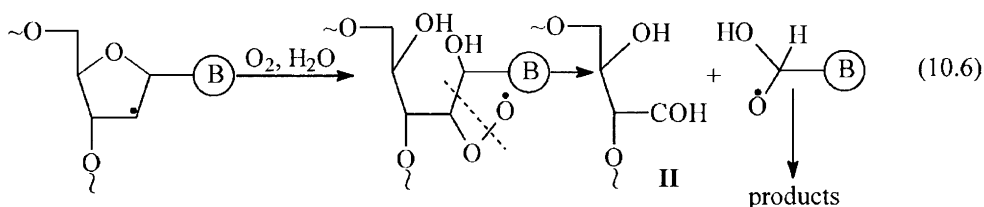
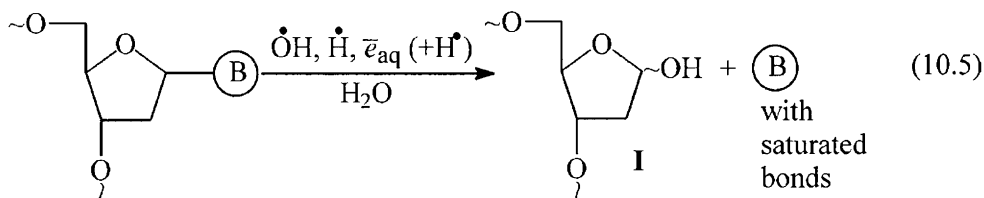
The formation of alkali-labile sites in DNA

Studying radiolysis of dry samples and frozen-up aqueous solutions of DNA by ESR method, the investigators have found out that sugar fragment radicals in DNA are not registered in these systems. Moreover, the occurrence of free bases, modified nucleosides and breaks in sugar-phosphate chain [1] among radiolysis products in the case of DNA solution irradiation indicates the primary damage of sugar unit of the polymer. In the nucleotide, the sugar unit contacts with water molecules of the hydrate layer and, therefore, compared with the base is less protected against the impact of $\cdot\text{OH}$ radicals (H_2O^+).

The radical yield in sugar, irradiated individually, is by an order of magnitude higher than the yield of radicals from the bases. At irradiation of nucleosides and nucleotides ESR spectrum of base radicals is registered, which yield approaches the yield of carbohydrate radicals. In the irradiated DNA, the yield of “sugar” radicals approaches zero (ESR data), and the base radicals dominate; the yield of breaks is an order of magnitude lower than that of the base dissociation [1].

Therefore, it may be suggested that during DNA irradiation in nucleotide an electron is transmitted from 2-deoxyribosyl primary radical to the base [11]. Analyzing the structure of recognized products of the radiation-modified DNA sugar chain at irradiation of its solutions or cells (alkaline-labile 2-deoxyribose residues, the so-called alkaline-labile sites in the polymer composition) – I, II, III, IV [1], see reactions (10.5), (10.6), (10.7), (10.8) – it may be concluded that radiolysis products II, III and IV are formed as a result of primary alkyl radicals $\cdot\text{C1}$, $\cdot\text{C2}$, $\cdot\text{C3}$; $\cdot\text{C4}$ [12]. In the case, if $\cdot\text{OH}$ radicals attack C–H bonds by C3 and C5 atoms, β -bonds are hydrolytically split in the radicals formed or these radicals convert by type of α -elimination of water

(Chapter 8) with occurrence of breaks in the sugar-phosphate chain (reactions (10.9) and (10.10)).



The reactions (10.6) – (10.8) reflect the processes of primary alkyl radicals $\cdot\text{C}_1$, $\cdot\text{C}_2$ and $\cdot\text{C}_4$ conversions, related to unpaired electron transmission from 2-deoxyribose radical to the base. The initiating stage of the processes (10.7) and (10.8) is formation of an intermediate complex, an ion-radical pair. As is observed from the literature, the rate of radiolytic conversions of radicals in the presence of ions (in the composition of ion-radical pairs) is by one to two orders of magnitude higher than the radical reaction rate proceeding under usual conditions [13 – 16]. For the chain

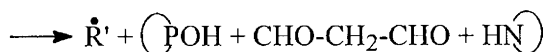
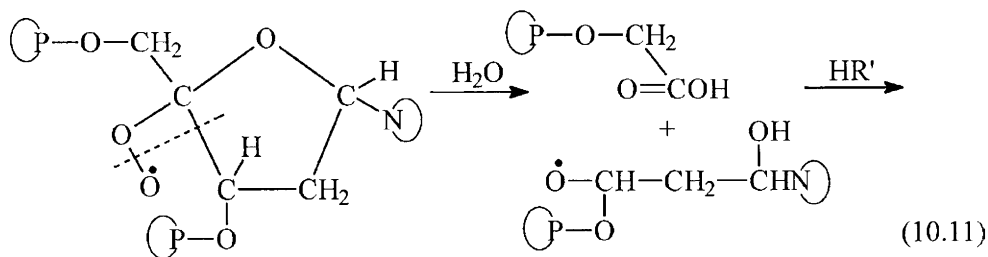
processes with participation ion-radical pairs at 77 K, \bar{e} plays the role of the chain carrier [13].

Note that the product I is formed as a result of nitrogen base damage in the nucleotide, in primary base radical conversions (the radicals-adducts of $\bullet\text{OH}$, $\bullet\text{H}$ and \bar{e}). The product II is detected only at DNA irradiation in the presence of molecular oxygen. Basing on the analysis of ESR data, obtained for irradiated model compounds, which are carbohydrates (Chapter 8), the product II formation may be related to conversions of $\text{C2OO}\bullet$ type peroxide radical by the reaction (10.6).

Products III and IV contain a carbonyl group $>\text{C}'1=\text{O}$. It may be suggested that both these compounds with the carbonyl group by $\text{C}'1$ are formed in single-type conversions of radicals with unpaired electron at $\text{C}'1$ atom: III – directly from $\text{C}'1$; IV – from $\text{C}'4$, which isomerizing with $\text{O}-\text{C}'1$ bond break in the furanose cycle forms $\bullet\text{C}'1$ radical. Both these radicals demonstrate hydrolytic splitting of $\text{C}'1-\text{N}$ bond and, consequently, $>\text{C}'1=\text{O}$ carbonyl group formation.

The possibility of glycoside bonds hydrolysis in $\bullet\text{C}'1$ type radicals has already been indicated [17]. It has been noted that the glycoside bond hydrolysis rate at transition from intact molecules to radicals increases by 8 – 9 orders of magnitude. If this conclusion is extended to $\text{C}'1-\text{N}$ glycoside bond in the DNA structure, according to the data from [18] for DNA solutions with pH 2.4, as transiting to macroradicals of $\bullet\text{C}'1$ and $\text{H}\bullet\text{C}'1$ types the rate constants of these bonds hydrolytic splitting should reach the level of $k = 10^4 \text{ s}^{-1}$.

For $\bullet\text{C}1$ and $\text{H}\bullet\text{C}1$ type radicals containing aglucon with an aromatic structure, the rate of N-glycoside bond hydrolysis should be higher even at neutral pH due to additional polarization of N-glycoside bond due to a significant shift of the spin density to the aromatic ring. For example, for benzyl and oxybenzyl radicals, splitting on carbon exo-atoms protons equals 1.640 and 1.517 mT [19], whereas for methyl radical it is ~ 2.3 mT. Thus about 1/3 part of the spin density in these radicals is concentrated at the aromatic ring. This is the reason why N-glycoside bond in nucleotide $\bullet\text{C}1$ and $\text{H}\bullet\text{C}1$ radicals becomes much more polarized, the excessive positive charge being devoted to $\bullet\text{C}'1$. Taking into account that some part of water molecules forming the “structured water” in the native polymer structure neighbors the N-glycoside bond, one may suggest that due to such structural organization of DNA occurrence of unpaired electron at $\bullet\text{C}'1$ gives an opportunity to form a radical-ion pair, in which OH^- plays the role of anion. This anion interacts



Thus, finally, 2-deoxyribosyl derivatives with carbonyl groups (aldehyde or keto-group) – potential apurine or apyrimidine sites – occur in DNA, and modified bases, the molecular products of base H-adduct conversions, are released to the solution [12]. At rendering alkaline irradiated DNA solutions, cells or tissues in these three types of DNA sites and those, occurred in DNA structure by the reaction (10.4), phosphoether bonds are hydrolyzed and, therefore, SB are formed in the sugar-phosphate DNA backbone. These four types of molecular products of 2-deoxyribosyl modification in the DNA structure represent alkaline-labile sites (ALS) of the polymer [7]. Single-stranded breaks (SB) formed at rendering alkaline the irradiated systems are usually called secondary (additional) in relation to the primary SB, detected immediately after irradiation of DNA, solutions, cells or tissues without their preliminary alkalization [1]. The formation of primary SB is due to conversions of 2-deoxyribosyl macroradicals $\cdot\text{C}'3$, $\cdot\text{C}'5$ and $\cdot\text{C}'4$ (in the presence of molecular oxygen), proceeding by the reactions (10.9) – (10.11) [11, 21] and is accompanied by free base release from nucleotide, modified in DNA.

The scheme for SB formation suggested was composed basing on ESR data on compounds modeling DNA fragments with respect to the fact, registered at irradiation of DNA solutions: simultaneously with one SB formation in the polymer chain, one undamaged base is released [22].

As calculated per 1 cell and 1 Gy, the mean radiation-chemical yield of SB in DNA at irradiation of cells equals 750 ± 250 , whereas ALS yield is three times lower (Table 10.4).

Table 10.4

DNA degradation in irradiated cells [23]

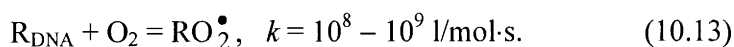
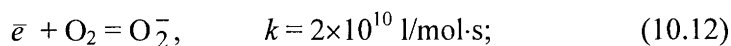
Type of damage	Number of damages, cell/1Gy	
	Data range	Mean value
Single-stranded breaks	500 – 1,000	750 ± 250
Alkaline-labile sites	200 – 300	250 ± 50
Sugar damages	800 – 1,600	1,200 ± 400
Base damages	1,000 – 2,000	1,500 ± 500

As mentioned above, the significance of hydrated electron for damaging sugar fragment is minimal (its reactivity, compared with $\cdot\text{OH}$ radical, in relation to carbohydrates is about 10 – 50 times lower [10]). Apparently, in the case of humidified DNA (DNA B-form – water concentration in the hydrate layer is 30% higher than in C-form), electron is stabilized by water molecules of the hydrate layer of the polymer near 2-deoxyribosyl. Obviously, this increases the electron lifetime, which promotes its transition to nitrogen bases (anion-radicals of bases are formed) or involvement into recombination reactions with any free radicals of DNA.

It has been shown [24, 25] that as DNA interacts with low energy electrons (below 15 eV), it may perform their resonance capture (during 10^{-15} s) with formation of intermediate molecular anion, accompanied by C–H bond splitting in 2-deoxyribosyl and subsequent sugar-phosphate chain break. The yield of this process is low – below 0.001 per 1 captured electron.

10.4. OXYGEN EFFECT

As molecular oxygen is present in the solution, \bar{e}_{hydr} and primary radicals of nitrogen bases (OH-, H- and electron adducts) enter reactions with it forming peroxide radicals:



If molecular oxygen concentration in the irradiated system (DNA solution or any microarea of the cell) is rather high, then resulting the reaction (10.12) hydrated electron is eliminated from the primary interactions with DNA bases. In the radicals ROO^\bullet formed by the reaction (10.13) peroxide groups are located at pyrimidine bases and, supposedly, guanine.

The first stage of peroxide radical conversions is formation of hydroperoxides $ROOH$ by the substitution reaction as follows:



In the structure of irradiated DNA pyrimidine base hydroperoxides were chromatographically determined [26], and their properties were studied on model systems by chemiluminescence method [27]. Spontaneous hydroperoxide dissociation (reaction (10.15)) initiates chain processes proceeding by the free-radical mechanism:



in accordance with the sequence of reactions (10.1), (10.13), (10.14), (10.16) that is the reason for post-irradiation degradation of DNA. The effect of post-irradiation degradation of DNA in solution may reach ~50% of the total effect. If irradiated DNA solution is added with an acceptor of oxidative radicals ($\bullet OH$, RO^\bullet), myoinositol, for example, in a rather high concentration, the yield of post-irradiation degradation of the polymer is reduced approaching zero [28, 29].

The conversions of the primary radicals of nucleic acids with unpaired electron at the sugar fragment are studied much better than conversions of nitrogen base macroradicals.

In the absence of molecular oxygen, radicals formed from sugar unit of nucleic acids by the reaction (10.1) are involved in the reactions, which may be divided into two groups according to radiolysis data on carbohydrates, nucleosides and nucleotides:

- 1) primary radical conversions within a single monomeric unit;
- 2) reactions involving two radicals and proceeding with unpaired electron transfer to neighbor fragments of the polymer.

The first group includes the following processes:

1. Radical isomerization reactions with cycle disclosure by C–O and C–C bonds and carbonyl group formation. For RNA, C'2–C'3 bond break is possible. As a result, the phosphoether bonds should also be broken;
2. β -elimination reactions analogous to β -elimination of water (refer to Chapter 8) with respect structural features of sugar 2-deoxyribosyl unit. It may be suggested that such conversions predominantly involve radicals with unpaired electron, localized at C'5 and C'3 atoms. During these reactions H atom is detached from C'4 atom, phosphoether bonds break and end phosphate groups are formed, 3- and 5-phosphate ones, respectively. The same end groups must also be formed due to α -elimination of phosphate groups and H-atoms detachment with them from C'4 atom.

Radical \bullet C'1 conversions in DNA and RNA are different, because hydrogen atoms in methylene unit (C₂H₂) have lower mobility than H atom of oxymethylene unit in ribose. Apparently, in DNA, in radical \bullet C'1 the bond $>$ C'1–N is hydrolyzed, and this process is accompanied by $>$ C'1OH groups formation and free nitrogen base release. The formation of free bases was detected at radiolysis of DNA precursors and DNA solutions [22]. As follows from the above-said, at radiolysis of RNA, its nucleosides and nucleotides β -elimination of 5'-phosphate group, and β - and α -elimination of the nitrogen base may be provided by primary radical \bullet C'1 and \bullet C'2 conversions.

The second group of reactions consists of:

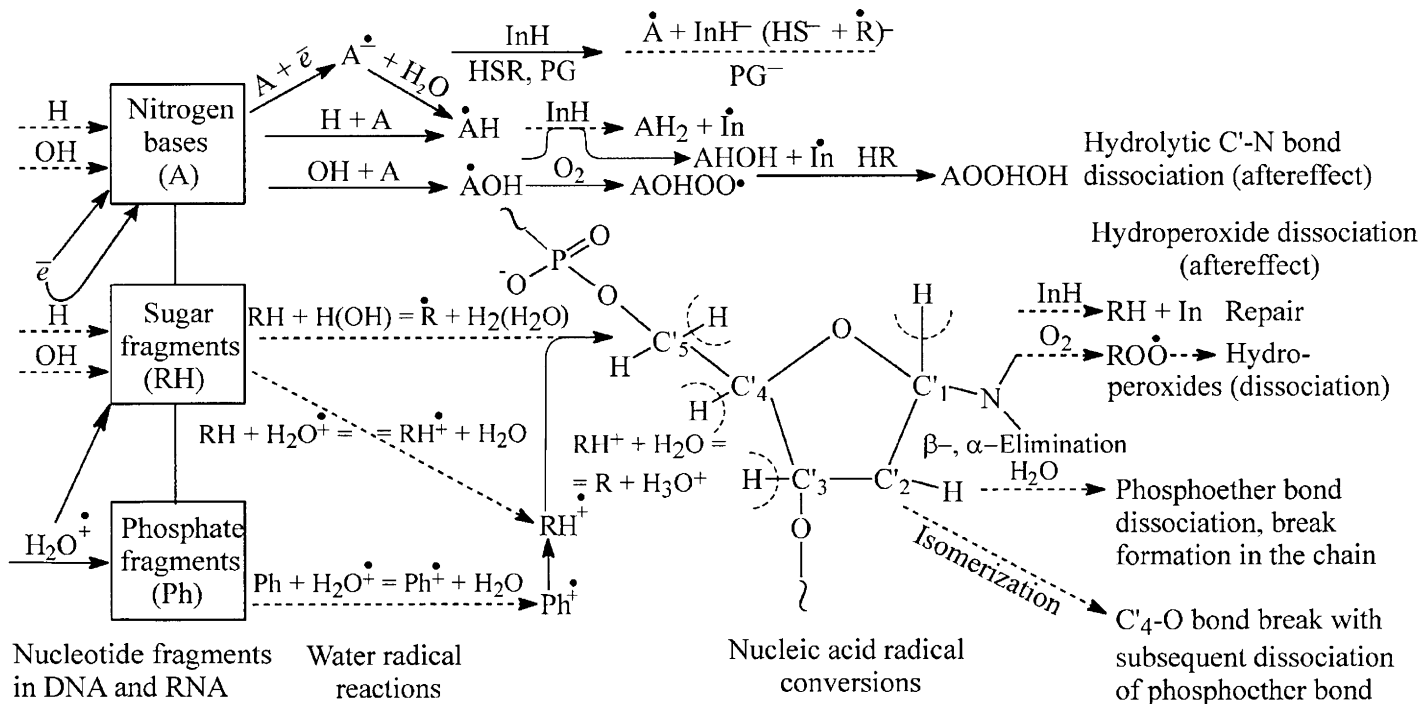
1. Radical recombination reactions capable of inducing crosslinking of molecular chains. If one of the radicals is \bullet H, a stereoisomer (an epimer) of the initial sugar may be formed (see the next Section for details). Such products are detected at radiolysis of frozen-up carbohydrate, glucoside, nucleoside and nucleotide solutions. The probability of epimerization product yield increases with transition to DNA, because bulky radicals are formed in this case, and their reaction with mobile H atoms is less probable due to steric factor.
2. Radical disproportionation reactions, in which compounds with carbonyl groups should be formed, for example, deoxyketosugars detected in the radiolysis of DNA solutions and even at radiolytic

degradation of DNA, irradiated in the composition of deoxyribonucleoprotein (DNP) – the natural DNA and histone proteins (Chapter 11).

In the presence of molecular oxygen, the mechanism of primary radical conversions is modified by their interaction with O_2 , forming peroxide radicals. Such radicals were registered at radiolysis of frozen-up carbohydrate, oligo- and polysaccharides and DNA solutions. However, a reliable recognition of unpaired electron localization site at the damaged unit (sugar fragment or nitrogen base) by ESR data is not possible yet. As follows from analysis of chemical products of DNA radiolysis, the composition of products and changes in the yields of single and double breaks at transition from solution radiolysis in the absence of molecular oxygen to radiolysis of solutions containing molecular oxygen, occurrence of peroxide radicals and, correspondingly, hydroperoxides at the sugar unit of DNA is quite possible.

The analysis of the radiolysis data for low-molecular analogues of nucleic acid sugar fragment indicates that in the current system formation and accumulation of final radiolysis products is defined by competition between conversions of primary radicals of the sugar fragment. Only very rapid first order conversions of the primary radicals may compete with the process of peroxide radical formation (reaction (10.4)). The formation of peroxide radicals and subsequent formation of hydroperoxides ROOH from them should cause break of C–C bonds neighbor to the peroxide group. Actually, the yield of DNA strand breaks at irradiation in solutions in the presence of molecular oxygen is higher compared with DNA irradiation in the absence of molecular oxygen.

Phosphate unit damage in nucleotide is induced by participation of radicals $\cdot OH$ or their precursors H_2O^+ in reactions with phosphate. As shown on the example of the study of radiolytic properties of frozen-up aqueous solutions of phosphoric acid and glucose in phosphoric acid, the system of variable composition modeling radiolysis of the sugar-phosphate fragment of nucleotide, the yield of carbohydrate radicals increases with gradual increasing concentration of dissolved sugar in the phosphate matrix from 0.15 to 6 M (Chapter 8, Figure 8.1b). Hence, total yield of radicals (of phosphate and glucose) formed at 77 K does not change. It is worthy of note that in 1 M glucose solution the quantity of radicals from sugar equaled ~70%, whereas in 2 M solution about 100%. Since phosphate-ion concentration in these solutions



Scheme 10.1

equals 4.5 M, one may conclude that in the carbohydrate-phosphate system with the component ratio 1:1, i.e. analogous to nucleotide structure, only sugar component radicals are formed. It may be suggested that, primarily, in this system a phosphate cation-radical is formed, and at 77 K the hole migrates from phosphate to glucose with further deprotonation of the sugar cation-radical formed in reactions with water molecules or, for example, phosphate radical reacts with carbohydrate molecule:



where RH is carbohydrate molecule.

Therefore, a conclusion can be made that initially occurred damage at the phosphate fragment (unpaired electron) of nucleotide is finally localized at the carbohydrate fragment.

Currently existing data allows for presenting a diagram of the basic routes describing formation and conversions of the primary radicals in DNA, irradiated in aqueous solution (see Scheme 10.1).

Free-radical mechanisms of DNA radioprotection

Similar to proteins (Chapter 7), at the primary stages of radiation degradation of DNA free-radical mechanisms of its radioprotection are subdivided as follows: the competing mechanism for water radicals and the mechanism of free-radical reaction (FRR) inhibition [30].

Realization of the competing mechanism for water radicals between a radioprotector (RP) and biopolymer (BP) depends on the observation of the condition of preferable interaction between water radicals and the radioprotector. In the case of $\bullet\text{OH}$ radicals, the following ratio should be observed:

$$k(\bullet\text{OH} + \text{RP}) \times [\bullet\text{OH}] \times [\text{RP}] \gg k(\bullet\text{OH} + \text{BP}) \times [\bullet\text{OH}] \times [\text{biopolymer}],$$

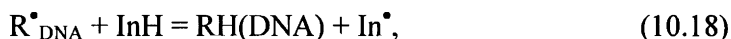
where $k(\bullet\text{OH} + \text{RP})$ is the rate constant of the reaction between $\bullet\text{OH}$ radical and RP.

By analogy, biopolymer may be protected against the action of the reduction component of water radiolysis on it – \bar{e}_{hydr} and $\bullet\text{H}$. If molecular oxygen is present in the irradiated system, the latter capturing these two

particles (\bar{e}_{hydr} and $\bullet\text{H}$), eliminates them from the reaction. Hence, less active free radicals, superoxide-ion O_2^- and superoxide radical HO_2^\bullet , are formed. Therefore, for the purpose of preventing the interaction between these superoxide radicals and DNA in the irradiated cell, substances also reacting with superoxide radicals or enzymes "utilizing" these radicals, superoxide dismutase, for example, should be used as radioprotectors.

There is an additional condition for implementing the protective mechanism using radioprotectors. In general, radicals of additives, formed in the primary acts, or molecular products of their radiolysis must not react with biopolymers. But if the radicals of the additives or final products of their radiolysis react with the biopolymer and, therefore, accelerate its degradation, then such additives should be belonged to the class of radiosensibilizers.

Realization of the FRR inhibition mechanism is implemented by free-radical substitution reactions [31, 32]:



In the present case, it is suggested that $\text{R}^\bullet_{\text{DNA}}$, RO^\bullet , and ROO^\bullet are the base radicals.

The contribution of each reaction to the total effect of DNA radioprotection is nonequivalent and depends on the radiation conditions (primarily, in the presence or in the absence of molecular oxygen), macroradical origin (the site of unpaired electron localization at the base and, apparently, at 2-deoxyribosyl) and the inhibitor molecule (its reactivity in relation to radicals). For example, the process (10.18) may only be realized in the absence of molecular oxygen. For DNA radicals, the rate constant of this reaction equals $10^7 - 10^8$ l/mol·s (cystamine) and $10^4 - 10^6$ l/mol·s (screened phenols) [32]. If the irradiated system contains molecular oxygen, all $\text{R}^\bullet_{\text{DNA}}$ radicals reacting with it ($k = 10^8 - 10^9$ l/mol·s) transit to peroxide radicals, which then will react with InH (the reaction (10.20)). Maximal rate constants of the reaction (10.20) vary within the range of $10^6 - 10^8$ l/mol·s with respect to the fact, how hindered the access of InH to peroxide radical is and what the origin of the inhibitor is. In the case of screened phenols, the rate constant varies within the range of $10^4 - 10^6$ l/mol·s, whereas for compounds with double bonds (quinines, for example) they are 1 - 2 orders of magnitude

higher. Similar situation of the reactivity in relation to alkoxy radicals is observed (the reaction (10.19)). However, it should be taken into account that RO^\bullet radicals are formed at peroxide dissociation by the reaction (10.15), and in irradiated cells and tissues peroxides effectively interact with glutathione peroxidase. As a consequence, stationary concentration of alkoxy radicals in these systems is minimal. Hence, the contribution of the process (10.19) into the cell radioprotection effect is also minimal.

Nevertheless, the yield of DNA degradation in solutions in the post-irradiation period, induced by decomposition of peroxides formed at irradiation and proceeding of the reactions in the presence of oxygen and reaction proceeding by the free-radical mechanism ((10.15), (10.1(5)), (10.16), (10.13), (10.14)), may reach 50% of total effect of the radiation degradation of biopolymer [28, 29].

As shown in the study of DNA solution radiolysis, macroradical repair by the reaction (10.18) with formation of the initial compound is possible in the only case, if unpaired electron in this macroradical is localized at 2-deoxyribosyl. Hence, if in the macroradical formed the unpaired electron is localized at the nitrogen base, then in the reaction between this radical and the inhibitor the initial structure of the molecule may not be reduced, and modified nitrogen base with saturated bonds is formed. No repair of primarily damaged molecule of biopolymer happens. In the DNA molecule, modified in this manner, N-glycoside bond is hydrolytically split (reaction (10.4)), and apurine or apyrimidine site (ALS) – the place of potential break in the sugar-phosphate chain in DNA – is formed (see Chapter 13 for details).

If in the DNA radical unpaired electron is localized at the nitrogen bond, then resulting the reaction (10.18) a damage “representing” unpaired electron is eliminated at this site in the macromolecule (the radical is recombined), and the double bond in the base is replaced by a single one. Hence, the initial structure of the macromolecule is not reduced. In this case, as well as at processes (10.19) and (10.20) the effect of radioprotection is only implemented via elimination of DNA macroradicals (replacing them, low activity inhibitor radicals are formed) and, therefore, their reactions leading to polymer degradation are prevented.

As unpaired electron is localized at 2-deoxyribosyl of DNA, the reaction (10.18) reduces the initial structure of the macromolecule (strictly speaking, this represents the radioprotection effect [10]) or produces 2-deoxyribosyl residue epimers (C'1-, C'3-, C'4-stereoisomers) [33, 34]. The interaction between FRR and these three types of sugar radicals should result in

the conformation change (disposition of atoms in the space) of the sugar fragment and, therefore, the entire macromolecule [35].

It has been proved [33] on the example of frozen-up ribose solution radiolysis (77 K) that the conformation of sugar molecule may be changes by radiation. Radicals formed at the interaction of $\cdot\text{OH}$ with the sugar molecules by the reaction (10.5) and \bar{e}_{st} were recognized. As irradiated by visible light or at heating irradiated samples up \bar{e} releases from the trap and recombines with sugar radical decreasing their concentration:



After defrosting the irradiated samples, among basic molecular products of ribose radiolysis, lyxose, arabinose and xylose were detected (see Chapter 8, Figure 8.24)). It should be noted that ribose epimer synthesis by the reaction (10.21) under conditions of monosaccharide irradiation in a rigid messenger (frozen-up aqueous solution, $T = 77$ K, migration of photoannealed electron in the system) takes place.

Analogous results in formation of initial deoxyribosyl epimers are observed at irradiation of frozen-up nucleotide (thymidine) solution [34]. After defrosting the irradiated samples, among thymidine radiolysis products, epimers by C3 and C4 carbon atoms were detected: 1-(2-deoxy- β -D-*treo*-pentofuranosyl)thymine and 1-(2-deoxy- α -L-*treo*-pentofuranosyl)thymine.

In the case of DNA solution γ -irradiation even at room temperature and so much at irradiation in the nucleosome composition, B-DNA (possessing a crystalline structure [36]), realization of elementary acts of 2-deoxyribosyl radical conversions by reactions (10.21) seems to be quite real. Firstly, due to the fact that crystalline DNA "fixes" the macroradical structure during some time, enough for proceeding of this radical recombination with the electron. Secondly, as mentioned above, the electron formed has no reactivity in relation to cyclic 2-deoxyribosyl, but is only stabilized by it and, therefore, as the recombinant is preserved in the irradiated system longer than hydrated electron. Moreover, C1-, C3- and C4-stereoisomers of 2-deoxyribosyl residue of DNA, irradiated in the cell, may also be formed due to an ability of variable valence metal ions, present in the native DNA, to act as recombining agents (electron donors) in relation to 2-deoxyribosyl radicals [35].

Thus, the formation of 2-deoxyribosyl epimers in DNA may be realized at the cell irradiation either in the presence of radioprotectors or without them

(as some background process [35]). Note that this very process may be one of the reasons for changing DNA conformation [37].

10.5. ABOUT MOLECULAR MECHANISMS OF RADIATION MUTAGENIC ACTION

By definition, mutations (spontaneous or induced by ionizing radiation, for example) represent jump-like changes in chromosomes, inherited and definitely affecting various signs of the organism (biochemical, physiological, and morphological). With respect to the measurement unit or the primary origin, mutations are subdivided into gene, chromosomal and genome ones [2, 38, 29].

Gene (point) mutations are stable changes of nucleotide type or location in DNA molecule within the coupled triplet (in 1 nm radius). The formation of point mutations does not disturb entity of the chromosome, and its protein component is not involved.

Chromosomal mutations represent rearrangements of chromosomes; intrachromosomal (separation, duplication or 180° inversion of any area of the chromosome) and interchromosomal rearrangements, which is the exchange of fragments between unpaired (nonhomologous) chromosomes.

Gene mutations are the change of the number of chromosomes.

From positions of the molecular ideas of interest on the reason for mutations, radiation-induced in the organism, according to common opinion, the occurrence of point mutations is related to loss of bases or their modification in DNA composition, induced by ionizing radiation. Hence, either full loss of complementary properties (specific coupling) in the composition of DNA (coupling with any of four bases happens: pyrimidine hydroperoxides, glycols, some products of purines degradation) or modified bases display some coupling specificity. For example, uracyl and hypoxanthine (cytosine and adenine deamination products) formed at DNA duplex “construction” couple with adenine and cytosine, respectively. At the places of occurrence of such radiolysis products the meaning of DNA codons is changed and, therefore, the protein synthesis controlled by mutated genes may proceed with single substitutions of amino acids.

It is the author’s point of view that another reason for point mutations is the primary damage of the sugar fragment of DNA – the formation of alkyl

radicals and then molecular products of their conversions – 2-deoxyribosyl epimers by C'1, C'3 and C'4 atoms. This statement is based on the test results of the radiolysis of frozen-up aqueous solutions of monosaccharides and thymidine (195 K), when macroradicals in a rather rigid matrix are stable, and $\cdot\text{OH}$ radicals and \bar{e} formed from water are mobile [33, 34]. As mentioned in the previous Section, under these conditions alkyl radicals may react with electrons and, recombining, form epimers. For DNA, the structure of the polymer itself plays the role of “rigid matrix” for 2-deoxyribose residue radicals. The occurrence of alkyl radicals and 2-deoxyribosyl epimers in the DNA structure must change orientation (deviation of N-glycoside bond and displacement of functional groups) of nitrogen base in the nucleotide in accordance with rehybridization of orbitals (initial fragment : radical : epimers = sp^3 : sp^2 : sp^3). According to computer modeling data, the highest deviation (up to 50°) is observed for the bases in the case of $\cdot\text{C1}$ radical (duplicating for epimers), and the lowest deviation (0°) is observed for $\cdot\text{C5}$ radical (Figure 10.3) [37, 40]. Figure 10.3 explains the mechanism of epimers formation in the nucleotide (a – initial nucleotide, b – radical, c – epimers). If the repair enzymes miss such changes in the structure of modified nucleotide in DNA molecule, then coupling of bases containing a stereoisomer in the nucleotide with extracanonical (by Watson-Crick) bases may proceed in the subsequent acts of DNA replication (the duplex formation). The base coupling only depends on the fact if hydrogen bonds manage to form between them e.g. if the distances in atomic pairs N...N and N...O in fall within the range of 2.74 – 3.15 Å [36, 37]. Hereof, a conclusion is induced about a possibility of occurrence of such types of gene mutations as transitions and transversions at the initial damaging of the sugar fragment of DNA [35, 37].

The launching mechanism of chromosomal mutation, as follows from their title, is related to the formation of breaks in the sugar-phosphate backbone of DNA. More than 60-year investigations of the radiation chromosomal aberrations (CA) allowed for determining the dependence of CA formation on the mitotic cycle stage (G1 – presynthetic stage; S – DNA synthesis stage; G2 – post-synthetic stage) under the effect of ionizing radiations. For example, in G1 phase the chromosome behaves itself as a single effective strand – the DNA molecule (the same is the break and exchange unit). In the G2 phase, the chromosome is represented by two chromatids, each behaving oneself as an independent break and exchange unit, and now the chromosome responses to the radiation impact as a structure consisting of two effective strands. Such

chromosome rearrangements are called aberrations of the chromatid type [38, 39].

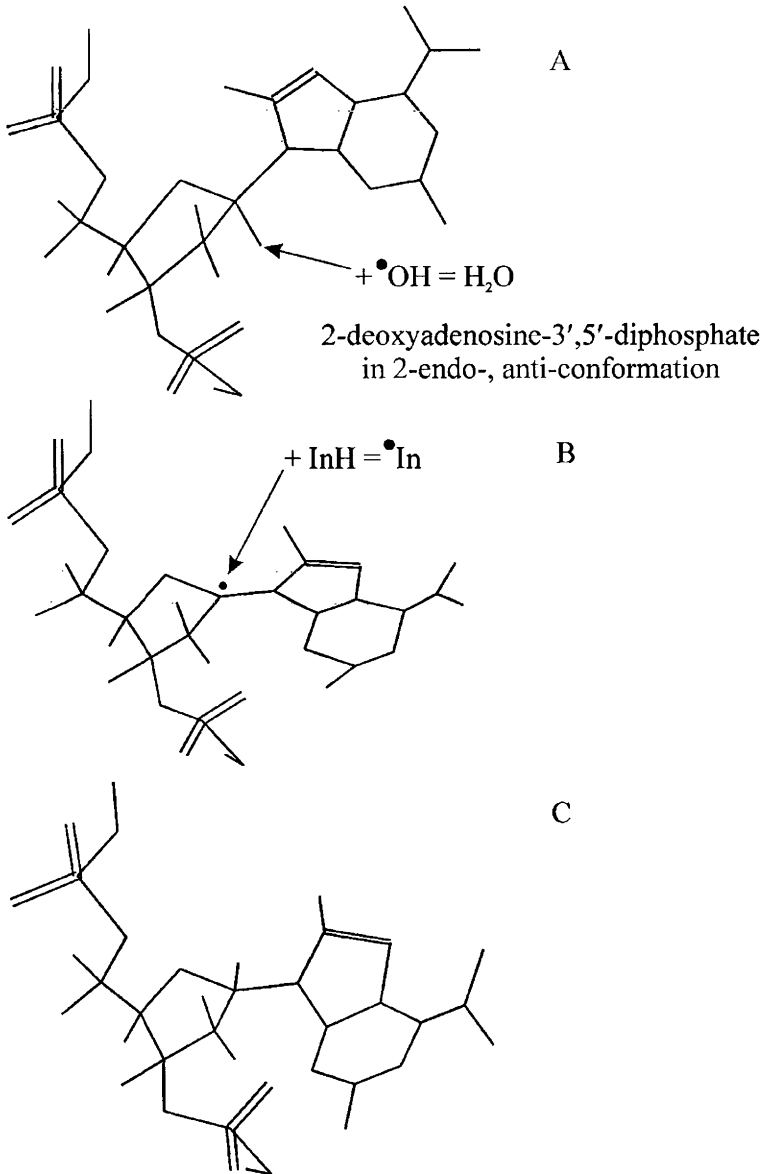


Figure 10.3. 3D model of nucleotide: epimers formation

The ESR data obtained for irradiated DNA and compounds modeling some fragments of it induce a conclusion that the base and sugar fragment modifications (including formation of breaks in the sugar-phosphate backbone) and, consequently, formation of potential mutation sites, both point and chromosomal, in DNA are initiated by free-radical mechanisms. Therefore, to decrease (if not to prevent) the yield of mutations of the first two types, radioprotectors should be used, possessing free radical acceptor properties and competing with DNA for water radiolysis products and, thus, acting as FRR inhibitors (antioxidants for irradiated biological system, if molecular oxygen is present in it).

However, it should be noted that application of FRR inhibitors may promote an increase of C1-, C3- and C4-stereoisomer yield and subsequent increase of the point mutation frequency of the "sugar origin" compared with the background one (for example, at cell irradiation in the absence of InH). Actually, some tests performed on drosophila flies and mice indicated that their irradiation in case of the presence of substances possessing InH (radical acceptor) properties in their organisms led to an increase of the point mutation frequency, as compared with irradiation under usual conditions [39]. If in this case point mutations were provided by modifications of nitrogen bases, then transition to irradiation in the presence of InH would decrease the yield of point mutations (as well as the yield of base degradation products and break formation in the sugar-phosphate backbone) [35].

To conclude the Chapter, let us emphasize that beside the common ideas about the occurrence of gene (point) mutations of DNA due to the initial modification of bases in the macromolecule structure, the possibility of occurrence of potential sites for point mutations in it due to primary damage of 2-deoxyribosyl (H detachment radical formation and their conversion to 2-deoxyribose residue epimers) should also be taken into account. The changes in the base disposition in space due to occurrence of 2-deoxyribose stereoisomer in DNA replication acts may lead to formation of hydrogen bonds with extracanonical (by Watson-Crick) bases and potential sites for point mutations (transversions and transitions).

REFERENCES

1. Ryabchenko N.I., *Radiation and DNA*, Moscow, Atomizdat, 1979, 192 p. (Rus)
2. Amigarova M.I., Duzhenkova N.A., Krushinskaya N.P., Mochalina A.S., Savich A.V., and Shal'nov M.I., *Primary Radiobiological Processes*, Moscow, Atomizdat, 1973, 336 p. (Rus)
3. Kudryashov Yu.B., *Radiation Biophysics (Ionizing Radiation)*, Moscow, FIZMATLIT, 2004, 448 p. (Rus)
4. Rakhmanov A.S. and Sharpatyi V.A., *Doklady AN SSSR*, 1972, vol. **203**(5), p. 1126. (Rus)
5. Dobryakov S.N., Mikhadjidinova D.R., and Sharpatyi V.A., *Proc. All-Union Conference "Magnetic Resonance in Biology and Medicine"* May 1990, Moscow, Izd. ICP AS USSR, p. 15. (Rus)
6. Dobryakov S.N., Il'yasova V.B., Mikhadjidinova D.R., and Sharpatyi V.A., *Biofizika*, 1986, vol. **31**(6), p. 573. (Rus)
7. Teoule R., *Int. J. Radiat. Biol.*, 1987, vol. **51**(4), p. 573.
8. Fuciarelli A.F., Wegher B.J., Blakely W.F., and Dizdaroglu M., *Int. J. Radiat. Biol.*, 1990, vol. **58**(3), p. 397.
9. Zakatova N.V., 'Radiolytic conversion of DNA in aqueous solutions', *Candidate Dissertation Thesis*, Moscow, Institute of Electrochemistry AS USSR, 1973, 102 p. (Rus)
10. Sharpatyi V.A., *Radiation Chemistry of Biopolymers*, Moscow, 1981, Energoizdat, 168 p. (Rus)
11. Sharpatyi V.A., *Radiats. Biol. Radioekol.*, 1997, vol. **37**(4), p. 508. (Rus)
12. Koritsky A.T. and Sharpatyi V.A., *Khimia Vysikikh Energiy*, 1991, vol. **25**(4), p. 354. (Rus)
13. Kovalev M.D., Koritsky A.T., and Sharpatyi V.A., *Khimia Vysikikh Energiy*, 1991, vol. **25**(4), p. 354 – 356. (Rus)
14. Koritsky A.T. and Zubkov A.V., *Khimia Vysikikh Energiy*, 1968, vol. **2**(6), p. 544. (Rus)
15. Koritsky A.T., Karatun A.A. *et al.*, *Khimia Vysikikh Energiy*, 1986, vol. **10**(5), p. 406. (Rus)
16. Myers D.J., Gardner P.D., Stroebel G.G. *et al.*, *J. Amer. Chem. Soc.*, 1973, vol. **95**(17), p. 5832.

17. von Sonntag C.V., *Adv. Carbohydr. Chem. Biochem.*, 1980, vol. **37**(2), p. 7.
18. Kochetkov N.K., Budovsky E.I., Sverdlov E.D., Simukova N.A., Turchinsky M.F., and Shibaev V.N., *Organic Chemistry of Nucleic Acids*, Moscow, Khimia, 1970, 720 p. (Rus)
19. Fischer H., *Z. Naturforschung*, 1965, Bd. **8**(5), S. 488.
20. *The Energy of Chemical Bond Break. Ionization Potentials and Affinity to Electron*, Ed. V.N. Kondrat'ev, Moscow, Nauka, 1974, p. 351. (Rus)
21. Kuzurman P.A. and Sharpatyi V.A., *Radiats. Biol. Radioekol.*, 1998, vol. **38**(2), p. 147. (Rus)
22. Swarts S.G., *Proc. Congress "Radiation Research 1895-1995"*, vol. **2**, Eds. U. Hagen, D. Harder, H. Jung, Ch. Streffer, Wurzburg/DBR, 1995, p. 208.
23. Pryakhin E.A., "Dynamics of changes in DNA repair in bone marrow cells of mice irradiated by ^{90}Sr ", *Candidate Dissertation Thesis*, Moscow, MSU, 1997, 135 p. (Rus)
24. Michael B.D. and O'Neil P., *Science*, 2000, vol. **287**, p. 1603.
25. Boudaiffa B., Cloutier P., Hanting D., Huels M.A., and Sanche L., *Science*, 2000, vol. **287**, p. 1658.
26. Scholes G. and Weiss J., *Nature*, 1960, vol. **185**, p. 305.
27. Zhizhina G.P., Zybina D.L., Kruglyakova K.E., and Emanuel N.M., *Doklady AN SSSR*, 1964, vol. **158**(4), p. 935. (Rus)
28. Kruglyakova K.E., Nikolaeva N.V., Zakharova N.A., and Emanuel N.M., *Doklady AN SSSR*, 1964, vol. **157**(2), p. 979. (Rus)
29. Zakatova N.V. and Sharpatyi V.A., *Doklady AN SSSR*, 1971, vol. **200**(5), p. 1378. (Rus)
30. Sharpatyi V.A., "Primary mechanisms of radiation damaging of biologically urgent molecules: DNA, protein, DNP, polysaccharides", *Doctor Dissertation Thesis*, Moscow, ICP AS USSR, 1972, 419 p. (Rus)
31. Emanuel N.M., *Proc. MIOP*, 1963, vol. **7**, Izd AN SSSR, p. 73. (Rus)
32. Sapezhinsky I.I., *Biopolymers: Kinetics of Radiation and Photochemical Conversions*, Moscow, Nauka, 1988, 214 p. (Rus)
33. Kochetkov N.k., Kudryashov L.I., Chlenov M.A., Sharpatyi V.A., Nadjimiddinova M.T., Nikitin I.V., and Emanuel N.M., *Doklady AN SSSR*, 1968, vol. **183**(2), p. 376. (Rus)

34. Sharpatyi V.A., Cadet J., and Teoule R., *Int. J. Radiat. Biol.*, 1978, vol. **33**(5), p. 419.
35. Sharpatyi V.A., *Radiobiologia*, 1992, vol. **32**(2), pp. 180 – 193. (Rus)
36. Zenger V., *The Principles of Structural Organization of Nucleic Acids*, Ed. B.K. Vainstein, Moscow, Mir, 1987, 584 p. (Rus)
37. Kuzurman P.A. and Sharpatyi V.A., *Khimia Vysokikh Energyi*, 1999, vol. **33**(5), p. 347. (Rus)
38. Alikhanyan S.I., Akif'ev A.P., and Chernin L.S., *General Genetics*, Moscow, 1985, 448 p. (Rus)
39. Mosse I.B., *Radiation and Inheritance*, 1990, Minsk, Universitetskoe Izd., 208 p. (Rus)

Chapter 11. Chromatin DNP radiolysis

11.1. COMPOSITION AND STRUCTURE OF DNP COMPLEX

Chromatin deoxyribonucleoprotein (DNP) is a natural complex based on DNA (30 – 40 wt.%) and proteins (30 – 50% - histones; 4 – 33% – nonhistone proteins). The quantity of proteins in DNP and the size of DNA molecules vary within a wide range with respect to the extraction method and the object origin.

Table 11.1

Histone fraction content in calf tissues, %

Fraction	Thymus	Intestine	Spleen	Lung	Cerebrum	Liver	Endometrium	Kidney
H1	19.5	18.9	24.1	21.1	20.4	18.7	16.3	20.5
H4	18.3	17.6	23.1	15.8	16.1	20.7	17.3	20.0
H2A	18.1	19.2	14.4	19.3	15.7	14.0	16.9	11.8
H2B	24.6	22.9	26.9	27.8	22.7	32.4	28.4	26.7
H3	19.6	21.3	11.5	16.0	25.2	15.3	20.7	21.9

The methods of biochemical analysis allowed for dividing histones into five fractions (Table 11.1). Primarily, histones are block structured: they demonstrate dense grouping and block arrangement of charged and hydrophobic amino acids, respectively. DNP in the cell nuclei is a part of more complicated complex, which is chromatin, the chemical substrate of chromosomes, from which DNP is extracted. Judging by description of cell nucleus treatment techniques, frequently in physicochemical investigations chromatin rather than DNP is used. Chromatin represents chromosomes, uncompact in the interphase nucleus (interphase is an intersect of the mitotic cycle between one mitosis end and beginning of another one).

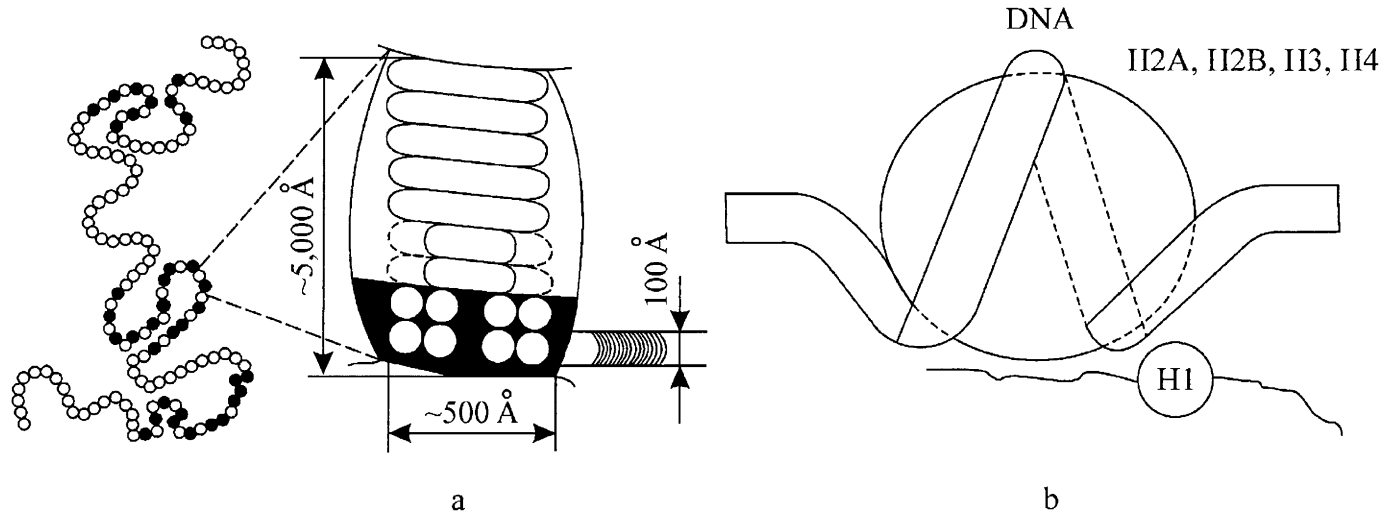


Figure 11.1. Chromatin structure model in the cell nucleus and DNP packing (DNA $MM \sim 2 \times 10^8$, $\sim 10^6$ Å long) within its subunit
 a – interphase chromosome; b – monosome [1]

Figure 11.1 shows supermolecular and molecular organization of eukaryote chromosome and chromatin as an assembly of nucleosomes (monosomes). Nucleosome diameter is about 100 Å. It contains DNA fragment 140 – 230 nucleotide pairs long ($MM > 10^5$). The monosome chain is bound by DNA strands 15 Å in diameter and 140 Å long, occupied by nonhistone proteins.

Each nucleosome (the cor-particle) represents a globule formed by 4 histone proteins (pairs of 4 histone molecules H2A, H2B, H3, H4 form an octamer). DNA is located at the external surface of the globule (in nucleosome DNA exists in B-conformation, 20 Å in diameter). Histone H1 is located at the top, linked to DNA coil. In the cor-particle DNA forms 1.75 coils, has 146 pairs of nucleotides and represents a supercoil with 27 Å step. Globular particles are located as far as 30 – 70 Å from one another [1].

Histone proteins contain abundant basic amino acid residues (totally, histones contain about 20 amino acids). C-terminal areas of H2A, H2B, H3 and H4 are hydrophobic ones (possess the secondary coil structure), and N-terminal areas are hydrophilic (basic) ones.

DNA packing in nucleosome is provided by electrostatic interaction of negatively charged phosphate groups of DNA with cationic Lys and Arg groups, located at the surface of the globular part of the histone octamer [2]. Cationic groups of N- and C-terminal areas of histone molecules (preferably H3 and H4 histones) additionally stabilize the structure of nucleosomes. The protein fragment is bound to DNA fragment by covalent phosphoether and phosphoamide bonds. Chelate bonds with participation of bivalent metals participate in the bond between the protein fragment and DNA fragment by adenine bases. There are ideas about tertiary and quaternary DNP structures – the supercoils.

11.2. BASIC RADIOLYTIC EFFECTS

Generally, radiolytic properties of DNP in solutions are determined by the level of DNP structural organization, which, in turn, depends on the ionic strength of the solution, DNP concentration and the environment pH. As affected by radiation DNP molecular mass changes due to formation of breaks and crosslinks in DNA and histone chains, and DNA–histone bonds break. These facts predetermine the change of macromolecular properties of the entire

DNP. Irradiation of DNP solutions induces formation of radiolytic degradation products of both DNA and histone fragment.

Deamination is one of the basic processes of DNP radiolysis, in which both fragments are involved. Table 11.2 shows that this process (studied by ammonia formation, Conway [3]) is stipulated by modification of the functional groups having nitrogen atom (amino, guanidine, imino groups etc.), the protein fragment of DNP complex: $G(\text{NH}_3)$ values obtained at DNP and histone irradiation (in both cases, histone concentrations are similar) are comparable.

Table 11.2

Ammonia yield (G , analysis by Conway) in aqueous solutions of DNP, DNA and histone, saturated with O_2 , $T = 300 \text{ K}$ [3]

Irradiated solution	$G(\text{NH}_3)$
0.055% DNP + 0.7 M NaCl	4 ± 0.5
0.09% DNA	0.58 ± 0.05
0.033% histone + 0.7 M NaCl	4.7 ± 0.5

Table 11.3

The yield of chromophore group degradation products in DNA fragment at DNP irradiation in solutions at different temperatures [4]

DNP composition (DNA, histone), its concentration, origin of saturating gas	77 K	195 K	273 K
DNP (1 – 1.7), 0.6% air	0.30 ± 0.10	1.2 ± 0.1	1.8 ± 0.2
DNP (1 – 1.7), 0.6% air + 0.2 M inositol	0.50 ± 0.10	–	–
DNP (1 – 1.7), 0.6% argon	0.40 ± 0.10	–	–
DNP (1 – 2), 1.8% air	0.57 ± 0.15	1.4 ± 0.1	3.1 ± 0.3
DNP (1 – 2), 1.8% air + 0.2 M inositol	0.77 ± 0.15	–	2.2 ± 0.2
DNP (1 – 2), 1.8% argon	0.66 ± 0.15	–	–
DNP (1 – 2), 1.8% argon + 0.2 M inositol	0.70 ± 0.25	–	–
DNP (1 – 1), 2.3% air	1.00 ± 0.20	–	–
DNA 0.2%, air	–	–	1.7 ± 0.2

Similar to radiolysis of DNP individual components – DNA (Chapter 10) and protein (Chapter 7), the yield of any product of these fragments radiolysis at irradiation of DNP solutions depends on the biopolymer

concentration. For example, the yield of chromophore group degradation products in DNA (double bonds in the bases) increases with DNP concentration (Table 11.3).

Primary radiolysis processes, the role of water radical

The products from both fragments are formed under the effect of water radicals, and their yield depends not only on the conditions of competing for water radicals of each active site of DNP fragments. As comparing data on the study of amino acid residue degradation in histone, irradiated individually or in DNP composition, induced by $\cdot\text{OH}$ radicals (irradiation of solutions in the presence of molecular oxygen, the electron acceptor), it follows that DNA fragment has a different effect on the degradation of amino acid residues in the histone fragment. Once, degradation is sensibilized (arginine, glycine); in another case, it protects them from degradation (phenylalanine, histidine, leucine, serine). It is worthy of note that in both cases, total degradation yield of the histone fragment is the same ($G = 1.6$). Generally, data on the primary processes of DNP radiolysis in aqueous solutions e.g. on the role of water radicals in DNP degradation, sites of their attacks and macroradical conversions were obtained by the method of the intermediate product registration – radicals, implemented using ESR technique at low temperature. For example, as comparing the yields of radicals, detected at irradiation of frozen-up aqueous solutions containing no DNP and solutions of the same composition in the presence of DNP, a decrease of the yield of radicals, \bar{e}_{hydr} and $\cdot\text{OH}$, stabilized at 77 K may be observed. Hence, their yield also decreases with increasing DNP concentration in solution. Vice versa, the yield of radicals from DNP increases. Therefore, even at 77 K during irradiation radicals \bar{e} and $\cdot\text{OH}$ (or H_2O^+) are involved into the reactions with dissolved DNP. Table 11.4 shows the yields of radicals, the sum of radicals and biopolymer radicals, registered in DNP solutions of various concentrations, aerated and evacuated, irradiated at 77 K. The yield of the primary radicals of biopolymer is independent of the presence or the absence of molecular oxygen in the solution.

Table 11.4

 $G(R)$ in DNP and DNA solutions at 77 K [4]

DNP composition (DNA:histone), concentration and saturating gas origin	$G(\Sigma R^{\bullet})$	$G(R^{\bullet}_{\text{biopolymer}})$
DNP (1:1.7), 0.6%, air	0.6	0.08
DNP (1:1.7), 2.3%, vacuum	0.8	0.5
DNP (1:1.7), 9%, air	1.2	0.8
DNP (1:1.7), 9%, vacuum	1.3	1.0
DNA, 1.56%, air	0.8	0.4

Table 11.5

 $G(\text{deamination})$ in aqueous DNP solutions irradiated at 77 and 195 K (in brackets) [4]

DNP composition (DNA:histone), concentration and the origin of saturating gas	$G(\text{ammonia})$, by Conway	
	In the absence of $\bullet\text{OH}$ radical acceptor (inositol)	In the presence of $\bullet\text{OH}$ radical acceptor (0.2 M inositol)
DNP (1:1.7), 0.6%, air	0.15 ± 0.05	0.09 ± 0.01
DNP (1:1.7), 0.6%, argon	0.04 ± 0.02	0.02 ± 0.01
DNP (1:1), 1.08%, air	0.30 ± 0.03	0.10 ± 0.03
DNP (1:0.8), 1.4%, air	(0.32 ± 0.02)	(0.13 ± 0.07)
DNP (1:1.6), 1.4%, air	0.03 ± 0.10	0.16 ± 0.02
DNP (1:1.6), 2.3%, air	0.30 ± 0.15	0.33 ± 0.04
DNP (1:1.6), 2.3%, argon	0.45 ± 0.05	0.03 ± 0.03
DNP (1:1), 2.3%, air	0.30 ± 0.03	0.32 ± 0.01
Histone, 0.6%, air	(0.42 ± 0.07)	(0.18 ± 0.06)
	0.01 ± 0.001	0.01 ± 0.002
DNA, 0.6%, air	(0.06 ± 0.006)	(0.04 ± 0.01)

The predominant role of water radicals in the DNP degradation is clearly displayed in the comparison of radiation-chemical yields of deamination – one of the most important processes of DNP radiation degradation – obtained for DNP solutions irradiated in liquefied nitrogen (when \bar{e} are mobile) and at 195 K (when both \bar{e} and $\bullet\text{OH}$ are mobile). Table 11.5 shows these values and $G(\text{deamination})$ for the case of histone and DNA irradiation. Similar to the case of the liquid-phase radiolysis at low-temperature irradiation of DNP solutions, deamination is related to histone fragment

degradation: for the radiolysis of 0.6% histone solution and 1.08% DNP solution (histone concentration is the same in these systems), $G(\text{deamination})$ values are equal. Deamination happens due to participation of both electron and $\bullet\text{OH}$ radical in the reaction: as transiting from 77 to 195 K, $G(\text{deamination})$ value abruptly decreases in the presence of $\bullet\text{OH}$ radical acceptor – myoinositol (at irradiation, when $\bullet\text{OH}$ radicals are mobile e.g. at 195 K).

As follows from the comparison of $G(\text{deamination})$, recorded for the same liquid solutions, DNA as a fragment of the DNP complex affects deamination proceeding in the histone fragment, initiated by \bar{e} and $\bullet\text{OH}$ radicals.

Data in the Table 11.5 obtained at the study of solutions saturated with an inert gas or molecular oxygen indicate a significant influence of oxygen on the deamination process. Since the presence of molecular oxygen has no effect on the primary radical yield (see Table 11.4), note that molecular oxygen participates in their conversions that affects the yield of the final products of DNP radiolysis.

11.3. ON THE ORIGIN OF DNP RADICALS

ESR spectra of aqueous solutions of DNP and histone, irradiated at 77 K, are similar by shape and are characterized by overlapping ESR bands of several types of radicals (Table 11.6). The following conclusions can be made:

- 1) a six-component band is detected in ESR spectra of DNP and histone solutions;
- 2) ESR spectra of histone solutions has a quintet band;
- 3) similar to DNA solutions, as DNP solutions are irradiated by light with $\lambda = 300$ nm or annealed after irradiation in the presence of molecular oxygen, their spectra change.

An octet of $\bullet\text{TH}$ radical is registered (Figure 11.2). In this case (annealing), $\bullet\text{TH}$ radical concentration gives about 70% of the initial concentration of DNP radicals. Data shown allowed for a conclusion that the formation and conversions of radicals in one of the DNP fragments are affected by another one, and the presence of histone in DNP sensibilizes the yield of radicals in the DNA fragment ($\bullet\text{TH}$ type radicals).

Table 11.6

Radicals recognized by ESR spectra in irradiated (60 kGy) DNP and histone solutions [5]

Radical	The number of HFS components	ΔH , mT	Total width, mT	Suggested structure	Temperature range of radical detection
R ₁	5.1:4:6:4:1 or	2	9	$-\text{CH}_2\text{CH}^\bullet\text{CH}_2-$	Histone, 77 – 190K
R' ₁	1:2:2:2:1 and	2	9	2H (1.9 mT) + 1H (3.9 mT)	
R'' ₁	1:2:1	2	4	2H (1.9 mT)	
R ₂	6.1:3:4:4:3:1	2.3	12.5	$^\bullet\text{CH}_2\text{CH}_2-$	Histone, 77 – 235 K
R' ₂	6.1:3:4:4:3:1	2.1	11.2	$^\bullet\text{CH}_2\text{CH}_2-$	DNP, 77 – 160 K
R ₃	2.1:1	1.5	2.5	$=\text{C}^\bullet-\text{O}^-$	DNP, histone, 77 – 160 K
R ₄	3.1:2:1	2.3	–	2H	DNP (low), up to 160 K
R ₅	2.1:1	–	2.2	Anion-radical	DNP, 77 – 190 K
R ₆	8.1:3:5:7:7:5:3:1	2	14	TH [•]	DNP, 77 – 190 K
R ₇	Asymmetric line $g_{\parallel} = 2.029$; $g_{\perp} = 2.029$	–	5	ROO [•]	DNP, histone, 150 – 205 K
$^\bullet\text{OH}$	2, asymmetrical doublet	4	10.5	$^\bullet\text{OH}$	DNP, histone, 77 – 120 K
\bar{e}_{st}	1, singlet; $g = 2.001$	–	1	$^\bullet e_{\text{st}}$	DNP, histone, 77 – 100 K

Table 11.7

Radiation-chemical properties of histone amino acids at 77 and 300 K [5]

Amino acid	Histone composition, C (mol%)	$G(R^*)$ at 77 K	Damage level, CG	ΔH_{\max} at 77 K, mT	$G(-AA)$ in DNP solution	$G(-AA)$ in histone solution
Arginine	8.3	1.2	10	14	0.35	0.16
Lysine	14.4	1.1	15.8	13	0.28	0.31
Histidine	1.7	0.26	0.44	8.4	0.04	0.13
Asparaginic acid	4.8	0.4	1.92	6	–	–
Asparagine	–	–	–	6	0	0
Glutamic acid	8.3	0.4	3.32	13.5	–	–
Glutamine	–	–	–	6	0	0
Serine	6.1	0.4	2.44	2	0.05	0.13
Tyrosine	2.5	0.06	0.15	2	0.15	0.16
Threonine	5.6	3.4	19.0	9	0.10	0.09
Alanine	13.8	1.4	19.3	3.5	0.12	0
Valine	6.0	2.4	10.1	10	0.5	0.10
Glycine	8.5	2.3	19.5	2.7	0.15	0.04
Isoleucine	4.0	–	–	–	0.07	0.10
Leucine	7.7	1.2	9.2	4.5	0.01	0.26
Methionine	1.0	0.6	0.6	3.4	0.04	–
Proline	5.4	1.0	5.4	5.2	–	–
Phenylalanine	1.9	0.3	0.57	4.3	0.05	0.09
Cysteine	0.6	0.5	0.3	12.0	–	–

Note: * $G(-AA)$ represent radiation yields of each amino acid degradation

The presence of DNA in nucleoprotein complex may also present an explanation of some differences in spectral characteristics of histone fragment radicals (Table 11.7).

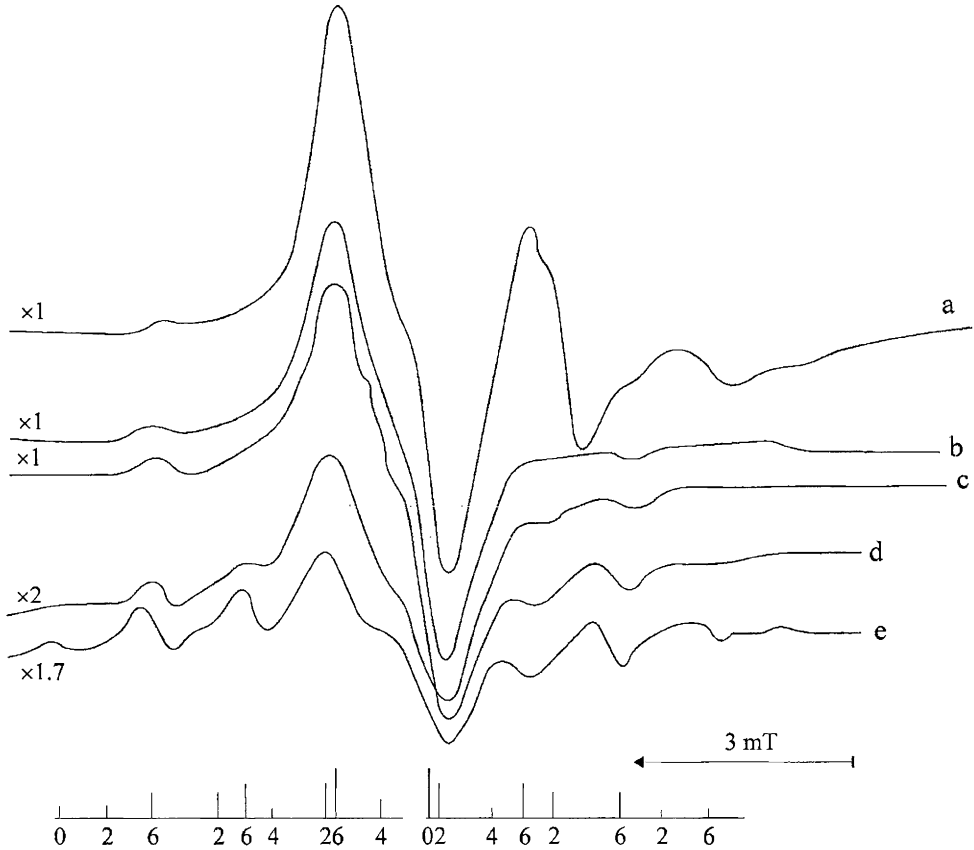


Figure 11.2. ESR spectra of DNP solutions (2.1 wt.%) from calf thymis, irradiated (60 kGy) in the absence of molecular oxygen at 77 K, recorded at 77 K immediately after the irradiation (a) and annealing of the samples at room temperature during different time periods: b – 9 s; c – 14 s; d – 18 s; e – 30 s [5]

A conclusion about unpaired electron localization sites in some DNP primary macroradicals, detected at 77 K, can be made basing on the comparison of radiation-chemical characteristics of low-molecular components

of the nucleoprotein complex with the ESR data. Let us discuss this point in more detail.

Table 11.7 shows $G(R^\bullet)$ values – the number of radicals formed at absorption of 100 eV with deduction of $G(\bar{e}_{st})$ – registered at low-molecular radiolysis of amino acids in the histone structure, and the ESR spectrum width for these radicals. Columns 2 and 4 of the Table show the amino acid composition of histone (mol%) and the damage level of amino acid residues, i.e. a relative contribution of each amino acid into total formation of histone radicals. This value is the product of $G(R^\bullet)$ multiplication by molar fraction of amino acid. Data shown in column 4 indicate that according to radiation-chemical properties, 8 of 19 studied amino acids with the contribution of 5 conditional units should be considered.

As comparing ESR spectrum width of irradiated amino acids and biopolymers – histone and DNP with respect to radiation-chemical properties of amino acids, one may conclude that the localization sites of unpaired electron in histone and DNP are lysine and arginine amino acid residues. Data on deamination of amino acids, histone and DNP in frozen-up solutions allows for a conclusion that one of the basic DNP macroradical types is formed at the electron attack on protonated end amino and guanidine groups of lysine and arginine amino acid residues of histone with subsequent ammonia and guanidine detachment. This type of R_2 radicals (Table 11.6) is characterized by six-component ESR band. The hyperfine structure (HFS) of this band is explained by the interaction between unpaired electron and four protons $\Delta H_{\beta_1} = 2(\Delta H_{\beta_2} = \Delta H_{\alpha})$. According to rather approximate estimation, radicals with the six-component ESR line give about 30% of total quantity of macroradicals.

The main difference in ESR spectra of irradiated histone and DNP is that in the first case, the ESR spectrum recorded at 77 K contains a quintet band. Due to this band overlapping in the central part by ESR bands of other radicals and, primarily, a triplet (R_4) with approximately the same splitting (1.9 mT), it appeared impossible to get a ratio of the component intensities in the ESR bands under discussion. One might suggest (as an alternative explanation) that the registered ESR band is at triplet (1:2:1, $\Delta H \sim 1.9$ mT) of doublets (1:1, $\Delta H = 3.9$ mT). Apparently, a conclusion about the origin of this radical can be made basing on, firstly, radiation-chemical properties of amino acid residues in histone, irradiated in the aqueous solutions and in DNP structure and, secondly, total ESR band widths for individual amino acid components and peptides, irradiated under the same conditions (Table 11.7). In Table 11.7, the last two columns show yields of amino acid residue degradation at irradiation of histone

and DNP aqueous solutions. If one suggests that at low-temperature radiolysis $\cdot\text{OH}$ radicals participate in addition by double bonds and H detachment at attack of C–H bonds in amino acid residues in the case, when $\cdot\text{OH}$ radicals are formed directly at these functional groups, a conclusion can be made that unpaired electron is localized on histidine, proline, serine, leucine (type R_1 and R'_1 radicals) and phenylalanine (type R''_1 radicals). The damage level of these amino acid residues (except proline, which degradation was not studied) significantly decreases at transition from histone to DNP solution. Moreover, the quantitative analysis of the amino acid composition recorded after defrosting the irradiated DNP solutions under the conditions of radical detection, the greatest degradation level was observed for lysine, arginine and aromatic amino acid residues. With respect to the fact that amino groups of lysine and arginine amino acid residues in DNP participate in formation of bonds with negatively charged phosphate groups, and radicals from lysine amino acid residues, for example, are formed at amino group detachment (after electron capture by them), it may be assumed determined that such primary processes are the reason for the bond break between DNA and histone, i.e. the bonds of the electrostatic type. As a result of water radical attack on aromatic rings of amino acid residues, oxy-products of substituted diphenols and semiquinones of these diphenols type are formed. These processes were discussed in the previous Chapters for the case of radiolysis of phenylalanine, tyrosine, and tryptophan. The products of radiolytic conversion of aromatic amino acids may react with compounds present in solutions. In this case, it may be suggested that the intermediate products, such as all types of semiquinone radicals, derived from tyrosine or phenylalanine, may react with DNA fragment, inducing any damages in it (conformational variations, strand breaks, etc.). Such effects were registered at radiolysis of DNA solutions in the presence of modified aromatic amino acids (3,4-deoxyphenylalanine). Since these amino acid residues in the histone fragment of DNP are disposed near DNA, the great role of the processes with participation of semiquinone radicals in the DNA fragment modification is obvious.

11.4. DNA FRAGMENT DEGRADATION

The conversions touching upon the DNA fragment in the irradiated DNP in aqueous solutions may be judged about at irradiation of radiolytic

effects, stipulated by degradation of each component of the nucleotide: nitrogen bases – 2-deoxyribose and phosphate ones. In the experiments, double bond breaks in nitrogen bases (chromophore groups)¹, accumulation of sugar fragment degradation product, the analogue of malonic aldehyde, a compound with the end group $-\text{HCOPCH}_2\text{CHO}$ forming a dyed complex with thiobarbituric acid with $\lambda_{\text{max}} = 532 \text{ nm}$, and formation of phosphate-ions determined by the reaction with ammonium molybdate, were registered.

At the irradiation of DNP aqueous solutions, conditions, at which one type or another of water radiolysis products (\bar{e} , $\cdot\text{OH}$, $\cdot\text{H}$) is preferably involved into the reaction, it is determined which particular water radicals attack the DNP fragments. It is of interest to compare data on radiolysis of aqueous and frozen-up DNP solutions at 77 and 195 K. For example, at 77 K mostly $\cdot\text{H}$, \bar{e} and component $\bar{e} \dots \text{H}_2\text{O}^+$ pairs are involved in the reactions with the dissolved substances, if dissociation of water molecules into ions has happened near any functional group of the biopolymer. Beside these particles, at 195 K $\cdot\text{OH}$ radicals are involved into the reactions, which are mobile at this temperature. The study of radiolysis at 273 K gave an opportunity to significantly eliminate the post-irradiation processes, which have made the picture of the primary effects more complicated.

Tables 11.3 and 11.8 show yields of chromophore group degradation and accumulation of DNA fragment sugar-phosphate unit degradation products, registered under different conditions of DNP solution irradiation (different temperature of irradiated solutions, in the presence of molecular oxygen and other additives – radical $\cdot\text{OH}$ acceptors, etc.). The comparison of data from Tables 11.3, 11.4 and 11.8 indicates that one of the main processes of DNA radiolytic degradation in the DNP composition in frozen-up aqueous solutions is degradation of nitrogen base chromophore groups: $G(-\text{chromophore groups})$ is comparable with total yield of radicals, registered at 77 K.

The yield $G(R_{\text{biopolymer}})$ increases with DNP concentration in the solution within the measurement accuracy proportionally to the concentration. The total yield of radicals increases to a lower extent, specifically in the case of higher concentrated DNP solutions (Table 11.4); hence, the relative part of $\cdot\text{OH}$ radicals in total concentration of the radicals significantly decreases.

¹ The analysis was performed by the spectrophotometry method for DNA solutions after deproteinization (histone removal) of DNP and strand separation in DNA.

Table 11.8

The yields of radiolysis products at irradiation of DNP and DNA aqueous solutions at 77 K (55 kGy) [4]

DNP composition (DNA:histone), its concentration, saturating gas origin	$G(\text{MA})$	$G(\text{PO}_4^{3-})$	$G(\text{organic phosphate})$
DNP (1:1.7), 0.6%, air	0.0014 (+ 15%)*	0.02 (+ 100%)*	0.025
DNP (1:1.7), 0.6%, air + 0.2 M inositol	0.0004	0.013	–
DNP (1:1.7), 0.6%, argon	0.0014 (+ 10%)*	0.01 (+ 150%)*	0.025
DNP (1:1.7), 0.6%, argon + 0.2 M inositol	0.001	0.002	–
DNP (1:1), 2.3%, air	0.003	0.03	0.25
DNA, 1.56%, air	–	0.2	0.45

Note: * Additional release of products into the solution after irradiation removal – the post-effect.

Similarly, the yield of other radiolysis products also increases with the DNP concentration in solution. Therefore, registered processes of DNP radiolytic degradation under current irradiation conditions are induced by radical products of water radiolysis. In these processes \bar{e} and $\cdot\text{OH}$ radicals (H_2O^+) are involved.

Similar to the liquid-phase radiolysis, the yield of carbohydrate-phosphate DNA fragment degradation products in the DNP composition is by 1.5 – 2 orders of magnitude lower compared with the yields of nitrogen base degradation products. The comparison of the data on accumulation of the radiolysis products under discussion, obtained from DNA at DNP and DNA individual exposure to radiation under identical conditions indicates that the presence of histone in the complex structure affects degradation of the nucleotide components.

The comparison of chromatin DNA and DNP solution radiolysis (Tables 11.9 and 11.10) indicates that the sugar-phosphate DNA backbone degradation yield in the DNP composition is three times lower than at irradiation of individual DNA [1]: histone in DNP and chromatin competes with DNA for $\cdot\text{OH}$ radicals (inositol is $\cdot\text{OH}$ acceptor).

Table 11.9

DNA degradation in chromatin DNP solutions ([DNA]:[histone] = 1:1.7) and individually (5 kGy, air, $T = 273$ K) [6]

Irradiated solution	$G(\text{chromophore group})$	$G(\text{breaks})$
0.2% DNA	1.7 ± 0.2	0.3
0.2% DNA in DNP solution, 0.7 M NaCl	1.8 ± 0.2	0.1

Table 11.10

DNA degradation in chromatin solutions (10.5 kGy, air, 273 K)

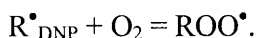
Irradiated solution	$G(\text{DNA degradation}) \times 10^5$ *
0.037%	7
0.037% chromatin + 0.05 M inositol	2.5

Note: * The yield was determined by comparison of the areas enclosed in densitometric curves of electrophoregrams [6]

The oxygen effect

As mentioned above, the yield of primary radicals from DNP is independent on the presence of molecular oxygen in solution. However, the yield of carbohydrate-phosphate chain of DNA (see Table 11.8) and histone fragment (see Table 11.5) degradation products depends on this factor. The experiments on annealing of DNA solutions, irradiated at 77 K, indicated that as biopolymer radicals recombined in the samples containing molecular oxygen, immediately peroxide radicals (ROO^\bullet) were formed, and their concentration increased in the temperature range of 163 – 203 K. Similar to irradiated DNA solutions (Chapter 10), in the samples containing no molecular oxygen in this temperature range thymine structure radicals (typical octacomponent ESR band, Figure 11.2) instead of peroxide radicals were registered.

Thus, it should be noted that molecular oxygen manifests its effect at the secondary stage of the radical conversion of biopolymer only:



The formation of type ROO^\bullet radicals and their conversions may represent an explanation for changes in the yield of the final products in aerated DNP

solutions compared with solutions saturated with an inert gas. As shown by data in Tables 11.5 and 11.8, the yield of the basic radiolysis processes (deamination, sugar-phosphate chain degradation – phosphate ion release) depends on the presence of molecular oxygen in solution, inositol injection to the DNP solution prior to irradiation and temperature of the solution irradiated. This dependence may be explained by the fact that the change of irradiation conditions affects conversions of macroradicals.

The role of DNA in histone degradation

In chromatin, DNA 7-fold decreases the yield of breaks in polypeptide chains of histones H1, H2 and H3 and has no effect for histone H4 (Table 11.11) [6, 7]. The presence of inositol in solution has no effect on H1 and H4 degradation. This means that degradation of these fractions is initiated by participation of the electron.

Table 11.11

The yield of radiation degradation of histone, irradiated in deaerated aqueous solutions in the chromatin structure and individually [6]

0.03% histone in the chromatin structure, 2 kGy, 273 K (the same in brackets + 0.05 M inositol)			0.25% histone (from calf thymus), 0.9 kGy, 300 K (the same in brackets + 0.05 M inositol)	
$G(-\Sigma)$	0.022 ± 0.002	(0.015 ± 0.002)	0.55 ± 0.03	(0.35 ± 0.03)
$G(-H1, H1A)$	0.006 ± 0.001	(0.005 ± 0.001)	0.24 ± 0.02	(0.15 ± 0.02)
$G(-H2)$	0.003 ± 0.001	(0.0015 ± 0.0005)	0.18 ± 0.03	–
$G(-H3)$	0.0035 ± 0.001	(0.002 ± 0.001)	0.12 ± 0.03	–
$G(-H4)$	0.01 ± 0.001	(0.008 ± 0.001)	0.05 ± 0.02	(0.02 ± 0.02)

Equal values of chromophore group degradation in individual DNA and chromatin structure (Table 11.9) allows for an additional conclusion that H atom transmission from the protein to DNA base radicals is also possible (to TH^{\bullet} radicals [6] by the reaction (13.6), in particular). In this case, the role of InH in relation to DNA in chromatin is played by the protein fragment.

11.5. ON THE MECHANISM OF RADICAL CONVERSIONS

As follows from the data obtained in the studies of radiolysis of DNA and the compounds modeling its separate fragments (refer to Chapters 4 and 10), the unpaired electron in primary DNA radicals is localized on the damaged sugar fragment and nitrogen bases. As indicated in the previous Chapter, the sites for $\cdot\text{OH}$ radical attack in 2-deoxyribofuranose fragment of DNA represent C–H bonds at all carbon atoms; hence, alkyl radicals are formed, among which C'1, C'3, C'4 and C'5 – with the highest yield. Primary macroradicals of the carbohydrate fragment may enter the following reactions: β - and α - (in the acidic environment) elimination of water, hydrolytic splitting of β -bonds, isomerization with C–O and C–C bond break in the anhydrocarbohydrate cycle (Chapter 8). In the case of DNA 2-deoxyribosyl, the radical reactions of the β -elimination of water type may represent an explanation for occurrence of end 3'- and 5'-phosphate groups in irradiated DNA and experimentally observed fact that the yield of 5'-phosphate groups gives the three fourth part of the total quantity of registered phosphate groups and free inorganic phosphate, as well as formation of breaks in the sugar-phosphate backbone and nitrogen base release (Chapter 10).

Similar to irradiation of DNA solutions [8] and the cells themselves, after alkalization of irradiated DNP solutions an additional phosphate ion and the so-called organic phosphate release is observed (Table 11.8). The phosphate ions are released from either nucleotides with modified nitrogen bases containing saturated bonds after C'1–N bond hydrolysis and modified nitrogen base detachment or nucleotides with the sugar chains, modified by radiation, which contain double bonds in β -position in relation to the phosphoether bonds. With respect to the fact that in this case also no additional end 3'- PO_4^- and 3'-OH groups are formed, one may conclude that, generally, inorganic phosphate is released by the β -elimination reaction.

The presence of oxygen in the solution affects conversions of primary macroradicals. Peroxide radicals formed are able to react with one another and undamaged molecules of the biopolymer. In the first case, formation of a compound with keto-groups and H_2O_2 , registered at the liquid-phase DNA radiolysis. In the second case, hydroperoxides are formed. Hydroperoxide groups are localized at both nitrogen bases and, apparently, carbohydrate fragment.

As shown for radiolysis of aqueous DNA solutions, hydroperoxides of DNA with OOH-group at the nitrogen bases with respect to their type dissociate by two mechanisms: hydrolytic or radical-chain. Formed in the second case, RO^\bullet and $^\bullet\text{OH}$ radicals react with the biopolymer molecules. As a result of these reactions, DNA degrades (the molecular mass decreases and a compound analogous to malonic aldehyde in the post-irradiation period is released (Chapters 6 and 10)). Protein present in the DNP composition abruptly decreases the yield of hydroperoxides and the rate of hydroperoxide degradation in the post-irradiation period. In the latter case, RO^\bullet and $^\bullet\text{OH}$ radicals are preferably captured by protein molecules.

On the features of DNP radiolysis

The study of chromatin DNP radiation degradation mechanism in solutions has determined three DNP-specific radiolytic effects:

- a) labilization of DNA-protein bonds in chromatin;
- b) unpaired electron transfer from primarily formed protein radical to DNA;
- c) occurrence of new chemical bonds between DNA and protein complex fragments – the DNA-protein type crosslinks [1, 9 – 11].

As low-molecular chromatin solutions are irradiated (a set of nucleosomes up to 8 units, DNA *MM* up to 600,000), it is found that beside DNA and protein degradation, in this natural complex, impacted by $^\bullet\text{OH}$ radicals, the DNA-protein bonds are also labilized. The yield of free DNA to the solution depends on [DNA]:[protein] ratio in chromatin. It increases with chromatin concentration in solution in the range of studied concentration from 0.04 to 0.18 wt.% (DNA concentration, Table 11.12) [10].

For example, in the case of solutions, the yield of this process, determined with respect to the mean molecular mass of DNA in chromatin ([protein]:[DNA] = 2.5:1), for [DNA] = 0.04 wt.% equals 0.0007, which is comparable with the yield of DNA-protein crosslinks in the same sample of chromatin [10]. As transiting from chromatin solutions saturated with argon to these saturated with nitrogen oxide, the yield of DNA-protein bond labilization increases twice.

Table 11.12

The increase of free DNA yield ($\pm 10\%$) to the solution at dissociation of chromatin samples, irradiated in Ar, compared with nonirradiated ones. Dependence of the effect on [protein]:[DNA] ratio in the sample

Chromatin (DNA) concentration in irradiated solution, %	Irradiation dose, kGy	[protein]:[DNA] ratio	Free DNA concentration in solution, n ($\mu\text{G/ml}$)	(n/DNA) $\times 10^2$
0.04	5	2.5:1	95	24
0.075	5	2.4:1	80	11
0.075	10	2.4:1	180	16
0.18	10	1.3:1	110	6
0.1	10	1.1:1	15	1.5

In 1960ies, the studies of low-temperature radiolysis of chromatin DNP solutions have indicated that the initial ESR spectrum, recorded at 77 K for a sample irradiated in liquefied nitrogen (low expanded doublet), resembles the spectrum of protein radicals. As heated up to 180 K, this sample demonstrates a spectrum mostly belonged to thymine H-adduct radicals (typical octa-component ESR band) [12, 13].

The observed effect of the ESR spectrum shape change is explained as follows. In chromatin DNP solution irradiated at 77 K, electrons and cation-radicals (electron holes) are formed and, therefore, only electrons are mobile in this case. Both fragments of the DNP complex (DNA and protein) compete for capturing the electrons formed. In this case, the ratio of molar concentrations in the DNP complex is [DNA]:[protein] $\sim 1:7$. Since reactivity of protein and DNA molecules in relation to electron is approximately the same, practically all electrons released at irradiation are captured by the protein fragment and then transmitted (at annealing) to DNA fragment [14].

In aqueous solution, DNA damage in the chromatin structure is induced by degradation (or modification) of nitrogen bases, which is easy to register due to decay of appropriate chromophore groups (double bonds in the bases) and break formation in DNA chains (Table 11.9).

Histone proteins in the DNP structure make no obstacles for chromophore group degradation, but effectively protect DNA from break

formation in the sugar-phosphate chains, induced by $\cdot\text{OH}$ radicals (Table 11.10).

As mentioned above, in irradiated chromatin solution DNA protects histone proteins from break formation in the polypeptide chain in histone fractions H1, H2A, H2B, H3, but does not protect H4 fraction from degradation (Table 11.11). Fractions H1 and H4 degrade due to electron impact. It is also observed that at the ratio of monomeric units equal $[\text{DNA}]:[\text{protein}] \sim 1:7$, initially, electrons in chromatin are captured by protein, and the registered effect of histone degradation prevention by DNA fragment is induced by unpaired electron transition from histone to DNA. In the case of histone H1, the transition of electron to DNA happens at the stage of anion-radical formation. This conclusion correlates with the ESR measurement data. For example, the occurrence of $\text{TH}\cdot$ type radicals at annealing of the sample irradiated at 77 K (a two-stage process: electron interacts with thymine; T^- formed in the interaction with water is protonated, and radical $\text{TH}\cdot$ is formed). In DNP, $\text{TH}\cdot$ yield is high compared with DNA solution (equal DNA concentrations are compared) [14].

Speaking about unpaired electron transition from histones H1 and H4 to DNA and subsequent formation of $\text{TH}\cdot$ radicals, one may suggest that such process of e^- migration is possible at the nucleosome sites, where amino acid residues locate near thymines (for example, they participate in the hydrophobic interaction with CH_3 -groups of thymines) or at the sites possessing hydrogen bonds between imino groups of the protein peptide bonds and $\text{O}=\text{C}4$ oxo-groups of thymines. Then a protein anion-radical ($-\cdot\text{C}(\text{O}^-)-\text{NH}-$ doublet HFS, Table 7.3) occurring at thymine double bond $\text{C}5=\text{C}6$ may play the role of anion-radical.

11.6. DNA-PROTEIN CROSSLINK FORMATION

In γ -irradiated chromatin solution (fragmented, low-molecular) after protein separation from DNA by adding a detergent (0.6% sarcosyl) to irradiated solution, electrophoretic analysis of DNA detects a new polymer consisting of DNA and protein fragments. To put it differently, at chromatin irradiation, DNA-protein crosslinks are formed in it [11]. Table 11.13 shows results of measurements of this product yield at chromatin radiolysis with respect to the origin of gas saturating the solution. For example, if the yield of

DNA-protein crosslinks in chromatin is assumed equal 1 at the solution saturation with argon (hydrated electron and $\cdot\text{OH}$ radicals are reagents), then at transition to solution saturated with Ar and N_2O mixture (the duplicity of $\cdot\text{OH}$ radicals is the reagent) the yield of crosslinks increases significantly. Chromatin irradiation in the presence of inositol produced no additional peak (band) on densitograms. This means that DNA-protein crosslinks in chromatin are generally formed due to $\cdot\text{OH}$ radical participation in the reactions.

Table 11.13

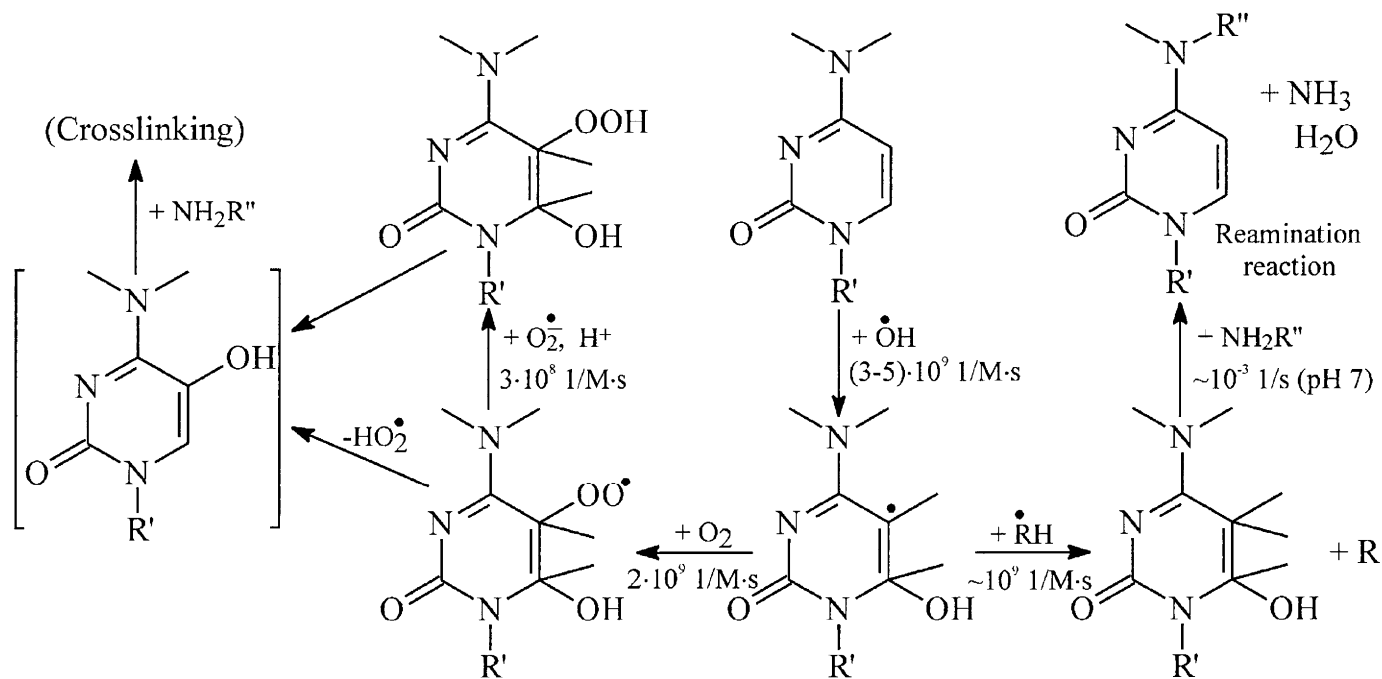
The formation of DNA-protein crosslinks in chromatin irradiated in solutions (0.03%, 40 kGy, 273 K) [5]

Gas or gas mixture saturating the solution	Ar	O_2	$\text{N}_2\text{O} + \text{Ar}$	$\text{N}_2\text{O} + \text{air}$	$\text{N}_2\text{O} + \text{O}_2$
Reagents	$\bar{e}_{\text{aq}}, \cdot\text{OH}$	$\cdot\text{OH}, \text{O}_2, \text{O}_2^-$	$2\cdot\text{OH}$	$2\cdot\text{OH},$ little O_2	$2\cdot\text{OH},$ O_2
Number of crosslinks (arb. un.)	1	0.4	1.4	1	0.7

The intensity of the DNA-protein polymer peak increases with the irradiation dose.

Data in Table 11.13 show that the yield of crosslinks in the presence of oxygen is minimal: $G(\text{crosslinks}) = 0.4$. In the presence of superoxide dismutase in solution ($1.6 \times 10^{-7} \text{ M}$) the yield of DNA-protein crosslinks is the same as in irradiated deaerated solutions [6, 7]. The number of crosslinks in the solution saturated with molecular oxygen increases in the after-irradiation period (48 h or longer) and reaches its maximum, observed in chromatin solutions, saturated with an inert gas. Thus, a conclusion can be made that the processes of crosslink and hydroperoxide formation are mutually exclusive; after hydroperoxide dissociation, the number of crosslinks in chromatin increases.

It is worthy of note that in the studied range of chromatin concentration (from 0.03 to 0.18 wt.% as recalculated per DNA) the yield of crosslinks in chromatin increased with DNA concentration in it only to a definite value (0.04 wt.%). At further increase of DNA concentration the yield remained constant, thus demonstrating the indirect action of irradiation ($\cdot\text{OH}$ radical action): $G(\text{crosslinks}) = 0.0006$ (Ar saturated solutions) [10]. In chromatin solutions of the same concentrations, saturated with nitrogen oxide, the yield of crosslinks was also constant by 40% exceeding the level, observed in the previous case.



Scheme 11.I

Turning back to radiolytic labilization of DNA–protein bonds in chromatin, note that despite the comparable values of their yield and the yield of crosslinks in chromatin, according to the criterion of concentration dependencies both these processes are of somewhat different “origin”: labilization of DNA-protein bonds with free DNA release into the solution most likely falls within the framework of direct action of irradiation on this system, and the DNA-protein crosslink formation – within the framework of classical ideas about indirect action of radiation. The observed linear concentration dependence of DNA-protein bond labilization in chromatin may be explained by relation of this process to water molecule ionization act proceeding directly in the hydrate layer of the polymer. Taking into account the fact that in the presence of nitrogen oxide in chromatin solution the yield of both processes significantly increases (both are induced by $\cdot\text{OH}$ radicals), it may be concluded that start-up process of the DNA-protein bond labilization is preceded by deprotonation of water cation-radical, formed in the hydrate layer of biopolymer.

The Scheme 11.I generalizes the investigation results on the formation of DNA-protein crosslinks, cytosine-lysine ones, as shown in the analysis [11]. At the first stage, as $\cdot\text{OH}$ radicals attack C5=C6 double bonds in cytosine, cytosine OH-adducts are formed. These radicals, with respect to the fact if molecular oxygen is present in the current microarea of the cell nucleus or not, may convert to peroxide radicals and then to hydroperoxides (and then crosslinks are not formed) or at the interaction with any reducing agent – to cytosine 4-exo-N-alkyl-6-oxy-5,6-hydro-derivative. Further on, Cyt-Lys crosslink between DNA and protein fragments is formed by the so-called reamination reaction [15], in which an amino group of the previous molecular product of radiolysis and amino group of histone lysine residue, with ammonia release. For example, such crosslinks may occur at the nucleosome sites, where lysine amino group is linked by the hydrogen bond to O=C6 keto-group of guanine, geometrically complementary in relation to cytosine, attacked by $\cdot\text{OH}$ radicals by C5=C6 bond.

The analysis of these data [8, 9, 14, 16] allowed for a suggestion that the most probable site for Cyt-Lys crosslink formation – “2” in nucleotide “55” of 5'-chain of DNA and at “16–20” quintet of the basic amino acid residues of histone H4. It should be noted that the Cyt-Lys crosslink may also be formed under the effect of H atoms. It is also suggested that another type of the DNA-protein crosslinks may also be formed in chromatin. As shown by the

estimation, total yield of the DNA-protein crosslinks does not exceed the one thousandth part of chromophore DNA group yield [17, 18].

Concluding the discussion, let us note that both effects of chromatin irradiation (damage transfer from protein to DNA and DNA-protein crosslink formation) are realized only due to specific structural organization of the fragments of this natural complex: potential reagents – the residues of corresponding amino acids in the protein fragments and functional groups of DNA bases – are located neighbor to one another in the nucleosome. This is the only reason for a possibility of realizing such multistage processes as electron transfer from the protein to thymine base and forming thymine derivative or cytidyl OH-adduct converting to the derivative with saturated bonds [15].

The conclusion about the predominant role of the structural organization of such biological system as chromatin at specific conversions of the fragments in this complex, initiated by ionizing radiation action, may also be spread upon the radiation degradation of other components of the cell – the complexes of various macromolecules or oligomers.

In this connection, a significant influence of radiolysis on biopolymer-structured water on degradation of both these polymers and their complexes should be emphasized. For instance, the transition from B- to C-form of DNA (the hydrate cover of C-DNA contains less water than B-DNA) is accompanied by two-time decrease of the single-stranded break yield in the sugar-phosphate backbone and transforming activity of DNA [19]. Both these effects are related to decrease of the structured water content at the transition from B- (92%) to C-form (57 – 66%) and the change of the spatial organization of hydrate layers of macromolecules. In the first case, via water molecules the hydrate layer of DNA realizes hydrogen bonds between O2 atoms of pyrimidines and N3 atoms of purines of complimentary bases, whereas the other part of water molecules fills tetrahedral coordination covers of water molecules participating in formation of hydrogen bonds mentioned. In the second case, water molecules in the hydrate layer form “strands” linking the phosphate groups to one another [20].

As a result of water radiolysis in biopolymer-structures hydrate layers, for example, in the case of polysaccharides, the yield of macromolecule degradation increases by many times compared with the situation observed for irradiation of the same compounds with lower concentration of adsorbed water in them (Chapter 8).

Such experimental data on radiolysis of the structured systems induce a new opinion on the problem of biopolymer radioprotection and indicate that previously formulated task of DNA or chromatin structure protection in the cell nucleus is far from resolution even at the primary, physicochemical stages of their radiation damage, and requires new approached to be properly resolved.

REFERENCES

1. Andrianov V.A., Akhrem A.A., Pisarevsky A.N., and Spitkovsky D.M., *Radiation Biophysics of Chromatin DNP*, Moscow, Atomizdat, 1976, 222 p. (Rus)
2. Khrapunov S.N., Sivolob A.V., and Berdyshev G.D., *Biophysics*, 1983, vol. **28**(4), p. 573. (Rus)
3. Zakatova N.V., "Radiolytic DNA conversion in aqueous solutions", *Candidate Dissertation Thesis*, Moscow, Institute of Electrochemistry AS USSR, 1973, 102 p. (Rus)
4. Zakatova N.V. and Sharpatyi V.A., *Radiobiologia*, 1977, vol. **17**(1), p. 3. (Rus)
5. Sharpatyi V.A. and Golubeva N.P., *Ibid*, 1977, vol. **17**(2), p. 200. (Rus)
6. Zakatova N.V. and Sharpatyi V.A., *Ibid*, 1984, vol. **24**(1), p. 60. (Rus)
7. Sharpatyi V.A. and Zakatova N.V., *Proc. 6th Symposium on Radiation Chemistry*, Budapest, 1986, p. 791.
8. Teoule R., *Int. J. Radiat. Biol.*, 1987, vol. **51**(4), p. 573.
9. Amiragova M.I., Duzhenkova N.A., Krushinskaya N.P., Mochalina A.S., Savich A.V., and Shal'nov M.I., *Primary Radiobiological Processes*, Moscow, Atomizdat, 1973, 336 p. (Rus)
10. Voznesenskaya O.S. and Sharpatyi V.A., *Radiobiologia*, 1991, vol. **31**(1), p. 52. (Rus)
11. Zakatova N.V. and Sharpatyi V.A., *Radiobiologia*, 1984, vol. **24**(4), p. 499. (Rus)
12. Kirby-Smith J.S., *Radiat. Res.*, 1960, vol. **2**(Suppl.), p. 668.
13. Flexander P., Lett J.T., and Ormerod M.G., *Biochim. Biophys. Acta*, 1961, vol. **51**, p. 207.
14. Sharpatyi V.A., *Radiation Chemistry of Biopolymers*, Moscow, Energoizdat, 1981, 158 p. (Rus)

15. Kochetkov N.K., Budovsky E.I., Sverdlov E.D., Simukova N.A., Turchinsky M.F., and Shibaev V.N., *Organic Chemistry of Nucleic Acids*, Moscow, Khimia, 1970, 720 p. (Rus)
16. Ryabchenko N.I., *Radiation and DNA*, Moscow, Atomizdat, 1979, 192 p. (Rus)
17. Michael B.D. and O'Neil P., *Science*, 2000, vol. **287**, p. 1603 - 1604.
18. Boudaiffa B., Cloutier P., Hanting D., Huels M.A., and Sanche L., *Science*, vol. **287**, p. 1658 - 1660.
19. Kondakova N.V., "Development of biotest systems for studying the damaging action of ionizing radiation and searching for biologically active substances with anti-radiation properties", *Doctor Dissertation Thesis*, Moscow, 2000, N.M. Emanuel IBCP RAS, 291 p. (Rus)
20. Senger V., *The Principles of Structural Organization of Nucleic Acids*, Ed. B.K. Vainstein, Moscow, Mir, 1987, 584 p. (Rus)

Chapter 12. Radiolysis in the cell. Primary stages of radiolysis

12.1. PROBLEMS IN DESCRIBING RADIATION-CHEMICAL PROCESSES PROCEEDING IN THE CELL

For applied radiobiology, the description of radiolysis in a cell – to put it differently, the description of chemical processes proceeding in a cell, exposed to ionizing radiation, and inducing a set of biochemical responses in it – would mean resolving of one of the most urgent questions: control for radioprotection processes or, vice versa, cell death stimulation.

The solution of this question is limited by sensitivity of currently present registration methods for radiolytic effects at the initial stages of radiation damage. However, the decision is a suitable selection of model systems for studying their radiolysis and reasoned transfer of these results on the living cell. In this relation, a comparison of investigation results on the primary radiation-chemical processes on the systems with permanently complicating organization seems to be perspective:

biopolymers – some structures of cell organelles – organelles – entire cell.

Transition from one organization level to another and, correspondingly, validity of data transfer to more complicated structure must be controlled using biological tests (the control for functioning of the above-mentioned organization level structures).

It is obvious that such approach to the brought up question must prefer the methods, which realization techniques cause no damage of the object entity. Among physicochemical methods, ESR and luminescence methods should be predominant.

By now, the data obtained on the primary stages of radiolytic processes proceeding in the cell are scanty. Nevertheless, they should be discussed, because such information might be used as a basis for deeper study of the radiation degradation mechanisms for chemical components of the cell.

The previous discussion of radiolytic properties of biologically active compounds, biopolymers, cell components, tested individually or in natural complexes, might induce a conclusion that the same processes (specifically for

primary stages of the radiation impact on the systems) must proceed in biopolymers immediately at living cell irradiation. However, it seems to be of interest to find direct proofs for the radical formation induced by radiation in the cell and track their conversions in the native system. Beside relatively low sensitivity of existing physicochemical registration methods for primary and intermediate radiolysis products in the cell, the difficulties at such direct measurements are due to the necessity of their implementation for low radiation doses (i.e. at extremely low concentrations of intermediates in the system), because native systems may endure low doses only. As impacted by high doses, the living cell cannot normally function anymore. Clearly the Nature has seen about elimination of irradiation consequences in the living cell using various repair systems.

Data on the primary radiation-chemical processes in the cell, obtained for systems more complicated than a biopolymer, but less complex than the living cell, allows for detecting the role of primary radiolysis products, radicals, in particular, in the cell damage, determining the damage localization sites in the cell structures and observing for their conversions. Such data were obtained at low-temperature irradiation of plant cells, more precisely, lyophilized cells (chlorellas) and frozen-up animal tissues. Consideration of the first of these objects is of interest due to chlorella being not only a cell, but a protozoon, too, existing individually in the Nature and adapting to the environmental conditions.

12.2. LOW-TEMPERATURE RADIOLYSIS OF CHLORELLA CELLS

Chlorella cells of various strains (see Table 12.1 for characteristics) were cultivated in a mineral or organic medium. The suspension of cells was removed from the cultivation vessel 8 – 9 h after the process initiation. The cells were separated from the medium by centrifuging, rinsed with distilled water and after extraction from the solution by subsequent centrifuging placed to cuvettes for measuring luminescence. In these cuvettes cells were dried in a vacuum case at room temperature during 16 – 18 h. Thereafter, the samples were placed to liquefied nitrogen and irradiated by a cobalt source. Irradiated samples were placed to thermolumiprinting device, where they were heated up to room temperature, where using a photoamplifier luminescence was measured.

Table 12.1

Characteristics of chlorella strains used [1]

Strain	Cell size, mm	Medium	Cultivation conditions
<i>Chlorella pyrenoidosa</i> Strain 211/8v	5 – 7	Mineral	Light and darkness alteration
<i>Chlorella miniata</i>	1 – 2	-//-	-//-
<i>Chlorella</i> sp. Cernay	2 – 3	-//-	-//-
<i>Chlorella vulgaris</i> Strain green	5 – 7	Mineral or organic	-//-
<i>Chlorella vulgaris</i> * Strain white	5 – 7	Organic	Darkness

Note: * Contains about 10% of chlorophyll.

During such measurements, carried out on irradiated cells, the regularities similar to the case of simple organic compounds were determined. These results indicate the affinity of primary radiolytic processes in the objects under discussion and allowed for correctness of the approach to selection of the investigation models for radiolysis of the native systems and suitability of the methods used for the observation for primary processes.

Let us dwell on the investigation results of radiolytic properties of chlorella cells, obtained by luminescence and ESR methods.

Isothermoluminescence of chlorella cells

After irradiation in liquefied nitrogen an isothermal luminescence (ITL) of the cells at 77 K. Figure 12.1 shows typical ITL curve. Here at the right hand linear anamorphosis I_0/I as the time function is shown, where I_0 is the luminescence intensity at the beginning of irradiation; I_t is the intensity at time t [1].

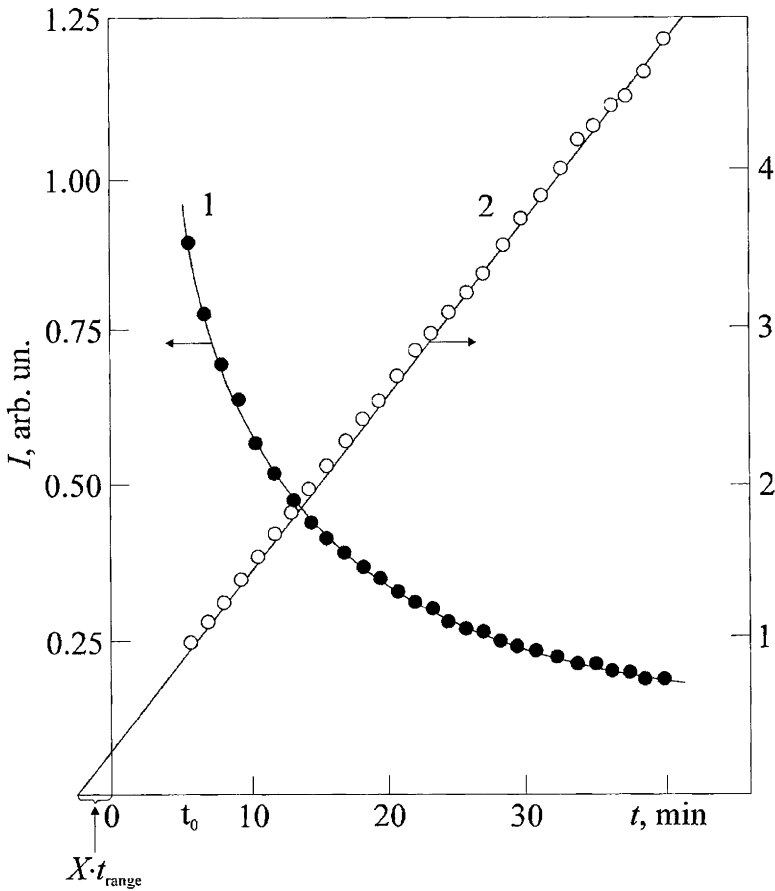


Figure 12.1. Isothermoluminescence curves for *Chlorella pyrenoidosa* cells (5 kGy dose): 1 – observed in the experiment; 2 – its linear anamorphosis

Clearly this function obeys a hyperbolic dependence, also observed in the case of simpler organic systems:

$$I_0/I = 1 + a(t - t_0), \quad (12.1)$$

where t_0 is the first measurement time; a – is the rate constant depending on the irradiation time and time passed after irradiation termination till the measurement beginning. The cross point of the line with the abscissa axis gives

time of the immediate dose perception by the sample. Previously, it has been shown on the example of organic compounds that for the irradiation period shorter than 1 min, $1/a = t_0$; for the irradiation period in the range between 1 and 30 min, the following expression is obtained:

$$1/a = t_0 + xt_{\text{irrad}}, \quad (12.2)$$

where $x = 0.25$. Table 12.2 shows changes of indices a and x with respect to the irradiation duration at constant dose intensity.

Table 12.2

Values of indices characterizing ITL

Dose, kGy	a	x	$xt_{\text{irrad}}, \text{min}$
2.5	0.16	0.07	6.5
5	0.11	0.19	7.7
10	0.09	0.14	11.5
22.5	0.07	0.10	16.7

For all studied chlorella strains, equations (12.1) and (12.2) demonstrate the same indices a and x at the same irradiation time.

The data obtained for the cells, compared with the results of investigation carried out on simple organic compounds, are explained by recombination of cations and captured electrons (the latter move due to the tunneling effect), the change of traps filling with electrons and subsequent $\bar{\epsilon}_{\text{st}}$ distribution by the sample irradiation time.

A conclusion about electron participation in ITL of chlorella cells is confirmed by the test results on the measurement of luminescence intensity of irradiated cells at 77 K after exposure to filament lamp radiation: unfiltered and filtered light, with filters transparent for $\lambda > 410 \text{ nm}$ and $\lambda > 1,100 \text{ nm}$. In all cases, compared with unlighted samples, after five minute-long lighting of irradiated cells the ITL intensity decreases by 30%, approximately. These results show that similar to organic (nonpolar) compounds, IR radiation is the effective in relation to electrons present in the traps.

Radioluminescence of chlorella cells

As cells irradiated in liquefied nitrogen are heated up (at annealing), luminescence ignition was observed (Figure 12.2). Chlorella cells of all studied strains luminesce in the temperature range of 80 – 210 K. As shown in the Figure, the majority of strains possess approximately identical shape of the luminescence curves (Figure 12.2a). RTL curves of *Chlorella vulgaris* cells (green and white strains) possess low differences, obviously related to the chlorophyll content.

A maximum of luminescence is observed in the range of 100 – 110 K. The intensity of this peak is changed with the irradiation dose. As affected by light, the peak intensity decreases by 20 – 30%. Hence, the electrons captured in traps represent recombining particles responsible for the origination of the basic peak. At higher temperature, several peaks of luminescence (more diffused and possessing lower intensity than the first peak intensity) are registered. For various strains, locations of these peaks on the curves are different. It may be suggested that this is stipulated by the structural features of the samples (cell strains) used.

12.3. ELECTRON SPIN RESONANCE (ESR) OF IRRADIATED CHLORELLA CELLS

As chlorella cells are irradiated in liquefied nitrogen, radicals are registered [2]. Figure 12.3a shows ESR spectra of chlorella cells, irradiated at 77 K, recorded at 77 K or higher temperature. It is obvious that the spectrum changes with temperature increase (at the sample annealing) and in the temperature range of 185 – 205 K become asymmetrical. As shown by the analysis, this happens due to the occurrence of ESR bands, belonged to allyl type radicals, formed as a result of primary macroradical conversions – the radicals formed from damaged carbohydrate chains (refer to Chapter 8). Figure 9.3 shows the so-called decoding of the ESR spectrum below the curves – the location of ESR band components of recognize radicals. The location of ESR band components for the allyl type radicals is denoted as R_A . The conversions of primary macroradicals to secondary ones with formation of the allyl type radicals are testified about by the measurement data on the radical

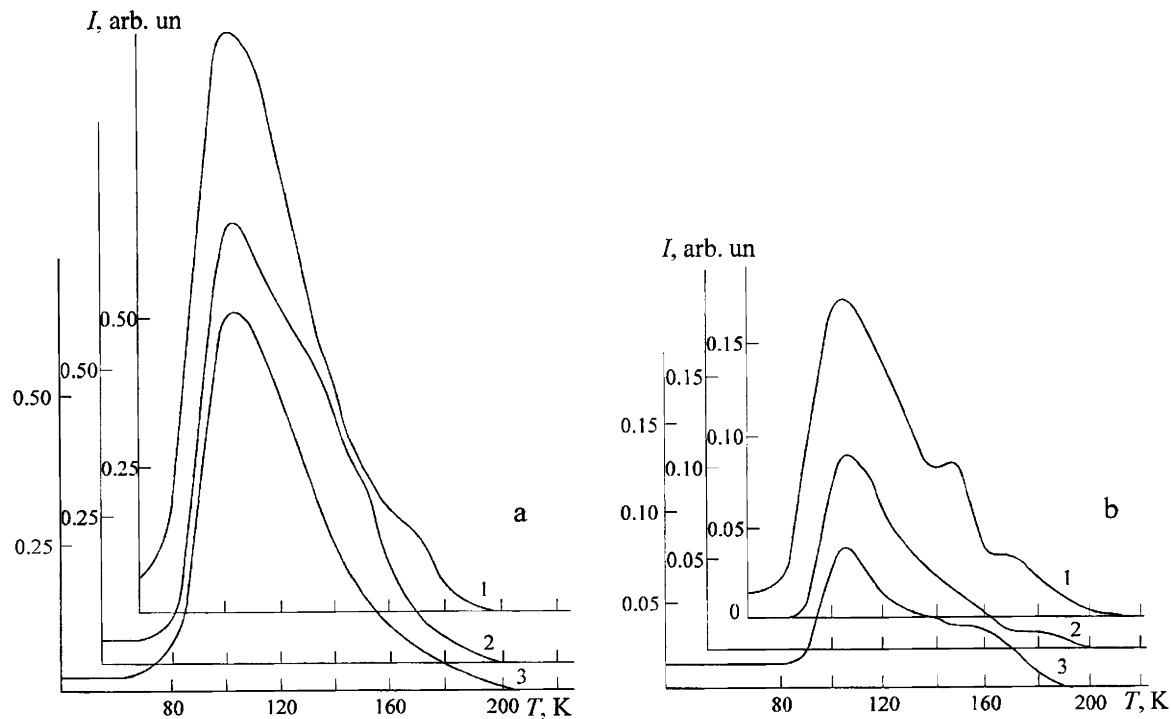


Figure 12.2. Luminescence curves (radiothermoluminescence – RTL) of chlorella cells of various strains, irradiated at 77 K (5 kGy)

a: 1 – *Chlorella pyrenoidosa*; 2 – *Chlorella* sp. Cernay; 3 – *Chlorella miniata*;

b: 1 – *Chlorella vulgaris*, all mentioned strains were cultivated in the mineral medium; 2 – *Chlorella vulgaris*, white; 3 – *Chlorella vulgaris*, green, the strains were cultivated in the medium containing glucose and vitamins

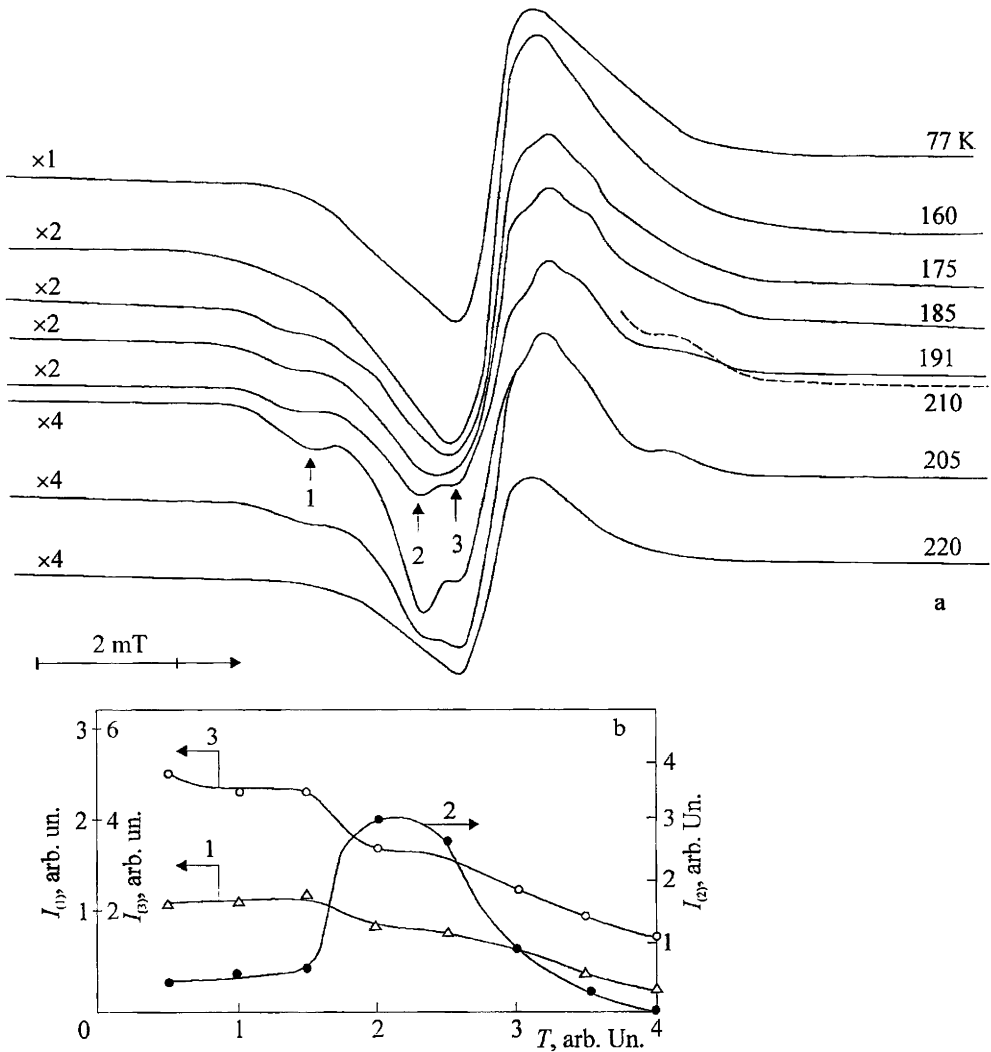


Figure 12.3. The annealing of chlorella cells (lyophilized at room temperature), irradiated at 77 K (10 kGy):
a – ESR spectra of cells (UHF intensity is about 1 MW); *b* – the concentration change of primary macroradicals (1 and 3) and the allyl type radicals, R_A (2)

concentration at the sample heating up (Figure 12.3b). As the intensity of the components 1 and 3 decreases, the intensity of the component 2 increases, i.e. concentration of the secondary radical (the allyl type one) increases.

The discussed changes in ESR spectra of irradiated cells are not observed in the case, when chlorella cells were cultivated in the presence of a detergent, which damages the cell cover. Regarding the facts that the plant cells, including chlorella cells, contains up to 50% in the covers, the difference in the radical conversions might be explained by formation of the allyl type radicals in the entire covers – polysaccharides forming the cover carcass. Hence, at long-term contact (3 days under experimental conditions) of cells with the detergent this carcass is destroyed, the conformation of polysaccharide molecules change, and at irradiation no allyl type radicals are formed.

An additional approach following from current observations reads that one of the reasons for the radiation damage of cells, plant at least, is destruction of the cover due to formation and conversion of the primary radicals at C–H bond break in polysaccharides, which form the cover carcass. Hereof, a method for protecting these cells basing on the data from Chapter 8 may be recommended: they should be cultivated in a medium containing substances, absorbable by the cover and able to react with the primary radicals of polysaccharides by the mechanism of free radical reaction inhibitors (by N.M. Emanuel).

12.4. LOW-TEMPERATURE RADIOLYSIS OF ANIMAL TISSUES

In the animal tissues irradiated at liquefied nitrogen temperature, free radicals were registered using the ESR method. Figure 12.4 [3] shows ESR spectra of the mouse thymus sample, γ -irradiated at 77 K (5 kGy). The spectrum at the left hand was recorded at 77 K immediately after irradiation ($P_{\text{UHF}} = 107 \mu\text{W}$, $M = 3.2 \text{ G}$); at the right hand, ESR spectra of recognized radicals are shown: TH^\bullet (“thymine” structure), $\text{TH}^\bullet_{\text{T}}$ – computer designed with HFS constants at corresponding protons: 20.8 and 36.7 G; A^\bullet – fatty acid residues of lipids; Q^\bullet – ester bond break in phospholipids and triacetyl glycerols; R_s^\bullet – ascorbic acid; ROO^\bullet – peroxide; $^*\text{S1}$ – polypeptide protein backbone. The ESR spectra are specified in ref. [3].

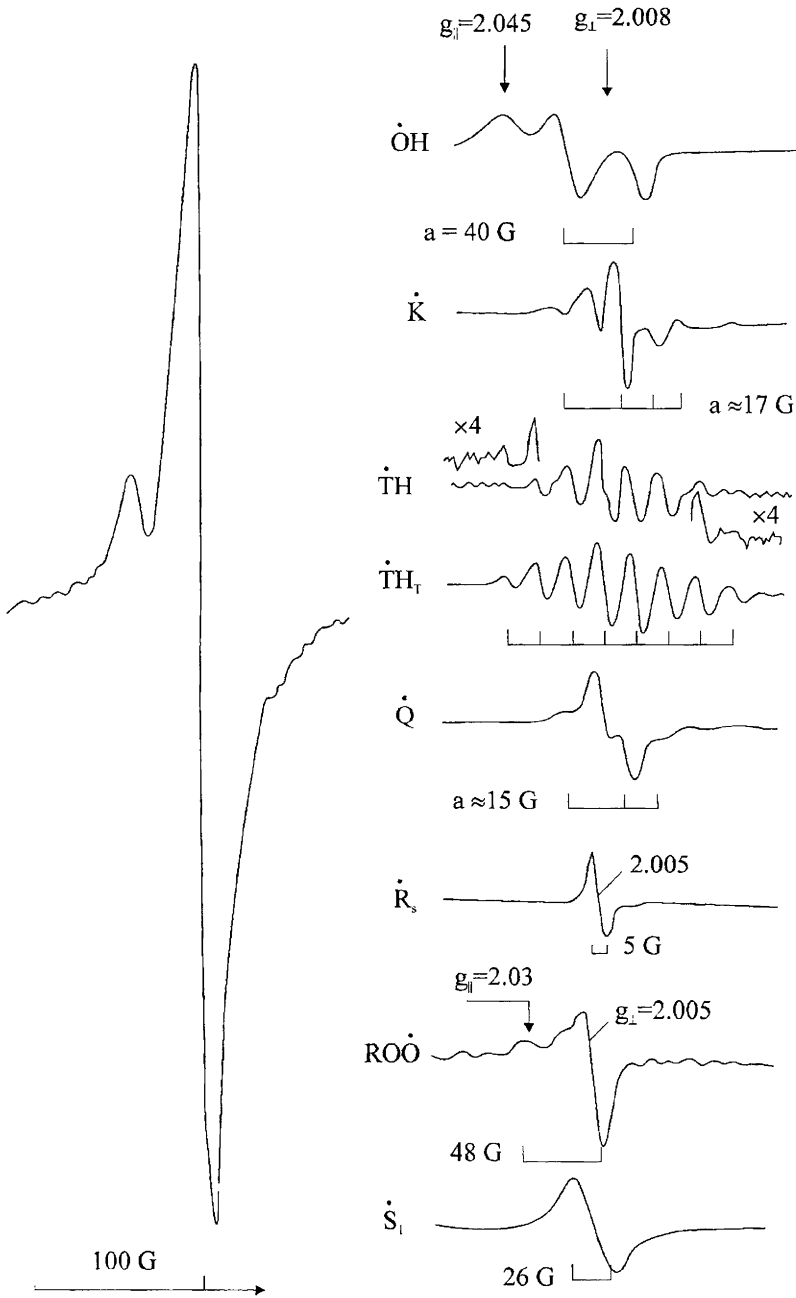


Figure 12.4. ESR spectra of γ -irradiated thymus sample in mice [3]

The analysis of ESR spectra allowed for determining some features of radical formation and conversions at low-temperature irradiation of tissue samples.

1. Frozen tissues represent heterogeneous systems. At 77 K, $\cdot\text{OH}$ radicals are detected in them. At annealing of irradiated samples these radicals recombine, hence, no changing (no increasing) concentration of other radicals, stabilized under these irradiation conditions. In glassy-like solutions of carbohydrates, for instance, at $\cdot\text{OH}$ radical recombination, sugar radicals were formed (Chapter 8). It may be concluded that in the case of frozen-up tissue, $\cdot\text{OH}$ were formed and stabilized in ice, crystallized as a separate phase at sample freezing up in the liquefied nitrogen.
2. In the tissue samples radicals of the main cell structures are registered: DNA, proteins, membranes (Table 12.3 [3]). If prior to irradiation the tissue samples were evacuated, then under annealing conditions in the temperature range of 160 – 180 K TH^\bullet type (the “thymine” structure) radicals were formed. Their parameters were shown before in the discussion of the data on low-temperature irradiation of frozen-up aqueous solutions of DNA and DNP (Chapters 10 and 11). The yield of TH^\bullet radicals depends on DNA content in the tissue, which is the reason for its radiosensitivity [4]. The change in the yield of TH^\bullet type radicals with respect to the type of irradiated tissue may be explained by DNA accessibility degree in the DNP composition for electron attack (in the absence of molecular oxygen), as well as the degree of DNA structure defectiveness.
3. If the tissue is irradiated in the liquefied nitrogen in the presence of molecular oxygen, under annealing conditions a formation of peroxide radicals is observed so frequently, the higher oxygen content in the tissue is. In this case, TH^\bullet type radicals may not be registered. ESR spectrum characteristics indicate that in the presence of oxygen in the tissues at the thymine base in DNA two types of peroxide radicals are formed [5]: TO_2^- and THO_2^\bullet .

Generally speaking, ESR measurements, carried out on frozen-up tissues, reflect the result of the so-called combined impact of γ -quanta and low temperature rather than radiolysis processes. The results of quantitative

measurements depend on the sample freezing mode, e.g. on the fact to higher or lower extent ice crystals, “dry” components of the cell and solid solution are extracted as a separate phase (refer to Section 4.2). The freezing mode also defines molecular oxygen content in each homogeneous part of the irradiated heterogeneous system. If we take into account the various microzones of frozen-up tissue are differently humidified, it is no wonder that as transiting from sample to sample the relative yield of radicals from biopolymer components of the cell and water ($\cdot\text{OH}$ and $\bar{\nu}_{\text{st}}$) changes.

Nevertheless, the data on the conversion mechanisms for free radicals, stabilized in tissues at low temperature, are rather urgent, because they allow for understanding the main directions of the radiation degradation of “isolated” chemical components of the cell, which are biopolymer. If a possibility of intermolecular interaction between these structures is taken into account, the mechanisms mentioned may be applied to the real cell.

12.5. ON THE ORIGIN OF FREE RADICALS IN IRRADIATED PLANT TISSUES

At low-temperature irradiation of evacuated samples (wood, straw, potato jacket and tubers) ESR spectra interpreted as a product of ESR spectra overlapping for the main components of the plant cell with predominant contribution of ESR spectra from irradiated cellulose radicals (doublet and triplet HFS, Chapter 8), are registered. In wood samples, irradiated at room temperature, beside cellulose radicals (65%), radicals with unpaired electron localized at the aromatic fragment in lignin (a singlet with $\Delta H = 0.83$ mT, $g = 2.0039$ [6]). In the irradiated potato jacket radicals possessing a singlet band with approximately the same characteristics are registered [7].

The accumulation of radicals in potato jacket and cellulose, irradiated at 77 K (Whatman type paper, 3% humidity) follows the dependence

$$C = C_{\infty}(1 - e^{-kD}) \text{ (refer to Chapter 1)}$$

with approximately the same parameter $k = 0.34$ Mrad⁻¹ [7]. Therefore, it may be concluded that the “phase composition” of these systems, in which radicals are stabilized at 77 K, is equal.

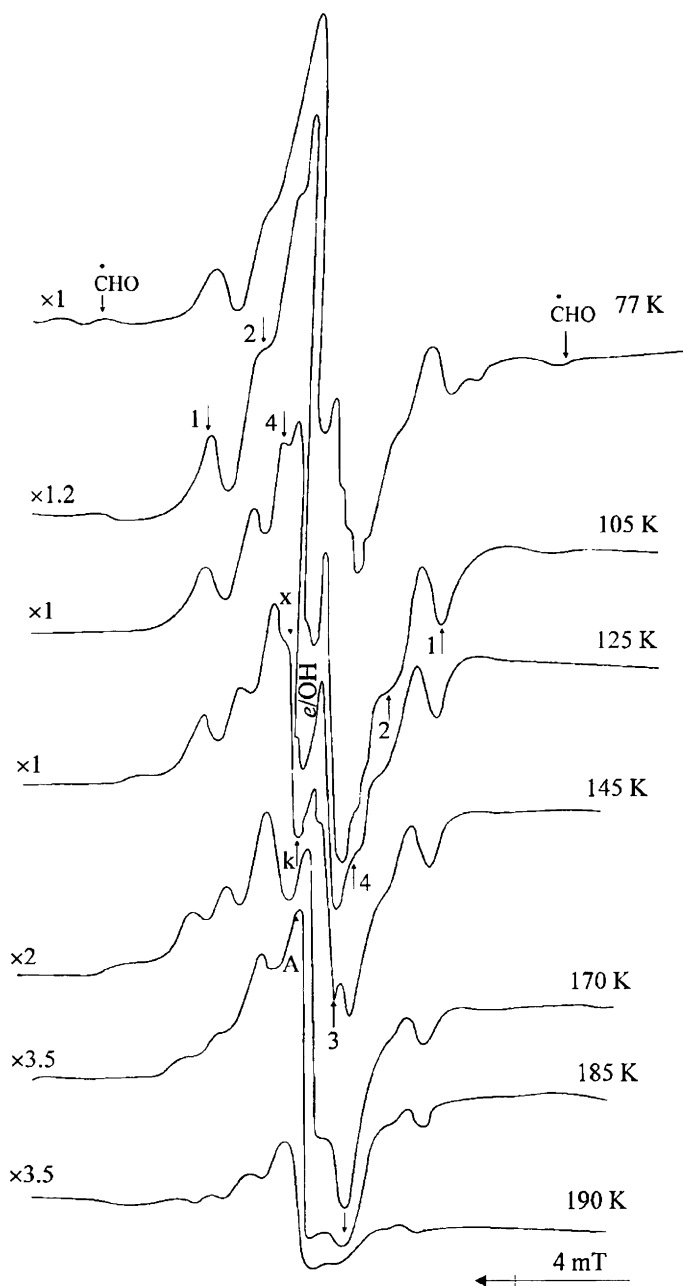


Figure 12.5. ESR spectra for irradiated potato (refer to the text)

Table 12.3

Radicals in potato, irradiated at 77 K, recognized by ESR spectra, and their characteristics [7, 8]

Radicals, suggested site of free valence localization	Number of HFS components, a (mT)	ESR band width, ΔH (mT)	g -factor	Temperature range of recording, conversion reaction, notes
$\cdot\text{OH}$	2, 4	10.5	$g_{\parallel} = 2.055$ $g_{\perp} = 2.0096$	77 – 105 K, 20% ΣR , $\cdot\text{OH} + \text{HR} = \text{H}_2\text{O} + \text{R}\cdot$, $2\cdot\text{OH} = \text{H}_2\text{O}_2$
$\dot{\bar{e}}_{\text{st}}$	1	1	2.001	77 – 145 K, 30% ΣR , $\dot{\bar{e}} + \text{R}(\cdot\text{C4}) \xrightarrow{+\text{H}^+} \text{RH}$ (epimers is galactose)
$\text{R}_1 (\cdot\text{C5})$	3; 3 – 3.2	7 – 7.4	2.003	77 – 185 K (low at 190 K), $\text{R}_1 \rightarrow \text{R}_A + \text{H}_2\text{O}$
$\text{R}_2 (\cdot\text{C4}, \cdot\text{C6}, \cdot\text{C2})$	3; 2 – 2.6	4.5 – 4.8	2.003	$-\text{O}\cdot\text{C4}< \rightarrow >\cdot\text{CH} + \text{O}=\text{C}<$ (keto-group)
$\text{R}_3 (\cdot\text{C3}, \cdot\text{C1})$	2; 2	2.2	2.003	77 – 170 K, $\cdot\text{C3} \rightarrow \text{R}_A + \text{H}_2\text{O}$ (β -elimination of water); $\cdot\text{C1} \rightarrow \text{R}_A + \text{H}_2\text{O}$
$\text{R}_4 (\cdot\text{C1})$	2; 2.5	2.8 – 3.2	2.003	77 – 185 K (low at 190 K), $>\cdot\text{C1}-\text{O}-\text{C4H}< \rightarrow >\text{C}=\text{O}$ (acid) + $\text{CH}<$
$\cdot\text{CHO}$	2; 12	12.5 – 13	2.00	77 – 125 K, 1% ΣR , $\cdot\text{CHO} + \text{HR} = \text{CH}_2\text{O} + \text{R}\cdot$
$\text{R}_{\text{ac}}(\text{R}-\cdot\text{C}=\text{O})$	1	0.4	2.0009	125 – 145 K, $\text{R}-\cdot\text{C}=\text{O} \rightarrow \text{R}\cdot + \text{CO}$
$\text{R}_A[-\cdot\text{COHC}(=\text{O})-, -\text{CHC}(=\text{O})]$	2; 1.2	1.7	2.0067	< 145 – 190 K, $\sim 30\% \Sigma(\text{R}_1, \text{R}_2, \text{R}_3)$, $\text{R}_A \rightarrow$ keto-, deoxyketo-groups

At low-temperature irradiation of potato tubers free radicals typical of the potato component “structures” are formed and stabilized: starch, cellulose, water (ice). Figure 12.5 shows ESR spectra of potato tuber, irradiated by 45 kGy at 77 K, recorded at 77 K immediately after irradiation and after annealing at temperature, indicated at the right of the spectrum. Table 12.3 shows the main types of free radicals, recognized by these spectra, ESR spectrum parameters, observation conditions and possible radical conversion reactions [7, 8].

Three experimental facts should be outlined:

- a) recognition of formyl radical by typical doublet ESR line (with ~12.5 mT splitting);
- b) \bar{e}_{st} accumulation at 77 K with higher yield;
- c) detection of formaldehyde and galactose (glucose epimers by C4, refer to Chapter 8 for the mechanisms of carbohydrate epimers formation) among molecular products after potato tuber defrosting, irradiated at 77 K.

The specific features of the low-temperature radiolysis of potato tuber body are the following:

1. High yield of water radicals – $\cdot\text{OH}$ and \bar{e}_{st} – 50% $\Sigma R\cdot$;
2. Even in the presence of molecular oxygen no peroxide radicals were detected at annealing of potato tuber samples, irradiated at 77 K (contrary to that how it happens at annealing of frozen-up aqueous solutions of polysaccharides, irradiated in the presence of molecular oxygen).

Both these facts and specifically \bar{e} stabilization in irradiated tuber with high yield indicates that polysaccharides present in the tuber bind water (about 80%) so tightly that at the sample freezing it appears in the structured state, and the entire systems is glassy-like. To put it differently, no free water is present in the tuber, which would be able to crystallize with formation of a separate phase, if the sample is placed to the liquefied nitrogen.

Taking into account this fact (the existence of the glassy-like polysaccharide-water system in the tuber) and following the conclusions made in Chapter 8 on the predominant role of the structured water radiolysis in humidified polysaccharides, one may imagine why relatively low irradiation

doses may induce so significant changes of physicochemical and organoleptic properties of potato at its radiation treatment [8].

To conclude the discussion, it should be mentioned that the data on the low-temperature radiolysis of the cells and tissues indicate the radiolysis regularities, similar to simple organic systems. This is no wonder, because primary radiation-chemical processes in these systems with high water content are identical. Hence, one may decide that the solution of such problems as, for example, radioprotection of the cell or sensibilization of degradation processes require the use of approaches similar to the radiation impact on biopolymers.

In this connection, the analysis of test results obtained at the cell level [9] for the final effect of DNA radioprotection (single-stranded break formation was tested) in the presence of various alcohols and SH-containing compounds in a wide concentration range is worthy of the note. As is shown, the irradiation of L 5178 Y cell suspensions in the presence of mercaptoethanol (MET) in a wide concentration range in the cultural medium is generally performed (65 – 67%) by the mechanism of competing for $\cdot\text{OH}$ radicals (the indirect effect of radiation): the yield of DNA breaks gradually decreased with increasing MET concentration in the suspension. Since some intermediate concentration, at its further increase, this yield remained unchanged. Hence, the maximal effect of radioprotection reached 86% [10].

REFERENCES

1. Sharpatyi V.A., Bayen M., Kieffer F., Rode A., and Apacheva L.M., *J. Chim. Phys.*, 1977, vol. 73(3), H. 376.
2. Sharpatyi V.A. and Apacheva L.M., *Izv. AN SSSR, Ser. Biol.*, 1979, No. 3, p. 458. (Rus)
3. Pulatova M.K., Rikhireva G.T., and Kuropteva Z.V., *Electron Spin Resonance in Molecular Radiobiology*, Moscow, Energoatomizdat, 1989, 232 p. (Rus)
4. Zhizhina G.P., Bunina E.F., Skalatskaya S.I., and Sharpatyi V.A., *Doklady AN SSSR*, 1985, vol. 281(6), p. 1466. (Rus)
5. Bunina E.F. and Sharpatyi V.A., *Izv. AN SSSR, Ser. Biol.*, 1988, No. 1, p. 137. (Rus)
6. Filonenko Yu.A., "Free radicals in radiation-chemical and chemical conversions of wood components", *Candidate Dissertation Thesis*, Moscow, IChP RAN, 1993. (Rus)
7. Korotchenko K.A. and Sharpatyi V.A., *Izv. VUZov. Pishchevaya Tekhnologia*, 1987, No. 2, p. 58.
8. Korotchenko K.A., Talanova D.A., and Sharpatyi V.A., *Izv. VUZov. Pishchevaya Tekhnologia*, 1986, No. 4, p. 19.
9. Ryabchenko N.I., *Radiation and DNA*, Moscow, Atomizdat, 1979, 192 p. (Rus)
10. Rainbow A.J. and Howes M., *Int. J. Radiat. Biol.*, 1977, vol. 13(2), p. 191.

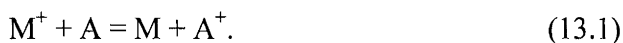
Chapter 13. The effects of radioprotection and sensibilization of radiation degradation of biopolymers in aqueous solutions

13.1. GENERAL PRINCIPLES OF ORGANICS RADIOPROTECTION IN THE CONDENSED PHASE

The radiation degradation of substances, irradiated individually or in solutions, is the result of chemical reactions, induced by formation and conversions of ionized and excited molecules and radicals, derived from them. In this connection, injection of additives – the compounds capable of reacting with the above-listed primary radiolysis products – into the irradiated system must significantly affect the depth and route of radiolytic processes in the irradiated system.

This principle of the radioprotective action of the additives may be illustrated by the examples from M.F. Romantsev monograph on radiation chemistry of organic compounds in non-aqueous solutions [1]. The action mechanisms of such substances-protectors (antirads) are not complicated by the hydration effects and are manifested, so to say, purely.

As a mixture of carbohydrates is irradiated, positive charge is transferred from radiolized substance-donor (M) to the substance-protector (A), the charge acceptor. Hence, a deviation from linearity for the mixture component dependence between radiation-chemical yield of M *degradation* (or, for example, H₂ accumulation) and concentration is observed. For instance, as a mixture of two compounds of the composition shown in Table 13.1 is irradiated, a relation between the radioprotection effect against the charge donor degradation by the charge acceptor and their corresponding ionization potentials (*I*) is observed. In this case, radioprotection proceeds by the positive charge transfer mechanism:



This process is possible under the condition $I_M > I_A$. This mechanism of the positive charge transfer may also explain radioprotection of poly(methyl methacrylate) in the presence of compounds, shown in Table 13.2.

Table 13.1

Ionization potentials for non-aromatic carbohydrates radiolized in the mixture [1]

Donor (M)	I_M , eV	Acceptor (A)	I_A , eV
<i>n</i> -Hexane	10.17	Neohexane	10.04
--	10.17	2,3-Dimethyl butane	10.00
--	10.17	Diisopropyl alcohol	10.15
--	10.17	Diisopropyl ester	9.3
Cyclopentane	10.51	2,3-Dimethyl butane	10.00
2-Methylpentane	10.09	<i>n</i> -Octane	9.99

Table 13.2

The ratio of reaction rate constants k_1/k_2 and ionization potentials for charge acceptors preventing poly(methyl methacrylate) (PMMA) degradation, $I_{PMMA} = 10.5$ eV [1]

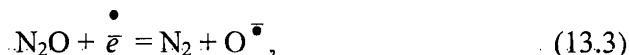
Additive	k_1/k_2 , M ⁻¹	I , eV
Tetramethylphenylene diamine	68.5	6.6
Diphenylamine	56.0	7.25
Paranitroaniline	52	7.7
Stilbene	46	7.95
Tetrachloroquinone	42	—
Naphthalene	30	8.10
Benzophenone	24	9.45
Benzoic acid	10	9.5
Trinitrobenzene	5.5	—

Table 13.2 shows the ratio of the reaction rate constants k_1/k_2 and ionization potentials I for positive charge acceptors preventing M degradation. Clearly k_1/k_2 is higher for a compound with the minimal ionization potential.

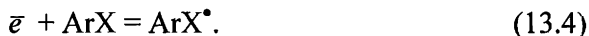
Electron transfer

The example of radioprotection via electron transfer from M to A may be the case of cyclohexane and aromatic additive (ArX) mixture radiolysis in

the presence of N_2O . Hence, the yield of N_2 , formed in the reaction below, decreases:



due to \bar{e} capture by the aromatic additive:



and prevention of the electron recombination with the cation-radical (13.2) with subsequent degradation of M substance.

The analogous mechanism of radioprotective action of the additives is manifested in the case of cyclohexane and aromatics mixture radiolysis. The protective action of A and the electron affinity energy of it (Q_A) correlate well with one another. In the general case, at radiolysis of a mixture of RH and an additive-protector (A) at the following reaction proceeding:



the protection effect is reached under the condition:

$$E_{RH^{\bullet+}} + Q_A > I_{RH^{\bullet+}}.$$

Table 13.3

The change in $G(H_2)$ at n -heptane radiolysis ($I_{RH} = 10.35$ eV) in the presence of aromatic substances with respect to their affinity to electron Q_A , ionization potential, and triplet excitation energy E_T

Compound	Q_A , eV	I , eV	E_T , eV	$\Delta G(H_2) = G_0(H_2) - G_A(H_2)^*$
Naphthacene	–	6.88	1.26	1.26
Anthracene	1.19	7.38	1.86	0.5
Pyrene	0.87	7.50	2.08	0.5
Acetophene	–	–	3.18	0.3
Naphthalene	0.65	8.10	2.62	0.2
Benzene	0.54	9.21	3.66	0.1

Note: * $\Delta G(H_2)$ values show $G(H_2)$ decrease in the presence of the additive in 10^{-4} M concentration.

Hence the highest probability is observed for the radioprotection, implemented under the condition that the substance A possesses the highest affinity energy to the electron (Table 13.3 [1]). The last column of Table 13.3 shows yields of molecular hydrogen decreasing in the presence of a protector (the radioprotection effect). Clearly the highest efficiency is displayed by the substances increased affinity to electron.

Excitation energy transfer

Beside the mentioned effects of radioprotection implemented via the charge transfer from the donor M to the protector A at the mixture irradiation, a possibility of radioprotection due to the excitation energy transfer should be taken into account. It is common knowledge that about 50% absorbed energy of the ionizing radiation is consumed for formation of the excited states of molecules in the irradiated system. In the radiation-chemical processes of biopolymer conversion, the excited states of the molecules and, foremost, molecules in the triplet state (which possess longer lifetimes, up to 10^{-1} s) are of high urgency. Therefore, energy in the system may be redistributed more effectively even at acceptor concentrations within $10^{-5} - 10^{-6}$ M.

There are several mechanisms for excitation energy transfer between the system components, one of which is the exchange-resonance energy transfer. Hence, the triplet state energy levels of the acceptors must be lower than corresponding ones of the donors. For example, this is realized at benzene (M) – naphthalene (A) system irradiation. The data on the hydrogen yield change at heptane radiolysis in the presence of aromatic compounds indicate the highest efficiency of protecting additives possessing the lowest E_T (refer to Table 13.3).

13.2. ON RADIOPROTECTION OF BIOPOLYMERS AT PRIMARY PHYSICAL STAGES OF RADIOLYSIS

In the previous Section we have discussed the most general cases of organics radiolysis and the effects of protectors preventing degradation of the irradiated compounds at the primary stages of radiolysis, which precede formation of the radicals. It is unambiguous that the mechanisms of

radioprotection under consideration may also be implemented in the case of aqueous solutions of biopolymers. However, their tracking is much complicated by the solvent polarity and hydration effects of both initial substances and intermediate radiolysis products.

Radiation chemistry of biopolymers is determined by the presence of peptide bonds and aromatic rings in amino acid residues (proteins) and nitrogen bases (DNA, DNP). The molecules containing the above-listed groups of atoms possess lower ionization potentials and excitation energies. At the same time, organic compounds used as radioprotectors in applied radiobiology include heteroatoms, such as sulfur and selenium, into the above-mentioned groups of atoms. All these components included in the molecules promote a decrease of ionization potentials and excitation energies of the molecules by 3 – 5 eV compared with the molecules having saturated bonds and containing no heteroatoms.

Taking into account that the radioprotectors are mostly effective as injected to the animal organism prior to irradiation, it should be noted that the competing mechanism between the protector and biopolymers forming basic structures of the cell, charges and excitation, are of high importance for radioprotection of the cell. The specific feature of radiation-chemical properties of biopolymer such as DNA is the presence of a regulated structure of nitrogen bases, united into the complementary pairs and forming “stacks”. The mentioned structure of the biopolymer makes possible migration of charges and excitation by the macromolecule.

Some ideas about a possibility of the charge migration by the system of nitrogen bases in DNA may be obtained from the analysis of ionization potentials of DNA nitrogen bases and their analogues, shown in Table 13.4. Adiabatic I was determined using a spectroscopic technique – by the Rydberg series limit of the banded spectra of molecules. The limit corresponds to a transition between zero oscillation levels of the main energy states of a molecule and an ion. Vertical I was determined by an electron impact method.

This value is higher than I (adiabatic) by the energy of oscillation excitation of the ion (the vertical ionization potential was called so due to observance of the Frank-Condon principle). Here the absolute values of these parameters are not so urgent as the descending sequence of I_{ion} , because we consider a possibility of the charge migration not only in the biopolymer crystal, but also in the solution. Data from the Table allow us for an assumption of the route for possible charge migration, occurring, to say, at the biopolymer irradiation towards decreasing potential of nitrogen base ionization. For

example, in the crystalline DNA and, apparently, in solutions the positive charge (i.e. unpaired electron of the cation-radical) must migrate from thymine to cytosine or adenine and localize on the guanine base. Moreover, if we consider the effect of DNA protection by positive charge migration mechanism, the radioprotector must have the following ionization potential: $I_{\text{ion,adiab.}} < 7.77 \text{ eV} \times I(\text{adiab.})$ or $I_{\text{ion,vert.}} < 8.24 \text{ eV} \times I(\text{vert.})$ or lower for aqueous solutions considering correction for hydration effects of molecules and ions, respectively.

Table 13.4

Ionization potentials of nitrogen bases of nucleic acids and their analogues [2]

Compound	I (adiabatic), eV	I (vertical), eV
Uracyl	9.32	9.00
Thymine	8.87	9.11
Cytosine	8.68	8.94
6-Methylcytosine	8.38	—
Isocytosine	8.44	—
5,6-Dihydrothymine	9.68	—
Imidazole	8.67	—
Purine	0.12	0.52
Adenine	8.26	8.44
7-Methyladenine	8.18	—
9-Methyladenine	8.04	—
Xanthine	8.55	8.89
Caffeine	7.94	—
Hypoxanthine	8.44	8.89
7-Methylipoxanthine	8.42	—
Guanine	7.77	8.24

As studying the initiated luminescence in DNA and DNP using photolytic methods, migration of the excitation energy by these structures was detected. These biopolymers possess various fragments in their composition absorbing light in the wavelength range from 200 to 350 nm. The light emission bands in these polymers are correspondingly shifted to the long-wave region, from 350 to 500 nm, approximately. The data from the literature allowed for a conclusion that in the case of mixture of the compounds

including nitrogen bases, the energy migration by triplet excited state levels of the bases in the DNA molecule is possible. In DNA molecules with undamaged structure the luminescence sites are thymine bases. According to radiothermoluminescence data, the luminescence sites in irradiated polycrystalline DNA and DNP preparations are thymine and adenine nitrogen bases. Note also that for estimating the energy migration routes of both singlet and triplet excitation types by these biomacromolecules, a dependence of luminescence characteristics on their structure, the solvent origin, and medium pH should be taken into account.

Thus, radioprotectors injected to the irradiated system as the excitation energy acceptors must have lower triplet excitation energy levels compared with protein molecules (determined by carbonyl groups of peptide bonds, aromatic and sulfur-containing and amino acid residues) and DNA (thymine and adenine).

13.3. THE EFFECTS OF RADIOPROTECTION AND RADIO-SENSIBILIZATION OF BIOPOLYMER DEGRADATION AT THE STAGES OF RADICAL FORMATION AND CONVERSION

The questions of biopolymer radioprotection by free-radical mechanisms were partly discussed in the previous Chapters at consideration of the results of radiolytic studies of proteins, polysaccharides, DNA and their natural complexes. Concluding consideration of the ideas about radioprotection of biopolymers in aqueous solutions, let us indicate realization of two basic mechanisms in these systems: the competition mechanism of radioprotectors for water radicals and the action mechanism of free-radical reaction inhibitors.

The realization of the competition mechanism for water radicals between the radioprotector and biopolymer depends on the observation of preferable proceeding of water radical reactions with the radioprotector (RP). For example, in the case of $\cdot\text{OH}$ radicals the following inequality was observed:

$$k_{\text{OH}+\text{RP}} \times [\cdot\text{OH}] \times [\text{RP}] \gg k_{\text{OH}+\text{BP}} \times [\cdot\text{OH}] \times [\text{biopolymer}],$$

where $k_{\text{OH}+\text{RP}}$ is the rate constant of $\cdot\text{OH}$ radical reaction with radioprotector. Similarly, the biopolymer should be protected from the effect of reductive

water radiolysis component. Hence, if molecular oxygen is present in the irradiated system, it captures electron and promotes O_2^- formation, and a radioprotector injected must react with O_2^- in order to prevent its interaction with the biopolymer.

Clearly all these conditions for radical reactions with dissolved substances may be realized in rather diluted solutions. The data shown in Tables 5.1 and 5.2 on the rate constants of water radiolysis product reactions with the components of biopolymers and radioprotectors allow for the estimation of possible radioprotection at irradiation of one system or another.

An additional condition for implementation of the protective mechanism of the additives is the following. Generally, the radicals formed from additives in the primary chemical acts or the products of their radiolysis must not react with dissolved biopolymers, i.e. the additive radicals or products of deeper radiolytic conversion of the additives must not be inert in relation to biopolymer molecules. Hence, if the radicals of dissolved additives or radiolysis products of these substances react with the biopolymer and, therefore, accelerate biopolymer degradation in the solution, such additives belong to radiosensibilizers.

Post-irradiation processes

Despite the presence of a radioprotective additive in the biopolymer solution, one is unable to fully protect biopolymer molecules against the water radical attacks according to the indirect radiation mechanism and, the more so, against the biopolymer radical formation by the direct effect of irradiation. Moreover, in the majority of real cases, the biopolymer solution irradiation is performed in air, i.e. in the presence of molecular oxygen. In this case, the macroradicals formed are involved in the reactions with molecular oxygen forming peroxide radicals. In the case of proteins, DNA, Polysaccharides and DNP unstable peroxide compounds are formed. Their degradation is the reason the observed degradation of biopolymers after the end of solution irradiation, i.e. the reason for so-called post-irradiation processes.

The biopolymer degradation in the post-irradiation processes may give high yields comparable with these of radiolytic processes (for example, in the case of DNA; Chapter 10). As shown for the majority of cases of biopolymer

Table 13.5

The yield of radiolysis products* (arbitrary units) of thymidine (de-T) at the irradiation of frozen-up aqueous solutions at 77 and 195 K under different irradiation conditions [3]

Concentration and irradiation conditions	de-TH ₂	de-T (OH) ₂	de-TT	T	TH ₂	G(-chr. gr.)	G(MA)×10 ³
0.0001 M, 0.1 MGy, vacuum, 77 K	0.3	0.4	0.4	0.4	–	–	–
0.0001 M + 0.5 M CH ₃ OH, vacuum, 77 K	2.1	0	0.9	0.5	0	–	–
0.0001 M, 0.56 MGy, 195 K	6.9	0.6	4.8	0.8	–	0.002	0.004**
0.0001 M + 0.5 M N ₂ O, vacuum, 195 K	0	3.0	1.8	3.9	0	0.002	0.012**
0.01 M, 0.56 MGy, 195 K	1.6	0.7	0.7	0.7	0.2	0.15	9
0.01 M + 0.01 M cysteine, 0.56 MGy, vacuum, 195 K	2.0	0.4	0.3	0.4	0.2	0.17	5
0.01 M, 0.56 MGy, air, 195 K	1.6	0.6	1.6	0.7	0.2	0.17	9
0.01 M + 0.01 M cysteine, 0.56 MGy, air, 195 K	2.0	0.6	0.6	0.4	0.2	0.17	6

Notes: * Designation: de-TH₂ – dihydrothymidine; de-T(OH)₂ – dihydroxy-dihydro-(5,6)-thymidine dimer; In TT, thymidine T dimer is innine; TH₃ is dihydrothymine; G(-chr. gr.) is the yield of chromophore group degradation (42 kGy); G(MA) is the yield of malonic aldehyde (42 kGy).

** G was determined at high doses (> 350 kGy).

radiolysis, the degradation of their hydroperoxides proceeds by the free-radical mechanisms. Therefore, proceeding of the post-radical reactions may be prevented by adding free-radical reaction inhibitors to the irradiated solution (Chapter 6, Figures 6.3, 6.6).

Free-radical reaction inhibitors are injected before irradiation, in concentrations not very high in order to avoid radiolytic reactions, but enough for proceeding of the following reactions:



The analysis of the investigation results on radiolytic properties of DNA indicates that in DNA macroradical reactions with InH of (13.6) type the initial compound may be synthesized exclusively, when free valence in this radical is localized at 2-deoxyribose unit. Hence if the free valence in newly formed macroradical is localized at nitrogen bases, the reaction between this radical and the inhibitor does not reduce the initial structure of the molecule. Subsequently, modified nitrogen bases with saturated bonds are formed. The repair of initially damaged biopolymer molecule is suppressed. In such modified DNA molecule, C'1-N bond is hydrolyzed, and after modified nitrogen base detachment 2-deoxyribose unit is hydrolytically degraded, which is accompanied by a polymeric sugar-phosphate chain break.

Table 13.6

The yield of chromophore group degradation and malonic aldehyde analogue accumulation at irradiation of frozen-up DNA and DNP aqueous solutions [3]

DNP composition, concentration and irradiation conditions	$G(-chr. gr.),$ $\pm 20\%$	$G(MA),$ $\pm 10\%$
0.34% DNA, 0.14 MGy, Ar, 77 K >> + CH ₃ OH (0.5 M)	0.035	0.0006
	0.1	0.0002
0.25% DNA, 0.05 MGy, Ar, 195 K >> + cysteine (0.01 M) >> + nitrous oxide (0.05 M)	0.2	0.002
	0.25	0.0002
	0.3	0.003
DNP (1:1), 0.36%, 0.16 MGy, Ar, 77 K >> + CH ₃ OH (0.5 M)	0.013	0.0007
	0.1	0.0001
DNP (1:1.7), 0.55%, Ar, 0.05 MGy, 195 K >> + cysteine (0.01 M) >> + nitrous oxide (0.05 M)	0.1	0.001
	0.4	0.0003
	0.1	0.003

Tables 13.5 and 13.6 show the results of the yield measurements for various radiolytic processes at irradiation of frozen-up aqueous solutions of thymidine, DNA and DNP under the conditions allowing for registering the primary stages of radical formation and conversions. These processes are induced by participation of a single electron (irradiation at 77 K) and an electron and $\cdot\text{OH}$ radical (irradiation at 195 K) in the reactions. As indicated by the above data, the presence of various additives in these systems: electron acceptors (nitrous oxide, molecular oxygen) and $\cdot\text{OH}$ radical acceptor (methanol), affects the yield of radiolysis products.

The yields decrease, if this product is formed at the participation of water radical, captured by the competing additive acceptor, in the reaction. For example, in the case of DNA and DNP radiolysis, the formation of a compound – malonic aldehyde analogue – is suppressed in the presence of $\cdot\text{OH}$ radical acceptor, methanol (Table 13.5). On the contrary, in the presence of nitrous oxide, due to $\cdot\text{OH}$ radical involvement in the reactions, the yields of free thymine (due to 2-deoxyribose fragment degradation), the products of thymidine hydroxylation (Table 13.5), and malonic aldehyde in DNP (Table 13.6) increase.

The presence of cysteine in the solution irradiated at 77 K does not affect the yields of chromophore group degradation in the irradiated systems and radiolysis products, stipulated by participation of electron (dihydrothymidine) in reactions with nitrogen bases in solutions unsaturated with oxygen. Vice versa, the yield of sugar fragment degradation in the presence of cysteine decreases (MA, inorganic phosphate in DNA and DNP solutions; the yields of thymidine dihydroxy-derivatives and free thymine). In the presence of molecular oxygen, cysteine affects the yield of free thymine (Table 13.5). The effects mentioned can be easily explained by cysteine manifestation of free-radical inhibitor processes in these systems, i.e. the protector properties at the stages of radical conversions by the reactions (13.6) – (13.8):



Therefore, no wonder that chromophore groups degrade as a result of both thymine C=C double bond attack with subsequent reaction of $\cdot\text{H}$ -adduct formed with cysteine and $\cdot\text{OH}$ radical attack on thymine base double bond with

subsequent reaction between $\cdot\text{OH}$ -adducts and cysteine. In the presence of oxygen, chromophore groups also degrade (Chapter 11). In this case, cysteine reacts with either $\cdot\text{H}$ - and $\cdot\text{OH}$ -adducts or peroxide radicals.

Thus, the inhibitors reduce the initial structure of the primary DNA molecule via participating in (13.6) type reactions exclusively with macroradicals having an unpaired electron localized at the sugar fragment. Analogous processes proceed at radiolysis of polysaccharides and proteins (with $\text{R}\alpha^\bullet$ type radicals, in particular, see Chapter 7). This process of biomacromolecule primary structure reduction may only be characterized as the repair process (the process of non-enzymatic repair). The reaction (13.6) between DNA macroradicals, in which unpaired electron is localized at nitrogen bases, with macroradical $\cdot\text{H}$ - or $\cdot\text{OH}$ -adducts do not reduce the initial structure of these damaged fragments of macromolecules, whence modified nitrogen bases – the products with saturated bonds – are formed. In this case, as well as in the processes (13.7) and (13.8), the radioprotection effect is implemented via DNA macroradical elimination (low-active inhibitor radicals are formed instead), and their reactions inducing the polymer degradation are prevented.

To implement radioprotection by the mechanism of free-radical reaction inhibitors in the case of biopolymer irradiation, it is necessary that reactions (13.6) – (13.8) produce In^\bullet inhibitor radicals inert to the primary polymer. These reactions and protector types are studied quite well. Among them natural (glutathione, cysteine) and synthetic (cysteamine) compounds containing sulfhydryl groups and spatially hindered phenols should be mentioned. Some of them are widely used as radioprotectors in radiobiology and medicine.

Table 13.7 shows reaction rate constants for radicals formed from a protein – human serum albumin (HSA) – with some compounds, which protector properties have been studied in radiobiological tests on animals. Obviously, cysteamine possesses the highest reactivity. However, radioprotection at the animal level may not be reduced to the only manifestation of the inhibition mechanism by (13.6) – (13.8) reactions.

Note that RP application for the purpose of DNA protection by the competition mechanisms for water radicals and FRR inhibition does not mean the necessity of accumulating extra-high RP concentrations in the cell (as it is usual for *in vitro* tests, when DNA concentration is exceeded by orders of magnitude), in order to suppress unwilling processes. It is emphasized [6 – 9] that the effect of DNA radioprotection may also be obtained in the case, when

RP is already localized at the potential damage site. Such sites in the macromolecule are H–C bonds in 2-deoxyribosyl and double bonds in nitrogen bases of the polymer, subject to $\cdot\text{OH}$ radical attack (Chapter 10). Hence, radioprotection by the competition mechanism for water radicals is realized [10], and if a radical site is formed in DNA, RP molecule linked to the DNA backbone may act as the FRR inhibitor. It is common knowledge that the application of chitosan as the radioprotector is the most effective, if it is injected to the organism prior to irradiation impact [11].

Table 13.7

Reaction rate constants for protein radicals and some radioprotectors [5]

Compound	Rate constant, $\text{M}^{-1}\text{s}^{-1}$
Cysteamine	4.6
Thiourea	2.9
Cysteine	2.6
AET	1.7
APT	1.6
Glutathione	1.3
4-Oxy-3,5-di- <i>tert</i> -butylphenylamine	0.6
Sodium sulfite	0.6
Sodium thiosulfate	0.6
Mercamine disulfite	0.4
2-Propyl-6-methyl-3-oxopyperidine	0.3
Aniline	0.2
Ascorbic acid	0.1
5-Methoxytyramine	0.0
Glucose	0.0

For example, such situation may be realized in the case of using diamines containing sulfhydryl groups as radioprotectors: RP links to the DNA backbone by its amino groups, whereas sulfhydryl groups implement their antiradical activity [6]. The essence of the radioprotection effect is not in capturing water radicals by sulfhydryl groups, but also stabilization of double-stranded DNA helix due to additional chemical (or hydrogen) bond formation between RP and biopolymer functional groups prior to irradiation. Such compounds play the role of something like “clips” of the double-stranded structure of the polymer [6 – 8]. Double-stranded DNA helix degradation is

related to the occurrence of primary 2-deoxyribosyl macroradicals (Chapter 10). The multistage process of primary macroradical conversions in carbohydrates (polysaccharides, Chapter 8) up to formation of final molecular products proceeds in the time range of $10^{-9} - 10^{-7}$ s. For DNA, it is suggested that 2-deoxyribosyl radical conversions fit the same time range. Finally, at the moment of enzymatic repair systems functioning initiation in the cell (the characteristic time of radiation damage repair by cells takes from several minutes to several hours [12]), all molecular products of radiolysis are synthesized, breaks in the sugar-phosphate backbone are formed and the role of the protectors (clips) is obvious: they are to fix the polymer structure at least during the time mentioned.

The substances-clips are, for example, cystamine, cadaverine and putrescine [7], cysteine and glutathione – aliphatic diamines. All these substances are able to stabilize DNA structure by forming chemical bonds between positively charged (protonated) amino groups and negatively charged phosphate residues in the polymer nucleotides, similar to that proceeding in nucleosome between DNA phosphate groups and lysine and glutamine residues of histone proteins [13] or at DNA-polylysine complex formation [14]. As mentioned above, locating near DNA, sulfhydryl groups in such substances-clips manifest their radical activity via reactions with water $\cdot\text{OH}$ radicals and macroradicals.

For chitosan (effective at injection into the organism before the irradiation) at the study of liquid-crystal dispersion formation from the DNA-chitosan complex in the polyethylene glycol containing solutions, it has been shown that the ligand amino groups separated by 5.15 Å gap, are next but one fixed to negatively charged phosphate residues [15, 16]. Five amino sugar chitosan residues ($MM = 1,000$) cover the area of 20 Å (occupying about 2.8 pairs of bases) of DNA.

As suggested, cystamine, cysteine and glutathione are also fixed to DNA phosphates by their amino and imino groups (more precisely, to oxygen atoms carrying negative charge) and, therefore, fix the double-stranded helix. The rest functional groups of these compounds capture water radicals and are able to react as InH. As follows from the data in Chapter 9, in the case of chitosan, glucosamine residues serve as $\cdot\text{OH}$ radical (the attack sites are H–C bonds in oxymethylene units) and \bar{e}_{hydr} (the attack sites are amino groups) acceptors. If 2-deoxyribosyl radicals are also formed in the presence of molecular oxygen (peroxide and hydroperoxide from both the sugar fragment and the bases), then the effectiveness of the reactions (13.7) and (13.8)

proceeding (hydroperoxides dissociate into RO^\bullet and $^\bullet\text{OH}$) is provided by the structural factor: the reagents are formed nearby one other.

In the case of compounds with disulfide bonds (cystamine, cysteine), two alternatives of radioprotective action of these compounds is possible: \bar{e}_{hydr} capture by disulfide bond (the competing mechanism with DNA for electron) and unpaired electron transfer from the primary DNA macroradical (the initial damage) to disulfide bond of a ligand. In both cases, as capturing electron disulfide bond breaks with sulfhydryl group and a radical with unpaired electron at sulfur atom (thyl radical) formation. This process was also detected in the case of radiation degradation of disulfide bond saturated protein – wool keratin – using the ESR method (Chapter 7). Further on, the thyl radical is able to react with C5=C6 double bonds in pyrimidines and by C8 in purines with protector–DNA covalent bond (crosslink) formation [9]. The duration of thyl radical interaction with the double bond of pyrimidine is comparable with the mentioned times of 2-deoxyribosyl radicals. The quantity of DNA–protector crosslinks increases with the irradiation dose, and the effectiveness of the polymer radioprotection also increases [9].

Basing on general ideas, it may be suggested that provision of the DNA double-stranded helix preservation may be related to formation of a clip along the sugar-phosphate chain (within one strand of the polymer) or across it – between two strands. Testing of hypothesis on implementation of InH properties by the clipping substance (one of its functional groups) via modeling attachment of protectors' amino groups to phosphate groups and possible interaction between 2-deoxyribosyl radicals and disulfide and sulfhydryl groups of the clipping substances is positive: both processes are possible – macroradical oxidation in DNA and H atom transfer from InH (cysteamine) to macroradical [17].

DNA-ligand “clips” may also occur due to hydrogen bond formation between amino, imino, sulfhydryl, hydroxyl or oxo-groups of the ligand-protector and appropriate functional groups of nitrogen bases or oxygen O4 in 2-deoxyribosyl. Therefore, a delightful prospect occurs: selecting compounds, both natural and synthetic, distribute functional groups – radical acceptors in different microareas of DNA “surface” before irradiation for the purpose of future controlling the conversions of 2-deoxyribosyl radicals.

Taking into account all the above-said about the mechanisms of radiolytic conversion of substances in aqueous solutions with participation of radicals and the effect of additives on these processes, let us consider total action of radioprotectors on the example of a molecular model rather similar to

the native system – the radiolysis of DNP aqueous solution in the presence of molecular oxygen (the model developed in 1976 by D.M. Spitkovsky *et al.*) [18]. Aqueous solutions of 0.03% DNP and a radioprotector with the concentration from 0.002 to 0.01 M with respect to their solubility were irradiated. The protectors under study (sulfur-containing – MPA, AET, MEL; tryptamines; nitriles; gallates) have the functional groups promoting the increased reactivity of these compounds in relation to water radicals: aromatic rings, C=C, C=N etc. double bonds. Moreover, the compounds with sulfhydryl groups may serve as FRR inhibitors. Therefore, under current irradiation conditions the processes of formation and conversion of radicals discussed and participation of protectors in these reactions are possible. Studied in the work were characteristics of the radioprotective action of various substances, widely applied by biochemists and radiobiologists. Registered in the tests was the so-called critical dose, as absorbing which DNP loses the ability to form fibers in the presence of a protector and in the absence of it in the irradiated solution. For all substances, the values of the so-called dose increasing factor (*DIF*, representing the ratio of critical doses in the presence of the protector and without it) were determined. As indicated, the highest efficiency is possessed by gallates (*DIF* = 14 – 40) and compounds with sulfhydryl groups (*DIF* = 21 – 30).

The data obtained for this model system correlate with the ideas on realization of to mechanisms of radioprotective action of radioprotectors injected into the solution, which are the radical acceptors: the competition mechanism for primary radicals and solvent radicals and the inhibition mechanism for macroradical conversions.

Thus, the highest protection of biopolymer molecules at radiolysis of its aqueous solutions should be implemented by a set of additives having properties of radical acceptors and free-radical reaction inhibitors. Hence, it is implied that the main process of biopolymer radiation degradation proceeds by the free radical mechanism. Beside the above-considered radioprotective action of the radioprotectors mentioned, a possibility of their protective action observed at additional structuring of the biopolymer (currently, chromatin DNP) due to formation of original “clips”, the additional bonds holding the entire DNP structure with no regard to formation of single- and double-stranded breaks in the DNA fragment.

On the mechanism of radiosensibilization of the substance degradation in solutions

Turning back to the primary stages of the radiation degradation of biopolymers in solutions, let us dwell on the mechanism of conjugated (according to M.A. Proskurin [19]) radical acceptors. The statements of this concept were discussed in Chapter 5. Here, let us just emphasize that the presence of various functional groups in the molecules of natural polymers, which may be acceptors of both reductive and oxidative components of the water radiolysis, creates conditions for additional injection of $\cdot\text{OH}$ and $\cdot\text{H}$ radicals or $\bar{e} \text{H}_2\text{O}^+$ into the reactions, usually recombining in diluted solutions. Hence, total quantity of radicals involved into the reaction equals two-fold higher number of pairs of these radicals or radiolyzed water molecules, i.e. four pairs in diluted solutions or eight pairs in concentrated solutions. Apparently, only in the case of polysaccharides not all radiolyzed water molecules are involved into the reactions, because as observed from the data on reactivity, the main reagents in relation to carbohydrates are only oxidative $\cdot\text{OH}$ radicals (see Table 5.1). Electron manifests low activity in relation to cyclic-shaped carbohydrates. Therefore, if polysaccharide radiation degradation processes should be stimulated or initial polymers should be modified, different additives – the electron acceptors forming radicals in reactions with the electron, reacting similar to $\cdot\text{OH}$ radicals or OH-groups. This compound is nitrous oxide: as interacting with the electron its molecule dissociates with formation of $\cdot\text{OH}$ and nitrogen inert to substances. Radicals $\cdot\text{OH}$ react with the molecules of the initial irradiated compounds, due to which the yield of radiolytic conversion of the latter increases (by two times). Similarly, the radiolysis of polysaccharides in the presence of molecular oxygen may be presented. As capturing electron O_2 forms $\text{O}_2^{\bar{e}}$ radicals able to react with other polymer radicals formed at $\cdot\text{OH}$ radical attack on the macromolecules. As a result, hydroperoxides occur then dissociating to radicals, which is accompanied by increasing yield of polysaccharide degradation.

Another example of the sensibilizing action of the additives at radiolysis is presented by the application of nitrate-ion, the effective electron acceptor. Radical formed in the reaction with nitrate-ions may also react with dissolved biopolymer; hence, the radiosensibilization effect should be expected.

Moreover, the examples of sensitizing action on radiolytic degradation of biopolymers in primary stages of radiolysis may be presented by the data on DNA and DNP degradation, as well as their basic fragment – the nucleotide – under low-temperature irradiation conditions (Tables 13.5 and 13.6). Thus, as comparing the yields of thymidine radiolysis products induced by electron participation (dihydrothymine, Table 13.5), the yield of chromophore group degradation products in DNA and DNP (Table 13.6) at the attack of electrons (because at the irradiation in liquefied nitrogen only electrons are mobile), a sharp (three – seven-fold) increase of these values in the radical $\bullet\text{OH}$ acceptor – methanol – is observed. Similarly, in the presence of nitrous oxide the yield of thymine radiolysis products, initiated by the oxidative component participating in the reaction with it, increases. In this case, the yield of dihydroxythymidine increases by five times rather than twice as required specifically for the reaction of \bar{e} “conversion” to $\bullet\text{OH}$ (reaction (13.3)). The same happens in the case of electron capture by cysteamine at DNA and cysteamine solution irradiation at 77 K. In this case, the yield of $\bullet\text{OH}$ radicals two-fold increases (Table 13.8).

Table 13.8

Concentration of radicals (10^{18} radical/g) and its variation in DNA and cysteamine (CAM) aqueous solutions, irradiated at 77 K, at annealing (in brackets $\bullet\text{OH}$ radical concentrations are shown)

T, K	Annealing time, min	[R \bullet] in DNA and CAM solutions	[R \bullet] in CAM solutions	[R \bullet] in DNA solutions
77	–	1.80 (1.3)	0.84 (0.8)	1.33 (1)
115	4	0.51	0.26	–
153	8	0.31	0.15	0.17
173	8	–	0.21	–
193	8 – 10	0.21	0.16	0.21
193	30	0.25	–	0.14

In the three systems under discussion, in the presence of low concentrations of the radical conjugated acceptors additional pairs of radicals $\text{H}_2\text{O} + \bar{e}$ or $\bullet\text{OH} + \bar{e}$, usually recombining at radiolysis of one of dissolved substances, are involved into the reactions.

The effect of sensibilization

The effect of sensibilization of radiolytic degradation of compounds (radiosensibilization) is reached at injection of additives into their solutions. In this case, one of two mechanisms of such additives manifests itself:

1. As injected into the solution of any compound, the substance “transforms” inactive component of water radiolysis in relation to that compound to the active one manifesting the same action, as “non-transformable” active component of radiolysis does (for example, in the case of \bar{e}_{hydr} inactive in relation to carbohydrates in the presence of nitrous oxide). Hence, in the limit (at the step on the concentration curve) the yield of dissolved compound degradation products must increase at least two-fold.
2. Sensibilizing action of additives relates to the effect of conjugated action of the radical acceptors (by M.A. Proskurin). As reacting with one of the components of water radiolysis primary product pair (ionized H_2O^+ , H_2O^\cdot or \bar{e} and excited $^\cdot\text{OH}$ and $^\cdot\text{H}$), the additive removes it from recombination process with a particle-companion and the “opposite” conjugated component of water radiolysis is involved in the reaction with the main dissolved compound.

The first mechanism of radiosensibilization is realized at radiolysis of 0.01 M carbohydrate solutions saturated with nitrous oxide. Carbohydrates degrade under the influence of $^\cdot\text{OH}$. The yield of their degradation products in the presence of N_2O is about to-fold higher. For another example the process of DNA inactivation in solutions with concentration from 10^{-4} to 0.1 mol% may be accepted. In N_2O saturated solutions, the yield of DNA inactivation increases twice compared with the solution saturated with an inert gas ($G_{\text{inactivation}} = 1.9 \times 2 = 3.8$).

The second mechanism of radiosensibilization is purely demonstrated at radiolysis of comparatively simple systems, such as aqueous solutions containing nitrate and phosphate ions, \bar{e} and $^\cdot\text{OH}$ radical (H_2O^+) acceptors. Total yield of primary radicals formed from these ions equals ~ 7 . As aqueous solutions of organics are radiolyzed, the observation for manifestation of these primary processes of radiosensibilization is complicated by secondary reactions, the reactions between intermediate products of additives radiolysis

and the initial substance molecules, in particular. The yield of degradation products of the latter becomes greater than 8 in the range of concentrations corresponding to the use of the maximal quantity of radicals – the water radiolysis products. For example, in the case of glucose and its nitrate, glycerol and its nitrate radiolysis, the maximal yield is 12 – 13 nitrate ions (in the range of concentrations corresponding to steps at the concentration curves of G). It is obvious that nitrate ions react with the radicals formed in $\cdot\text{OH}$ reactions with glycerol and glucose reducing them to nitrite-ion.

Analogous sensibilization mechanism is realized at radiolysis of S-(2-aminoethyl)-thiuronium sodium salt solution in the presence of molecular oxygen. This compound is the common radioprotector, which radiolysis was studied in a wide concentration range (from 10^{-5} to 0.01 M). The concentration curve of the degradation product yield shows two steps in the ranges of 10^{-4} – $3 \cdot 10^{-4}$ M and $5 \cdot 10^{-3}$ – 0.01 M, where the radiation-chemical yield of the degradation products reach 9 and 17 per 100 eV absorbed, respectively. They correspond to involvement of ionized and excited water molecule conversion products into the reaction under the suggestion that both $\text{O}_2^{\bar{\cdot}}$ and HO_2^- , formed in this system, possess the same oxidative equivalent and, similar to $\cdot\text{OH}$, are involved in the reactions with S-(2-aminoethyl)-thiuronium.

As estimating the sensibilizing action of molecular oxygen in organic compounds' solutions and, of course, biopolymers, one should take into consideration a possibility of hydroperoxide formation, which decay may promote degradation of the initial compounds. Such processes of post-irradiation degradation of protein, DNA and polysaccharides were recorded by different methods. For example, in the post-irradiation period DNA degradation yield in aqueous solutions reaches values comparable with these determined directly at irradiation (Chapter 6).

CONCLUSION

We have discussed the foundations of the radiation-chemical conversions of biopolymers in aqueous solutions. To conclude the discussion, it is appropriate to bring up the following questions: what is the prospect of radiation chemistry for biopolymers and what is the use of the data on the

radiation degradation mechanism of biopolymers, radiation medicine, for example?

Primarily, the investigation results on radiolytic properties of three classes of biopolymers (proteins, polysaccharides and nucleic acids) allow for detecting the sites in these molecules, sensitive to the action of ionizing irradiation – the place of unpaired electron localization in appropriate macromolecules. Moreover, the basic routes of macroradical conversions with formation of several final products (radiolytic effects) are tracked in these biopolymers and their natural complexes. These data on the radiolytic conversion mechanism of biopolymers form the basis for the control of radioprotection processes and degradation radiosensibilization of one polymer or another.

As applied to radiobiology, such questions may be resolved taking into account nucleic acid and protein conversions in the cell (cell radioprotection, radiation therapy: radiation treatment of cancer cells –DNA degradation by C–O–P and C–C bonds, repair system enzymes' degradation – the protein degradation).

As applied to polysaccharides, analogous tasks occur at resolving such questions as waste utilization of food and forest industries, and agriculture (radiation degradation as a method for decreasing molecular mass of cellulose, for example, for subsequent hydrolysis and production of sugars and glucose for cattle forage, wood property modification, etc.). As the mechanism of radiation degradation and modification of polysaccharides is tightly related to the question of sterilization of various materials, medicinal preparations and articles from cellulose, starch-containing food preservation – potato, flour, grain (see Chapter 8 for details).

The list of branches requiring data on the primary stages of biopolymer radiolysis mechanism may be significantly extended, if we consider not only water-soluble polymers. However, the data on the radiation degradation mechanisms of such systems are rather scanty in the literature yet.

Considering urgency of the investigation results of biopolymer radiolysis, a methodological disadvantage should be mentioned. Usually, such investigations were implemented by a single method only, and the test conditions applied by different groups of scientists may hardly be compared. Therefore, the value of such works for determining the radiolysis mechanism of particular object is diminished. Hence, a necessity of future coordination of efforts of different scientific groups, standardization of the sample

(biopolymer) irradiation conditions and selection of the objects for investigation most typical of these classes of compounds are desired.

Concluding the analysis of data on free-radical mechanisms of biopolymer radiation degradation, let us discuss in brief the question of radioprotection of a cell or an organism by chitosan, which is biopolymer. As found in radiobiological investigations, chitosan is one of highly effective radioprotectors. At intravenous injection to mice recalculated per 20 mg/kg 15 – 30 min prior to irradiation by 8 kGy (the minimum absolutely lethal dose), the compounds with molecular mass from 10,000 to 70,000 increase survivability of animals to 73% [11]. Chitosan is produced from chitin (see Chapter 9) [20]. Compared with other radioprotectors, chitosan application for this purpose is preferable due to biocompatibility and ability to biodegrade to glucosamine or N-acetylglucosamine in incompletely deacetylated chitin preparations – animal and human metabolites. Toxic properties of chitosan are observed only at doses exceeding that used for radioprotection by 1,000 times [21].

Suggesting predominance of the indirect action mechanism of ionizing radiation damaging a cell or an organism, let us manage to discover the role chitosan as a radioprotector of DNA and membranes – two main cellular targets [22].

Chitosan as DNA radioprotector

Primarily, it should be mentioned that chitosan is able to penetrate into the cell and, consequently, bind to DNA. As shown in *in vitro* tests [15, 16], DNA may form a complex with chitosan. Nanoparticles sized within 100 – 250 nm, possessing 35.6 wt.% DNA and 64.4 wt.% chitosan are formed due to electrostatic interaction between protonated amino groups of the ligand and negatively charged phosphate groups at the optimal ratio equal $N/P = 3 - 8$ (at 100 $\mu\text{g/ml}$ chitosan concentration) [23]. The formation of such particles showing N/P ratio equal 4 and sized within the range of 400 – 600 μm (200 $\mu\text{g/ml}$) was also detected in another system, obtained during preparation of anti-caries vaccine from DNA (in the presence of chitosan) and plasmid pGJA-P/VAX [24]. It is shown that the transfection effectiveness depends on the type of the studied cells [24]. A possibility of chitosan penetration through cytoplasmic membrane of various cells is also indicated [25].

In a complex with DNA in the cell, chitosan may act as free radical capturer (Chapter 9), similar to the case of sulfur-containing amines – radioprotectors [6]. The latter are also bound by amino groups to phosphate DNA (more precisely, to negatively charged oxygen atom in phosphate [26]).

Similar to other macromolecules (proteins, lipids, glycoproteids), pino(endo)cytosis is the basic mechanism of chitosan penetration into the cell. The length of chitosan macromolecules in the maximum efficient preparation efficiency (at $MM = 10,000 - 70,000$ [11, 27]) correlate with typical sizes of vesicles (from 50 to 1,000 nm) for polymer molecules at pinocytosis. Times of prior to irradiation chitosan injection to animals for the purpose of obtaining the maximal radioprotection effect [11] correlate with the times of penetration of the macromolecules mentioned into the cell at endocytosis and the ligand-receptor accosiate formation (up to dozens of minutes [28]).

On membrane radioprotection by chitosan

As we suggest that similar to the case of DNA we are speaking about prevention of free radical (water and alkyl radicals) impact on the main structures of the membrane, the following two factors should be taken into account:

1. what fragments of the membrane chitosan molecule is bound to;
2. what types of membrane damages chitosan prevents.

Practically all membranes of the animal cell contain phospholipids with negatively charged heads – phosphate groups, with which chitosan amino groups associate. As indicated, the degree of their bonding to phosphate groups of membranes also affects both the solution pH and molecular mass of chitosan. The interaction between chitosan and the membrane lipids is testified about by the change of bilipid layer structure at this site [29]. The investigation results of low-temperature radiolysis of liposome dispersion aqueous solutions indicates the formation of radicals from lipids and the significant decrease of their yield in the presence of radioprotector – one of spatially hindered phenols, injected to the liposome lipid bilayer before irradiation [30]. These data allow for a suggestion that chitosan linking to lipid phosphates may serve as the free radical capturer, \bar{e} and $\bullet\text{OH}$, in particular.

Proteins represent the second basic component of the membranes. As regards to the type of the cell, their concentration in the membranes varies from 25 to 75%. The function of membrane integral proteins (which is of interest for us) is transmission of substances to the cell, required for its functioning. The system of lipoprotein and glycoprotein receptors – subunits in the integral protein structure – controls the substance structure process. Radiation disturbs the structure and functioning of integral proteins. Hence, anything may penetrate through the damaged membrane into the cell: antigens and toxins, for example. As observed in investigations of the bat cell macrophages (RAW264.7) [31, 32], aminoglucose residues of chitosan associate with the receptors of immunoglobulins specific to mannose by the complement system (key–lock). Hence, it may be concluded that interacting with receptors of the current immunoglobulin (the protein fragment of glycoprotein), chitosan prevents the attack of free radicals on them and preserves them for consecutive functioning – the recognition of antigens. In this case, we are speaking about preservation of the organism immunity, suppressed by the radiation impact.

Thus the presence of chitosan at the membrane may prevent (or decrease) the change of structural organization of the lipid bilayer and the integral protein receptor degradation under the impact of ionizing radiation.

The above data on chitosan inspire a certainty that the maximal radioprotection of the human organism may be reached at the application of acceptors for free radicals generated by ionizing radiation.

REFERENCES

1. Romantsev M.F., *Chemical Protection of Organic Systems Against Ionizing Radiation*, Moscow, Atomizdat, 1978. (Rus)
2. Orlov V.M., Smirnov A.N., and Varshavsky Ya.M., *Molecular Biology*, 1977, vol. 11(1), p. 222. (Rus)
3. Sharpatyi V.A., Cadet J., and Teoule R., *Int. J. Radiat. Biol.*, 1978, vol. 33(5), p. 419.
4. Sharpatyi V.A., *Radiation Chemistry of Biopolymers*, Moscow, Energoizdat, 1981, 168 p. (Rus)
5. Sapezhinsky I.I., *Biopolymers: Kinetic Study of Radiation and Photochemical Conversions*, Moscow, Nauka, 1988, 216 p. (Rus)

6. Eyduş L.H., *Physicochemical Grounds of Radiobiological Processes and Protection Against Irradiation*, 2nd Edition, Moscow, Atomizdat, 1979, 216 p. (Rus)
7. Vladimirov V.G., Krasil'nikov I.I., and Arapov O.V., *Radioprotectors: Structure and Function*, Kiev, Naukova Dumka, 1989, 264 p. (Rus)
8. Kondakova N.V., "Biotest-system design for studying the damaging action of ionizing radiation and searching for biologically active substances with anti-radiation properties", *Doctor Dissertation Thesis*, Moscow, IBChPh RAS, 2000, 291 p. (Rus)
9. Kondakova N.V., Sakharova V.V., Ripa N.V., Rebrov L.B., Mandrugina A.A., and Fedoseev V.M., *Radiats. Biol. Radioekol.*, 2002, vol. 42(5), p. 503. (Rus)
10. Kudryashev Yu.B., *Radiation Biophysics (Ionizing Irradiation)*, Moscow, FIZMATLIT, 2004, 448 p. (Rus)
11. Il'in L.A., Andrianova I.E., and Glushkov V.A., *Radiats. Biol. Radioekol.*, 2004, vol. 44(2), p. 176. (Rus)
12. Hoffman J., *Cancer Induced by Low Dose Irradiation: Independent Analysis of the Problem*, Ed. E.B. Burlakova and V.N. Lystsov, Socioecological Union, 1994, vol. 1, pp. 18–3. (Rus)
13. Khrapunov S.N., Sivolob A.V., and Berdyishev G.D., *Biophysics*, 1983, vol. 28(4), p. 573. (Rus)
14. Zenger V., *The Principles of Structural Organization of Nucleic Acids*, Moscow, Mir, 1987, 584 p. (Rus)
15. Nechipurenko Yu.D., Vol'f A.M., Salyanov V.I., and Evdokimov Yu.M., *Zh. ETF*, 2004, vol. 125(1), p. 103. (Rus)
16. Evdokimov Yu.M., Salyanov V.I., Krylov A.S., Nechipurenko Yu.D., and Vol'f A.M., *Biofizika*, 2004, vol. 49(5), p. 789. (Rus)
17. Kuzurman P.A. and Sharpatyi V.A., *Chemical and Biological Kinetics: New Horizons (on the 90th Anniversary of Academician N.M. Emanuel)*, Ed. E.B. Burlakova, S.D. Varfolomeev, G.E. Zaikov and A.E. Shilov, Moscow, Khimia, 2005. (Rus)
18. Andrianov V.T., Akhrem A.A., Pisarevsky A.N., and Spitkovsky D.M., *Radiation Biophysics of DNP Chromatin*, Moscow, Atomizdat, 1976, 224 p. (Rus)
19. Proskurin M.A., *Doklady AN SSSR*, 1960, vol. 135(6), p. 1446. (Rus)
20. Stepanenko B.N., *Chemistry and Biochemistry of Carbohydrates (Polysaccharides)*, Moscow, Vysshaya Shkola, 1978, 256 p. (Rus)

21. Tsygan V.N., Zhogalev K.D., and Nikitin V.Yu., *BAD Market*, 2002, No. 2, p. 1. (Rus)
22. Burlakova E.B. and Shishkina L.Ya., *The Questions of Natural and Modified Radiosensitivity*, Ed. M.M. Konstantinova and A.M. Kuzin, Moscow, Nauka, 1983, p. 29. (Rus)
23. Mao Hq., Roy K., Troung-Le Vl., Janes Ka., Lin Ky., Wang Y., August Jt., and Leong Kw., *J. Control Release*, 2001, vol. 70(3), p. 399.
24. Li Yh., Fan Mw., Bian Z., Chen Z., Zhang Q., and Yang Hr., *Chin. Med. J. (Engl.)*, 2005, vol. 118(11), p. 936.
25. Prabaharan M. and Mano Jf., *Drug Deliv.*, 2005, vol. 12(1), p. 41.
26. Kuzurman P.A., and Sharpatyi V.A., *Radiats. Biol. Radioekol.*, 2006, vol. 46 (in print). (Rus)
27. Mori T., Murakami M., Okumura M., Kadosawa T., Uede T., and Fujinaga T., *J. Vet. Med. Sci.*, 2005, vol. 67(1), p. 51 – 56.
28. Varfolomeev S.D. and Gurevich K.G., *Biokinetics*, Moscow, Grand, 1999, 720 p. (Rus)
29. Fang N., Chan V., Mao Hq., and Leong Kw., *Biomacromolecules*, 2001, vol. 2(4), p. 1161.
30. Paramonov D.V., Trofimov V.I., and Knyazev A.A., *Khimia Vysokikh Energiy*, 2004, vol. 38(2), p. 113. (Rus)
31. Han Y., Zhao L., Yu Z., Feng J., and Yu Q., *Int. Immunopharmacol.*, 2005, vol. 5(10), p. 1533.
32. Feng J., Zhao L., and Yu Q., *Biochem. Biophys. Res. Commun.*, 2004, vol. 317(2), p. 414.

This page intentionally left blank